

**Solid organic matter in UK aquifers:
its role in sorption of organic contaminants**

Hannah Steventon-Barnes

A thesis submitted to the University of London
for the degree of Doctor of Philosophy

Department of Geological Sciences
University College London

September 2000

ProQuest Number: U642575

All rights reserved

INFORMATION TO ALL USERS

The quality of this reproduction is dependent upon the quality of the copy submitted.

In the unlikely event that the author did not send a complete manuscript and there are missing pages, these will be noted. Also, if material had to be removed, a note will indicate the deletion.



ProQuest U642575

Published by ProQuest LLC(2015). Copyright of the Dissertation is held by the Author.

All rights reserved.

This work is protected against unauthorized copying under Title 17, United States Code.
Microform Edition © ProQuest LLC.

ProQuest LLC
789 East Eisenhower Parkway
P.O. Box 1346
Ann Arbor, MI 48106-1346

Abstract

A major control on the attenuation of organic contaminants dissolved in groundwater is their sorption onto solid organic matter (OM) in the rock. Sorption modelling is currently based on the *amount* of solid organic carbon in the rock. However, there are very few available data on the total organic carbon (TOC) content in common UK geological materials. A significant new set of TOC measurements on a range of important formations is presented. Methods to measure TOC in geological, especially carbonate-rich, samples are reviewed and evaluated.

The impact of the *type* of OM on its sorption capacity is not understood. Non-linear isotherms measured on seven samples (of Lincolnshire Limestone, Glacial Till from Norfolk and unconsolidated deposits) had a wide range of organic carbon normalised distribution coefficients (K_{OC} from 7.85 l/g to 767 l/g at 0.01 g/l trichloroethene). This indicates the impact of characteristics of the OM.

Bulk geochemistry and micro-morphology characteristics of the OM that could be important predictors for sorption capacity are investigated and identified. Organic matter has been isolated, and the isolation technique evaluated. The major element composition of the isolated OM has been determined; elemental results were found to correlate with results of a pyrolysis analysis applied to whole rock samples. Morphological analysis of microscope slides of isolated organic matter provided information on the physical types (visually) and size (by image analysis) of the organic particles. Measured K_{OC} values correlated with the elemental H/O content of the sample's OM and with the pyrolysis measurements, but not with morphological results.

The effect of selected empirical isotherms on solute transport was simulated: use of an accurate distribution coefficient is essential, but non-linearity was found not to make a major impact on arrival results. Recommendations are made for the improvement of sorption modelling, and for appropriate analysis methods to supply relevant data on the type of OM in this context.

Table of Contents

Abstract.....	2
Table of Contents	3
List of Tables	8
List of Figures.....	9
Acknowledgements.....	13
 1. INTRODUCTION	 15
1.1 Aims of the research	15
1.2 Structure of the thesis.....	17
 2. LITERATURE REVIEW OF ROLE OF TOC IN SORPTION.....	 19
2.1 Introduction.....	19
2.2 Sorption isotherms	19
2.2.1 Freundlich and linear isotherms.....	19
2.2.2 Langmuir isotherm	21
2.3 Sorption of hydrophobic chemicals	22
2.3.1 Sorption to low organic carbon materials	23
2.3.2 Effects of water chemistry	25
2.3.3 Breakthrough curves show early arrival and tailing	25
2.4 Sorption variation with material type.....	26
2.4.1 Oxygen content or polarity index	26
2.4.2 Aromaticity.....	27
2.4.3 Conceptual models for isotherms	29
2.5 Summary.....	31
 3. MEASURING TOTAL ORGANIC CARBON CONTENT	 33
3.1 Introduction.....	33
3.2 Review of TOC measurement methods	34
3.2.1 Literature review	34
3.2.2 British Standard Methods.....	37
3.3 Methods used by commercial laboratories	38
3.4 Method evaluation	40
3.4.1 AIC analysis detection limits and precision.....	40
3.4.2 Interlaboratory comparison of TOC analysis.....	42
3.4.3 Dissolved Organic Carbon in acid.....	43
3.4.4 Comparison of acid evaporation and filtration	44
3.5 Conclusions and Recommendations	48
3.6 Summary.....	50

4.	GEOLOGY AND HYDROGEOLOGY OF UNITS SAMPLED	51
4.1	Introduction.....	51
4.2	The Chalk geology and hydrogeology	51
4.3	Lincolnshire Limestone geology and hydrogeology	52
4.4	Triassic Sandstone geology and hydrogeology	57
4.5	Sites A and B	57
4.6	Glacial Till geology and hydrogeology.....	58
4.7	Lower Coal Measures.....	59
4.8	Summary.....	59
5.	TOC IN UK AQUIFER AND AQUITARD MATERIAL	60
5.1	Introduction.....	60
5.2	Chalk.....	64
5.2.1	Upper and Middle Chalk	64
5.2.2	Lower Chalk	67
5.2.3	Previously published work	68
5.2.4	Summary of TOC in Chalk.....	69
5.3	Lincolnshire Limestone	69
5.3.1	Oxidised Lincolnshire Limestone.....	70
5.3.2	Unoxidised Lincolnshire Limestone.....	72
5.3.3	Redox blocks	73
5.3.4	Summary of TOC in Lincolnshire Limestone.....	74
5.4	Triassic Sandstone	75
5.5	Unconsolidated deposits	77
5.5.1	Site A.....	77
5.5.2	Site B.....	78
5.5.3	Conclusions	79
5.6	Glacial Till.....	80
5.6.1	North Sea Drift.....	80
5.6.2	Lowestoft Till.....	81
5.6.3	Summary of TOC in Glacial Till.....	84
5.7	Lower Coal Measures.....	84
5.8	Lower Greensand.....	85
5.9	Jurassic Mudrocks: Oxford Clay, Kimmeridge Clay and Lower Lias.....	85
5.10	Conclusions.....	86
5.11	Summary.....	87

6.	CHARACTERISATION OF ORGANIC MATTER.....	89
6.1	Introduction.....	89
6.2	Methods used.....	90
6.2.1	Isolation of organic matter.....	90
6.2.2	Geochemical analysis	92
6.2.3	Morphological analysis	94
6.3	Conclusions and Summary.....	105
7.	ORGANIC MATTER GEOCHEMISTRY: RESULTS AND DISCUSSION..	107
7.1	Introduction.....	107
7.2	Isolation of organic matter.....	107
7.3	Elemental content of isolated organic matter	110
7.4	Inorganic content of isolated organic matter.....	115
7.5	Stable carbon-isotope content of isolated organic matter	118
7.6	Rock-Eval pyrolysis of whole rock samples.....	120
7.7	Summary.....	127
8.	ORGANIC MATTER MORPHOLOGY: RESULTS AND DISCUSSION	128
8.1	Introduction.....	128
8.2	Organic matter characterisation results	128
8.3	Particle size analysis	133
8.3.1	Image analysis results	133
8.3.2	Made ground AIC distribution with particle size	137
8.4	Summary.....	140
9.	MEASURING SORPTION: METHODS USED	141
9.1	Introduction.....	141
9.2	TCE as a contaminant	141
9.2.1	TCE properties	141
9.2.2	Trichloroethene use	142
9.2.3	Case examples of trichloroethene contamination	143
9.3	Methods to measure sorption.....	144
9.4	Literature review of trichloroethene sorption.....	145
9.5	Method applied	146
9.5.1	Methanolic Solutions.....	146
9.5.2	Batch sorption procedure	148
9.5.3	Loss into headspace.....	151
9.5.4	GC-MS analysis.....	152
9.6	Conclusions and Summary.....	153

10. SORPTION: RESULTS AND DISCUSSION	155
10.1 Introduction.....	155
10.2 Sorption isotherms	156
10.3 Correlation with geochemical characteristics	162
10.4 Correlation with physical characteristics	164
10.5 Summary.....	165
11. COMPUTER MODELLING	167
11.1 Introduction.....	167
11.2 Retardation factor	168
11.3 Bio1d simulations.....	171
11.4 Sensitivity to inputs.....	175
11.5 Conclusions and summary	178
12. CONCLUSIONS	179
REFERENCES.....	182
APPENDICES:	
A. TOC ANALYSIS METHODS.....	193
A.1 Commercial laboratories' method details.....	193
A.2 Wolfson Geochemistry Laboratory, UCL.....	195
A.3 Commercial Laboratories Surveyed.....	196
B. DISSOLVED ORGANIC CARBON IN ACID.....	197
B.1 Method	197
B.2 Results.....	197
C. ACID-EVAPORATION PRE-TREATMENT METHOD	199
D. MEASURED AIC CONTENT	201
D.1 Upper Chalk.....	202
D.2 Lower Chalk.....	206
D.3 Lincolnshire Limestone from Quarry exposures.....	207
D.4 Unoxidised Lincolnshire Limestone.....	217
D.5 Triassic Sandstone	220
D.6 Site A.....	222
D.7 Site B.....	223
D.8 Lower Coal Measures.....	230
D.9 Bure Catchment Glacial Till.....	232
D.10 Morley Glacial Till.....	237

E.	ORGANIC MATTER ISOLATION	238
E.1	Method details.....	238
E.2	Mineral matter in residues.....	239
E.3	Loss of organic matter.....	239
E.4	Use of HCl with HF.....	240
E.5	Drying	240
E.6	Slide preparation.....	241
F.	RESULTS FROM POINT COUNTING.....	242
F.1	Repeated counts on the same slide.....	242
F.2	Counts on duplicated slides of the same sample.....	243
F.3	Impact of density.....	244
F.4	Lincolnshire Limestone	244
F.5	Glacial Till	245
F.6	Site B.....	245
G.	TCE ANALYSIS.....	246
G.1	TCE analysis method details.....	246
G.2	Standards.....	246
G.3	Blank values	247
H.	RESULTS OF SORPTION EXPERIMENTS.....	250

List of Tables

Table 1: Summary of TOC analysis methods used by commercial laboratories	39
Table 2: Total organic carbon results from Laboratory C and UCL	42
Table 3: Organic carbon lost in solution in hydrochloric acid.....	44
Table 4: Total organic carbon compared to acid-insoluble carbon results	46
Table 5: Descriptions of Lincolnshire Limestone Formation Members	53
Table 6: Permeability and interconnected porosity of Lincolnshire Limestone.....	55
Table 7: Organic carbon data provided in Consim	62
Table 8: Summary of AIC in Upper Chalk	66
Table 9: Summary of AIC in Middle Chalk.....	66
Table 10: Summary of AIC in Lower Chalk.....	68
Table 11: Summary of AIC in oxidised Lincolnshire Limestone	70
Table 12: Summary of AIC in unoxidised Lincolnshire Limestone	72
Table 13: Summary of AIC in Triassic Sandstone.....	75
Table 14: Summary of AIC in samples from Site A.....	77
Table 15: Summary of AIC in samples from Site B	79
Table 16: Analyses of dark, light and bulk glacial till fractions	82
Table 17: Sulphur and AIC in glacial till layers	83
Table 18: Summary of AIC in Glacial Till	84
Table 19: Summary of AIC in Lower Coal Measures	85
Table 20: Summary of new AIC determinations	87
Table 21: Precision of counting based upon classification of 300 particles	98
Table 22: Replicate particle classification and counts	99
Table 23: Isolation of organic matter	108
Table 24: Summary of recovery of carbon in isolated OM.....	108
Table 25: Elemental composition of kerogen, humic acid and fulvic acid.....	110
Table 26: Elemental analysis of isolated organic matter	114
Table 27: Inorganic geochemistry of isolated OM residues.....	117
Table 28: Stable carbon isotope results	119
Table 29: Rock Eval analysis results	122
Table 30: Rock Eval analysis results including S ₃ data	125

Table 31: Mean components in organic matter each material type.....	132
Table 32: Chemical and physical properties of trichloroethene.....	141
Table 33: Molar fractionsof methanol and TCE in water	147
Table 34: Descriptions of samples used in sorption experiments.....	148
Table 35: Range of equilibrium trichloroethene concentrations.....	156
Table 36: Range of K_{OC} values measured.....	159
Table 37: Freundlich isotherms fitted to the experimental data.....	160
Table 38: Langmuir isotherms (per gram solid)	160
Table 39: Measured sorption and geochemical data.....	162
Table 40: Properties used in simulations	172
Table 41: Isotherms used in simulations.....	172
Table 42: Input values used for made ground.....	176
Table 43: Input values used for weathered glacial till	176
Table 44: Total and Inorganic carbon measured in blanks	198
Table 45: Acid-soluble organic carbon as a percentage of original sample weight...	198

List of Figures

Figure 1: K_d values as a function of the organic carbon content	23
Figure 2: Total organic carbon results measured by Laboratory C and UCL	43
Figure 3: Apparent loss of organic carbon with inorganic carbon content	48
Figure 4: Sampling locations	63
Figure 5: AIC in Upper Chalk, Layer de la Haye.....	65
Figure 6: AIC in Upper Chalk, Banterwick Barn.....	65
Figure 7: AIC in Middle Chalk, Banterwick Barn.....	66
Figure 8: Negative correlation of AIC with $CaCO_3$, Banterwick Barn.....	67
Figure 9: AIC in Lower Chalk, Thriplow	67
Figure 10: AIC and TC in oxidised Lincolnshire Limestone, Brauncewell Quarry	71
Figure 11: AIC in oxidised Lincolnshire Limestone, Leadenham Quarry	71
Figure 12: AIC and TC in unoxidised Lincolnshire Limestone, Longholt core	72
Figure 13: AIC, AIS and TS in redox block, Brauncewell Quarry	74
Figure 14: AIC in Sherwood Sandstone, Middlesbrough core	76

Figure 15: AIC, TC and TS in Triassic Sandstone, Gamston Core	76
Figure 16: AIC, TC and TS in Site B Borehole 9D	78
Figure 17: AIC and clay in North Sea Drift, Primrose Farm	81
Figure 18: AIC and clay in North Sea Drift, Pages' Farm	81
Figure 19: AIC and TS in Lowestoft Till, Morley	82
Figure 20: Black wood	95
Figure 21: Brown wood	95
Figure 22 a and b: Examples of fine plant material	95
Figure 23: Pollen grain	95
Figure 24: Degraded humic matter	96
Figure 25: Fine amorphous matter	96
Figure 26: Rarefaction curve showing impact of additional points counted	97
Figure 27: Effect of density of slide solution on classification and abundance	99
Figure 28: Impact of 'Smooth' and 'Sharpen' image analysis tools	101
Figure 29: Image analysis of concentric images	102
Figure 30: The range of particle size distribution data	103
Figure 31: Area analysis of five images at magnification $\times 20$, Slide N1,5	104
Figure 32: Area analysis of six images at magnification $\times 40$, Slide N1,5	104
Figure 33: Effect of density of slide solution on particle size distribution	105
Figure 34: Van Krevelen diagram of kerogen types	111
Figure 35: Correlation between sodium content and residue unaccounted-for	118
Figure 36: HI correlation with H/C for glacial till samples	123
Figure 37: HI plotted against H/C for all samples	124
Figure 38: Atomic O/C against Tmax	124
Figure 39: Covariance of HI and OI with atomic ratios	126
Figure 40: Covariance of HI/OI with H/O atomic ratio	126
Figure 41: Components in organic matter from Lowestoft Till samples	129
Figure 42: Components in organic matter from North Sea Drift samples	129
Figure 43: Components in organic matter from Lincolnshire Limestone samples	130
Figure 44: Components in organic matter from Site B samples	130
Figure 45: Photomicrographs of selected smear slides of isolated organic matter	131
Figure 46: Particle size distribution of Glacial Till samples	135

Figure 47: Particle size distribution of Lincolnshire Limestone and Site B samples	136
Figure 48: PSD of particles and organic carbon content in made ground sample	137
Figure 49: Photograph of made ground from 2m bgl, retained on 19 mm sieve	138
Figure 50: Photograph of made ground from 2m bgl, between 12.7 mm and 16 mm	139
Figure 51: Photograph of made ground from 2m bgl, between 16 mm and 19 mm..	139
Figure 52: Concentration change in batch reactors over time.....	151
Figure 53: Sorption isotherms.....	157
Figure 54: Sorption isotherms, with logarithmic scale	157
Figure 55: Sorption isotherms, per gram organic carbon.....	158
Figure 56: Sorption isotherms per gram organic carbon, with logarithmic scales.....	158
Figure 57: Variation of K_{OC} with solute concentration.....	159
Figure 58: Plot of C_w against C_w/C_s	161
Figure 59: Relationship between K_{OC} and geochemical results.....	162
Figure 60: Correlation of Freundlich N with K_{OC} and H/O	164
Figure 61: Sorption plotted with morphological type content and % passing $0.6\mu m$	165
Figure 62: Variation of R with n and TOC for a linear isotherm.....	168
Figure 63: Variation of Freundlich retardation coefficient with concentration	169
Figure 64: Variation of R with TOC for varying Freundlich N	170
Figure 65: Variation of R with Freundlich N for varying TOC	170
Figure 66: Concentration profiles from Bio1d simulations	173
Figure 67: Results of parameter changes	177
Figure 68: Lithological log of Banterwick Barn Upper and Middle Chalk core	204
Figure 69: Key to lithological and other symbols used in Figure 68	205
Figure 70: AIC, TS and TC in oxidised Lincolnshire Limestone, Harmston Quarry	209
Figure 71: AIC, AIS and TS in redox block 1 from Harmston Quarry.....	210
Figure 72: AIC, AIS and TS in redox block 2 from Harmston Quarry.....	210
Figure 73: AIC, TS and TC in oxidised Lincolnshire Limestone, Ropesley Quarry .	213
Figure 74: AIC in oxidised Lincolnshire Limestone, Walcott Quarry.....	216
Figure 75: AIC in samples from BH 1, Site A.....	222
Figure 76: AIC in samples from BH 2, Site A.....	222
Figure 77: AIC in samples from BH 3, Site A.....	222
Figure 78: AIC in samples from BH 4, Site A.....	222

Figure 79: AIC, TC and TS in Site B Borehole 2D	223
Figure 80: AIC, TC and TS in Site B Borehole 4D	224
Figure 81: AIC, TC and TS in Site B Borehole 5D	224
Figure 82: AIC, TC and TS in Site B Borehole 6D	225
Figure 83: AIC, TC and TS in Site B Borehole 8D	226
Figure 84: AIC, TC and TS in Site B Borehole 10D	228
Figure 85: AIC, TC and TS in Site B Borehole 11D	228
Figure 86: AIC, TC and TS in Site B Borehole 12SA	229
Figure 87: AIC, TC and TS in Site B Borehole 13S	229
Figure 88: AIC in Borehole A, Lower Coal Measures	231
Figure 89: AIC in Borehole C, Lower Coal Measures	231
Figure 90: AIC in Borehole E, Lower Coal Measures	231
Figure 91: AIC in Borehole G, Lower Coal Measures	231
Figure 92: AIC and clay in North Sea Drift, Bates Moor Farm	234
Figure 93: AIC and clay in North Sea Drift, Crabgate Farm	235
Figure 94: AIC and clay in North Sea Drift, Ropers Farm	236
Figure 95: Decrease in TCE contamination in blanks with repeated analysis	247
Figure 96: TCE peak areas in blanks, compared to peak areas of preceding samples	248
Figure 97: TCE peak areas in blanks, compared to peak areas of preceding blanks	248

Acknowledgements

Prof. John McArthur conceived and supervised the project. The author would also like to thank the following people and organisations for their assistance:

For sample provision: CH2M-Hill; Dr. Alison Murphy and Dr. Ian Jarvis, Kingston University; Geoff Williams and colleagues at the British Geological Survey; Dr. Simon Bottrell, University of Leeds; Philippa Scott of ICI Technology; Entec (UK) Ltd; Dr. Kevin Hiscock, Dr. Mike George and Lucy Robson, University of East Anglia; and Aspinwall and Co. Representatives of many commercial laboratories and consultancies supplied information for the survey of TOC analysis methods.

For assistance in or access to facilities: Tony Osborn (for some sample preparation and AIC analysis) and Sarah Houghton (for GC-MS analysis) in the Wolfson Geochemistry Laboratory; Dr. Alex Kim for some AIC analysis results; Prof. Alan Lord and Jim Davy for assistance with organic matter isolation in the Micropaleontology Unit; Dr. Paul Bown for use of equipment for image capture; Dr. Dave Matthey for assistance with CHN and C-isotope analysis, Royal Holloway University of London; Janet Hope and colleagues in the Physical Geography Laboratory, UCL. Rock-Eval pyrolysis measurements were made by the Newcastle Research Group, Newcastle University. Oxygen content was analysed by Elemental Microanalysis Ltd.

For informative and / or enjoyable discussions, either in person or by email: Jane Dottridge (formerly of UCL); Prof. Richelle M. Allen-King (University of Washington State); Prof. John Barker (UCL); Dr. David Jolley and colleagues at the Centre for Palynology, University of Sheffield on organic matter identification and characterisation; Prof. Mike Hoare (Department of Biochemical Engineering, UCL), and Dr. Rudi Zauner (Department of Chemical Engineering, UCL) on particle size distribution analysis; Prof. David Kinniburgh and Daren Goody (British Geological Survey) and many others.

Jeremy Steventon-Barnes is thanked for so much support, help and for proof-reading the whole thesis; Dr. Alan Steventon is thanked for information and proof-reading parts of the thesis. Friends too numerous to mention by name are thanked for their forbearance.

This thesis is dedicated:

to my parents,
Alan and Judy Steventon,
without whose support and inspiration
I would not have started this work;

and to my husband,
Jeremy Steventon-Barnes,
without whose support and encouragement
I would not have finished it!

1. Introduction

Anthropogenic organic chemicals are significant groundwater contaminants. Their transport through the ground is controlled by a number of factors, which include the groundwater flow, and retardation processes experienced by the chemicals. One retardation mechanism is the partitioning of the organic chemicals from the water onto or into the solid rock material (sorption). As sorption processes remove organic contaminants from solution, they can mitigate or delay the threat of organic contaminants in groundwater. For hydrophobic organic contaminants, the solid organic matter in the rock materials is considered to be the main sorbent. The extent and mechanism of sorption processes and the nature of the solids to which the chemicals sorb are poorly understood. Data on the amount and distribution of organic matter in these rocks and the sorptive capacity of the organic matter are therefore of great importance.

It has previously been proposed that, when the total organic carbon (TOC)¹ concentration of the solid material is above 0.1%, the sorption of organic solutes is dependent on the TOC content. Much current modelling of sorption of hydrophobic chemicals assumes that the extent of sorption (or distribution coefficient, K_d) is solute-specific, and is linearly proportional to the aqueous concentration of the solute chemical and to the TOC content of the sorbent. The distribution coefficient normalised to the TOC content (K_{oc}), is therefore considered to be constant for all materials and specific to each solute. All solid organic carbon is assumed to behave identically with respect to sorption. Potential differences in extent or linearity of sorption between different types of organic carbon in different materials are completely disregarded.

1.1 Aims of the research

This research aims to increase the understanding of the role of solid organic matter in sorption of hydrophobic contaminants. To achieve this overall aim, the following questions have been investigated:

1. What are the TOC contents of UK aquifer and aquitard materials? How appropriate are the TOC analysis methods for these materials?
2. Is K_{oc} independent of the sorbent, or does it vary between materials?

¹ TOC as used here is identical to fraction of organic carbon (foc), and is given as a percentage.

3. If K_{OC} varies between materials, can this variation be related to geochemical and / or morphological properties of the solid organic carbon in the materials?
4. If K_{OC} varies between materials, does this variation impact significantly on the results of contaminant transport models and the predicted mitigation of potential groundwater threats?

Since the organic carbon concentration is considered to be an important control on the sorption of organic contaminants, it is a necessary input for contaminant transport modelling, and for understanding the fate of contaminants and their interactions with the rocks. Published TOC data for the UK is very sparse. TOC values are frequently estimated with little better than an educated guess. Alternatively TOC may be measured on samples, but no standard analytical technique is applied and there is little or no understanding of the implications of the different techniques used. The impact on TOC analysis results of the carbonate content of the samples was investigated. Previous studies of TOC analysis methods have used low carbonate materials. The first question above was addressed by:

1. analysing TOC in many UK materials and compiling over 1000 previously unpublished TOC measurements from six material types, including major aquifers (the Chalk, Lincolnshire Limestone and Triassic Sandstone);
2. compiling details of analytical techniques applied by major commercial testing laboratories; and
3. investigating analytical techniques experimentally to identify their precision and bias.

The potential variation of K_{OC} between materials, the second question raised, was investigated by performing batch sorption experiments on seven samples with varying material type and TOC. The results of these experiments were used to address the third and fourth questions.

To examine the relationship between potential variation in K_{OC} and the characteristics of the solid organic matter, the third question posed, required geochemical and morphological analysis of the solid organic matter, together with the results of the batch sorption experiments. Organic matter was isolated to quantify morphological (size and

type) and geochemical (elemental composition) differences. Morphological analysis included particle size analysis (by image analysis) and counting the abundance of classifications of organic matter on smear microscope slides. Geochemical techniques applied included elemental analysis of isolated organic matter and use of a pyrolysis technique on the whole rock samples.

The impact of K_{OC} variations on contaminant transport models was examined using computer simulations with commercial software to answer the fourth question. Empirical sorption isotherms gained during the research were simulated and their impact relative to isotherms generated from widely published K_{OC} values was investigated.

In many of the materials studied, much groundwater flow (and hence contaminant transport) is by fracture flow rather than matrix flow. Sorption may not significantly influence the arrival times or concentrations in such situations. However, study of such materials is important for two reasons: the relationship between solid organic matter and sorption can be studied, regardless of the large-scale physical hydrogeology of the formation; and in the field, matrix diffusion will enable sorption to occur, reducing solute concentrations and creating a store of contaminant with the potential to desorb if solute concentrations decrease, increasing remediation times.

1.2 Structure of the thesis

The methods used to answer the questions above and the results produced are presented and discussed in this thesis. Following this introduction (Chapter 1), published literature on the influence of organic carbon on the sorption of organic contaminants is reviewed (Chapter 2). Measurement methods to quantify total organic carbon (TOC) in rocks have been investigated (Chapter 3) and a method was selected to measure TOC content in major aquifer and other materials. The geology and hydrogeology of sampled units is reviewed (Chapter 4). The results of TOC analysis are presented in Chapter 5, which includes over 1000 unpublished TOC analyses together with published data to provide a compilation of TOC content in major aquifer materials, selected aquitard materials and samples of unconsolidated deposits and made ground.

Chapter 1: Introduction

Organic matter isolation techniques and methods for geochemical and morphological analysis of the organic matter are included in Chapter 6. Results from these investigations are presented and discussed in Chapters 7 (geochemical results) and 8 (morphological results).

Batch sorption experiments have been used to measure the sorption of an organic contaminant to seven samples. The methodology used is detailed in Chapter 9 and the results presented and discussed in Chapter 10. The significance of the results is examined by computer simulations discussed in Chapter 11. Chapter 12 draws conclusions and makes recommendations from the research.

2. Literature review of role of TOC in sorption

2.1 Introduction

In this chapter, formulae representing sorption isotherms are introduced (Section 2.2). Sorption of hydrophobic organic chemicals (HOCs) is related to the organic carbon content of the sorbent (Section 2.3), and the limitation of low total organic carbon (TOC) content on sorption of HOCs is examined. Research into the impact of variations in organic matter chemistry on its sorption behaviour is presented in Section 2.4.

Sorption is the uptake of species from solution by partitioning onto, or into, a solid. This includes adsorption (onto the surface) and absorption (within the matrix), but excludes desorption. Sorption leads to retardation of transport of the solutes, thereby increasing the time for a solute to reach a receptor. This increases time required to pump solutes from the ground in remediation schemes and decreases transformation rates such as biodegradation and volatilisation which do not affect sorbed chemicals (Allen-King *et al.*, 1996a, Schwarzenbach *et al.*, 1993).

A sorption isotherm represents the equilibrium partitioning of a chemical between solution and sorbed to solid, at a given temperature. Equilibrium models assume that the flow rate is sufficiently low for equilibrium to be attained. If this is not the case, a kinetic model is required, incorporating the rate of sorption, and rate of diffusion to sorption sites.

2.2 Sorption isotherms

2.2.1 Freundlich and linear isotherms

The Freundlich sorption isotherm is widely applied to sorption by geological materials of metals and organics, and is an empirical fit to experimental data. Therefore, extrapolation of the equation beyond the limits of empirical data should be avoided (Fetter, 1993).

Chapter 2: Role of TOC in sorption

The Freundlich sorption isotherm is:

$$C_S = K_F (C_W)^N$$

where [with dimensions]:

C_W = the concentration in solution [M/L^3]

C_S = the amount sorbed per unit mass of solid, in equilibrium with C_W [M/M]

K_F = the Freundlich coefficient (dimensions depend on N ; [L^3/M] when $N=1$)

N = a constant (dimensionless)

This can be linearised as $\log C_S = \log K_F + N \log C_W$

When $N=1$, the Freundlich isotherm represents a linear distribution ($C_S=K_d C_W$), with the C_S / C_W ratio constant at all concentrations and K_d being the linear partition coefficient. When $N<1$, the solute forms a spreading front, and as equilibrium solute concentration C_W increases the isotherm represents a decreasing ratio of sorbed to dissolved solute; at high concentrations (such as near a contamination source) the 'sorption capacity' of the solid is approached. When $N>1$, the solute forms a self-sharpening front with C_S/C_W increasing as C_W increases. At low concentrations, and over limited concentration ranges, a Freundlich isotherm approximates to a linear isotherm. Many sorption experiments have been at low concentrations over limited concentration ranges, and results interpreted as linear isotherms. However, researchers investigating higher concentrations over larger ranges have observed non-linear isotherms that fit the Freundlich isotherm (for example, Ball and Robert, 1991) and Freundlich N values between 0.777 to 0.956 have been reported (Xing and Pignatello, 1997). Thus, linear extrapolation from low to high concentrations can lead to significant overestimation of sorption.

Chapter 2: Role of TOC in sorption

The Freundlich sorption isotherm can be used to generate a retardation coefficient (r_f), representing the retardation of the solute relative to the groundwater velocity:

$$r_f = \frac{v_x}{v_c} = 1 + \frac{B_d K_F N C_w^{N-1}}{\phi}$$

where:

v_c = average linear water velocity

v_x = average linear velocity of solute front

and:

B_d = bulk density

ϕ = water filled porosity

For linear isotherms, when $N=1$, this simplifies to:

$$r_f = 1 + \frac{B_d K_d}{\phi}$$

2.2.2 Langmuir isotherm

The Freundlich sorption isotherm has no theoretical upper limit; as C_w increases, it predicts continual increases in sorption. Sorption may be conceptualised as binding to a finite number of sites, so there cannot be limitless sorption increase; when these sites are filled, there can be no more sorption. The Langmuir sorption isotherm is based on this concept:

$$\frac{C_w}{C_s} = \frac{1}{\alpha\beta} + \frac{C_w}{\beta}$$

where:

α = absorption constant related to binding energy (l/mg)

β = maximum amount of solute that can be sorbed by the solid (mg/kg).

The Langmuir isotherm is linearised by plotting C_w/C_s against C_s . It gives a retardation coefficient (r_{fL}) of:

$$r_{fL} = 1 + \frac{B_d}{\phi} \left(\frac{\alpha\beta}{(1 + \alpha C_w)^2} \right)$$

Some experimental studies have produced empirical data that can be fitted by a Langmuir curve with two straight line segments (Fetter, 1993), suggesting the existence of two types of sorption sites with different binding energies.

2.3 Sorption of hydrophobic chemicals

Hydrophobic organic chemicals (which exclude ionising organics) are sorbed by partitioning into or binding with low polarity solids. The main sorbent for hydrophobic chemicals is organic matter, usually quantified as organic carbon content. If all sorption is to solid organic carbon, the distribution coefficient (K_d) to the whole solid can be related to a distribution coefficient to organic carbon (K_{OC})¹ by the fraction of organic carbon (f_{OC}):

$$K_d = K_{OC} f_{OC}$$

This relationship does not allow for sorption to mineral surfaces, nor for variation in the sorptive capacity of the organic matter.

The fraction of organic carbon may be obtained from sample analysis or from limited published data (described in Chapters 3 and 4). For a particular chemical, K_{OC} may be obtained from published empirical results (such as Spitz and Moreno, 1996; Pankow and Cherry, 1996; Fetter, 1993; see also Section 6.4). K_{OC} is often related to the chemical's solubility (S) or its octanol - water partition coefficient (K_{OW}). Empirically determined relationships (Fetter, 1993, Allen-King *et al.*, 1996a) linking K_{OC} with K_{OW} or S may be extended to estimate K_{OC} for chemicals for which it has not been determined. It is preferable to use an equation determined from chemicals similar to that for which the K_{OC} is required; where this is not possible, the average or range may be used. The following examples of calculations of K_{OC} from correlations are for trichloroethene (TCE), which is the example contaminant used throughout this thesis. Fetter (1993) does not provide correlations based on experimentation with chlorinated hydrocarbons; the K_{OC} range calculated from correlation to K_{OW} (of 195 l) was 28 to 417 kg/l, and from correlation to solubility (of 1100 mg/l) was 56 to 316 kg/l. Allen-King *et al.* (1996a) provide correlations for non-aromatic halogenated compounds giving K_{OC} of 73 kg/l and 400 kg/l correlating to K_{OW} and solubility respectively. These compare well to published empirical K_{OC} values that are generally 50 to 500 kg/l (Section 9.4). K_{OC} may also be estimated from the molecular structure (the 'molecular connectivity index') of the chemical; for trichloroethene the calculated K_{OC} based on molecular structure (Fetter, 1993) was 95 kg/l. K_{OC} estimation from molecular structure can be amended to account for the

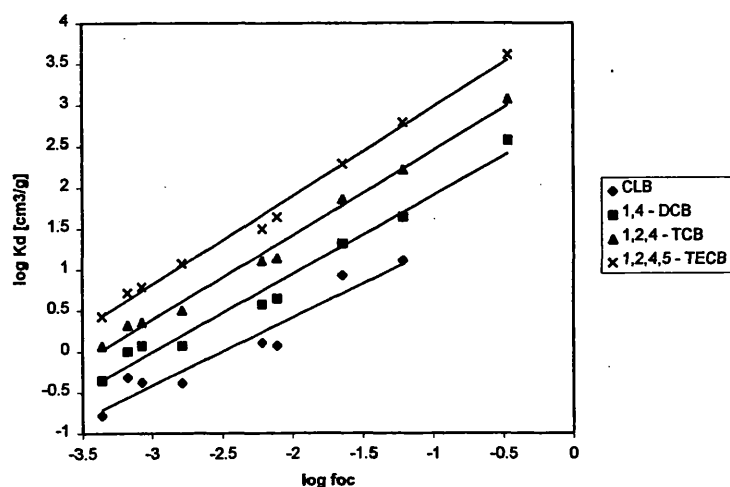
¹ K_{OM} , the sorption to organic matter may be used instead. %OM is approximately twice %OC.

for the molecule's polarity, but this has not been found to produce better results than methods based on K_{ow} or S (Allen-King et al., 1996a).

2.1.1 Sorption to low organic carbon materials

It is frequently assumed that over 0.1% TOC (i.e. f_{oc} of 0.001) is required for HOC sorption to be dependent on the TOC concentration. It appears that this concept of a 0.1% TOC 'cut-off' limit was developed in the early 1980s as researchers found that linear relationships between $\log K$ and $\log f_{oc}$ broke down as TOC dropped below a small value, around 0.1% (as illustrated in, for example, Figure 1; Schwarzenbach and Westall, 1981). Schwarzenbach *et al.*, 1993 claim that since mineral surfaces are polar, bonding with non-polar organic solutes is energetically unfavourable and thus minimal. Mineral surface sorption will be proportionally significant when TOC is low, such as in many aquifer materials. They state that sorption data appear to have correlated K_d and f_{oc} when TOC >0.1 to 0.2% (Schwarzenbach and Westall, 1981; Banerjee et al, 1985), and that at lower TOC mineral surface sorption becomes significant. However, they reference experiments involving the removal of organic carbon that indicate that the organic carbon continues to be significant in sorption of HOCs, even at very low TOC contents ($<0.1\%$ TOC). They conclude that the ratio of area of mineral surface to TOC determines the relative inputs of these two solids to HOC sorption. At TOC $<0.1\%$, sorption to mineral surfaces should be considered, but may not dominate, depending on properties of the sorbate and solid.

Figure 1: K_d values as a function of the organic carbon content
from Schwarzenbach and Westall, 1981



Ball and Roberts (1991) undertook experimental sorption studies on low organic carbon sandy aquifer material with TOC from 0.013% to 0.099%; ('low organic carbon' is widely used to refer to <0.1% TOC). Coarse size fractions had greater sorption capacity, with greater BET measured surface area and organic carbon content. Sorption was not reduced by removal of carbonate, nor was it changed by pulverisation of the samples. K_d for these samples was found to be over an order of magnitude higher than that predicted from the sample's TOC and previously published K_{OC} values. Ball and Roberts (1991) state that sorption differences were not related to organic carbon content, but that reasonable correlation between K_d and f_{OC} was found and organic dominated sorption may occur. They suggest that thin coatings of organic matter on mineral surfaces may affect sorption. They found isotherm non-linearity, which was attributed to heterogeneous sorption sites. However, it is suggested here that comparing the partition coefficients of samples with different depositional environments, geochemistry and other properties is unlikely to reveal strong correlation between f_{OC} and K_d because other influences on sorption (such as organic matter type) may outweigh the influence of the organic carbon content.

The lower TOC limit for organic carbon dominated sorption of HOCs is based on the point at which sorption of HOCs to mineral surfaces becomes significant compared to their sorption to organic matter. This is dependent on both the organic content of the solid, and on its inorganic geochemistry, as well as on the hydrophobicity or K_{OW} of the solute contaminant. At some TOC content [f_{OC}^*], sorption to OM is equal to sorption onto mineral surfaces. f_{OC}^* may be linked to K_{OW} and the surface area (S_a) of the solid (which is largely dependant on its clay content) by:

$$f_{OC}^* = \frac{S_a}{200(K_{OW})^{0.84}} \quad (\text{Fetter, 1993})$$

which gives f_{OC}^* of 0.0007 (TOC 0.07%) for TCE in a solid with a surface area of 12m²/g (typical of kaolinite clay soil). It is clear from this that the greatest impact of sorption to minerals will be in solids with low TOC and high surface area, such as from swelling clay content, and for solutes with low K_{OW} .

2.3.2 Effects of water chemistry

The following discussion is based on Allen-King *et al.* (1996a) who note that variations in natural water chemistry have little impact on degree of sorption. The increased solubility of organic compounds with increasing temperature would lead to lower sorption, but the environmental temperature range is very limited. Temperature variation between 9°C and 23°C has been found to cause K_d changes of less than 10% in most cases, with a maximum of 33% reported. pH effects have not been observed in experiments with non-ionic compounds. Increasing ionic strength can decrease solubility and therefore increase sorption, but this is a small effect. An ionic strength increase from distilled water to sea-water causes a sorption increase of about 20%. Organic contaminant co-solvents may compete with each other, and increase solubility, both effects leading to decreasing sorption. Increasing solubility due to presence of a co-solute is likely to have a significant effect only when the co-solute is >5% of the solution. Retardation may be decreased by dissolved organic matter and suspended colloidal material, which can sorb and transport organic contaminants. Surfactants present above a substance-specific critical level will increase the solubility of organic solutes. However, below the critical level, the surfactants will form a layer around organic matter leading to decreasing sorption of other organic solutes when the surfactants are non-ionic and anionic, and increasing sorption when the surfactants are cationic.

2.3.3 Breakthrough curves show early arrival and tailing

Field observations of both early solute breakthrough and solute tailing which will lead to faster receptor contamination and longer remediation times are attributed to pore-scale and field-scale effects. Such effects could include isotherm non-linearity (causing either early breakthrough or tailing, but not both concurrently), desorption hysteresis (causing tailing), and non-equilibrium sorption, which is considered the most important (Allen-King *et al.*, 1996a). Attaining sorption equilibrium is controlled by physical or chemical rate-limiting processes such as diffusion of the solute into stagnant water and slow reaction sites on the sorbent. Modelling non-equilibrium sorption requires knowledge of the rate of the rate-limiting step, and details of relevant physical characteristics of the system. Models fitted to experimental breakthrough curves usually result in non-unique solutions. Asymmetrical breakthrough curves observed for sorbing solutes but not

conservative solutes suggests the occurrence of intra-organic matter diffusion. Intra-particle diffusion may occur when organic matter (OM) is distributed throughout mineral particles. Spatial variability in hydraulic conductivity or K_d will also produce non-ideal breakthrough curves.

2.4 Sorption variation with material type

Sorption to organic matter in geological rocks is dependent on the characteristics of the organic matter itself. Mouvet *et al.* (1993), Bourg *et al.* (1993) and Mackay *et al.* (1986) found sorption properties that could not be related to TOC variations. Mouvet *et al.* (1993) found these differences were not linked to surface area, and concluded that some discrepancies between partition coefficient and TOC may be due to the nature of solid or dissolved organic matter.

If sorption of HOCs to organic matter is dependent to some extent on some characteristic of the organic matter, what might that characteristic be? All previous research has focused on the chemistry of the organic matter, concluding that the organic matter's polarity is important. Allen-King *et al.* (1997b) suggested that differences in K_{OC} between weathered and unweathered glacial tills are related to the oxidation state and hence lipophilic character of the OM. This was further developed by Binger *et al.* (1999), who found $\log K_{OC}$ to be linearly related to $\log H/O$ for a series of glacial tills with different extents of weathering. The $\log K_{OC} / \log H/O$ relationship in these samples was steeper than previously reported in shale and coal samples (Grathwohl, 1990).

K_{OC} increases have been associated with various changes in OM geochemistry, including: lower O content (Grathwohl, 1990; Huang and Weber, 1997); decreased polarity index (O+N)/C (Rutherford *et al.*, 1992; Xing *et al.*, 1994); increased aromaticity (Gauthier *et al.*, 1987; Murphy *et al.*, 1990). These are expanded in the following sections.

2.4.1 Oxygen content or polarity index

Enhanced sorption (by > 1 order of magnitude) to OM in unweathered shales and coals, compared to sorption to OM in recent soils, geologically young material and low-grade coals has been attributed to a lower content of oxygen-containing functional groups (Grathwohl, 1990). Increasing linear K_{OM} or K_{OC} has been non-linearly correlated to decreases in the (O+N)/C ratio (the polarity index, PI) of the solid (Rutherford *et al.*,

1992; Xing *et al.*, 1994). Lower oxygen content (as O/C ratio), greater condensation and chemical reduction, due to material age, resulted in greater sorption, together with more non-linear isotherms and greater sorption - desorption hysteresis (Huang and Weber, 1997).

These findings have been used to generate empirical relationships between elemental ratios and K_{OC} :

$\log K_{OC} = 1.52 \log (H/O) + 1.54$, for TCE (Grathwohl, 1990)

Other correlations are provided by Huang and Weber (1997) for phenanthrene at two concentrations (due to isotherm non-linearity). They relate isotherm non-linearity (as N in the Freundlich isotherm) to elemental content via

$N = 0.409 + 0.704 (O/C)$.

Such correlations have been suggested as mechanisms to calculate K_{OC} for other solutes in other materials: from the solute's K_{OW} and the material's measured elemental content (Grathwohl, 1990); or from solute's K_{OW} and the material's polarity index as calculated from measured K_{OW} and K_{OC} of another solute in that material (Xing *et al.*, 1994); or from the K_{OC} for two solutes in the same material, and the K_{OC} of one of them in another material (Rutherford *et al.*, 1992). Such approaches were claimed to provide a better match to experimental data than K_{OC} predictions from K_{OW} alone (Xing *et al.*, 1994).

Diagenetic changes usually result in decreasing H/C and O/C, and increasing polymerisation and condensation of organic molecules, leading to increasing K_{OC} . Conversely, weathering increases the O/C ratio: weathered shale was found to have sorption reduced by a factor of 30 compared to unweathered shale from same site (Grathwohl, 1990); O/C ratios were not measured.

While PI incorporates the polarity impact from the chemical composition, it ignores the impact on polarity of the molecule's configuration and structure. Effective polarity may also be influenced by the association of the OM with minerals.

2.4.2 Aromaticity

Sorption capacity of materials has been related to the polarity of the material (as O/C or (O+N)/C ratios), which in turn has been associated with the aromaticity of the material

(Xing *et al.*, 1994). Alternatively, some researchers have directly related sorption capacity with aromaticity (Gauthier *et al.*, 1987; Murphy *et al.*, 1990).

Gauthier *et al.* (1987) link the sorption of HOCs to dissolved humic and fulvic acids² with the acids' aromaticity, as measured by ¹³C nuclear magnetic resonance (NMR). The aromatic fraction correlated with the -COOH functional group content, the predominant oxygen containing group. Thus a correlation of sorption with aromatic carbon may be an indirect correlation with oxygen content. Excluding fulvic acids, which have a high proportion of -COOH groups, K_{OC} correlates with the H/C ratio. Oxygen content was not measured.

Murphy *et al.* (1990) built on investigations of Gauthier *et al.* (1987) and others on sorption to aqueous organic phases in which sorption coefficients have been related to the origin, molecular weight, polarity and molecular structure of the dissolved organic matter. Less polar organic substances with low O/C ratios showed greater sorption. OM may be transported as dissolved organic carbon from soil zone sources until it forms coatings on mineral grains (West *et al.*, 1994). Murphy *et al.* (1990) artificially created coated mineral grains, by deliberately sorbing well-characterised, consistent natural humic substances (purchased with known elemental analyses), to haematite and kaolinite. Sorption of organic solutes was found to be dependent on the type of humic substance; the most aromatic humic acid was the strongest sorbent. Sorption was also dependent on the mineral substrate, which controlled both amount of humic substances sorbed to the mineral, and also their sorption capacity for HOCs. The mineral substrate may control the variation of the sorption capacities by controlling the orientation and structure of the sorbed humic substance and thus affecting its surface area or accessibility. The non-linear Freundlich sorption isotherms measured had increasing gradient and linearity with the solute hydrophobicity. K_{OC} values were relatively insensitive to the estimated exposed surface area of the mineral sorbent, due to the low mineral sorption coefficient. Except at very low TOC content, K_{OC} values were also found to be relatively independent of TOC.

² Humic and fulvic acids are defined in Section 7.3 as soluble in alkali, with fulvic acids also soluble in acid.

2.4.3 Conceptual models for isotherms

The linear sorption isotherm can be conceptualised as dissolution of the solute in the organic matter, and can be analogised to organic solvent - water solute partitioning. The Langmuir isotherm represents binding of solute molecules to specific, identical sites in the sorbent. However, experimental determinations of sorption isotherms are best fitted by Freundlich isotherms, which have no clear theoretical basis. Can increased understanding of the impact on sorption made by organic matter type help us understand this isotherm? This section discusses a concept of sorption that relates observations to physical processes.

Sorption to soils has been found to become increasingly non-linear and competitive with increasing condensed nature of organic matter. Concentration-dependent heat of solution and evidence of an internal surface in solid organic matter (Xing and Pignatello, 1997) also discredit the model of linear partition analogised to dissolution. While solid geological OM is not a true polymer, it is macromolecular, and thus an analogy between man-made polymers and geological OM may be appropriate. Sorption to man-made organic polymers has been conceptualised by the 'dual mode model' or 'dual reactive domain model' (DRDM) (Xing and Pignatello, 1997), which has also been found suitable for explaining many non-ideal HOC sorption-desorption equilibria and rate phenomena. The polymers have glassy or rubbery structures, with glassy structures being more condensed with higher cohesive forces between polymers. Polymers change from glassy to rubbery at a compound-specific temperature. Sorption to the rubbery state is by dissolution, and to the glassy state by both dissolution (creating a linear partition) and 'hole filling' (creating a Langmuir partition). The dissolution domain could comprise many constantly changing dynamic sites, which behave as a liquid; conversely, 'holes' could be bounded by macromolecules with a rigid configuration. However, OM is highly heterogeneous, so it could be conceptualised as having many different glassy and rubbery components, with many different dissolution and hole filling sorption mechanisms, each with its own linear or Langmuir isotherm. It has been shown mathematically (Xing and Pignatello, 1997) that the isotherm created from multiple Langmuir terms is related to a

Freundlich isotherm³, and so the empirical application of Freundlich isotherms may have a theoretical basis. It would be impractical to use different isotherms to represent each of the multiple dissolution and hole filling processes occurring, so representing the sum of these processes with a single Freundlich isotherm is a useful simplification. The Freundlich non-linearity N term may be taken as a index of site energy distribution (shown mathematically, Xing and Pignatello, 1997) such that a smaller N , and greater non-linearity, relate to a broader energy distribution and greater contribution of the hole-filling mechanism.

Xing and Pignatello (1997) used sorption experiments to support the DRDM model. They found that the hole-filling mechanism accounts for most sorption to OM (using both single solute and competitive sorption experiments to divide sorption into a linear and a Langmuir component; 68% of sorption at low concentration was attributed to hole-filling, reducing to 45% at high concentration). The non-linearity (N) was unaffected by the removal of mineral phases with HCl and HF. Increased temperature (from 6°C to 90°C) increased the linearity of sorption. Following the polymer analogy, this occurred as the organic structures converted from glassy to rubbery. The sorption capacity decreased as holes became unavailable. The sorption of chlorinated benzenes to different organic matter fractions showed increasing non-linearity and increasing competitive effects with increased condensation of the OM. Non-linearity increases with reaction time, suggesting that hole-filling sorption is kinetically slower. Structurally similar sorbate molecules appear to compete more strongly, suggesting some degree of selectivity of sorption sites. The isotherm of a solute becomes more linear when in the presence of a strongly competing co-solute, suggesting that the co-solute fills potential holes but does not prevent dissolution-type sorption. Non-linearity and competitive effects correlate with internal microvoids, revealed by measuring BET surface area at 273K using CO₂ as the sorbate compared with the external surface area of the OM measured using N₂ at 77K.

Weber *et al.* (1998) investigated sorption - desorption hysteresis in the context of the DRDM. Hysteresis is possibly attributable to slow desorption or entrapment of sorbing

³ This is trivial, as the Freundlich curve is such that many curves will sum to produce it (Barker, pers. comm. 2000).

molecules within condensed organic matrices. Kerogen, characterised by ^{13}C NMR, is highly condensed OM; samples with high kerogen content reveal greater hysteresis, and sorption 1 to 2 orders of magnitude greater, than samples with more ‘younger amorphous humus’. Oxidised amorphous SOM micropores have changing shape and rigidity and interact with water to become swollen. Condensed pores are rigid; thermodynamic hysteresis is attributed to heterogeneous condensed micropores having different sorption and desorption energies.

2.5 Summary

- Sorption of a solute to a solid may be represented by isotherms relating sorbed concentration to dissolved concentration via solid and solute characteristics.
- Sorption of hydrophobic organic solutes is predominantly to solid organic matter; the contribution from other surfaces can be disregarded, except at very low organic carbon contents. Sorption is therefore normalised to the organic carbon content.
- ‘Solid organic carbon’ is usually considered to be consistent, and sorption coefficients to organic carbon are assumed to be solute dependent but not sorbent dependent. Linear sorption coefficients may be calculated from the solute’s solubility, K_{OW} , or from previous measurements.
- Sorption of HOCs over wide concentration ranges has been found to be non-linear, and is best fitted to a Freundlich sorption isotherm. Use of linear partition coefficients over a wide concentration range, or extension from experiments undertaken at dilute concentrations to modelling of high concentrations, will overestimate sorption at high concentrations.
- Solid organic matter is not consistent. The chemistry of the organic matter has been shown to affect sorption to it. K_{OC} is therefore sorbent dependent, and has been correlated to the oxygen content or polarity of the OM (as O/C or H/O, or (O+N)/C ratios), or its aromatic content. OM geochemistry has been shown to affect extent of sorption, sorption non-linearity and sorption - desorption hysteresis.
- The impact of the variations in OM type may be understood by conceptualising sorption using the ‘dual reactive domain model’, based upon sorption to polymers. This describes OM macromolecules as either glassy or rubbery structures with linear, dissolution-type sorption to both structures, and hole-filling sorption following

Langmuir isotherms to glassy structures. Summing multiple Langmuir isotherms can produce Freundlich isotherms, which commonly provide the best fit to empirical sorption data.

3. Measuring Total Organic Carbon Content

3.1 Introduction

This chapter discusses methods to analyse total organic carbon (TOC) content. Published literature is reviewed in Section 3.2, and Section 3.3 summarises and comments on methods used by commercial laboratories. The analytical method used for this research is discussed and evaluated in Section 3.4, including experiments to quantify the loss of organic carbon during pre-treatment for TOC analysis. Section 3.5 discusses some of the difficulties in measuring TOC, compares the methods, and presents some conclusions and recommendations.

The sorption of organic solutes to subsurface materials retards contaminant movement. The extent of such sorption is considered to be controlled largely by the TOC content of the material where it is greater than 0.1% (see Section 2.3.1). The correct quantification of TOC is therefore of great importance to accurate modelling and prediction of contaminant retardation by sorption.

Analysis for TOC commonly uses high temperature oxidation (HTO) with quantification of the carbon dioxide produced, or alternatively wet chemical oxidation with quantification of the excess oxidising agent. Samples analysed by HTO are prepared for analysis by removing their inorganic carbon, either by acidifying the sample and filtering to isolate the residue for analysis, or by acidifying the sample and evaporating to dryness to isolate the residue. Filtration of the acid risks losing organics dissolved in the acid whilst evaporating introduces problems due to incomplete removal of carbonate (Caughey *et al.*, 1995; Heron *et al.*, 1997).

The work reported in this chapter indicates that, whilst most published literature on TOC analysis methods recommends using evaporation of the acid during the carbonate removal step, this causes significant errors in the analysis of high carbonate samples due to the failure to remove all carbonate. Filtration of the acid from the sample is recommended for high carbonate materials, which include many major UK aquifers.

3.2 Review of TOC measurement methods

3.2.1 Literature review

The importance of TOC content in contaminant transport has led to the publication of a number of papers reviewing analysis methods. High temperature oxidation (HTO) after removal of carbonates by acidification is now regarded as the most appropriate TOC analysis method, due to the potential for incomplete oxidation during wet chemical oxidation. Ideally, acidification must both completely remove inorganic carbon and retain all the organic carbon, which two aims produce conflicting methods.

The Walkley and Black wet chemical oxidation method was compared to an automated coulometric method by Lee and Macalady (1989). Total carbon (TC) and inorganic carbon (IC) were determined, taking organic carbon as the difference. For the coulometric method TC was determined from CO₂ evolved by HTO, and IC was determined from CO₂ evolved from acidification of the sample with perchloric acid (ClHO₄). Incomplete carbonate removal and the potential for oxidation of organic carbon by the acid were detailed as drawbacks for IC analysis. Wet chemical oxidation was compared to HTO analysis following acidification of the sample in an interlaboratory study (Powell *et al.*, 1989), in which three laboratories analysed samples for TOC using the method of their choice. The one that used wet oxidation reported lower TOC values, indicating incomplete oxidation. Another, using acidification (with HCl) followed by carbon analysis by HTO, found higher TOC content than the third, potentially indicating incomplete carbonate removal. Powell *et al.* concluded (unsurprisingly) that '*standard methods of sample pre-treatment and analysis are required to increase the reliability of TOC analyses*', and that some discrepancies between laboratories were due to carbonate removal methods.

Churcher and Dickhout (1989) recommend analysis of carbon content of samples by HTO following carbonate removal by 30% HCl washed over the sample on a filter paper. They quantify organic carbon loss in the acid as less than 0.1% TOC, by analysing the filtrate. However, this potential for loss of organic matter dissolved in the acid has concerned later researchers (for example, Caughey *et al.*, 1995, Heron *et al.*, 1997) who stress the

importance of avoiding loss of acid-soluble organic carbon, but do not quantify likely losses. Dissolution of 5 to 45 % of the TOC in marine sediments (which might be expected to be more reactive, as they contain relatively young, labile organic matter) treated with phosphoric acid (H_3PO_4) have been reported (Froelich, 1980), and of 10 to 80% of TOC from bottom sediment, suspended organic material and dissolved organic material from a delta and bottom sediments from a continental shelf when using HCl, sulphuric acid (H_2SO_4) and nitric acid (HNO_3), compared to less than 2% when using H_2SO_3 (Gibbs, 1977).

To avoid the potential loss of organic matter dissolved in the acid, evaporation of the acid from the sample is recommended. Such a method was tested in an interlaboratory study (Caughey *et al.*, 1995), in which sulphurous acid (H_2SO_3) was repeatedly added to the sample in the combustion vessel (to avoid losses in transfer) and evaporated overnight at 40°C until at least 10% excess acid had been added and effervescence had ceased. Residual carbon was determined by HTO. Significant systematic errors between different laboratories were found, and Caughey *et al.* concluded that '*samples high in TIC [total inorganic carbon] and low in TOC present the greatest analytical difficulties, even when special care is taken during an interlaboratory study*'. While reasonably good interlaboratory agreement was found for TIC and total carbon (TC) values, TOC results were more scattered; often the sum of TOC and TIC results was greater than TC. Incomplete carbonate removal was reported as a source of bias in the TOC analysis. The only laboratory in the study reportedly successful in removing all the carbonate carbon had extensive prior experience in using the specified method. Additional problems reported included initial difficulties in obtaining H_2SO_3 uncontaminated with non-carbonate carbon and difficulties in grinding the samples without adding non-carbonate carbon contamination. Finer grinding of the sample was suggested to improve sample homogeneity and speed of carbonate dissolution (especially for slow dissolving carbonates such as dolomite).

A similar method for 'determination of nonvolatile organic carbon in aquifer solids after carbonate removal by sulphurous acid' designed to avoid the loss of organic matter dissolved in the acid, by using evaporation rather than filtration to remove the acid was

published by Heron *et al.* (1997). They comment that '*all TOC methods depend on efficient and complete carbonate removal prior to the TOC quantification step*'. They acidified the samples (mainly quartz sands, with inorganic carbon, where measured, less than 0.002%) in beakers either repeatedly with 2ml or once with 5ml of 0.73 M H₂SO₃ at 40°C for 24 hours. The residue was transferred into crucibles and TOC determined with a LECO® CS-225 C/S analyser. They reported large standard deviation on triplicate samples (with sample results well above the detection limit), which limits quantitative conclusions on the degree of carbonate removal. Heron *et al.* also emphasised the importance of running method blanks to test for carbon contamination from the acids used.

However, Heron *et al.* noted problems arising from incomplete removal of carbonates: analysis of samples spiked with additional carbonate produced a higher apparent TOC. In particular, siderite (FeCO₃) proved problematic: between 21% and 86% of siderite in spiked samples was removed, consistent with very slow siderite dissolution. Apparent TOC content in naturally 'carbonate-rich' samples⁴ (with over 1% inorganic carbon⁵) containing calcite and dolomite continually decreased with increased acid addition, indicating incomplete carbonate removal. Heron *et al.* concluded that their method is not suitable for samples containing slow-dissolving carbonates. The problems of incomplete removal of carbonate caused by this method may be more significant than avoiding loss of organic matter when filtering acid from the sample.

Allen-King *et al.* (1997a), using standard methods (Churcher and Dickout, 1989, Lee and Macalady, 1989, Caughey *et al.*, 1995) on samples with 0.004% to 4% inorganic carbon, comment that stronger acids than H₂SO₃ (such as HCl and HNO₃) are more likely to achieve complete carbonate dissolution, because H₂SO₃ is weak and available only at low concentrations. If a large number of applications are required, the analytical process will be lengthy. Allen-King *et al.* state that strong acids are unlikely to remove significant amounts of the kerogen⁶-rich organic matter in geological samples. H₂SO₃ is a corrosive

⁴ samples from Villa Farm.

⁵ which is much lower than carbonate-rich UK aquifer sediments; for example, virtually pure limestones such as the Chalk and Lincolnshire Limestone can contain almost 12% inorganic carbon.

⁶ 'kerogen' is defined in Section 6.2.1 as organic matter that is insoluble in organic solvents.

vapour, is available only at low concentrations and adds sulphur and carbon contamination, which interfere with some quantification methods and raise the detection level.

Current best practice is analysis of remaining carbon by HTO following removal of carbonate by acidification. Recent literature has concentrated on the retention of all organic carbon during the acidification stage, proposing removal of carbonates by addition of acid to a ground sample, with repeated evaporation and addition of the acid; H_2SO_3 has been considered ideal because it is least destructive to organic carbon, but stronger acids may be more successful in carbonate removal. However, there is a wide acknowledgement of the problem of incomplete carbonate removal in carbonate-rich samples, and no clear quantification of the impact of the resulting over-measurement of organic carbon relative to the loss of organic carbon when filtering acid from samples. All quoted literature focused on aquifer materials with relatively low carbonate content, while carbonate-rich limestones and chalks are common aquifer materials in the UK.

3.2.2 British Standard Methods

British Standard 7755: Part 3, Section 3.8, 1995 ‘Determination of organic and total carbon after dry combustion (elemental analysis)’ (BS 7755:3.8) requires the determination of the total carbon content of the sample to allow calculation of the excess volume of acid required for removal of the carbonate (assuming all carbon is present as carbonate). Hydrochloric acid (34% dilution of concentrated HCl) is added to the crucible with the weighed sample. After 4 hours the sample is dried, then analysed by HTO.

British Standard 1377: Part 3: 1990, ‘Soils for civil engineering purposes, Part 3. Chemical and electro-chemical tests’ includes ‘determination of the organic matter content’. This is based on the Walkley and Black wet chemical oxidation method, using dichromate oxidation. Sub-samples of a dried, crushed sample are used to determine the presence of sulphides and chlorides, which are eliminated from a further sub-sample prior to organic carbon analysis. Organic matter is oxidised by potassium dichromate ($\text{K}_2\text{Cr}_2\text{O}_7$) with concentrated H_2SO_4 . Excess dichromate is quantified by titration with ferrous sulphate (FeSO_4) after addition of distilled water, orthophosphoric acid (H_3PO_4) and

indicator. Titration results are converted to organic carbon content assuming 77% of the carbon in the organic matter is oxidised. The British Standard states that these figures will give correct results for natural organic matter, but does not state that they are based on averages, and therefore are not accurate for all materials. Dichromate oxidation oxidises an inconsistent proportion of the organic carbon. Any calculation converting OC oxidised to OC present in the sample is therefore based on an assumed proportion.

3.3 Methods used by commercial laboratories

The literature discussed in Section 3.2 revealed that there remains considerable discussion on the most appropriate method to measure TOC. Since this measurement is key to retardation modelling and since TOC is often obtained commercially, a review of methods employed by commercial laboratories was undertaken.

Commercial laboratories routinely used by major environmental consultants in Britain for TOC analysis were surveyed for details of their TOC analysis method⁷. Most laboratories provided a short method sheet. The test method details obtained from method sheets, supplemented by telephone conversations, are described in Appendix A, and summarised in Table 1 below. Clients rarely specify technical details for TOC test methods, and the test method sheets rarely include analytical details (specifically details of the acidification pre-treatment) that are suggested here to be critical to assess the accuracy of analysis. Most laboratories were unwilling to provide further information, citing commercial issues. One company claimed to follow BS 1377, one to follow an unidentified USEPA method; no others referred to standard methods.

⁷ The laboratories surveyed are listed in Appendix A, but to ensure confidentiality are not identified with their methods.

Table 1: Summary of TOC analysis methods used by commercial laboratories

<i>Laboratory</i>	<i>Oxidation method</i>	<i>Acid used</i>	<i>Removal of acid</i>
A	HTO	50% HCl	acid evaporated; then washed with water filtered on papers
B	HTO	unspecified	unspecified
C	HTO	hot and cold dilute and concentrated HCl	filtration on porous crucibles
D	HTO	under development	under development
E	HTO	H ₃ PO ₄	filtration
F	wet chemical	unspecified	not applicable
G	leach organic carbon from the sample in water and analyse dissolved organic carbon in the leachate ⁸		
H	wet chemical	not applicable	not applicable
Wolfson	HTO	dilute and if required concentrated HCl	filtration on porous crucibles

These methods fall into three groups: those based on wet chemical oxidation of the organic carbon (such as BS 1377); those based on high temperature oxidation, following removal of inorganic carbon; and the ‘leaching’ method used by Laboratory G.

The ‘leaching’ method will not dissolve all the organic carbon from the solid, and therefore cannot provide meaningful TOC results.

Two laboratories used wet chemical oxidation. As some forms of organic carbon are more amenable to wet chemical oxidation, not all the organic carbon in any sample is oxidised (Powell *et al.*, 1989). A percentage of organic carbon oxidised is assumed and applied to all samples analysed, although the proportion oxidised will be sample specific. This assumption prevents the wet chemical oxidation process from providing an accurate TOC value. As the methods were developed originally for TOC analysis of soil materials, containing younger and different organic carbon than rock materials, it is unlikely that the percentage corrections used apply accurately to aquifer samples.

Consistent with the discussion in Section 3.2, most laboratories surveyed use HTO of carbon in an oxygen stream to produce CO₂, which is quantified by infra-red detection.

⁸ This is what the laboratory claimed as their TOC analysis method in solids.

This method is expected to oxidise all the carbon present in a sample. The success of HTO for TOC analysis depends on the complete removal of inorganic carbon, without removal of organic carbon, prior to oxidation of the sample. This is achieved by acidification of the sample, and is discussed further in Sections 3.4.3 and 3.4.4. Each laboratory used a different procedure to remove carbonate, with different acids, drying temperatures and filtering or evaporating procedures. Two laboratories filter the acid from the sample, two remove the acid by evaporation and one would not disclose their procedure. Given the lack of consistency in methods applied by different laboratories, it is unsurprising that clients report little reproducibility between laboratories.

3.4 Method evaluation

The TOC analysis method (detailed in Appendix A) developed in the Wolfson Geochemistry Laboratory at UCL has been used for the past ten years. The removal of carbonates by acidification with filtration is followed by HTO. The filtration pre-treatment method has been selected for this research as it is more accurate for carbonate-rich materials than using evaporation to remove the acid (Section 3.4.3 and 3.4.4). As discussed in Section 3.2, the filtration may lose some organic carbon, so results are reported as ‘acid-insoluble carbon’ (AIC). However, there is little published data quantifying this effect, and these AIC results are usually treated as TOC (as in Pickering *et al.*, 1998, McArthur *et al.*, 1992, McLeod, 1998, Fretwell, 1999).

This method has therefore been evaluated by running comparative analyses with another laboratory (Section 3.4.2); by measuring the dissolved organic carbon (DOC) in acid filtered from samples (Section 3.4.3); and by running comparative analyses with an alternative method in which acid was removed by evaporation (Section 3.4.4). The accuracy of the method for samples with high carbonate content has been considered.

3.4.1 AIC analysis detection limits and precision

Blank samples, standards and duplicates were analysed during each analysis run to identify bias and contamination. The results of analysis of blanks indicate the detection limit, duplicates indicate the method precision and standards the accuracy.

During carbon and sulphur analysis, empty (‘blank’) crucibles are analysed and their carbon and sulphur content given as a percentage of a nominal input weight. Their carbon

content is found to be inversely proportional to the nominal input weight, indicating that the carbon is a fixed mass of contamination. Their mean carbon content was 3.5×10^{-6} g with a standard deviation of 2.8×10^{-6} g. Their mean sulphur content was 1.22×10^{-5} g with a standard deviation of 5.3×10^{-5} g. This represents a carbon content of 0.0005% and sulphur content of 0.0017% for a 0.7g sample (the most common sample weight). For a 0.7g sample, the detection limit, set at the mean plus twice the standard deviation, is 0.0013% carbon and 0.017% sulphur.

For AIC analysis the samples are pre-treated with acid in porous crucibles to remove carbonate. Empty ('blank') crucibles pre-treated identically were analysed for carbon content as a percentage of a nominal input weight. Over one hundred acid-washed blanks analysed during the course of the research have been reviewed. Their carbon content is inversely proportional to the nominal input weight, indicating that the carbon is due to an approximately constant amount of contamination, possibly from the atmosphere. The mean carbon content was 1.9×10^{-5} g, with a standard deviation of 2.4×10^{-5} g. For a 0.7g sample the contamination will add 0.0027% carbon. For 0.7g sample, the detection limit for AIC, set at the mean plus twice the standard deviation, is 0.0096%.

Calcite, carbon content 12.01%, was analysed frequently. Measured carbon was between 11.9% and 12.2%, with a mean of 12.0% and a standard deviation of 0.13% (i.e., 1% of the calcite's carbon content) indicating that 95% of analysis results will be within a relative 2% of the true value of the sample placed in the LECO®.

Approximately one in ten sample analyses were repeated. With rare exceptions the variation (the absolute difference between the results of duplicates divided by the mean of the results) was found to be under 10% for AIC and TS determinations, and under 5% for TC determinations. Errors introduced during the pre-treatment process cause greater variation in AIC determination. Sorption of sulphur dioxide (SO₂) internally to the LECO® equipment causes greater variation in TS determinations, despite commencing each run with combustion of high sulphur compounds to saturate the SO₂ sorbing sites.

Chapter 3: Measuring TOC

Calcite analysis indicates that the determination of carbon in the LECO[®] analyser is precise (to within 2% for 95% of results) and accurate; however, imprecision (less than 5%) is introduced by sample inhomogeneity (minimised by crushing and mixing the sample) and additionally (an extra 5%) by the pre-treatment process applied for AIC analysis.

3.4.2 Interlaboratory comparison of TOC analysis

To evaluate the UCL method, ten samples were analysed both by Laboratory C and at UCL. The samples were collected from cable percussion drilling at Site B (Section 4.6.2), and cover a wide TOC content range. They were analysed by the standard method of each laboratory (see Appendix A for method details). The very similar analysis methods differ mainly in the use of both hot and cold hydrochloric acid and the use of concentrated hydrochloric acid on all samples at Laboratory C. Results are shown in Table 2 and are plotted in Figure 2 below, on which the line of gradient one is shown. Where two analyses were undertaken at UCL the TOC shown is their mean.

Table 2: Total organic carbon results from Laboratory C and UCL

Sample Borehole	depth (m bgl)	TOC (%)	
		Laboratory C	UCL
4d	3.75	1.35	1.12
5d	5.45	3.37	3.29
8d	1.75	1.28	1.07
8d	5.05	0.32	0.29
9d	6.00	0.92	0.96
9d	6.80	0.17	0.19
9d	10.40	0.38	0.30
9d	10.80	0.28	0.22
9d	13.80	0.16	0.088
13s	3.10	3.11	2.51

bgl = below ground level

Figure 2: Total organic carbon results measured by Laboratory C and UCL

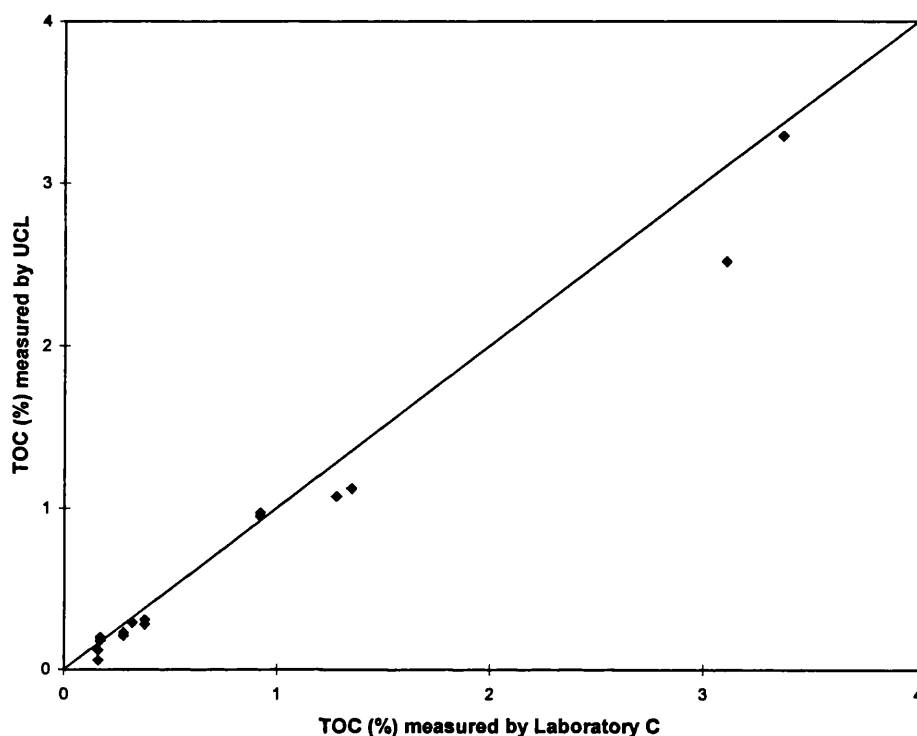


Figure 2 shows good agreement between the results from the two laboratories; minor differences probably result from sub-sampling. UCL results are, on average, a relative 13.7% below Laboratory C values. This bias may be introduced by slight differences in the methods, with more inorganic or organic carbon removed during the UCL acidification process. Calibration bias of the LECO® CS Analyser(s) (or other sample handling or preparation operations) could have the same effect.

Methods used by some other laboratories differ more significantly, for example with the acid removed by drying, rather than filtration. A full inter-laboratory comparison of TOC analyses would provide an interesting indication on the accuracy and precision of TOC results, but is beyond the scope of this review.

3.4.3 Dissolved Organic Carbon in acid

A major uncertainty in some methods is how much organic carbon is lost in filtered acid. To determine this, samples with a range of organic carbon and inorganic carbon contents were acidified on filter papers and the leachate tested for dissolved organic carbon (DOC). Method details are given in Appendix B and results in Table 3. Blank-corrected results are given as acid-soluble organic carbon (ASOC) as a percentage of the whole solid sample

weight and also as a percentage of TOC, where TOC is taken to be the sum of AIC and ASOC.

Table 3: Organic carbon lost in solution in hydrochloric acid

Sample description	AIC (%)	ASOC (%)	ASOC as % of TOC
Mudstone	3.09	0.51	14
Lower Chalk	0.038	0.0074	16
grey silty clay	0.96	0.13	12
red-brown sandy clay	0.3	0.032	9.8
Made Ground	7.5	1.5	16
Lincolnshire Limestone	0.16	0.028	15

Between 10 and 16 % of the TOC in these samples may dissolve in hydrochloric acid. Acid-insoluble carbon measured after the removal of acid by filtration will be an underestimate of TOC. Removal of acid by evaporation may prevent the loss of ASOC, but carbonate dissolution may be incomplete (Caughey *et al.*, 1995). Incomplete dissolution of chalk was observed despite using a 200% excess of acid for 20 hours.

The filter papers used retain 1.0 μm particles. LECO[®] filter crucibles used in AIC analysis have a pore size of 160 to 210 μm , nominally 210 μm , (Cook, pers. comm. 1999). Greater amounts of organic carbon may be lost through the larger pores of the LECO[®] crucibles.

3.4.4 Comparison of acid evaporation and filtration

To determine the difference between TOC measured in samples from which the acid has been evaporated and AIC measured by the UCL method with filtration of acid, samples were analysed after pre-treatment by both methods. Samples had a range of organic carbon and inorganic carbon and ratio of organic carbon to inorganic carbon; a carbon-free blank was included. Details of the method are given in Appendix C.

Results (Table 4) include analysis results following acid filtration (presented as AIC) and following acid evaporation (as TOC). Percentage loss is the difference between TOC and AIC, as a percentage of TOC. Inorganic carbon was calculated as the difference between TC and TOC. % deviation is the % deviation from the mean.

Chapter 3: Measuring TOC

For TC results, the % deviation from the mean is less than 2%, (excluding W9D2, % deviation up to 6%, for which high carbon content (21.5%) necessitated the use of relatively small quantities increasing the impact of sample heterogeneity). The low variability, together with consistent results for calcite analysis, indicate that the LECO® analysis introduces little error.

Much higher % deviation is seen in TOC and AIC analysis, indicating that both acid pre-treatment procedures introduce scatter (occasionally over 10%, generally under 5%). This is not unexpected, as all additional processes introduce additional errors. Excluding IGCR and W9D31.5, which have very low carbon, TOC values have a deviation from the mean of up to 14%, and AIC values of up to 12%, both with a mean deviation of 4%.

The carbon-free blank had AIC below the detection limit, but TOC much greater than the detection limit, indicating that carbon contamination occurred during the TOC pre-treatment process. If this was from the acid, the amount of contamination will be proportional to volume of acid used, and correction should be relative to acid volume. If the contamination was from the equipment or atmosphere, the absolute amount of contamination in each sample will be constant and correction should be by an absolute amount. TOC results have been corrected following both approaches, presented (Table 4) as TOC c1 and TOC c2 respectively. Both corrected and uncorrected values have been included as it is unclear which correction is appropriate. Correcting for contamination in TOC results reduces the apparent loss of organic carbon before AIC analysis. The loss of carbon in AIC, compared to the TOC values, has been recalculated using corrected TOC values (Table 4) but is not significantly altered.

Table 4: Total organic carbon compared to acid-insoluble carbon results

n.d. = not detected

sample	Description	TOC		AIC		TC		% Loss	IC %	TOC c1	TOC c2
		%	% deviation	%	% deviation	%	% deviation				
BB81-1	Chalk	0.0659	-4.0	0.0346	10.9	11.2	-0.3			0.0598	0.0594
BB81-2		0.0704	2.5	0.0276	-11.5	11.2	-0.3			0.0642	0.0639
BB81-3		0.0697	1.5	0.0314	0.6	11.3	0.6			0.0635	0.0633
BB81 - mean		0.0687		0.0312		11.2		54.6	11.2	0.0625	0.0622
W9D31.5 -1	Unconsolidated sand from industrial site B	0.0179	-9.2	0.0888	27.9	0.460	1.9			0.0134	0.0134
W9D31.5 -2		0.0219	11.1	0.0714	2.8	0.448	-0.7			0.0174	0.0174
W9D31.5 -3		0.0194	-1.8	0.0481	-30.7	0.446	-1.2			0.0149	0.0149
W9D31.5 - mean		0.0197		0.0694		0.451		-252.1	0.4	0.0152	0.0152
LL-1	Lincolnshire Limestone	0.401	-0.4	0.324	3.1	10.9	0.0			0.395	0.395
LL-2		0.410	1.8	0.310	-1.4	10.9	0.0			0.403	0.404
LL-3		0.397	-1.4	0.309	-1.7	10.9	0.0			0.390	0.391
LL - mean		0.403		0.314		10.9		22.0	10.5	0.396	0.397
NBAT2-1	Glacial Till	0.155	-1.2	0.175	8.7	1.87	0.0			0.151	0.148
NBAT2-2		0.159	1.4	0.159	-1.2	1.87	0.0			0.155	0.152
NBAT2-3		0.156	-0.1	0.149	-7.5	1.87	0.0			0.153	0.150
NBAT2 - mean		0.156		0.161		1.87		-2.9	1.7	0.153	0.150
NRF9-1	Glacial Till	0.265	-6.1	0.226	-4.8	9.55	0.5			0.261	0.259
NRF9-2		0.309	9.2	0.259	9.1	9.54	0.4			0.305	0.302
NRF9-3		0.274	-3.2	0.227	-4.4	9.43	-0.8			0.270	0.267
NRF9 - mean		0.283		0.237		9.51		16.0	9.2	0.279	0.276
LS-1	Kirtan Shale from within the Lincolnshire Limestone	2.95	10.2	1.71	2.0	9.27	-0.5			2.95	2.95
LS-2		2.31	-14.0	1.65	-1.6	9.39	0.8			2.30	2.30
LS-3		2.78	3.7	1.67	-0.4	9.29	-0.3			2.78	2.77
LS - mean		2.68		1.68		9.32		37.5	6.6	2.68	2.67
LSM-1	Kirtan Shale, ground in micronising mill	1.76	-1.9	1.64	1.7	9.56	-0.1			1.74	1.74
LSM-2		1.82	0.9	1.70	5.4	9.56	-0.1			1.79	1.79
LSM-3		1.82	1.1	1.50	-7.0	9.59	0.2			1.79	1.79
LSM - mean		1.80		1.61		9.57		10.3	7.8	1.77	1.77
W9D6-1	Silt from industrial site B	1.05	-1.8	0.957	-0.1	1.80	-0.9			1.05	1.04
W9D6-2		1.08	1.5	0.965	0.7	1.85	1.8			1.08	1.07
W9D6-3		1.07	0.3	0.952	-0.6	1.80	-0.9			1.07	1.06
W9D6 - mean		1.07		0.958		1.82		10.2	0.8	1.06	1.06
W9D2-1	Made Ground from industrial site B	20.4	-0.7	18.8	3.7	20.8	-3.3			20.4	20.4
W9D2-2		20.8	0.8	18.0	-0.7	22.8	6.0			20.8	20.7
W9D2-3		20.6	-0.1	17.6	-2.9	20.9	-2.8			20.6	20.5
W9D2 - mean		20.6		18.1		21.5	0	11.9	0.9	20.6	20.5
IGCR-1	ignited crucible	0.0048	8.2	n.d.		n.d.				-	-
IGCR-2		0.0041	-8.6	n.d.		n.d.				-	-
IGCR-3		0.0045	0.4	n.d.		n.d.				-	-
IGCR - mean		0.0046		n.d.		n.d.		-	-	-	-
IGCRM-1	ignited crucible, ground in micronising mill	0.0316	17.2	0.0111	-9.0	0.0145	-18.8				
IGCRM-2		0.0234	-13.2	0.0066	-45.9	0.0179	0.2				
IGCRM-3		0.0259	-4.0	0.0189	54.9	0.0212	18.7				
IGCRM - mean		0.0270		0.0122		0.0179		54.8	-0.0091	-	-

Chapter 3: Measuring TOC

AIC measurements are between 10% and 55% (mean 24%) lower than measured uncorrected TOC (excluding W9D31.5 and ICGR which contain very little or no organic carbon and glacial till NBAT, which shows no loss). Analysis of a carbon-free sample indicated that the TOC method introduced greater carbon contamination than the AIC method, but the contamination accounts for a small proportion of the excess carbon measured as TOC. Large excesses of acid, and long time periods for removal of the carbonate, were designed to remove all carbonate.

The range of carbon lost during filtration of the acid found in this experiment (10% to 55%) is greater than that measured by analysis of DOC in the acid filtrate (10% to 16%, Section 3.4.3).

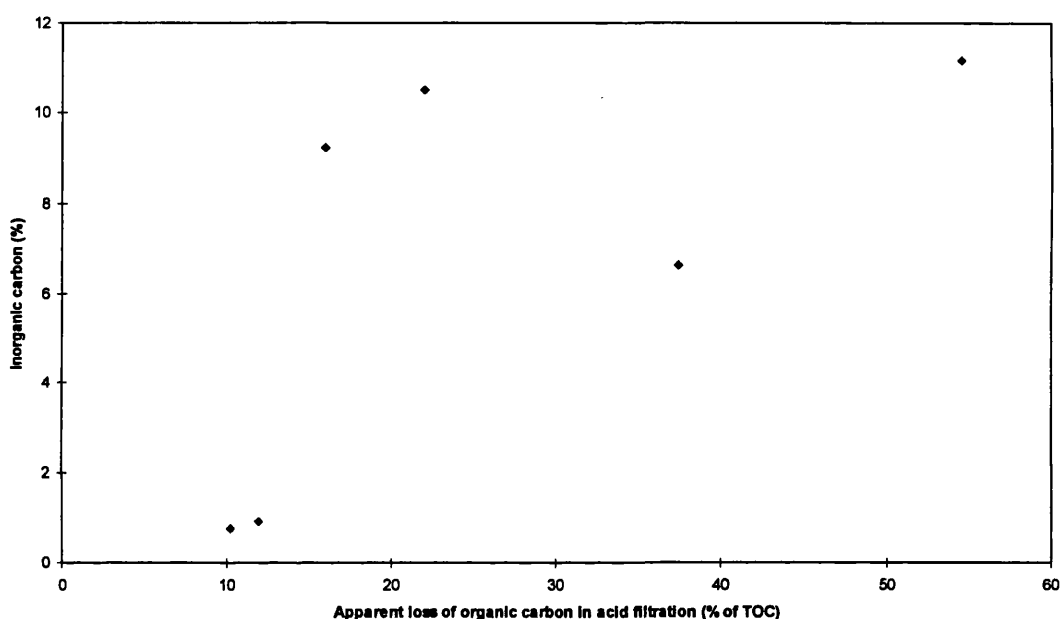
Incomplete removal of carbonates has been reported as a source of bias in TOC analysis (Heron *et al.*, 1997; Caughey *et al.*, 1995). During this experiment, effervescence quickly became almost imperceptible, dissolution continued with little sign and it is possible that not all carbonate had dissolved. Largest differences between TOC and AIC were observed in those samples with greatest IC content (see Figure 3). Higher 'TOC' values may be due to remaining carbonate, successfully removed during acid filtration.

The chalk sample included had a measured AIC of 0.03% and TOC of 0.07%. If the 0.04% difference was due to undissolved carbonate, it would represent less than 0.4% of the total carbonate of the sample. If it represents organic carbon lost before AIC analysis, it would account for over 50% of the total organic carbon present in the sample. These figures alone indicate that for a carbonate-rich / organic-poor sample very small amounts of inorganic carbonate remaining (residual carbonate of less than 0.5% of the whole rock carbonate) will lead to greater errors in TOC analysis than loss of over half the organic carbon. For such samples, complete carbonate removal is essential for accurate TOC analysis. It is therefore considered likely that much of the difference between TOC and AIC detailed above is due to traces of undissolved carbonate.

To examine this possibility, one sample and a carbon-free blank were very finely ground using a McCrone micronising mill, and the AIC and TOC analysis repeated using twice as much acid. The difference between TOC and AIC was reduced, confirming that the previous TOC values were elevated by remaining carbonate. Greater carbonate dissolution is attained by finer grinding and / or addition of more acid. It is not certain that carbonate

dissolution is complete in TOC analysis of the micronised sample, and the remaining 10% difference between AIC and TOC may be (partially) due to remaining carbonate in the TOC sample rather than loss of organic matter from the AIC sample. It was also found that finer grinding and addition of extra acid causes greater carbon contamination.

Figure 3: Apparent loss of organic carbon with inorganic carbon content



3.5 Conclusions and Recommendations

Acid-soluble organic matter will be lost if the acid is removed by filtration. In samples analysed as part of this research, TOC results following evaporation of the acid were 10% to 55% higher than AIC results from filtering acid. This potential problem has led others to recommend the removal of acid from the sample by evaporation. However, this research has supported previous publications in reporting that evaporation of the acid results in incomplete carbonate dissolution, especially in high carbonate samples and those containing slow-dissolving carbonates. Weaker acids, which are less likely to dissolve organic matter, are also less effective in dissolving carbonates (experience in the Wolfson Laboratory at UCL, also Powell *et al.*, 1989). The incomplete dissolution of carbonate has been found to cause a significant part of the higher values after evaporation pre-treatment.

Chapter 3: Measuring TOC

Previous research on TOC analysis methods has been largely undertaken on North American samples with relatively low carbonate content. Those studies have recommended the use of evaporation techniques to remove acid from the sample, to reduce loss of acid-soluble organic carbon. However, many UK aquifer materials have high carbonate content (frequently over 90% calcium carbonate content) and low organic carbon. The incomplete removal of carbonate carbon could produce a more significant source of error than the additional removal of acid-soluble organic carbon. It is therefore suggested that filtration is more appropriate for high carbonate samples.

Environmental consultants commissioning TOC analysis should request full test method details and be aware of the method's limitations and direction of bias. This recommendation is hindered as the method statements provided by most laboratories do not provide important details of the acid removal technique (evaporation or filtration), and most laboratories are reluctant or unable to provide such detail.

Commercial laboratories use a wide range of methods to analyse TOC. Whilst the majority of laboratories use high temperature combustion to determine the carbon content, pre-treatment of the samples to remove carbonate carbon follows various procedures. A standard and widely used method for analysis should be applied, and would benefit from incorporation into an interlaboratory comparison scheme (such as Aquacheck or Contest).

It has been found that analytical methods in which the acid used to remove carbonates is removed by filtration cause the loss of significant additional carbon, assumed to be organic carbon. However, it was also found that the higher results for TOC analysis associated with evaporation of the acid may be due to residual carbonate. It is therefore recommended that the method used for TOC analysis is detailed with any results.

Additionally, for analysis of TOC with evaporation of acid, the following points should be noted:

- to reduce sample heterogeneity and reaction time, samples should be finely ground; mechanical grinding is finer than manual grinding, but may introduce additional contamination;

- carbonate dissolution continues slowly for long periods after easily observable effervescence has ceased;
- samples free of organic carbon should be analysed as controls to measure contamination during the TOC pre-treatment process; other researchers (Caughey *et al.*, 1995) have found that H_2SO_3 may be a source of contamination;
- to decrease the potential for incomplete carbonate dissolution, acid should be added far beyond the point at which effervescence ceases. Many published methods, including BS 7755:3.8, dictate the volume of acid to be used dependent on sample weight and carbon content. Even a large stoichiometric excess of acid may be insufficient for complete carbonate dissolution before the acid evaporates.

Acid evaporation is found to be time-consuming, and therefore suitable only for small numbers of samples. Routine analysis of large numbers of samples would be more easily approached by a simpler means of carbonate removal. Whilst the method incorporating evaporation clearly results in higher TOC results, this work has shown that, for samples with high carbonate content, the difference may be due to incomplete carbonate dissolution associated with acid evaporation, rather than loss of organic carbon associated with acid filtration.

3.6 Summary

- Accurate determination of TOC uses high temperature oxidation after carbonate removal with acid.
- Acid added to the sample may be removed using filtration or evaporation: filtration results in the loss of acid-soluble organic carbon and hence under-estimation of TOC; evaporation from high carbonate samples, or those containing acid-resilient carbonates, frequently results in incomplete carbonate removal, and hence over-estimation of TOC.
- Errors due to acid-soluble organic carbon loss or incomplete carbonate removal may be 10% to 50%. However, it is impossible to divide such errors between the two error sources.
- No standard TOC analysis method exists. Frequently, those commissioning analysis are unaware of the analysis method, and hence unaware of its limitations.

4. Geology and hydrogeology of units sampled

4.1 Introduction

This chapter describes the geology and hydrogeology of samples analysed for their total organic carbon content. These include the Chalk, the Lincolnshire Limestone, the Triassic Sandstone and Glacial Till. The locations of the aquifers are shown in Chapter 5 on Figure 4. Greater detail is given for the Lincolnshire Limestone and Glacial Tills, which were selected for organic matter isolation and characterisation, using methods presented in Chapter 6.

4.2 The Chalk geology and hydrogeology

The Chalk is the UK's most important aquifer, present in south east England (Day, 1986). Its outcrop stretches from the Lincolnshire coast to the Dorset coast, dipping east from outcrop under overlying deposits towards the coast. The Chalk is divided into Upper, Middle and Lower Chalk, laterally continuous although varying in thickness. Thickness variations in the Upper Chalk (up to 400 m thick) are largely due to erosion; thickness variations in the Middle and Lower Chalk are partly due to sedimentation. Lithologically, the Chalk is a fine white, generally soft, microporous limestone mainly of organic origin, in which the grain-size of the finer planktonic coccolith debris may be less than 1 μm , and coarse shelly debris is usually 10 - 100 μm . Upper and Middle Chalk are mainly over 95% calcium carbonate; the Upper Chalk contains flint bands and randomly located flint nodules. The Lower Chalk contains a much higher proportion of clay minerals (commonly 20 to 35%, up to 60%), reducing its permeability.

Most Upper and Middle Chalk have 40 to 50% porosity; porosity in the Lower Chalk is typically 20 to 30%. Permeability within the matrix is low, typically 1 - 3%, due to the fine grained nature of the unit, but fractures and joints, widened by dissolution, provide a higher secondary permeability. As the development of fissures is related to water flow, Chalk permeability decreases with depth, and the Chalk aquifer (with usable permeability) usually relates only to the top 70 m or so of the geological unit. At outcrop, the Chalk's transmissivity (T) is typically 1 500 to 3 000 m^2/d , but in confined conditions with restricted circulation T may be as low as 15 m^2/d .

4.3 *Lincolnshire Limestone geology and hydrogeology*

The Lincolnshire Limestone is a major British aquifer, and is the principle source of water for an area of Lincolnshire used for intensive agriculture. In 1977, licensed groundwater abstraction was 150 000 m³/d (British Geological Survey, 1997). The unit has been selected for study owing to its significance as an aquifer, and because it contains significant and varying quantities of organic matter (up to 2.7% in shale layers). The Lincolnshire Limestone outcrop is approximately 120 km long, running roughly north - south between North Humberside and Kettering. The outcrop is between 3 and 5 km wide in the north and 6.5 to 8 km wide in the south (BGS, 1997). The Lincolnshire Limestone was deposited in the Middle Jurassic during a marine transgression (Kent, 1980). The formation dips east at 3° with a N-S strike in the northern area, and dips less than 1° with a SSW-NNE strike in the southern area (BGS, 1997). It thins eastwards from a maximum of 40 m thick at outcrop in the central region to less than 20 m thick, and extends about 50 m beyond the coastline to the east. It is crossed by a number of faults. The unit is underlain and overlain (where confined) by shale and mudstone-dominated formations (Bishop and Lloyd, 1990).

The Lincolnshire Limestone is lithologically varied, with facies types changing rapidly vertically, from ooid-dominated and skeletal grainstones and packstones to underlying wackestones, calcilutites, marls and shales. It can be divided into 'Upper' Lincolnshire Limestone, dominantly a coarse, shelly, cross-bedded oolite and 'Lower' Lincolnshire Limestone, mainly a fine-grained, micritic and peloidal limestone (BGS, 1997). In south Lincolnshire, the unit consists almost entirely of limestone, but an increase in terrigenous clastics is seen northwards, most clearly in the occurrence and increasing thickness of the Kirton Shale unit. Apart from the Kirton Shale, which appears in the north of the unit, but not the south, Emery and Dickson (1991) report a lack of major lateral facies change and, following Ashton (1980), divide the Lincolnshire Limestone into nine members, which are summarised in Table 5.

Table 5: Descriptions of Lincolnshire Limestone Formation Members

Member	Thickness	Description
Clipsham	4.78 m at type section	Primarily cross-bedded oolitic grainstones with subsidiary skeletal grainstones.
Sleaford	4.83 m at type section	Facies-diverse: mainly cross-bedded skeletal and oolitic grainstones. Ashton (1980) identified fining-upwards and coarsening-upwards rhythms and biothermal micrites.
Blankney	2.13 m at type section	Facies-diverse: chiefly oolitic or peloidal grainstones, with subordinate quartoze peloidal grainstones.
Metheringham	2.36 m at type section	Oolitic packstones and grainstones, sometimes with pisoids predominating over ooids. Ashton (1980) identified silty and argillaceous layers.
Kirton Shale	4.2 m at type section	Well-laminated marly-shale, with occasional argillaceous lime-mudstones.
Lincoln	1.85 m at type section	Dominantly oolitic and skeletal packstones and wackestones, this is the basal oolitic packstone or grainstone. It contains the Ropsley beds (0.84 m thick at type section), dominantly thinly-bedded lime mudstones, and the Scottlethorpe beds (2.1 m thick at type section), which range from oolitic packstones to lime mudstones.
Leadenham	3.05 m at type section	Thinly-bedded pure lime mudstones with thin clay or marl partings. Shelly, peloidal and oolitic lenses locally. Includes the Cathedral beds (about 0.9 m thick): alternating argillaceous limestones and shales, containing skeletal oncolites up to 15 mm diameter.
Greetwell	4.88 m at type section	Diverse oolitic and peloidal / pelleted wackestones and packstones, and more rarely grainstones. The Wragby bed (maximum thickness 1.52 m) is a thin clastic intercalation within the Greetwell Member.
Sproxton	1.6 m at type section	Silty lime mudstone. Ooids sparsely present in some cores. Up to 30% is dolomitised. Overlain by 0.3 m thick stiff, black, well-laminated clay.

(summarised from Emery and Dickson, 1991 and Ashton, 1980)

Chapter 4: Geology and hydrogeology of units sampled

Shales, marls and clays are present in the Lincolnshire Limestone mainly within two members (Table 5). The Kirton Shale forms a shale layer in the north of the unit about 4 m thick. The Leadenham Member also contains argillaceous beds, shales and thin clay or marl partings. Emery and Dickson (1991) published gamma-ray logs from 18 boreholes showing positive anomalies⁹ correlating with the Kirton Shale Member, the Leadenham Member, within the Greetwell Member and at many of the interfaces between members. Towards the south, the intensity of the anomaly associated with the Kirton Shale decreases; this is suggested to be due to a gradual transition of the Kirton Shale Member from a clay / clastic-rich facies into a pure limestone. This interpretation is consistent with observations that the Kirton Shale is replaced southwards by limestone (Ashton, 1980), and is supported by examination of lithological cores (Emery and Dickson, 1991). The hydrogeological importance of the shale is described below. The geochemical significance of the clay content of the layers in the context of this research is the correlation between clay content and higher organic carbon levels.

Groundwater in the Lincolnshire Limestone aquifer is unconfined at outcrop, but confined (often artesian) when overlain by low permeability deposits. Groundwater flow is eastwards, downdip from the outcrop, with a hydraulic gradient of about 1:300 (Greswell *et al.*, 1998). Recharge is largely from precipitation at outcrop either infiltrating through the unsaturated zone, or as 'rapid recharge' through swallow holes and fissures (Bishop and Lloyd, 1990). Local geology governs complex interactions between surface water and groundwater (BGS, 1997).

Abstraction takes place mainly from the confined region, where artesian conditions occur. In the south, abstractions are made up to 10 km east of the outcrop. The greater dip in the north means that the aquifer is too deep for abstractions over a few kilometres from the outcrop. Seasonal head differences can be large (up to 10 m at outcrop, Rushton *et al.*, 1982), as the aquifer responds rapidly to recharge when enhanced fractures allow runoff

⁹ Lithologies containing minerals with elements that undergo radioactive decay (such as potassium feldspars and many clay minerals) will produce a positive gamma-ray anomaly. Pure limestones which do not contain radioactive elements will give a negative anomaly.

to enter the aquifer quickly. Tracer tests near outcrop have showed flow velocities of hundreds of metres per day.

Pumping tests in the Lincolnshire Limestone reported in the Aquifer Properties Manual (BGS, 1997) gave an interquartile range for transmissivity of 259 to 2265 m²/d and for storage coefficient of 4.9×10^{-5} to 5.2×10^{-4} . Laboratory analyses have given an interquartile range for porosity of 13.1 to 21.6% and hydraulic conductivity of 4.99×10^{-5} to 4.39×10^{-4} m/d. Generally, permeability increases with porosity, especially at lower values. Fracture porosity is thought to be around 1% (BGS, 1997). Transmissivities are higher at outcrop than in the confined aquifer (Lloyd *et al.*, 1996).

Greswell *et al.* (1998) studied the physical properties of the Lincolnshire Limestone in a micro-scale laboratory and field investigation of a quarry. Exposure and boreholes revealed 24.8 m of Lincolnshire Limestone, from the Metheringham Member to the Sproxton Member. Their data showed wide ranges for both interconnected porosity and hydraulic conductivity that were dependent on the lithology (Table 6). The Kirton, Lincoln and Leadenham Members had low hydraulic conductivity and low interconnected porosity. This zone has been interpreted as an aquitard (see below) (Greswell *et al.* refer to Smith-Carrington *et al.*, 1983, and Moncaster, 1993).

Table 6: Permeability and interconnected porosity of Lincolnshire Limestone

Stratigraphic member	Metheringham	Kirton, Lincoln and Leadenham	Greetwell	Sproxton
Permeability (m/s)				
Number of samples	20	35	18	19
Mean	1.14×10^{-8}	7.58×10^{-10}	1.84×10^{-9}	9.53×10^{-10}
Minimum	1.13×10^{-10}	2.31×10^{-11}	3.85×10^{-10}	3.11×10^{-10}
Maximum	9.21×10^{-8}	1.50×10^{-8}	4.98×10^{-9}	6.50×10^{-9}
Porosity (%)				
Number of samples	68	119	51	48
Mean	16.8	10.6	12.5	15.6
Minimum	7.5	1.6	11.0	14.1
Maximum	34.1	23.5	13.9	17.2

(from Greswell *et al.*, 1998)

The Lincolnshire Limestone is often considered to be a dual porosity aquifer, with water storage in both the fissures and the matrix, and permeability provided by fracture flow in a

network of well-developed bedding-plane fractures and joints. Advection and dispersion of solutes are assumed to occur only in the fissures, and solute flux between the fissures and the matrix is controlled by matrix diffusion properties (Greswell *et al.*, 1998). The importance of matrix flow in the Lincolnshire Limestone aquifer is contested. Greswell *et al.* claim that matrix hydraulic conductivities are inconsequential for groundwater flow. They state that intergranular flow within the aquifer is insignificant and that the contribution made by the matrix to specific yield is insignificant because the small pore sizes require a very large suction to alter saturation significantly. The existence of reduced Lincolnshire Limestone in the centre of blocks between fractures indicates slow intergranular flow in matrix blocks. Low matrix permeabilities are measured in the laboratory (less than $6 \times 10^{-4} \text{ m day}^{-1}$). However, high sustained yields in the southern limestone imply that an extensive interconnected fissure system may be fed, to some extent, by intergranular flow and slow seepage from certain lithologies. Downing and Williams (1969) (quoted in BGS, 1997) suggest that as the mass of the rock in certain lithologies, such as oolites, is relatively porous, some intergranular flow takes place through these deposits.

Greswell *et al.* (1998) claim that the large contact area between fissure surfaces and groundwater in the fissures, together with the relatively high interconnected porosity of the matrix, mean that diffusive exchange between the mobile groundwater in fissures and the pore-water can be significant for contaminant retardation, by removing contamination from fissure flow. This is significant to this study, as matrix diffusion will enable sorption to organic matter within the matrix. This will reduce contaminant concentrations during diffusion out of the matrix, but extend the potential time period for contamination release as desorption occurs. Greswell *et al.* found that the effective matrix diffusion coefficients in the Lincolnshire Limestone of three tracer solutes were related to the interconnected porosity. Thermonuclear tritium (created after 1953, peak levels were 1963-1964) found in the pore-waters of the upper limestone in 1977 (Smith-Carrington *et al.*, 1983) indicates substantial diffusion exchange between the matrix pore-water and the fissure water.

Smith-Carrington *et al.* (1983) state that the Kirton Shale forms an aquitard, causing the limestones above and below the shale to act as separate aquifers to some degree. A significant vertical head difference across the unit is reported: groundwater in the lower limestones at some locations is under artesian conditions while the upper limestone aquifer is unconfined; in other places rapid groundwater flow through the base of the limestones can lead to perched water tables on the Kirton Shale. The conclusion that the Kirton Shale is acting as an aquitard is further supported by different groundwater chemistry reported in the Upper and Lower Limestones. The Kirton Shale was found to contain higher TOC levels than the other limestone members which may enable it to act as a zone removing contamination from the groundwater, as groundwater flows through it. However, with low permeability, such through flow may be limited.

Locally the Lower Lincolnshire Limestone may be confined by the Crossi Bed (the uppermost of several thin micritic limestones with clay partings which separate the Lower and Upper Lincolnshire Limestone in South Lincolnshire), indicated by upsurges of water during drilling (BGS, 1997).

4.4 Triassic Sandstone geology and hydrogeology

The Triassic Sandstones form the second most important aquifer in the UK, present in the Midlands and North-West England, and are important over much of northern Europe (Edmunds *et al.*, 1982). Deposits can be up to 1000 m thick. Triassic Sandstones in the UK include the Sherwood Sandstone Group. This aquifer exhibits dual permeability, with both fissure flow and intergranular flow important. Grain size varies between units. Permeability depends to some extent on the degree of cementation. Transmissivity (T) may be high (up to 1 500 m²/d) at outcrop where fissures are well developed, but lower in the confined aquifer (from 150 m²/d, generally 350 to 750 m²/d; Day, 1986).

4.5 Sites A and B

For reasons of commercial confidence, the industrial sites sampled are referred to as Sites A and B. The site locations, and details of their hydrogeology and geology cannot be given as this information is commercially sensitive; material descriptions are presented with the results. Samples from these sites represent a wide range of materials that may be encountered by infiltrating contamination including made ground.

4.6 Glacial Till geology and hydrogeology

The Glacial Tills of Norfolk largely form an aquitard rather than an aquifer. As such they are not a direct groundwater source, but they are relevant in this research owing to their potential to protect groundwater. The widespread tills in Norfolk overlie a significant area of the Chalk Aquifer and a substantial proportion of the recharge to the Chalk may penetrate Glacial Till cover: recharge to the Chalk through the till has been calculated to be between 20 and 40 mm per year, which is about 50 to 80% of total recharge (Jackson and Rushton, 1987; Klinck *et al.*, 1996). Thinner, more weathered deposits at valley margins allow greater recharge to the underlying deposits (Lloyd *et al.*, 1981; George *et al.*, in prep.). Glacial deposits in the UK also provide protection to the underlying Triassic Sandstone aquifer. As a consequence, the capacity of the till to attenuate contaminants is important. Due to their low permeability, clays such as tills may also be used as engineered landfill containment systems, in which situation their capacity to attenuate contaminant movement is paramount. Clay-rich glacial tills are widespread in Europe and northern North America, and frequently protect regional aquifers or are containment for waste deposits. However, little detailed hydrogeological research has been undertaken on these units (Hendry and Wassenar, 1999).

Glacial till in East Anglia was deposited by ice sheets in the Anglian, during the Pleistocene (Ehlers *et al.*, 1991). The East Anglian till deposits are generally divided into three types: Lowestoft Till, North Sea Drift and Marly Drift. Lowestoft Till (which includes Chalky Boulder Clay) is the predominant till lithofacies in East Anglia (Hart and Boulton, 1991) forming a largely continuous sheet in southerly areas and occurring in the East Midlands and much of central and south East Anglia. It is clay rich (with much reworked Jurassic Kimmeridge Clay), with many chalk and some flint clasts and other minor constituents, and a little sand. North Sea Drift (also known as Cromer Till), in northeast and north Norfolk, is sandy, with fewer chalk and flint clasts, and high quartz and quartzite content. Marly Drift occurs in north Norfolk; it is very chalk-rich and has been suggested to be a chalk-rich member of the Lowestoft Till (Ehlers *et al.*, 1991) or to comprise two components: North Sea Drift, and Lowestoft Till (Perrin *et al.*, 1973, 1979). Each till is lithologically varied, and contains a number of distinct units.

Hydraulic conductivity of 10^{-11} to 10^{-9} m / s has been measured in laboratory tests (Lloyd *et al.*, 1981). Higher hydraulic conductivity measured in the field, (4.5×10^{-7} to 6.4×10^{-9} m/s in weathered till and 1.2×10^{-11} to 8.0×10^{-8} m/s in unweathered till), includes fracture flow and flow through sand lenses (Klinck *et al.*, 1996). Isotopic signatures in North Sea Drift pore-water indicate that sand-rich layers contain some recent groundwater, but clay-rich tills contain older water (George *et al.*, in prep.). From this it is inferred that groundwater and solute transport in sand layers (which contain recent water) is by advection and in clay layers (which contain old water) is dominated by diffusion.

In fractured clayey deposits, dissolved contaminants may enter the matrix by diffusion (Parker *et al.*, 1994; Myrand *et al.*, 1992). The processes occurring within the matrix are therefore of importance. Clay layers below the water table may form barriers to flow of dense non-aqueous phase liquids (DNAPLs), such as chlorinated solvents. They will then be in contact with the 'pooled' DNAPL and with groundwater contaminated by it. It was observed in Chapter 4 that clay rich units tend to have higher TOC, and as such their potential for organic contaminant sorption is more significant than that of aquifers.

4.7 Lower Coal Measures

The Lower Coal Measures, where sampled, comprise interbedded mudstone and sandstone with units 15 to 50 m thick (Wright *et al.*, 1927) and have been described as a complex aquifer system (Mather *et al.* 1998).

4.8 Summary

- Six material types have been selected for acid-insoluble carbon analysis. These include the three major aquifers, a major aquitard, a minor aquifer / aquitard system and deposits underlying industrial sites.
- Three sets of geological materials have been selected for further investigation: a major aquifer; an aquitard; and made ground and unconsolidated samples that represent materials that may be encountered by industrial contamination. These represent a wide range of lithologies and depositional environments, and therefore were considered likely to contain organic matter displaying a range of geochemistry and morphology.

5. TOC in UK aquifer and aquitard material

5.1 Introduction

The organic carbon content of geological materials is an important control on the sorption of organic contaminants dissolved in groundwater, and it is generally considered that other sorbents are negligible when the total organic carbon (TOC) content is greater than 0.1% (see Section 2.3). TOC content is therefore a necessary input for organic contaminant transport modelling, and for understanding the fate of contaminants and their interactions with rocks. However, TOC data for common geological materials is very sparse, and users of such data frequently guess likely values (J. Dottridge, pers.comm., 1998).

An example of the limited TOC data available is the data set provided as suggested input parameters in the contaminant transport modelling software Consim (Golder Associates, 1999, Table 7) which comprises predominantly values from North America. The review by Stuart (1991) showed how little published data was available on organic carbon in British aquifers; it summarised that the Triassic Sandstone contains very low levels of organic carbon and significant quantities are present in the Lincolnshire Limestone. TOC in the Chalk was not quantified, but it was stated that it contained a wide range of types of organic materials. Durand (1980) reported world-wide average organic carbon concentrations of about 1% in clays and shales, 0.3% in carbonates and 0.2% in sands and sandstones, consistent with the finding that the finest grained sediments are usually richest in organic carbon. Durand also notes two minima in world-wide distribution of organic carbon with geological age, during the Silurian and the Triassic, which are attributed to variation in primary productivity due to climate change or variation in atmospheric carbon dioxide (CO₂).

To address this lack of data, more than one thousand new organic carbon content measurements have been made and are presented in this chapter¹⁰ The measurements were made using the method recommended in Chapter 3 (Section 3.4.2) for carbonate-rich samples. Samples were chosen to represent the media that form important pathways for contaminant transport.

¹⁰ Some measurements made by A. Kim are included here.

Chapter 5: TOC in geological material

Samples of the major aquifers have been analysed, comprising Chalk (Section 5.2), Lincolnshire Limestone (Section 5.3), and Triassic Sandstone (Section 5.4), as have unconsolidated deposits from two industrial sites (Section 5.5). Samples from the aquitards formed by clay in glacial till and mudstone from the Lower Coal Measures are reported (Sections 5.6 and 5.7 respectively) and published data from the Jurassic aquitards and Lower Greensand aquifer are summarised (Section 5.8 and 5.9 respectively). Sampling locations are shown in Figure 4.

The results show that organic carbon content in the Chalk and Triassic Sandstone is low, generally below 0.1%, and therefore unlikely to affect sorption. This is lower than reported in Durand (1980), possibly due to the different geological locations studied. The Lincolnshire Limestone has higher organic carbon content, mainly above the 0.1% threshold, with higher concentrations in interbedded shales and mudstones. Glacial Till and mudstones from the Lower Coal Measures had organic carbon content mainly over 0.1%, organic carbon concentration varying with grain size in the Glacial Till. Oxidative weathering decreases organic carbon concentrations in Glacial Tills, and decreases those in the Lincolnshire Limestone on a regional scale. Unconsolidated deposits showed varied organic carbon content, higher in fine grained materials; made ground materials sampled showed very high organic carbon content (up to 20%).

Table 7: Organic carbon data provided in Consim

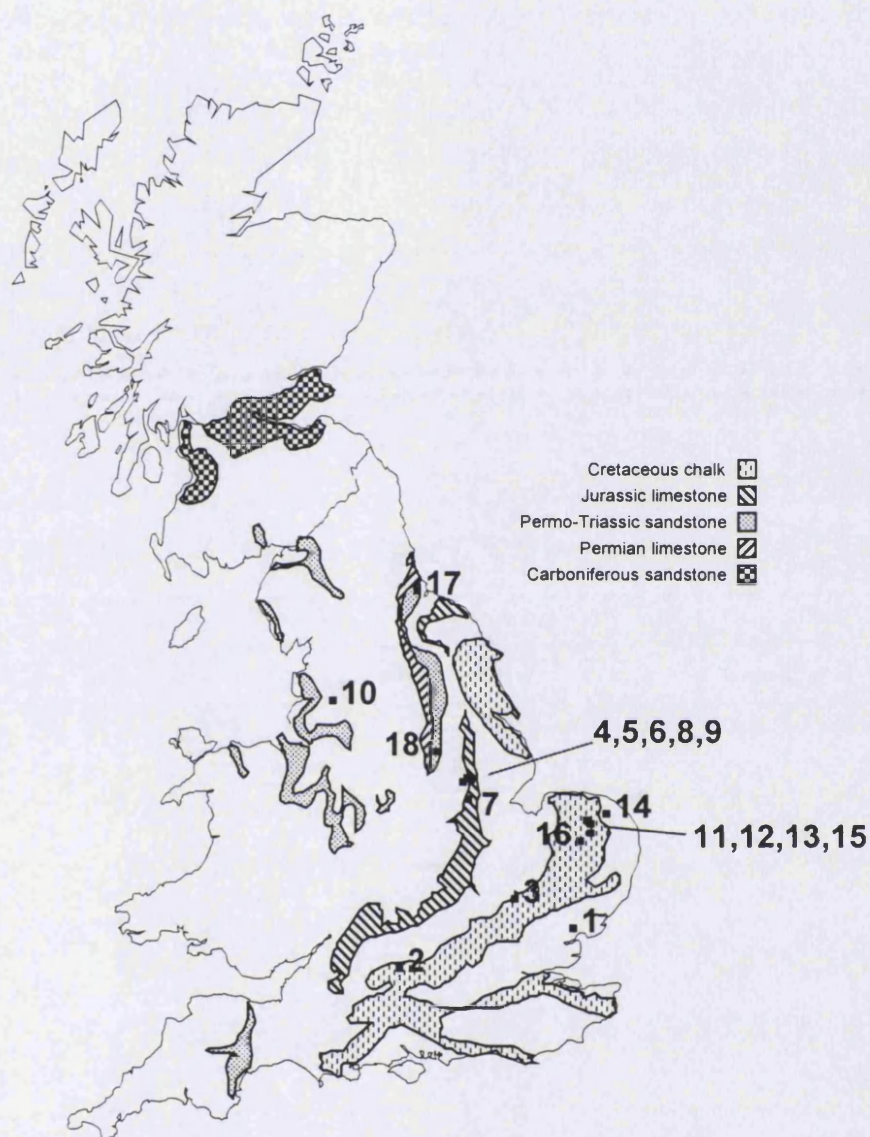
Substrate Type	Min (%)	Mean / Best (%)	SD (%)	Max (%)	Data Source
Glacio-fluvial sandy gravel	0.017	n.g.	n.g.	0.125	1
Glacio-fluvial Sand	0.021	n.g.	n.g.	7.3	1
Glacio-fluvial silty sand	0.07	n.g.	n.g.	0.8	1
Organic silt and peat (lacustrine)	10	n.g.	n.g.	25	1
Silt (lacustrine)	n.g.	0.11	n.g.	n.g.	1
Silt (aeolian)	0.058	n.g.	n.g.	0.61	1
Boulder Clay (glacial)	0.17	n.g.	n.g.	0.19	1
Fluvial Sand	0.053	n.g.	n.g.	0.57	1
Fluvial Silt	2	n.g.	n.g.	2.9	1
Sandy soil	0.02	n.g.	n.g.	0.25	7
Loam (soil-type)	0.2	n.g.	n.g.	8.6	8
Clay	1	n.g.	n.g.	10	9
Silt	1	n.g.	n.g.	10	9
Sand	0.01	n.g.	n.g.	0.1	9
Alfisol (or Pedalfer: leached soil)	n.g.	0.6	1	n.g.	3
Aridisol (or semi-desert soil, low in organics)	n.g.	0.5	0.5	n.g.	3
Entisol (or Azonal: young, well drained soil)	n.g.	0.7	1.2	n.g.	3
Inceptisol (or Brown forest, grey: young soil)	n.g.	1.5	2.3	n.g.	3
Mollisol (Chernozem: semi-arid, low humus)	n.g.	0.9	1.1	n.g.	3
Oxisol (or Laterite: soil with concret. Fe-oxide)	n.g.	1.1	1.4	n.g.	3
Spodosol (or Podzol)	n.g.	2.6	2.9	n.g.	3
Ultisol (lateritic soil)	n.g.	0.6	1.2	n.g.	3
Vertisol (or Grumusol: clay soils from Savannah)	n.g.	0.8	0.7	n.g.	3
Mercia Mudstone	0.01	0.34	n.g.	0.9	6
Sandstone (aquifer solids)	0.7	n.g.	n.g.	0.8	7

n.g. = not given.

Data sources as provided by Consim:

1. Wiedemeier, T. et al., 1995; Tech. protocol for implementing Intrinsic remediation with long-term monitoring for at. attenuation of fuel contam'n. dissolved in g'water. Vol. 1. Brooks AFB, Texas
3. Manrique, L.A. & Jones, C.A., 1991; Bulk density in relation to soil physical and chemical properties. Soil Sci. Soc. Am. Jnl., Vol. 55.
6. Sherwood, P.T. and Hollis, P.T., 1966; Studies of the Keuper Marl: Chemical properties and classification tests. Min. Trpt. Rd. Lab. RRL. Rpt. No. 41
7. Bourg, A.C.M. et al, 1992; A review of the attenuation of TCE in soils and aquifers. Qtly. Jn. Eng. Geol.
8. Soil Characteristics. 1995; Env. Sci. and Tech. Vol. 29, No. 8.
9. Rifai, H.S. and Hopkins, L.P., 1996; Natural attenuation toolbox. Dept. Env. Sci. Eng.

Figure 4: Sampling locations



Aquifer locations from Woodcock, 1994

Chalk cores	Limestone samples	Glacial Till cores	Triassic Sandstone
1 Layer de la Haye	4 Brauncewell	11 BatesMoor	17 Middlesborough
2 Banterwick Barn	5 Harmston	12 Crabgate	18 Gamston
3 Thriplow	6 Leadenham	13 Primrose	
	7 Ropesley	14 Roper	other cores:
	8 Walcot	15 Page's	10 Lower Coal
	9 Longholt	16 Morely	Measures

Site A and Site B confidential locations not shown.

5.2 Chalk

Chalk geology and hydrogeology is summarised in Section 4.2. 106 samples were obtained from three boreholes cored into the Chalk aquifer: Layer de la Haye, Essex, sampling Upper Chalk; Banterwick Barn, Berkshire, sampling Upper and Middle Chalk; and Thriplow, Cambridgeshire, sampling Lower Chalk.

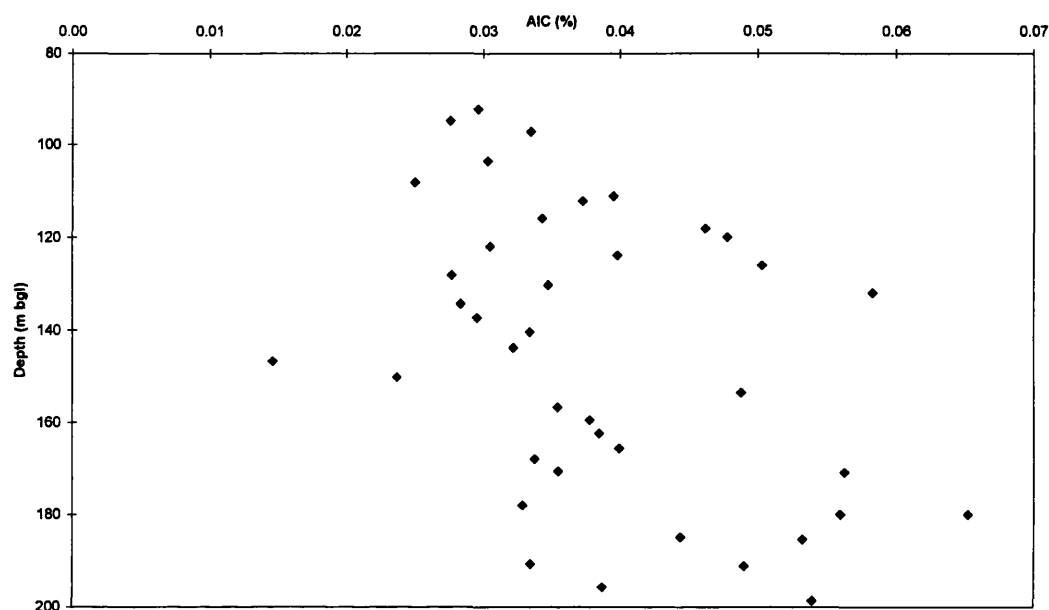
5.2.1 Upper and Middle Chalk

Upper Chalk rotary cored near Layer de la Haye, Essex, (approximate grid reference (GR) TL 971 196) sampled 108 m of chalk from 91.15 metres below ground level (m bgl), overlain by London Clay, Woolwich and Reading Beds, Thanet beds and the Bullhead Formation. The chalk was described as medium soft to hard, with putty chalk in places, with a decreasing number of fractures and flints with depth. The acid-insoluble carbon (AIC) content and descriptions of the samples are tabulated in Appendix D, summarised in Table 8, and illustrated in Figure 5.

A sub-sample obtained from a brown patch at 108.16 m bgl had AIC of 0.13% (excluded from Table 8), significantly higher than the adjacent white chalk material (AIC 0.024% to 0.036%). Grey chalk from 125.04 m bgl had AIC of 0.05% compared to 0.03% to 0.04% for adjacent white samples; this suggests that the grey colour observed does not relate to higher organic carbon. Samples of harder material showed no increase in AIC compared to softer samples.

Five cross-sections of core were studied to investigate whether the organic polymer drilling fluid used resulted in higher organic carbon at the core edges. No significant variation of AIC through the core was identified, indicating either that no contamination had occurred, or less probably, that a constant level of contamination permeated the core.

Figure 5: AIC in Upper Chalk, Laver de la Haye



The Banterwick Barn core (GR SU 513 775) sampled 97 m of Upper and Middle Chalk near Newbury, Berkshire; its inorganic geochemistry is detailed in Murphy *et al.*, 1997. The measured AIC contents are tabulated in Appendix D, illustrated in Figure 6 and summarised in Table 8. A log of the core is also included in Appendix D (Figure 68).

Figure 6: AIC in Upper Chalk, Banterwick Barn

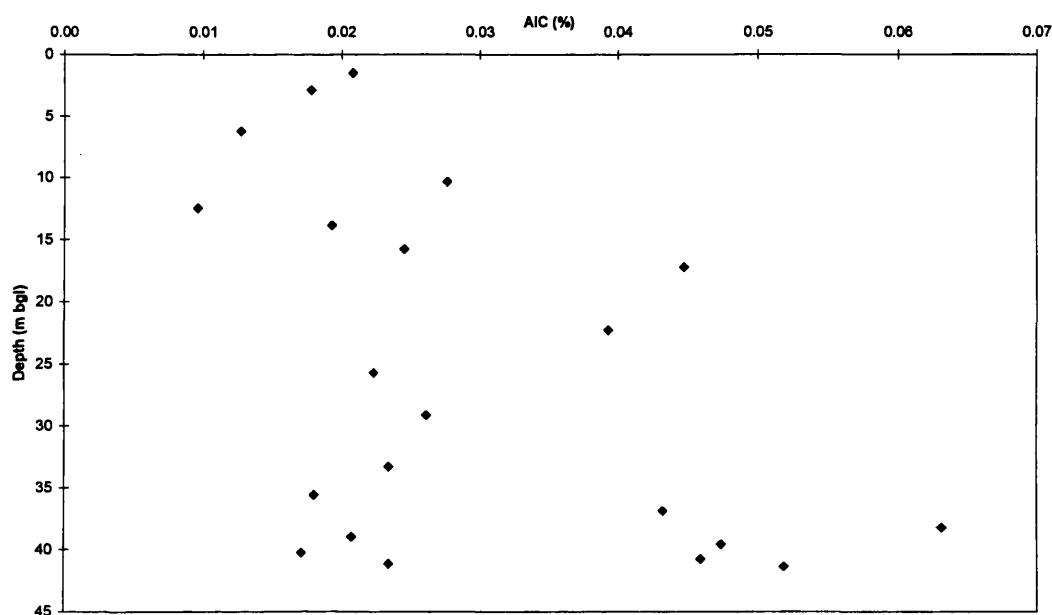
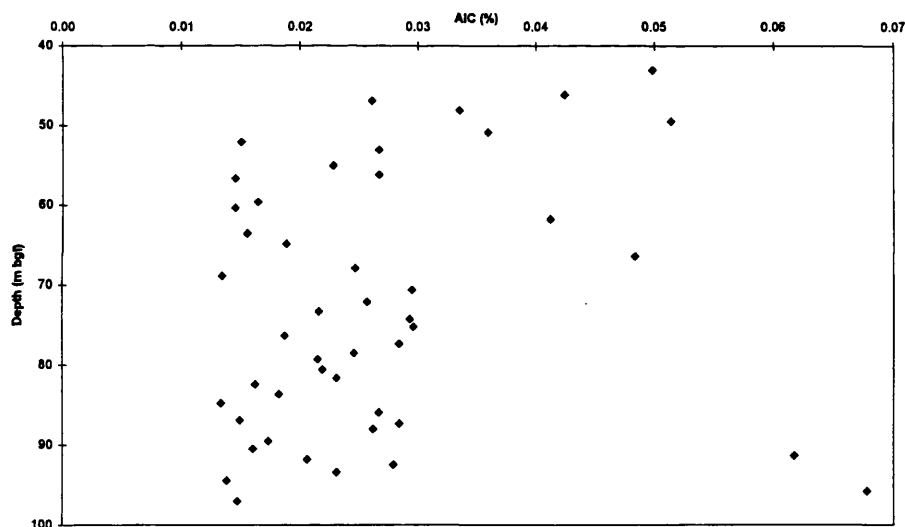


Table 8: Summary of AIC in Upper Chalk

Core	No. of samples analysed	Mean (%)	Maximum (%)	Minimum (%)
Layer de la Haye	39	0.039	0.065	0.015
Banterwick Barn (Upper Chalk material)	21	0.029	0.063	0.0096

Figure 5 and Figure 6 show fluctuations through the Upper Chalk cores without a clear trend, but possibly with increasing AIC with depth.

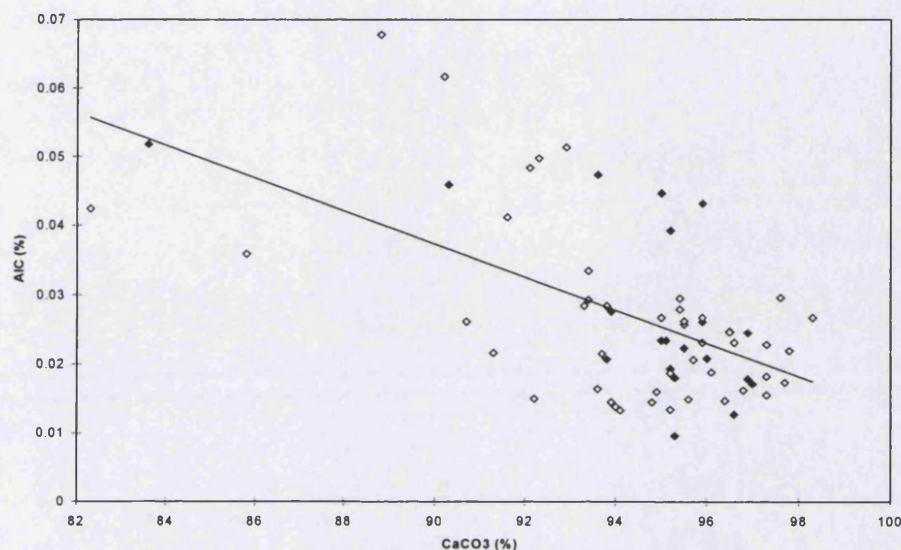
The Banterwick Barn core contained Middle Chalk below the Chalk Rock at approximately 40 m bgl. Results from AIC analyses of Middle Chalk are presented in Figure 7, summarised in Table 9 and tabulated in Appendix D.

Figure 7: AIC in Middle Chalk, Banterwick Barn**Table 9: Summary of AIC in Middle Chalk**

Core	No. of samples analysed	Mean (%)	Maximum (%)	Minimum (%)
Banterwick Barn (Middle Chalk material)	46	0.027	0.068	0.013

AIC content increases with decreasing CaCO_3 content in the samples from Banterwick Barn (Figure 8). Decreasing CaCO_3 is likely to be due to increasing clay content.

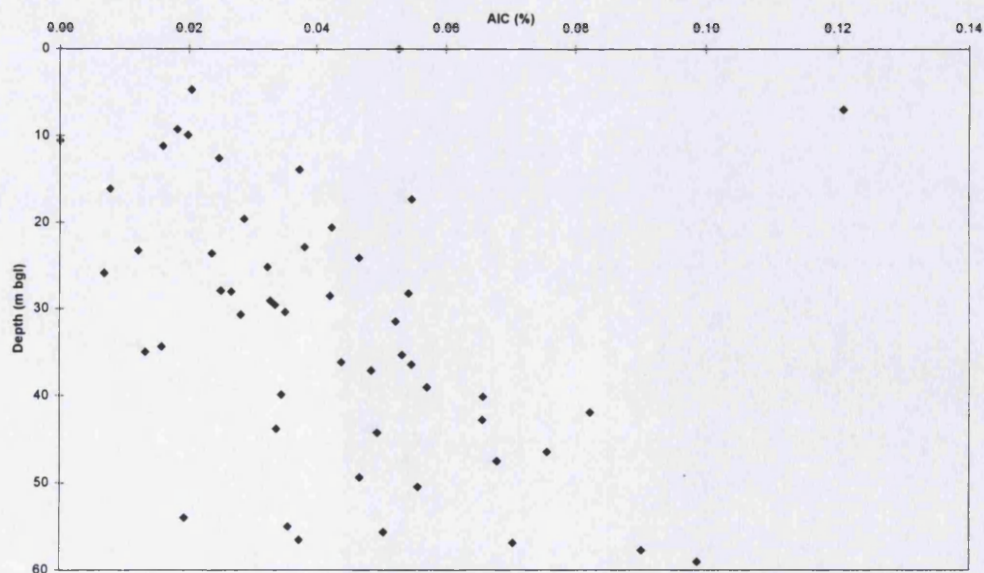
Figure 8: Negative correlation of AIC with CaCO_3 , Banterwick Barn



5.2.2 Lower Chalk

Lower Chalk material was obtained from the Thriplow core from Cambridgeshire (GR TL 446 446). AIC content and descriptions of these Lower Chalk samples are tabulated in Appendix D, illustrated in Figure 9 and summarised in Table 10.

Figure 9: AIC in Lower Chalk, Thriplow



These data indicate an increase in AIC content with depth, which may be associated with increasing clay content with depth in the Lower Chalk.

Table 10: Summary of AIC in Lower Chalk

Core	No. of samples analysed	Mean (%)	Maximum (%)	Minimum (%)
Thriplow	52	0.045	0.12	0.007

5.2.3 Previously published work

Whitelaw and Edwards (1980) and Pacey (1989) analysed various organic components from Upper and Middle Chalk samples, although neither report TOC content. Whitelaw and Edwards (1980) found carbohydrate¹¹ content in the Middle Chalk of 0.0065% to 0.03%, with an exponential decrease with depth. Upper Chalk samples had carbohydrate concentrations between 0.0002% and 0.02%. It was proposed that the carbohydrates were products of bacterial metabolism and suggested that variations between sites may be related to land use. Pacey (1989) found humic matter¹² to be between 0.01% in white chalks and 0.1% in clayey and phosphatic chalks. Fulvic acid content was estimated to be up to 20% of the humic matter. Less than 30% of the humic matter was amenable to direct extraction, the bulk (and all the bitumen¹³) being obtained after dissolution of the matrix. This was thought to indicate a diffuse distribution of organic matter in the chalks, with some intra-crystalline within the calcite, and some associated with the clays. Bitumen levels were 0.01% to 0.15%, usually similar to the humic acid content in the samples. Only small amounts of kerogen¹⁴ were found, as most of the conventional kerogen fraction was found to be alkali soluble after matrix dissolution.

Bein and Sandler (1983) determined organic carbon content with a LECO[®] analyser on the residue of hydrochloric acid dissolution from a series of Eocene chalks and cherts from Israel. The organic matter content of the chalks was found to be higher than that of chert, but analysis of extracted kerogen and humic acid indicated that the composition of

¹¹ Carbohydrate has many hydroxyl functional groups.

¹² Humic matter is the fraction of sedimentary OM that is soluble in basic solutions, and comprises both fulvic acids that are also soluble in acidic solutions and humic acids that are not.

¹³ Bitumen is organic material insoluble in basic solution and soluble in nonpolar organic solvent (Pacey, 1989).

¹⁴ Kerogen is organic matter in sediments that consists of large molecules and is insoluble in non-polar organic solvents.

the organic matter was similar. Total organic carbon ranged between 0.16% and 0.63% in the cherts, and 0.38% and 1.77% in the chalks.

5.2.4 Summary of TOC in Chalk

Upper and Middle Chalk have AIC content less than 0.1% (usually between 0.01% and 0.05%), fluctuating through the depth of the cores studied, showing no consistent trends. Locally higher AIC content appeared to correlate with small brown areas and with decreased CaCO_3 content. Lower Chalk has higher organic carbon content than Upper and Middle Chalk (AIC up to 0.12%), associated with higher clay content and darker appearance. Chalk AIC content is relatively low; organic carbon in the Chalk, especially in Upper and Middle Chalk, is unlikely to provide a significant sorbent.

5.3 Lincolnshire Limestone

The geology and hydrogeology of the Lincolnshire Limestone are summarised in Section 4.3. Little published work on organic carbon in limestones has been found. Lawrence and Foster (1986) extracted bitumen from a Lincolnshire Limestone series, and found low levels in oxidised areas (0.01% to 0.07%) and higher amounts (generally over 0.1%) in unaltered areas. Bishop and Lloyd (1990) state that organic carbon may form up to 5% by weight of the limestone, but do not provide the source of this data. Gehman (1962) measured TOC and bitumen for 346 Cambrian to late Tertiary limestones from various parts of the world. TOC ranged from 0.01% to 7%, with an average of 0.24%. Bitumens ranged from 3 to 6000 $\mu\text{g g}^{-1}$, with a mean of 98 $\mu\text{g g}^{-1}$. Values below average were found only in materials with predominantly non-skeletal grains. Organic carbon of 0.5 to 3% (by weight loss on heating) was reported in Late Precambrian limestones from Southern Norway (Tucker, 1983).

AIC has been measured in 514 Lincolnshire Limestone samples from six locations. Total carbon and sulphur have also been measured for many of these samples. Sample collection, preparation and analysis for all samples excluding some Longholt core were made by A. Kim, but results have not been discussed or presented elsewhere. Analyses from oxidised (weathered) samples obtained at or near the outcrop are presented in Section 5.3.1, followed by results from a core into the unoxidised zone of the limestone in Section 5.3.2. Selected sample sets are presented as examples here, and all results are

tabulated with additional figures and sample descriptions, in Appendix D. Section 5.3.3 includes analysis of samples taken across colour-change boundaries within large limestone matrix blocks, 10s of centimetres between fractures, called redox blocks, which indicate the extent of occurrence of oxidation. Many sample series contain interbedded marls, which were found to have higher organic carbon concentrations.

5.3.1 Oxidised Lincolnshire Limestone

The analysis of oxidised Lincolnshire Limestone obtained from five locations is summarised below (Table 11). These include samples taken from four redox blocks from three locations.

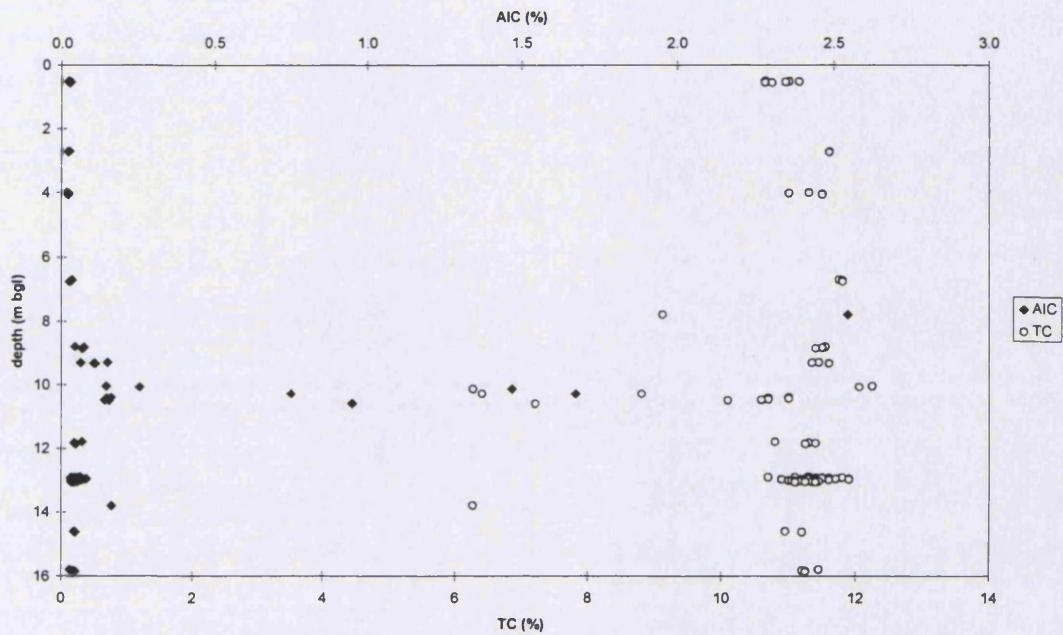
Table 11: Summary of AIC in oxidised Lincolnshire Limestone

Sampling location and grid reference	No. of samples analysed	Mean (%)	Maximum (%)	Minimum (%)
Brauncewell Quarry TF 028 518	81 including 33 from r.b.	0.147	2.545	0.0162
Harmston Quarry SK 991 618	42 including 27 from 2 r.b.s	0.0869	0.5845	0.01185
Leadenham Quarry: marl SK 964 524	7	0.187	0.25	0.13
Leadenham Quarry: limestone	35	0.026	0.052	0.010
Ropesley Quarry: limestone TF 002 365	52 including 14 from r.b.	0.0487	0.254	0.018
Ropesley Quarry: marl	3	1.031	1.515	0.381
Walcott Quarry near TF 130 566	123	0.163	2.22	0.019

r.b. = redox block

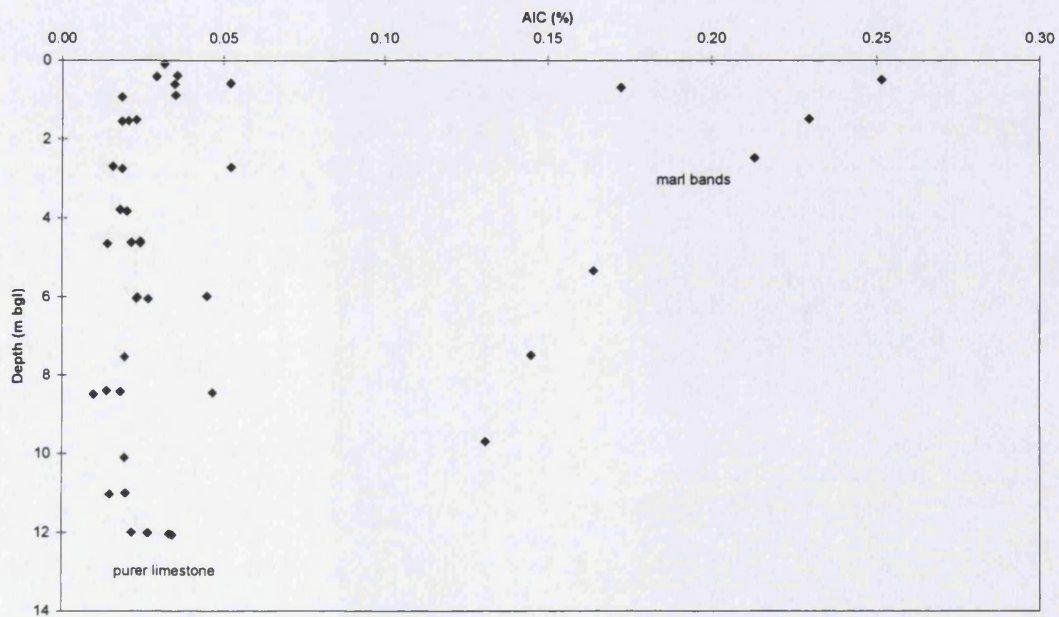
The data from Brauncewell Quarry (plotted against depth on Figure 10) show AIC mainly between 0.02% and 0.3%, rising to 2.5% in clay-rich bands. High AIC values correspond with reduced total carbon values, indicating correlation of increased organic carbon with higher clay content.

Figure 10: AIC and TC in oxidised Lincolnshire Limestone, Brauncewell Quarry



AIC concentrations from Leadenham (Figure 11) display two distinct series. Low organic carbon concentrations (between 0.010% and 0.052%) are found within purer limestone. Higher AIC concentrations (decreasing with depth from 0.25% to 0.13%) are mainly associated with thin red-brown marl (clay-rich) bands interbedded within the limestone.

Figure 11: AIC in oxidised Lincolnshire Limestone, Leadenham Quarry



Marl bands interbedded in the limestone at Ropesley Quarry were also found to have higher organic carbon concentrations (0.38% to 1.5% AIC) compared to the limestone (0.018% to 0.25%). Highest organic carbon concentrations in limestone are from samples adjacent to marl bands. At Walcott Quarry, limestone samples had 0.028% to 0.45% AIC, mainly below 0.15% while AIC in marl bands was between 0.073% and 2.2%.

5.3.2 Unoxidised Lincolnshire Limestone

115 samples were obtained from a core drilled anoxically into the unoxidised part of the aquifer at Longholt (GR TF 104 585) and immediately frozen in liquid nitrogen. AIC measured varies between 0.035% and 2.7%, with higher values associated with reduced total carbon measurements, indicating marl bands. These data are illustrated in Figure 12 and summarised in Table 12 below.

Figure 12: AIC and TC in unoxidised Lincolnshire Limestone, Longholt core

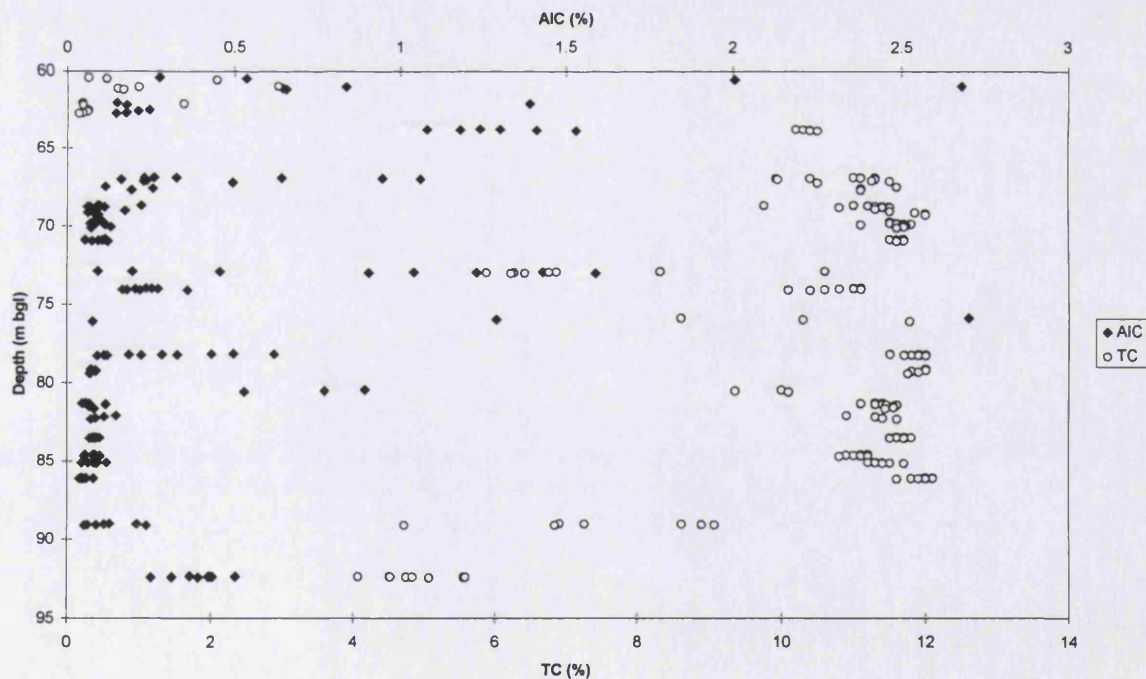


Table 12: Summary of AIC in unoxidised Lincolnshire Limestone

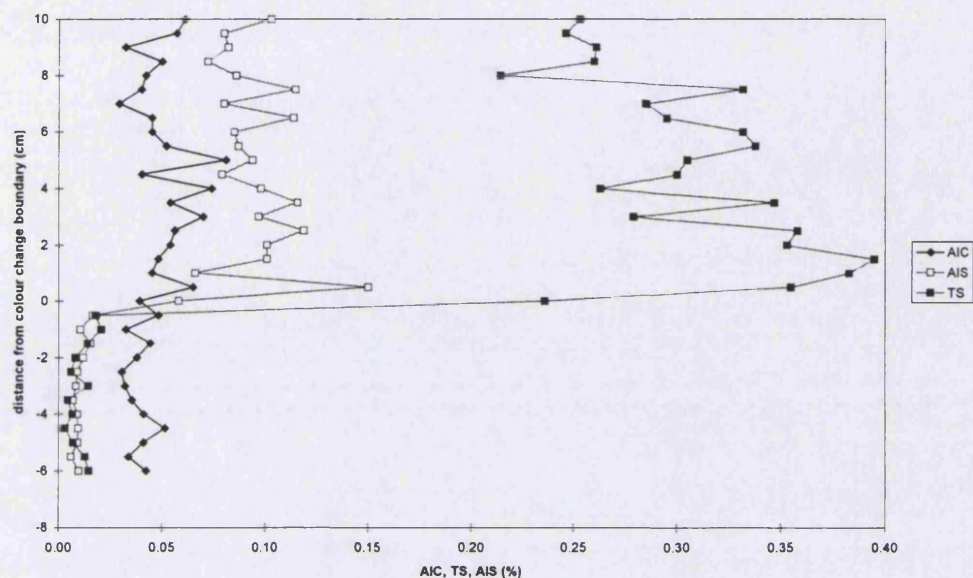
Sampling location	No. of samples analysed	Mean (%)	Maximum (%)	Minimum (%)
Longholt core	168	0.313	2.7	0.035

5.3.3 Redox blocks

Four 'redox blocks' were studied, which comprise blocks of limestone matrix containing a redox boundary in which a colour change in the material from blue-grey to beige-grey indicates a change from reduced to oxidised material. AIC, TC and TS were measured on samples taken at close intervals across the boundary. The data gathered from these blocks are included in the data tables for the appropriate quarry in Appendix D. The data from 33 samples at 5mm intervals across the redox block from Brauncewell are illustrated as an example (Figure 13), and data from other redox blocks are illustrated in Appendix D.

These samples indicate a clear decrease in sulphur content, and a possible, very small concomitant decrease in organic carbon across the redox boundary¹⁵. The colour change observed is probably due to the removal by oxidation of dark-coloured iron and sulphur-containing minerals (pyrite precursors). Acid-insoluble sulphur (AIS) is measured with AIC after HCl pre-treatment of the sample. It generally provides no meaningful information and is usually disregarded, as some of the total sulphur is removed in the acid treatment. It was found in these samples that the difference between AIS and TS in the oxidised part of these blocks is minimal, but in the unoxidised sections AIS is significantly less than TS. The sulphur that has been removed from oxidised sections comprises most of that removed from unoxidised sections during the acid pre-treatment process.

¹⁵ The null hypothesis of equal mean TOC for unoxidised and oxidised samples is rejected in favour of the alternative that mean TOC for unoxidised samples is greater than mean TOC for oxidised samples at greater than 95% confidence for most sample sets.

Figure 13: AIC, AIS and TS in redox block, Brauncewell Quarry

5.3.4 Summary of TOC in Lincolnshire Limestone

AIC measurements on Lincolnshire Limestone samples varied from 0.01% to 2.9%. The reduced limestone core had organic carbon between 0.035% and 1.5%, with a mean of 0.3%. Measurements from oxidised limestone were between 0.01% and 2.5%, with a mean of 0.1%, indicating lower AIC concentrations in oxidised limestone at and near outcrop, which may be due to oxidation by infiltrating waters (J. McArthur, pers. comm.; Kim *et al.*, undated).

Little change in AIC across redox boundaries was observed, whilst sulphur content decreased significantly in the oxidised sections. This suggests that in the Lincolnshire Limestone, the oxidation of sulphur-containing minerals drives the redox process. The solid organic carbon content is not as significantly affected by oxidation as the sulphur content. Reduction of organic carbon may occur in a different location to oxidation of sulphur-containing compounds (supported by the larger difference in AIC noted between the outcrop and reduced limestone).

Organic carbon in limestone samples is increased when in proximity to marl bands; the marl and shale bands have much higher organic carbon content, up to 2.3%. Much of the Lincolnshire Limestone, particularly marl bands, have sufficient organic carbon to potentially provide a significant sorbent for organic pollutants.

5.4 Triassic Sandstone

The geology and hydrogeology of the Triassic Sandstones are summarised in Section 4.4. Little analysis of organic carbon in sandstones has been published before. Analysis of Triassic sandstone samples from Yorkshire (unpublished British Geological Survey data, Stuart, 1991) showed little bitumen (generally less than 0.05%), with no detectable kerogen. Other samples from the same area had organic carbon content from 0.02% to 0.07%. Edmunds *et al.* (1982) state that organic matter was not detected in cores of Sherwood Sandstone from the East Midlands, UK, and was insufficient to be an energy source for heterotrophic bacteria, without providing any values. Carbonate content was given as 1 to 4%, with dolomite more prevalent than calcite. Higher values were measured by wet chemical oxidation in two Carboniferous Coventry Sandstone samples with TOC 0.7-0.8% (Bourg *et al.*, 1993). Stuart (1991) quotes organic carbon of 0.017% to 0.065% in sandstones from southern Ontario from 2m bgl to the water table, where dissolved organic carbon originating in the soil zone was suggested to be an important source in aquifers.

112 samples of Triassic Sandstone from two cores have been analysed. Sample preparation and analysis for the Gamston were made by A. Kim, but results have not been discussed or presented elsewhere. AIC is plotted against depth for Sherwood Sandstone Group strata from the Middlesbrough core (Figure 14) and for the Gamston Core (Figure 15). They are summarised in Table 13 and tabulated in Appendix D together with sample descriptions where available.

Table 13: Summary of AIC in Triassic Sandstone

Sampling location and grid reference	No. of samples analysed	Mean (%)	Maximum (%)	Minimum (%)
Middlesbrough Core NZ 503 250	53	0.017	0.071	0.001
Gamston Core approx SK 710 760	59	0.038	0.058	0.024

Triassic Sandstone samples analysed showed very low organic carbon content, consistently well below 0.1%, even in the clay-rich mudstone bands. It is unlikely that the

minuscule amount of organic carbon present in these deposits contributes measurably to hydrophobic sorption.

Figure 14: AIC in Sherwood Sandstone, Middlesbrough core

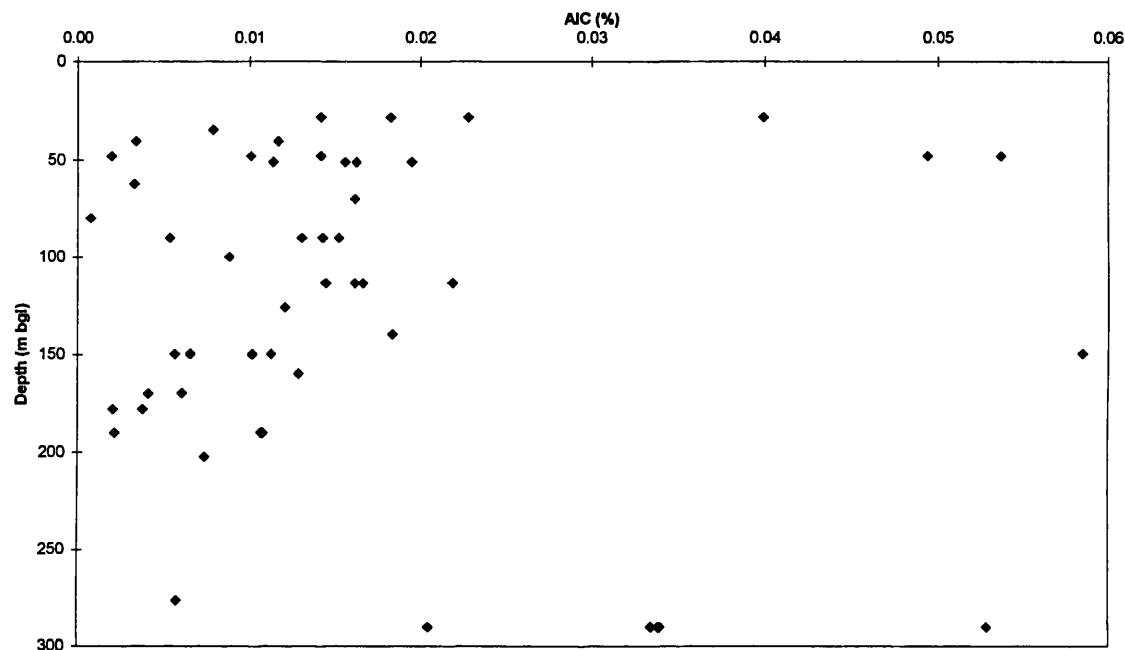
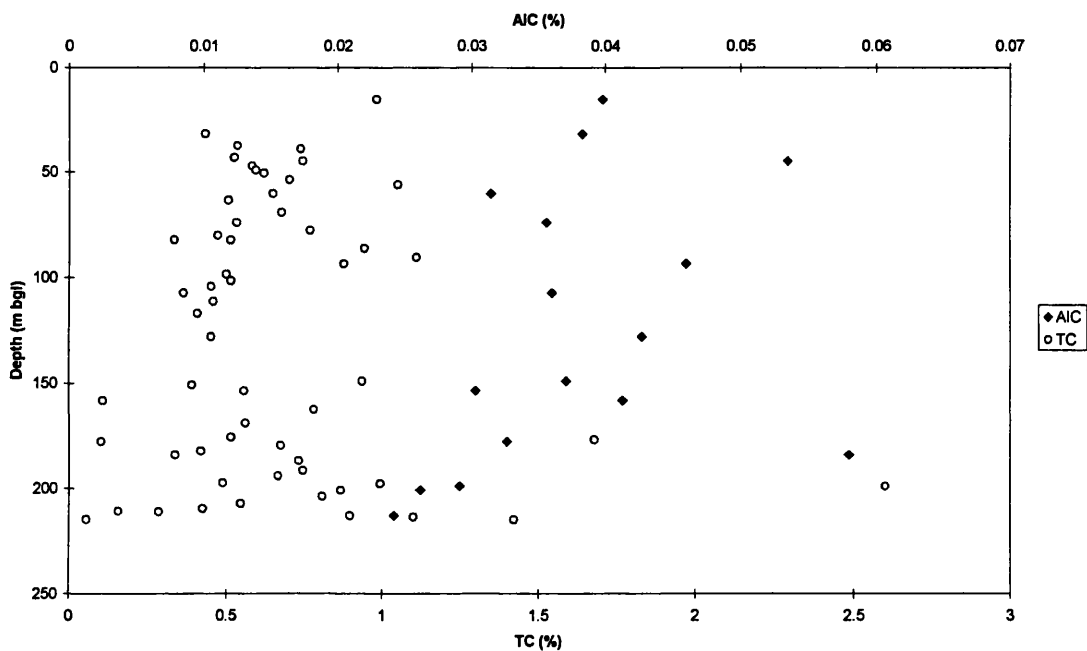


Figure 15: AIC, TC and TS in Triassic Sandstone, Gamston Core



5.5 Unconsolidated deposits

Much groundwater contamination enters the ground from the surface, for example, agricultural chemicals applied to the field surface or industrial chemicals spilt onto the site surface. The flowpath for these chemicals involves percolation through the anthropogenic and natural materials at and near the surface. The compositions of these materials depends on the locality and history of the site. The organic carbon distribution in unconsolidated deposits under two different sites has been investigated. These sites are described below as Site A and Site B. Locations and borehole logs cannot be given as this information is commercially sensitive.

5.5.1 Site A

23 samples were obtained by cable percussion drilling from four boreholes at Site A, which is situated near to an estuary. The analysis results are tabulated and illustrated in Appendix D and summarised in Table 14. Two different material types were sampled: sand and gravel in Boreholes (BHs) 1, 2 and 3, and below 5 m bgl in BH 4; silts dredged from the estuary bottom and deposited here in settlement ponds in BH 4 above 4 m bgl.

Table 14: Summary of AIC in samples from Site A

Material description	No. of samples analysed	Mean (%)	Maximum (%)	Minimum (%)
Sand and Gravel (BHs 1, 2, 3)	18	0.13	0.42	0.035
Estuarine silts (BH 4)	5	1.05	6.19	0.16

The samples contained visible organic fragments, including coal and root fragments. Organic components large enough to be removed were hand-picked from five sub-samples and analysed for total carbon and the remaining material analysed for AIC; these data were compared to AIC analysis of the whole sample. The data tabulated in Appendix D indicate that about half the organic carbon in the samples is present as particles of medium sand size and larger. Given that a significant amount of coal fragments of fine sand size was observed but not removed, it is likely that the majority of the organic carbon in the sampled sand unit at Site A is in discrete particles of fine sand size and larger.

Many of the sand samples had an AIC content over 0.1%, but may have a reduced impact in sorption of organic solutes because:

- much of the organic carbon is in the form of coal fragments of fine sand size and larger with a carbon content up to 77%. They therefore have a reduced surface area per unit mass than smaller particles.
- coal largely comprises mineralised carbon, and therefore may not form a strong sorbent for organic contaminants.

The estuarine silts had higher AIC with fewer large organic particles than the sand samples, due to their different depositional environment. However, the location of the samples on this site, in settlement ponds, means that they are unlikely to form part of a flow path for contaminants at this site, apart from contamination in the settlement ponds.

5.5.2 Site B

110 samples were obtained from Site B by cable percussion drilling. Sample descriptions, AIC content and (where obtained) TC and TS content are tabulated and illustrated in Appendix D and summarised in Table 15. Results from one borehole are illustrated on Figure 16 below; other results are illustrated on figures in Appendix D.

Figure 16: AIC, TC and TS in Site B Borehole 9D

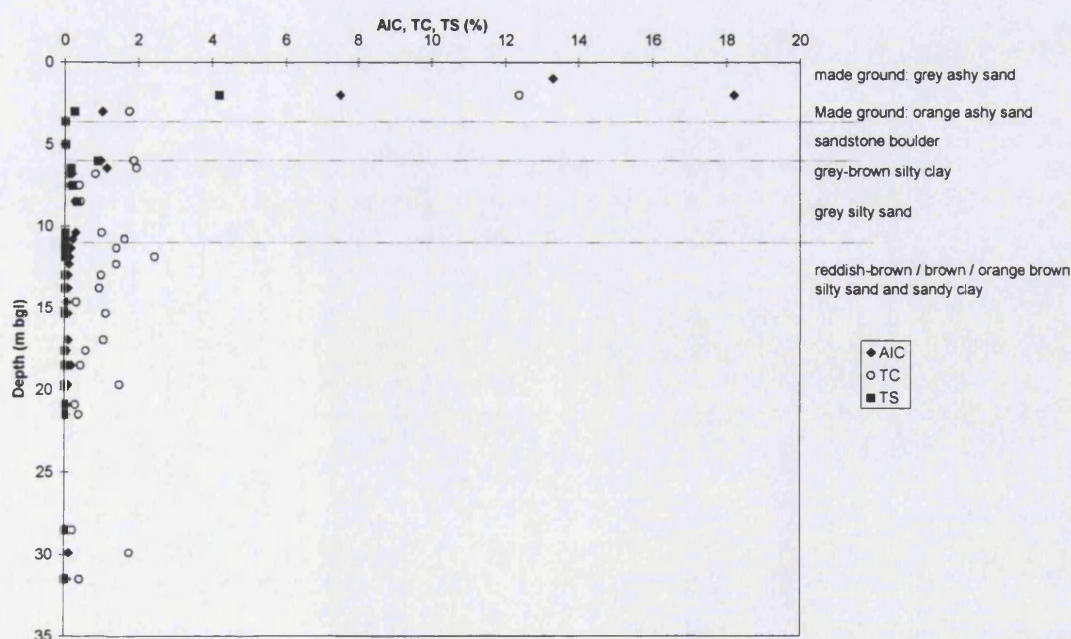


Table 15: Summary of AIC in samples from Site B

Material description	No. of samples analysed	Mean (%)	Maximum (%)	Minimum (%)
Made Ground	11	8.38	27.4	1.03
Made Ground: Sandstone Boulder	2	0.01	0.011	0.009
Grey / grey-brown / black silt and clay	23	1.38	5.5	0.19
Grey and grey-brown sand and gravel	11	0.37	1.21	0.062
Red-brown / brown clay and silt	33	0.24	1.33	0.06
Red-brown and brown sand and gravel	27	0.11	0.44	0.020
Brown clayey peat	3	15.3	23.8	9.9

The sample descriptions in Appendix D show that these material types are interlayered, and do not consistently occur at the same depth. These results indicate that made ground (excluding the sandstone boulder) has much higher AIC content than the other material types tested. In general, silts and clays had higher AIC than sands and gravels, consistent with the finding that finer grained materials have higher organic carbon content than coarser grained materials. The grey and grey brown materials (which were from shallower depths) generally had higher organic carbon than the red-brown and brown materials. As expected, the peat sampled in one borehole had high organic carbon content.

Many samples had visible fragments of organic material: silts and clays from shallow depths contained rootlets and fragments of roots; made ground samples contained many sand and gravel sized coal, slag and ash material. Frequent clinker (furnace residue) particles suggested that the made ground partially comprises furnace waste. Further investigations on samples from Site B, including the distribution of organic content with particle size for one made ground sample, are included in Chapters 8 to 10.

5.5.3 Conclusions

These samples from unconsolidated deposits show a huge range of AIC contents, in many cases sufficiently high to be expected significantly to sorb hydrophobic contaminants. Samples from Site B show variations in AIC with grain size and with material colour. Made ground samples had very high AIC content, with the exception of the sandstone boulder. However, much of the high AIC in these samples, as in sand samples from Site A, is associated with sand-size and larger particles, and therefore has a much lower

surface area, which may affect its availability for sorption, than finer organic material. Additionally, where organic particles are sufficiently large for visual inspection, they clearly comprise many different organic materials: rootlets and plant fragments, peat and coal fragments have all been noted. It is unlikely that all these different materials will have the same behaviour as sorbents.

5.6 Glacial Till

78 glacial till samples from two sample sets were analysed for AIC: five boreholes in the Bure Catchment, north Norfolk, sampled North Sea Drift; a borehole at Morley, north Norfolk, sampled Lowestoft Till. The geology and hydrogeology of the Glacial Till in Norfolk have been discussed in Section 4.6, and results of further analysis and experimentation on selected samples are presented in Chapters 8 to 10. The clayey glacial till deposits form an aquitard providing important protection to the major Chalk aquifer beneath.

5.6.1 North Sea Drift

46 samples were obtained from five boreholes drilled into the North Sea Drift in the Bure Catchment, north Norfolk (Bates Moor Farm, GR TG 040 250; Crabgate Farm, GR TG 105 280; Primrose Farm, GR TG 075 250; Roper Farm, GR TG 110 350; and Page's Farm GR 075 275). Additional investigation on these samples is discussed in George *et al.* (in prep.). The analytical results and sample descriptions are presented in Appendix D; AIC results are summarised in Table 18. Examples of AIC and clay profiles with depth are illustrated in Figure 17 and Figure 18 below and the remainder in Appendix D. Clay content is based on field observations (George, 1998). Samples from Crabgate Farm, Primrose Farm (Figure 17), Roper Farm and Bates Moor Farm appear to show positive correlation of AIC with clay content; no samples from these boreholes with low clay content have high AIC. This is expected, as higher TOC values are frequently associated with finer materials (Durand, 1980). Conversely, samples from Page's Farm (Figure 18) unexpectedly appear to show a negative correlation with clay content. A similar pattern is observed in the correlation of clay content with oxygen 18 and deuterium isotope measurements (George, 1998): a positive correlation is seen for samples from Crabgate Farm, Primrose Farm, Roper Farm and Bates Moor Farm, and a negative correlation for

samples from Page's Farm. This is attributed to weathering patterns: at the first four boreholes, higher grain size has allowed greater weathering to reduce the TOC content. At Page's Farm, artesian groundwater conditions have prevented water infiltrating downward, preventing oxidation of organic carbon. The wide AIC content range reflect the varying material types, especially with respect to weathering and grain size, within these North Sea Drift and Lowestoft Till materials.

Figure 17: AIC and clay in North Sea Drift, Primrose Farm

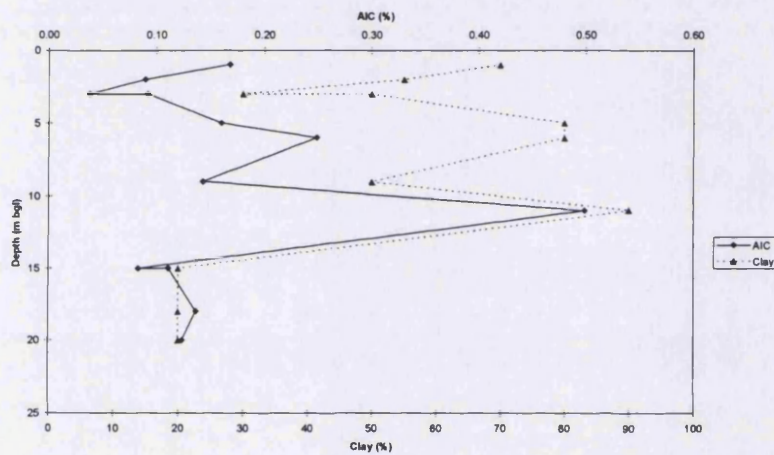
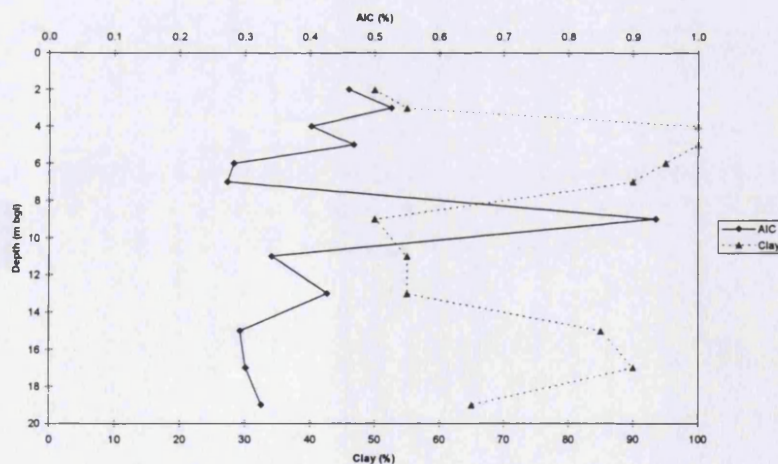


Figure 18: AIC and clay in North Sea Drift, Pages' Farm

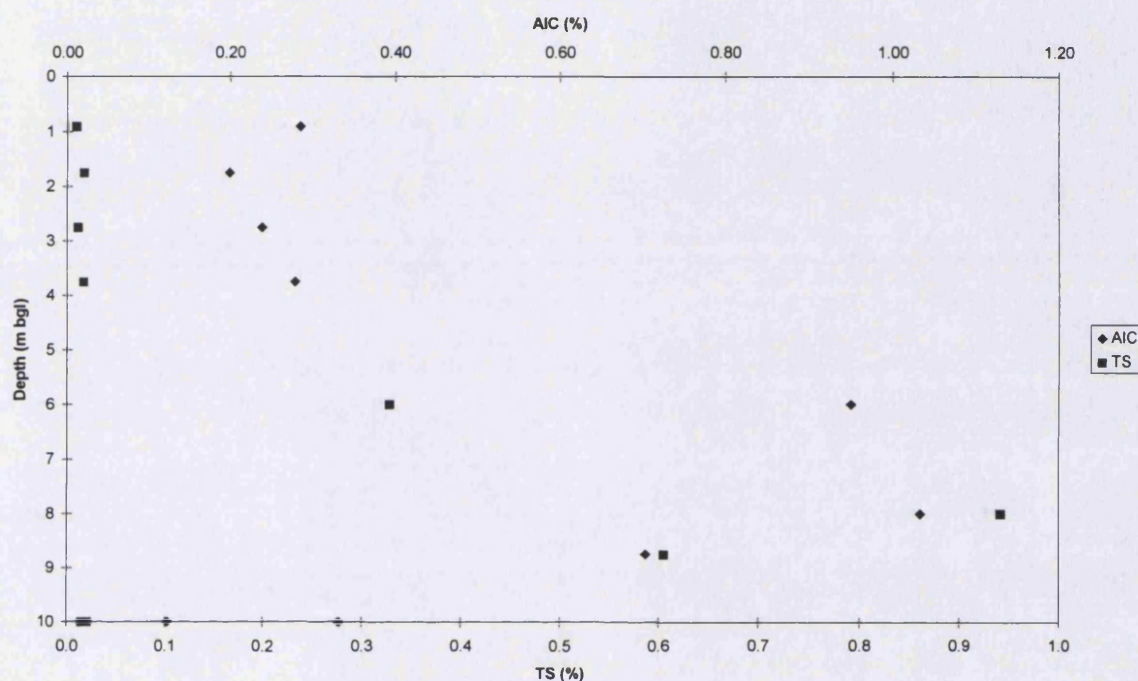


5.6.2 Lowestoft Till

Nine samples were obtained from a borehole drilled into the Lowestoft Till at Morley in north Norfolk (GR TM 062 989). Sample descriptions are given in Appendix D. The results are tabulated in Appendix D and illustrated on Figure 19 below. These samples

were found to be carbonate-rich; if all carbonate is calcium carbonate, it accounts for between 36% and 55% of each sample.

Figure 19: AIC and TS in Lowestoft Till, Morley



Samples above 3 m bgl (described as ‘mottled’) contained gravel-sized fragments of dark brown material. The dark brown and lighter coloured materials were separated and analysed (Table 16).

Table 16: Analyses of dark, light and bulk glacial till fractions

Sample (m bgl)	fraction description	TC (%)	TS (%)	AIC (%)	IC (%)
0.8-1	bulk rock sample	4.68	0.009	0.285	4.39
	dark brown material	1.33	0.0092	0.712	0.0077
	light material	5.7	0.0022	0.16	0.0039
1.5-2	bulk rock sample	6.09	0.017	0.199	5.89
	dark brown material	3.47	0.013	0.806	2.66
	light material	6.28	0.009	0.177	6.10
2.5-3	bulk rock sample	6.46	0.011	0.239	6.22
	dark brown material	1.25	0.0094	0.892	0.0114
	light material	6.53	0.0065	0.210	0.0355

Results in bold type indicate the mean of two analyses

These analyses show that the dark fractions have much higher AIC than whole rock samples and the ‘light’ coloured material had correspondingly slightly lower AIC. This indicates that the dark coloured, organic-rich material comprises a small percentage of the whole rock (approximately 20% for the 0.8 - 1.0 m bgl sample, and 4% for the samples

from 1.5 - 2 m bgl and 2.5 - 3.0 m bgl). This confirms the observation that the brown crumbs are rare, and shows that they have a minor impact on the AIC content of the whole sample.

The glacial till investigated comprises three distinct layers, described in Table 17, interpreted as the result of differential weathering and oxidation. Weathering from the surface has penetrated to a depth of between 5 and 6 m. Material with coarser grain-size and higher permeability material at 10 m has had a greater flow of oxidising water, and hence oxidation occurred within this layer. An intermediate unoxidised layer is characterised by a grey colour. AIC and TS show distinct changes between these layers (Table 17).

Table 17: Sulphur and AIC in glacial till layers

Depth (m bgl)	no. of samples	material description	sulphur (%)			carbon (%)		
			min.	max.	mean	min.	max.	mean
0 - 5	4	yellow, brown & orange clayey materials with flint and gravel	0.0090	0.017	0.25	0.20	0.29	0.25
6 - 9	3	grey clay	0.33	0.94	0.62	0.70	1.0	0.90
10	2	coarser-grained orange-brown silts and sands	0.015	0.020	0.018	0.12	0.33	0.23

The significant decrease in both AIC and TS in the upper and lower oxidised layers indicates that these elements have been removed by oxidation. If the oxidised layers had originally contained as much organic carbon as the central unoxidised layer, and if the reduction in organic carbon in the upper and lower layers is due solely to oxidation, the majority (over 70%) of the organic carbon formerly present was susceptible to oxidation. A change in organic carbon content across the oxidation boundary is not unexpected, although it was less marked in redox blocks in the Lincolnshire Limestone, and not observed in glacial till in Ontario (Robertson *et al.*, 1996, in samples with TOC between 0.05% and 0.2%, lower than that in Norfolk Glacial Till samples). Organic carbon in those deposits was concluded to be largely compounds resilient to oxidation. It is therefore suggested that a significant proportion of the organic carbon in these glacial till samples is in forms which are susceptible to oxidation. Some variation in organic carbon content in these glacial tills may be due to variations during deposition. The decrease in sulphur observed in the Morley Glacial Till samples suggests that sulphur-containing

compounds were oxidised to form water-soluble forms of sulphur that are subsequently dissolved (sulphur decrease with oxidation was also found by Robertson *et al.*, 1996).

The AIC content measured in these Lowestoft Till samples is comparable to those measured in North Sea Drift samples. Unlike the North Sea Drift samples, these samples did not exhibit a wide range of particle sizes; therefore, variation of AIC with clay content was not inspected. The North Sea Drift samples appeared to show a decrease in AIC with oxidation of the samples (George *et al.*, in prep) which is clearly confirmed by the results from these samples.

5.6.3 Summary of TOC in Glacial Till

A wide range of AIC content, with many areas of relatively high values, has been observed in glacial tills. AIC content is related to the weathering condition of the material, and possibly to the grain-size and variations in AIC content on deposition. The AIC measured in glacial till samples is summarised in Table 18.

Table 18: Summary of AIC in Glacial Till

Sampling location	No. of samples analysed	Mean (%)	Maximum (%)	Minimum (%)
Bure Catchment	71	0.251	0.947	0.033
Morley	9	0.460	1.033	0.123

5.7 Lower Coal Measures

Four boreholes drilled at Whinney Hill, near Accrington, Lancashire (GR SD 757 305) sampled Lower Coal Measures (BGS, 1971). Geology and hydrogeology are briefly commented on in Section 4.7. AIC data measured in the Whinney Hill core are tabulated with sample descriptions and figures in Appendix D and summarised in Table 19. These contain high levels of organic carbon. Comparable 2.8 to 11.3% TOC have previously been measured in Middle and Lower Coal Measures (Dobson and Kinghorn, 1987).

Table 19: Summary of AIC in Lower Coal Measures

Sampling location	No. of samples analysed	Mean (%)	Maximum (%)	Minimum (%)
Whinney Hill	52	2.17	7.26	0.38

5.8 Lower Greensand

McLeod (1998) analysed 78 samples from the Hythe Beds of the Lower Greensand, from a core drilled near Hindhead, Surrey. She found a mean AIC content of 0.04% in the top 65m, and higher and more variable concentrations in the lower 20m (from 0.03% to 0.19% AIC). Concentrations of over 0.34% were measured in three samples from the underlying Atherfield Clay aquitard.

5.9 Jurassic Mudrocks: Oxford Clay, Kimmeridge Clay and Lower Lias

Jurassic clays, particularly the Oxford Clay, form some of the most extensive aquitards in the UK, and are widely used for landfill liners. As such, they are frequently important in retarding contamination movement into aquifers.

Kenig *et al.* (1994) analysed the biogeochemistry of 165 samples of the Oxford Clay Formation and 5 from the underlying Kellaways Formation, sampled at eight locations in quarries and one core into the outcrop. Organic carbon content ranged from 0.5% to 16.6%, with a mean of 4.8%. TOC was higher in the Peterborough Member (Lower Oxford Clay) (mostly over 3%) than in the underlying Kellaways Formation and overlying Stewartby Member (Middle Oxford Clay), which both had less than 1.5% TOC. The Oxford Clay has significant potential to sorb organic contaminants. In the Peterborough Member, shales have high concentrations of TOC (and hydrogen index¹⁶ (HI) approaching 800), indicating preservation of hydrogen-rich organic material. Conversely, shell beds and calcareous and silty clay beds have lower TOC (and HI dropping below 100), indicating extensive oxidation of the organic matter.

Other surveys have reported TOC in 40 samples from the Peterborough Member from 2.54% to 9.44%, with a mean of 5.11% (Norry *et al.*, 1994); TOC in ten samples of

¹⁶ HI is a parameter produced by Rock-Eval pyrolysis, considered to be a proxy for the H/C ratio of the organic matter, and is discussed further in Section 7.6.

Oxford Clay was found to be from 1.03 to 12.36% (Ebukanson and Kinghorn, 1985, analysing samples from Southern England) who also measured between 0.99 to 20.48% TOC in 21 samples of Kimmeridge Clay and between 0.26 to 7.36% TOC in Lower Lias (limestone and mudstone / shale) samples. A trend of increasing organic content from the Lower Lias (up to 7.36%), through the Oxford Clay (up to 12.36%) to the Kimmeridge Clay (up to 20.48%) was observed (Ebukanson and Kinghorn, 1985), with TOC content related to both preservation in anoxic conditions and sedimentation rate with increased primary productivity.

5.10 Conclusions

UK aquifer materials in general have low organic carbon content: the organic carbon levels in Chalk and Triassic sandstone are unlikely to be sufficient significantly to sorb hydrophobic organic contaminants. The Lincolnshire Limestone contains more organic carbon, with much higher levels in interbedded shales and mudstones. In the Chalk and Lincolnshire Limestone, areas with higher clay content contain more organic carbon than purer material. Mudstones and Glacial Till had much higher organic carbon content: aquitards are likely to provide the most significant retardation due to sorption for hydrophobic organic contaminants. The wide range of organic carbon content measured in unconsolidated clays, silts, sands and gravels reflect their varying depositional and post-depositional processes. A significant amount of organic carbon in the made ground and unconsolidated sands analysed was found to be as sand and larger sized fragments. The AIC contents measured are summarised in Table 20.

Table 20: Summary of new AIC determinations

Material type	No. of samples	Mean (%)	Maximum (%)	Minimum (%)
Upper Chalk	60	0.036	0.065	0.0096
Middle Chalk	46	0.027	0.068	0.013
Lower Chalk	52	0.045	0.12	0.007
Oxidised limestone	333	0.12	2.55	0.010
Marl within limestone	10	0.44	1.52	0.13
Unoxidised Limestone	168	0.31	2.7	0.035
Triassic Sandstone	112	0.028	0.071	0.001
sands and gravels	56	0.17	1.2	0.020
silts and clays	61	0.74	6.2	0.06
Made Ground	11	8.38	27.4	1.03
Made Ground: Sandstone	2	0.01	0.011	0.009
Peat	3	15.3	23.8	9.9
Lower Coal Measures	52	2.17	7.26	2.17
Glacial Till	80	0.28	1.03	0.033

Organic carbon was found to be significantly depleted by weathering oxidation in glacial tills and to a lesser extent in the Lincolnshire Limestone, indicating differences in the availability of the organic material to redox reactions. This suggests that different organic material with different geochemical properties is present in these two geological units: the organic carbon in the glacial tills is more reactive than that in the limestone. These geochemical differences may also cause differences in the extent to which the organic material reacts with organic contaminants.

5.11 Summary

- Over one thousand samples have been analysed for their total organic carbon content, using HTO after pre-treatment to remove carbonate carbon by addition of dilute HCl with filtration. The results for this method are considered to be more accurate for high carbonate samples, and are reported as acid-insoluble carbon (AIC).
- All AIC values gathered are summarised in Table 20.
- Chalk and Triassic Sandstone were found to have low AIC, below 0.1%.
- AIC content in the Lincolnshire Limestone varied, mainly above 0.1%, with higher values in interbedded shales and marls. A small decrease in AIC was seen across colour change redox boundaries.

Chapter 5: TOC in geological material

- Glacial Till samples mainly had over 0.1% AIC content, which varied significantly depending on the weathering state of the samples, and also on the grain size of the samples.
- Unconsolidated sands and gravels had very varied AIC content, which were seen to be associated with material colour. Unconsolidated silts and clays had higher AIC content, largely above 0.1%, with a mean of 0.7%.
- Made ground sampled had very high AIC, with a mean of 8.4%, excluding a sandstone boulder which had AIC content typical of sandstones.
- AIC content can be weakly correlated with grain size and material colour, but varies too much for these to be used as predictors.
- AIC content in glacial tills decreases substantially with weathering, and to a lesser extent in the Lincolnshire Limestone.

6. Characterisation of Organic Matter

6.1 Introduction

It is proposed in this thesis that the capacity of a rock to sorb hydrophobic organic contaminants is controlled not only by its total organic carbon (TOC) content, but also by the physical or geochemical type of its organic matter (OM). Therefore, to discover how the type of OM influences sorption, and how that influence can best be predicted, characterisation of OM type is required.

This chapter describes the methods used for investigating and comparing the chemical and morphological characteristics of OM in ways that may prove useful in predicting its influence on sorption. Results of geochemical OM characterisation are given and discussed in Chapter 7, and results of morphological OM characterisation are given and discussed in Chapter 8. Organic matter can be typed both geochemically and morphologically; geochemistry may be undertaken either on the whole rock or on isolated or extracted¹⁷ OM, and may provide information on either the bulk characteristics of the whole OM, or on a fraction of the OM, or on specific compounds. For this study, geochemical information was gathered on the bulk characteristics of the OM, because the exclusion of specific fractions cannot be justified; presence and abundance of specific chemical molecules were not studied. OM typing and characterisation methods have been adapted from those used in palynological and petroleum studies. These methods have been applied to 43 samples from the Lincolnshire Limestone, Glacial Till from north Norfolk, and unconsolidated sediments and made ground from Site B; sample materials and the geology and hydrogeological context are described in Chapter 6.

Almost 25% (1.25×10^{16} tonnes) of the carbon in the global carbon cycle is organic carbon in sedimentary rocks (Killops and Killops, 1993). Organic matter (OM) in sediments is the degraded residue, after diagenesis, of organic matter inputs to the sediments from numerous sources, such as reworked secondary OM, and algal, plant and animal remains. Some OM may be imported into aquifers as dissolved organic carbon and deposited as

¹⁷Isolated OM is separated from the whole rock sample by removal of rock minerals by dissolution in acid; extracted OM is separated from the whole rock sample by dissolution of OM in organic solvents.

grain coatings (for example, West *et al.*, 1994). Made ground will also contain anthropogenic organic materials, and larger fragments of materials. Most OM was originally deposited under water. Terrestrially deposited OM is preserved mainly in peats. Biologically-driven diagenesis continues after burial. OM degradation releases simple molecules (CO_2 , CH_4 , H_2 , H_2O) leaving an aromatic carbon-rich residue (Durand, 1980). Further degradation of refractory OM in ancient sediments (>1 million years) may occur given changes in conditions such as weathering and redox changes or pressure and temperature increases (Tyson, 1995).

For elemental and isotopic analysis of the OM, it must be separated from other rock components: isolation was undertaken using HCl / HF dissolution (Section 6.2.1). Geochemical analyses (Section 6.2.2) comprised elemental and stable C isotope analysis on isolated OM, together with Rock-Eval pyrolysis, a method applied to whole rock samples, which was expected to provide proxies for some elemental data. OM morphology was characterised in slides of isolated OM, by classification into morphological types and by image analysis of the particle size distribution (Section 6.2.3).

6.2 Methods used

6.2.1 Isolation of organic matter

Solid organic matter is isolated by palynologists and petroleum geochemists for different reasons. They apply similar techniques to isolate organic matter (OM) by dissolving the mineral components of the rock sample using hydrochloric acid (HCl) to remove carbonate, sulphide, sulphate and oxide minerals (forming soluble chloride salts, water and gases including CO_2) and hydrofluoric acid (HF) to dissolve silicates (which form the gas SiF_4 and water).

Isolation techniques applied in palynology are described in Wood *et al.* (1996) and Traverse (1988). Similar techniques used in petroleum geochemistry to isolate kerogen¹⁸

¹⁸ Kerogen is organic matter that is insoluble in organic solvents and may be operationally described as the material remaining after treatment with both organic solvents and HCl and HF (Whelan and Thompson-Rizer, 1993; Senftle *et al.*, 1993).

are described by Durand and Nicaise (1980). These involve a series of HCl / HF / HCl applications, separated by washing with distilled water, which may be followed by density separation (typically at specific gravity (s.g.) 2.0). Thorough washing is required after HCl treatment before HF addition to remove calcium ions and prevent CaF₂ precipitation (Bostick and Alpern, 1977). In palynology, oxidation, sieving and staining are applied before slide mounting to reveal palynomorphs more clearly. Oxidation may be employed prior to heavy liquid separation to remove opaque sulphide minerals. Surfactants are used to remove clay materials. In petroleum geochemistry, the sample is dried for analysis. For petrographic examination of the residue, an aim is to recover particles sufficiently large for microscopic identification with minimal morphological change. This can conflict with the aim of isolation for geochemical purposes to recover and purify OM with minimal loss (Durand and Nicaise, 1980). Palynologists grind samples less finely than do geochemists, and will accept a greater residual mineral component.

For this study, a method was developed to remove mineral matter and concentrate OM from the samples for preparation of slides (for micro-morphological study) and dried residue (for geochemical analysis). Its success in concentrating organic matter was examined, both in removing all other components, and in retaining all the organic carbon. Sequential and repetitive leachings with HCl and HF, to remove carbonate and silicate minerals, were followed by a heavy liquid density separation to purify the resulting residues. This produced a float and a sink fraction. The method was adapted from palynological preparation techniques used in the Micropaleontology Unit at UCL, with the omission of sieving and oxidation processes in order to retain all particle sizes and to minimise alteration of the organic material. Slides of OM were made using OM suspensions in poly vinyl alcohol (PVA); wet preparations were found to be most successful. The procedure development and details are given in Appendix E.

The proportion of organic carbon from the original whole rock samples that was recovered in the floats was calculated by total carbon (TC) analysis of the floats and acid-insoluble carbon (AIC) analysis of the whole rock samples. The effectiveness of the heavy liquid separation was assessed by TC analysis of the sink fractions. The percentage of the whole rock organic carbon present in the final float and sink fractions is referred to as the

percentage recovery, which had a mean of 52% and is reported with the results in Chapter 7. The dried residues were analysed for elemental composition and carbon isotope ratios, and the slides analysed for particle type and size.

To assess the reproducibility of the isolation procedure, OM was isolated in duplicate subsamples from each of two samples of Lowestoft Till (for results, see Chapter 7). One pair of duplicates have less than 5% deviation from the mean in their elemental geochemistry (C, H, N, O, S analysis), and the other less than 9% deviation from the mean. These differences are largely due to differing non-organic content and are reduced to less than 2% and 4% and when taken as % of the CHNOS_{org} content of the samples. In terms of morphology, both pairs of duplicates show 9% or less deviation from the mean in amorphous matter abundance which forms 70% and 60% of the two samples.

6.2.2 Geochemical analysis

CHN analysis was undertaken using a Carlo-Erber analyser in which the gases liberated from the sample by high temperature oxidation (HTO), completed catalytically, are chromatographically separated in a capillary column. The N₂, CO₂ and H₂O peak areas at the thermal conductivity detector (TCD) are identified by arrival time and calibrated against an organic standard. The standard deviations of standards analysed during the sample run were 0.5% of the mean for N, 0.6% for C and 1.1% for H. Analysis both of blanks (empty capsules) given a nominal weight of 5mg (the mean sample weight used) and of a C, H and N-free sample were 0.00% ± 0.01% for N, 0.00% ± 0.01% for C (with a couple of exceptions) and 0.00% ± 0.00% for H, compared to sample results of 0.02% to 2.8% for N, 0.15% to 76% for C and 0.6% to 5.6% for H. Duplicate samples give C results with a deviation from the mean of less than 3% (mean 1%), for H of less than 4% (mean 2%) and for N less than 5% (mean 2.5%).

Sulphur analysis on most samples used HTO followed by infra-red quantification of SO₂ using the LECO[®] analyser as described in Section 3.4 and Appendix A. Samples analysed for S by LECO[®] also had C quantified by this method, in addition to quantification using the Carlo-Erber analyser. On samples where insufficient material was available for LECO[®] analysis, S was analysed by HTO (with tungstic oxide to ensure complete

combustion) followed by TCD in the Chemistry Department of UCL using a 240 Perkin Elmer elemental analyser set up specifically to run sulphur analyses. This had a detection limit of 0.5% and a deviation from the mean of less than 2% in duplicates. S analyses by these methods provided results that were in good agreement. Silicon content was analysed by the Brannock and Shapiro method, in which 100 mg of the sample was fused in lithium metaborate in platinum crucibles at approximately 850°C, dissolved in dilute hydrochloric acid, and the resulting solution analysed by the molybdenum blue method with calibration against standard rocks. The remaining elements were analysed by inductively coupled plasma - atomic emission spectrometry (ICP-AES) after dissolution of the sample in mixed strong acids.

Stable carbon isotope ratios were measured by mass-spectrometry of CO₂ after HTO to convert C to CO₂ and chromatographic separation of the evolved gases. Most duplicates were within 0.3‰ (typical analytical uncertainty), or within 1.2% of their mean.

The Rock-Eval analysis method can be summarised as follows: a whole rock or isolated kerogen sample is gradually heated in a helium stream to an intermediate temperature of 200 to 250°C; hydrocarbons already generated in the rock are volatilised, quantified by flame ionisation detection (FID) and the amount termed S₁. Temperature increase to 550°C causes degradation of the kerogen structure, producing gases which are quantified by FID, providing the S₂ value. On some equipment these gases may also be analysed by TCD, which analyses oxygen-containing compounds (CO₂ and H₂O), providing the S₃ value. For an accurate S₃ value, CO₂ generation from carbonate mineral decomposition must be avoided by temperature control, removal of carbonates prior to analysis or analysis of isolated kerogen. The S₃ function is often omitted. T_{max} is the temperature at which the S₂ peak reaches its maximum.

For this work 45 samples were analysed using a Delsi Rock Eval Oil Show Analyser, which does not provide an S₃ value. Fourteen of these samples were also analysed using an IFP Rock-Eval II analyser, which does provide S₃.

For the Delsi Rock Eval Oil Show Analyser, crushed whole rock samples were analysed under standard conditions: the furnace was heated from 300°C to 550°C at 25°C min⁻¹. Hydrocarbons evolved were quantified by flame ionisation detection (FID). The

equipment used omitted the S_3 function. Results were compared to a standard of powdered Kimmeridgian black shale (cross calibrated against the Norwegian Petroleum Directorate standard), which had mean S_1 of 0.33 mg/g (standard deviation 0.06), compared to its actual S_1 of 0.27 mg/g, mean S_2 of 13.18 mg/g (standard deviation 0.44) compared to its actual S_2 of 13.59, and mean T_{\max} of 430°C (standard deviation 1.76) compared to its actual T_{\max} of 430°C. The detection limit, taken as the mean of the blanks plus two standard deviations, was 0.06 mg/g for S_1 and 0.00 mg/g for S_2 excluding one very high value, compared to sample results of S_1 of 0.1 to 0.4 mg/g and S_2 of 0.02 to 2.5 mg/g. Analysis of blanks and carbon-free samples produced S_1 or S_2 components below the detection limit, and therefore immeasurable T_{\max} . Duplicates gave S_1 and S_2 values typically ± 0.06 mg/g, and $T_{\max} \pm 13^\circ\text{C}$. These are within the variations found in repeated analysis of the standard, but are large deviations from the mean for S_1 and S_2 (typically within 44% and 35%, up to 100% and 200% respectively) due to low absolute values. T_{\max} deviations from the mean for duplicates are typically within 3%, up to 20%.

The IFP Rock-Eval II analyser has an identical temperature programme. The hydrocarbons evolved are analysed by both FID and by TCD, which provides the S_3 value. The equipment is calibrated with a laboratory standard, and cross calibrated against a primary standard. The laboratory reports variation in T_{\max} of 3°C and the standard deviation of S_1 is 10%, S_2 is 5% and S_3 is 15%.

Discussion of the Rock-Eval method and its inherent problems is given in Section 7.6.

6.2.3 Morphological analysis

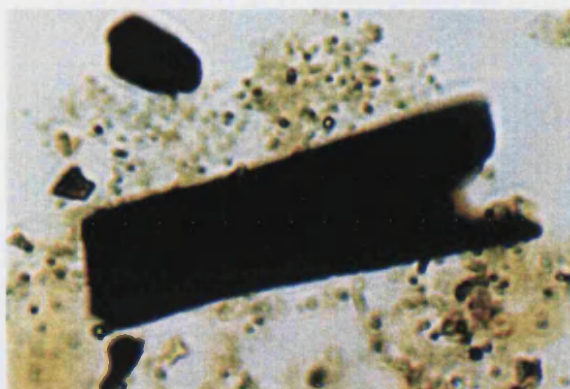
6.2.3.1 Classification and abundance

A classification has been developed to categorise components in the microscope slides of isolated OM from samples in this study. The categories used are described below:

Black wood (Figure 20) ('inertinite' in coal petrography) is opaque material which may be from forest fires or oxidised by groundwater or high temperature. Opaque mineral matter will be included. Some 'black' particles may be slightly translucent at the edges.

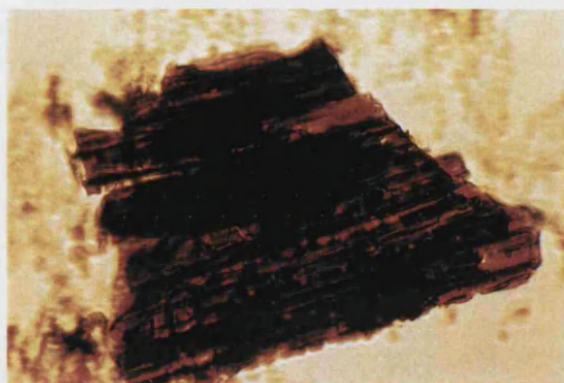
Brown wood (Figure 21) ('vitrinite' in coal petrography) is translucent, and is varied in colour, shape and size and internal structure.

Figure 20: Black wood



Magnification 1200

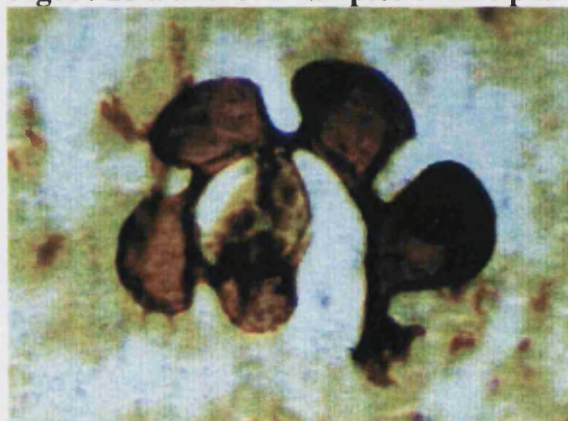
Figure 21: Brown wood



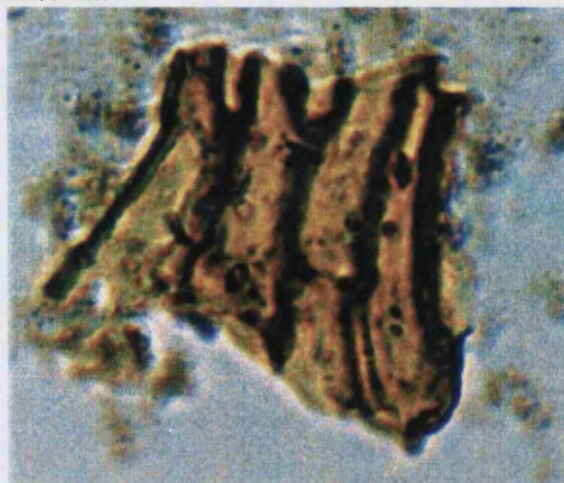
Magnification 400

Cortex, cuticle, other fine plant matter (Figure 22 a and b) contains relict or clear biological structure: cortex is fibrous or gauze-like in appearance; cuticles are rare and identified by stomata; 'other fine plant matter' comprises fine pale sheets.

Figure 22 a and b: Examples of fine plant material



foram lining
Magnification 400



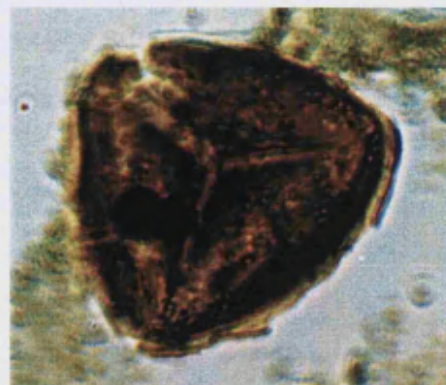
Magnification 300

Pollen (Figure 23) displays various structures which are multilayered with internal structure

Spores (not shown) are more uniform than pollen with less structure. They are frequently kidney-bean shaped or have tri-part symmetry.

Fungi and algae (not shown): fungi are long 'worm-like' shapes; algae are spiky.

Figure 23: Pollen grain

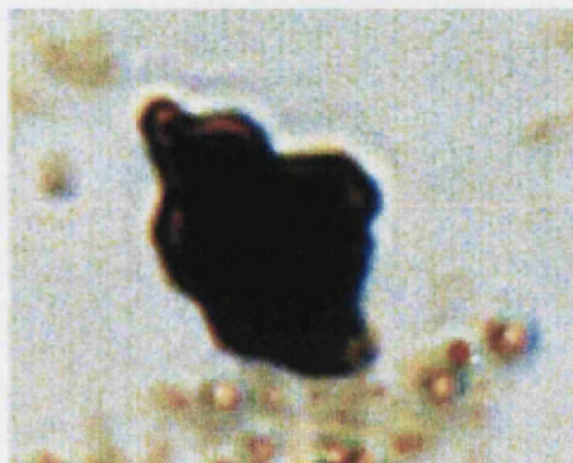


Magnification 250

Degraded matter (Figure 24): shapeless, brown or opaque particles which have distinct 'tattered' edges and may have some structure are categorised as degraded remains of black or brown wood. These may represent an intermediate degradation stage.

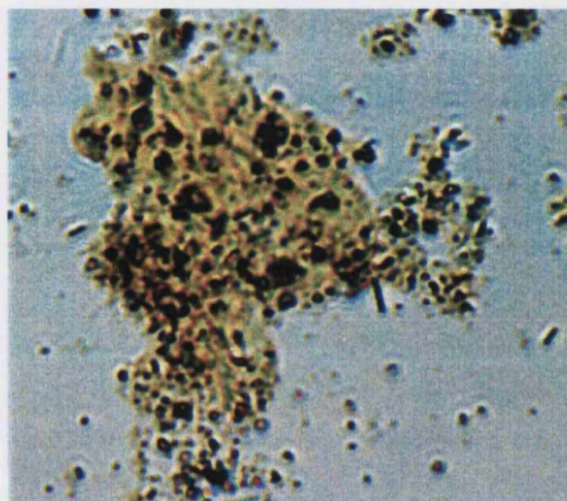
Amorphous matter (Figure 25) has no clearly defined shape, and may be finely dispersed or aggregated. Amorphous matter cannot be consistently distinguished as humic matter (granular) and sapropelic matter (fluffy, fluoresce under UV) without UV microscopy.

Figure 24: Degraded humic matter



Magnification 3800

Figure 25: Fine amorphous matter



Magnification 1400

Resin (not shown) is orange gellified amorphous matter.

Other (not shown) is the category for unidentified items or things that cannot be placed elsewhere.

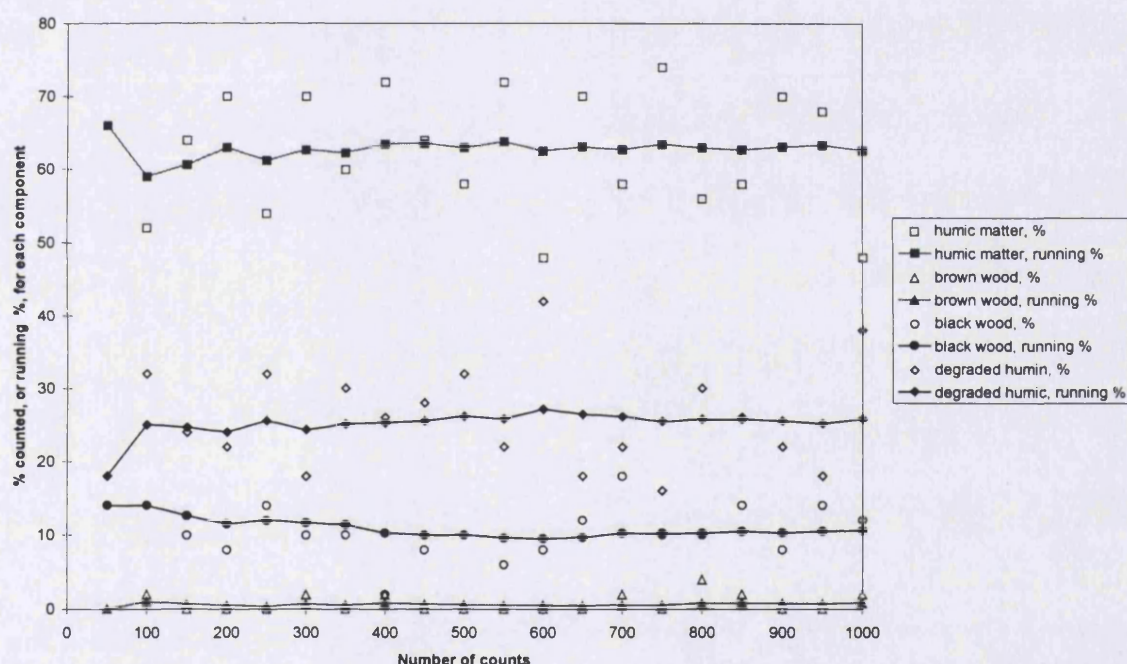
Minerals (not shown) are non-organic particles, and were excluded from both the number of particles counted and from the percentages.

To find the proportion of each category in each sample, strewn slides were point counted. For 300 locations on the slide the item under (or, in sparse slides, close to) the cross-hairs was categorised and tallied; locations with no item under the cross-hairs were passed over; mineral matter was tallied, but not included in the 300 point total. An automated stepping stage ensured locations were evenly distributed across the slide, decreasing susceptibility to distribution variation. 300 points counted represented typically 6 to 10 traverses, depending on the OM density. Points were 0.2 mm apart (the minimum possible with the stage used), approximately half the field of vision; traverses were separated by typically 1 to 3 mm, chosen to ensure coverage of the whole slide. Point counting

provides an estimate of the relative surface area covered by each category, not the number of particles in each category (as particles have different surface areas).

To determine the minimum number of counts required to classify OM for this study, a rarefaction curve was prepared for a slide of OM from made ground from Site B. This curve (Figure 26) shows apparent changes in total percentages with each additional 50 counts. There is decreasing fluctuation in the running percentages, with continuing variation in the % abundance in each 50 points. Little change in the total % abundance occurs after 300 counts, confirming that this is an appropriate number.

Figure 26: Rarefaction curve showing impact of additional points counted



According to Traverse (1988) 'The number of specimens that must be counted to achieve a desired standard deviation depends on the abundance of the least abundant form'. 200 counts (commonly used in palynological analyses) is often viewed as reliable for abundant forms. To gain data on categories present in small proportions, large numbers of specimens need to be counted. Subsequent increases in count numbers give decreasing additional reliability (as the standard deviation (s.d.) falls by a decreasing amount); there is a trade-off between time taken and improved accuracy. The precision with which the abundance of a proportion (%) of a component can be determined is a function of the

proportion itself and the number of counts made per slide. This is given for 300 counts of components present in different proportions (Table 21).

Table 21: Precision of counting based upon classification of 300 particles

Proportion (%)	Relative standard deviation (%)	Range of 66% of analyses i.e. ± 1 standard deviation
5	25	5 ± 1.25
10	17	10 ± 1.7
15	14	15 ± 2.1
20	12	20 ± 2.4
30	9	30 ± 2.7
40	7	40 ± 2.8
50	6	50 ± 3
60	4.5	60 ± 2.7
70	4	70 ± 2.8
80	3	80 ± 2.4

From figure in Traverse, 1988, p 490

An increase to, for example, 500 counts means a component that is 5% of the total has a s.d. of about 20%, so 66% of all analyses should lie in the range $5\% \pm 1\%$. The number of counts chosen reflects the proportion of components present and the accuracy to which the data is required. 300 counts will ensure that material present in as little as 1% will be seen (Bown, 1998). The observation of such low abundance is good for this work, which proposes that different types of OM will have different impacts on sorption.

Replicate counts on the same slide (Table 22) show reproducibility of the point counting technique. They clearly illustrate an increase in standard deviation with decrease in abundance, as expected from the statistics of sampling. Deviation may also be introduced by misidentification of particles. Whilst care was taken to avoid this, black wood, degraded humin and amorphous matter may form a continuum as various stages in the degradation process; categorisation of such particles is not always clear.

Table 22: Replicate particle classification and counts

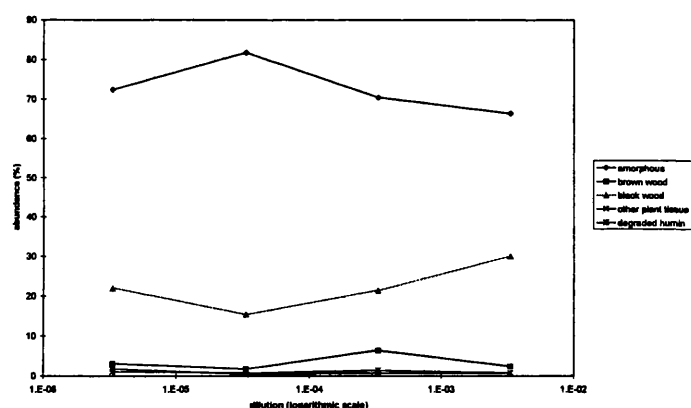
slide	item	humic matter	brown wood	black wood	plant tissue	resin	degraded humin	pollen	spores	mineral
w10d 2.0:1	Mean (%)	49.5	5.6	36.7	0.2	n.d.	7.9	n.d.	n.d.	15.0
	S.D. (%)	2.3	1.4	2.2	0.2	n.d.	1.8	n.d.	n.d.	5.2
	S.D. (as % of mean)	4.6	25.0	6.0	109.5	n.d.	22.4	n.d.	n.d.	34.8
NTY10-3	Mean (%)	73.2	12.4	12.2	1.5	n.d.	0.7	n.d.	n.d.	n.d.
	S.D. (%)	3.3	3.5	2.6	1.2	n.d.	0.8	n.d.	n.d.	n.d.
	S.D. (as % of mean)	4.5	28.6	21.3	81.6	n.d.	104.2	n.d.	n.d.	n.d.
LL 60.48	Mean (%)	23.4	27.2	36.0	4.0	0.6	4.9	3.7	0.2	n.d.
	S.D. (%)	10.9	4.7	9.2	2.1	1.0	4.7	2.6	1.2	n.d.
	S.D. (as % of mean)	46.4	17.4	25.5	52.4	n.i.	95.6	70.9	n.i.	n.d.

Abundance and standard deviation are for the sample, not the population

n.d. not detected

n.i. not included due to insufficient data

The density of OM suspended in the solution used to make slides affects the density of particles on the slide. Abundances in a series of five slides created at exponentially increasing dilution (decreasing particle density) indicated no significant density dependence (Figure 27). The OM in the most dense slide was about as dense as any of the slides. The OM in the least dense slide (at the greatest dilution) was too sparse to count, as insufficient particles were encountered.

Figure 27: Effect of density of slide solution on classification and abundance

6.2.3.2 Image analysis

As surface area of organic matter may be an important control on sorption, a method was sought to characterise the particle size distribution (PSD) on a microscopic level; this was achieved by image analysis of smear slides. *'Image analysis measurements of relative areas are the most accurate form of data in transmitted light work'* (Tyson, 1995)

'Particle shape and size can be measured easily and rapidly by image analysis methods'

which can provide shape and size parameters. Alternative PSD analysis methods such as Coulter counting and laser imaging were not used as practical limitations (including particle size range and material structure) would have created uncertainty in the resultant data. It was noted in Section 5.5 that the size of organic particles in some samples (notably made ground) varies on a macroscopic level; macroscopic particles (greater than about 1mm) are not retained in slide preparation.

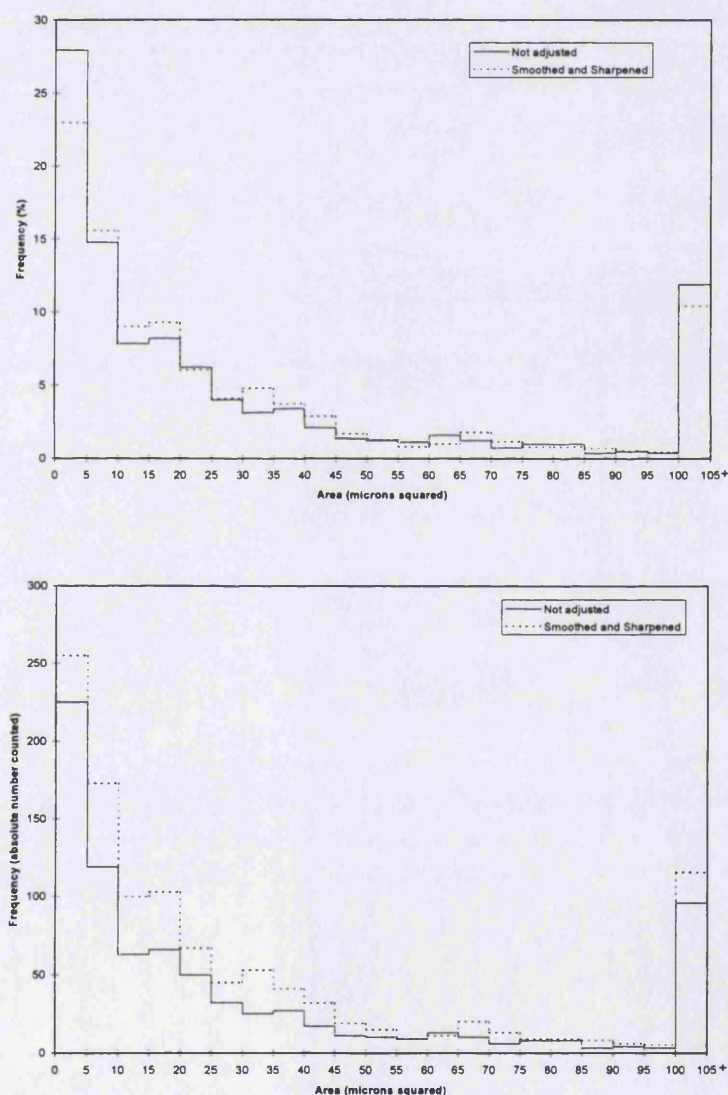
Strewn slides were viewed using objective lenses of magnifications $\times 5$, $\times 20$ and $\times 40$ and an optivar lens of magnification $\times 1$; the image fed to the video camera bypassed the ocular lens. $\times 20$ and $\times 40$ images were concentric with $\times 5$ images, which were randomly located. Images were captured for processing through a JVC KY F55B video camera to a Macintosh computer; each computer image was the average of eight video frames to reduce noise and receive the three colour inputs. Image analysis software was the public domain NIH Image program, version 1.61 (developed at the U.S. National Institutes of Health, available on the internet at <http://rsb.info.nih.gov/nih-image/>). Images were calibrated using a macro that relates the size of each pixel to the microscope magnification.

Thresholding differentiates particles from background on the basis of grey level. Objects identified by thresholding can be automatically counted and measured; measurements selected included the area of the particle (in square microns after calibration). Up to 8000 particles between 1 and 999999 pixels in size could be measured from each image. Particles touching the edge of the image were excluded, and interior holes were not included in the measurements.

'Sharpen' and 'Smooth' are noise filtering functions that may be used in conjunction to increase contrast and reduce noise. The effect of applying 'Smooth' followed by 'Sharpen' was investigated. PSD results for one image from a glacial till slide (at $\times 5$ magnification) are given first as percentage frequency, and second as absolute number of particles (Figure 28). Clearly details of many finer particles are merged or unidentified and so uncounted during the image manipulation, resulting in a greater percentage of

small (under $5 \mu\text{m}^2$) particles measured in the unadjusted image. However, fewer particles are identified in the unadjusted image (1610 compared to 2218 in the Smoothed and Sharpened image), indicating that the greater contrast enables the thresholding to recognise particles otherwise combined and measured as one particle, or ignored as background. However, the resolution limit is unchanged (just under $5 \mu\text{m}^2$) as it is dependent on the size represented by each pixel.

Figure 28: Impact of 'Smooth' and 'Sharpen' image analysis tools

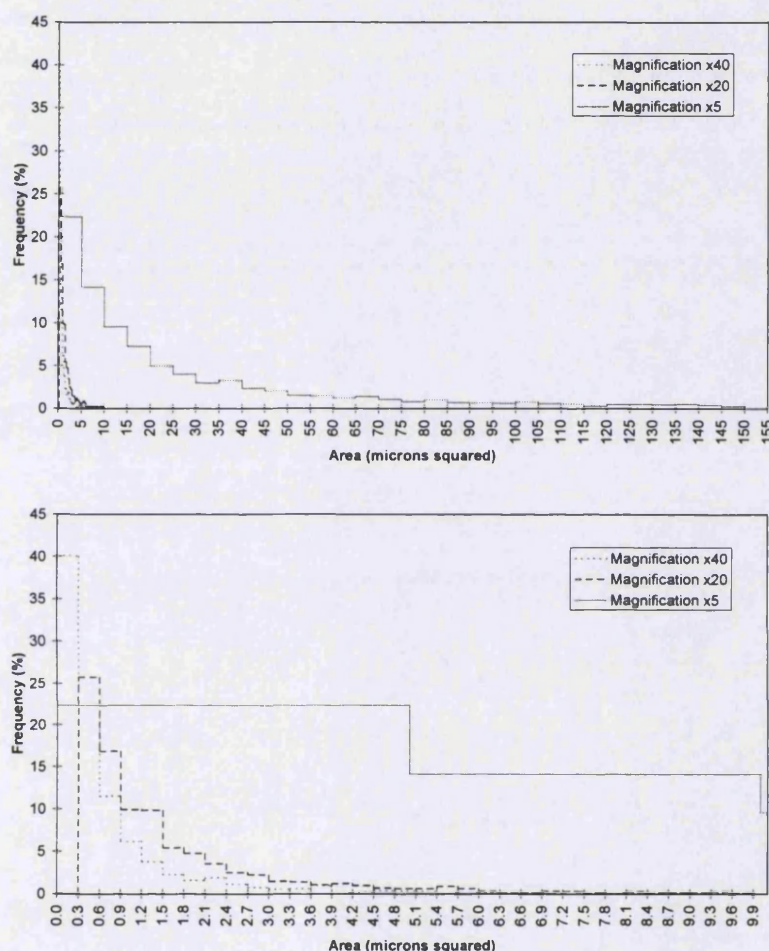


Smaller particles provide a greater contribution to total surface area per volume and may therefore be relatively more important sorbents than larger particles. They may also have different chemistry to large particles. Therefore, to prevent image manipulation losing or obscuring information on these smaller particles, all images were analysed unadjusted.

The PSD (mean of three separate images) from concentric images captured at $\times 5$, $\times 20$ and $\times 40$ magnifications is presented below, using two area scales.

Figure 29: Image analysis of concentric images

Three magnifications, plotted on two scales.



These data indicate that

- as expected, greater magnification enables resolution of finer particles (each pixel represented just under $5 \mu\text{m}^2$ at magnification $\times 5$, $0.31 \mu\text{m}^2$ at $\times 20$, and $0.078 \mu\text{m}^2$ at $\times 40$);
- there are a decreasing percentage of particles of increasing size; therefore,
- greater magnification enables resolution of many more, finer particles, thus decreasing the percentage frequency of the larger particles.

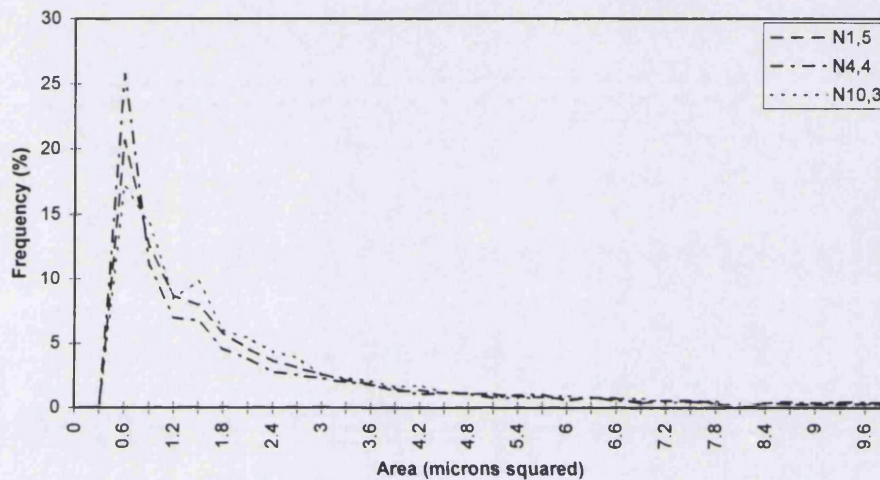
An 'absolute' PSD is not available using this method, because different magnifications provide different resolutions. There will always be a resolution limit (as with any method). The size of the field of the image will exclude larger particles. Lower magnifications allow a greater field of view, in which a greater number of larger particles

can be identified without them touching the edge of the image (and hence being excluded). Results from different slides can be compared at any given magnification.

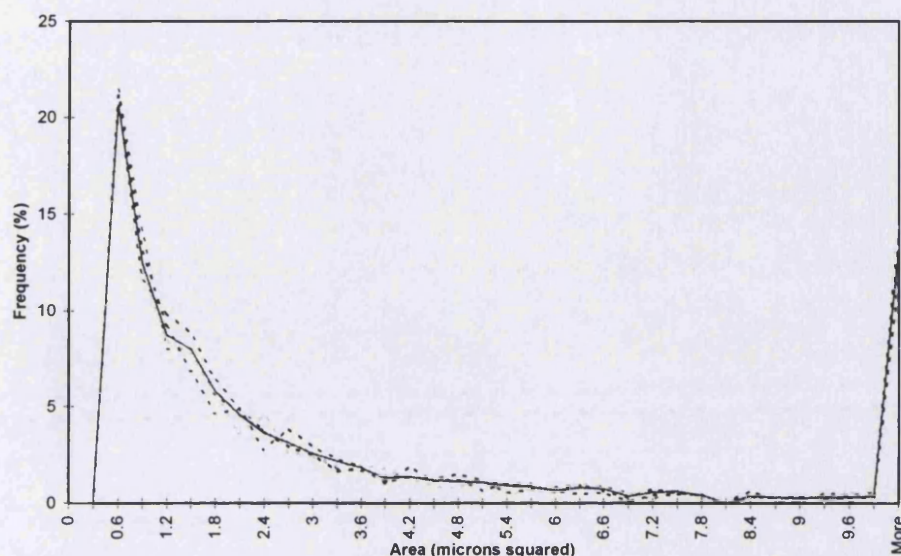
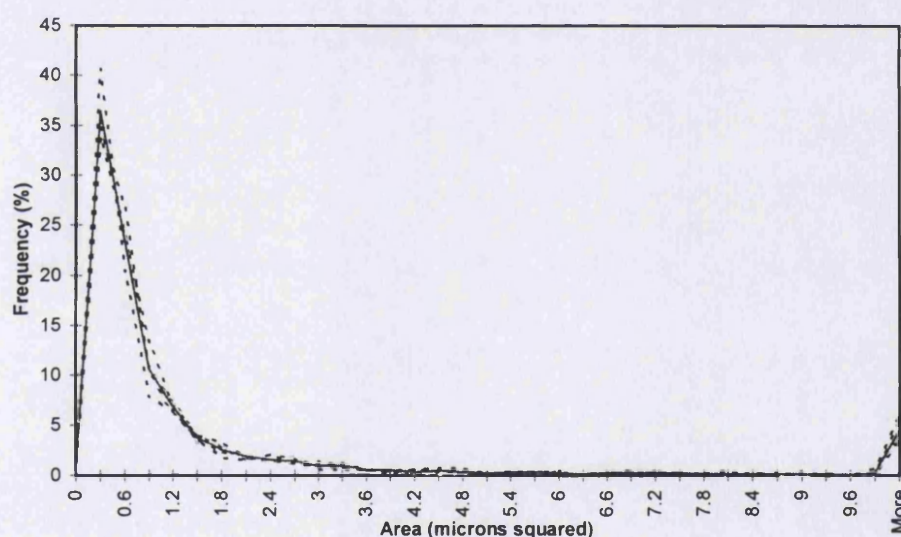
For the North Sea Drift Glacial Till samples, differences between samples are greatest at $\times 20$ magnification; the range of results at this magnification is illustrated in Figure 30.

Figure 30: The range of particle size distribution data

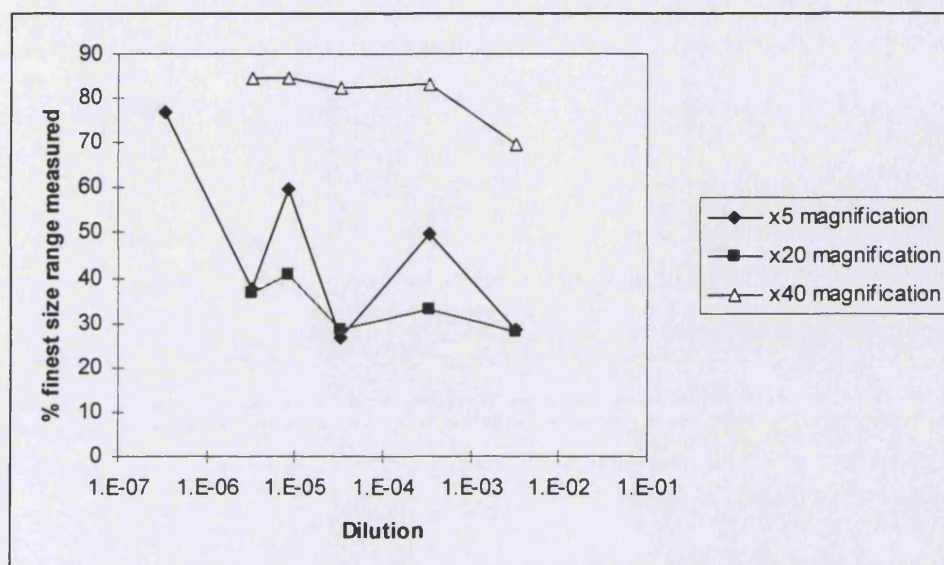
magnification $\times 20$



Five images at magnification $\times 20$ and six at magnification $\times 40$ were taken from different locations on a slide of North Sea Drift from 1 m bgl (Figure 31 and Figure 32 respectively, the solid line is the mean). They show little variation between different images from the same slide. For the analysis presented in Chapter 8, at least three images were captured from each slide.

Figure 31: Area analysis of five images at magnification $\times 20$, Slide N1,5**Figure 32: Area analysis of six images at magnification $\times 40$, Slide N1,5**

The particle size distribution of the five slides created at exponentially increasing dilution (decreasing particle density) had fluctuating, but in general, decreasing proportion of fine particles (Figure 27). Image analysis for PSD in the least dense slide was only possible at the lowest magnification, when more particles were encountered due to the larger field of vision. This suggests that PSD by image analysis is sensitive to the density of the OM on the slide. This could be estimated by eye only (from the appearance of the suspension and slide), and efforts were made to maintain consistent slide density.

Figure 33: Effect of density of slide solution on particle size distribution

6.3 Conclusions and Summary

Organic matter in rocks includes a wide range of chemical compositions and physical structures. A method has been developed to isolate organic matter from geological samples, removing as much non-organic matter and retaining as much organic matter as possible. It was found, however, that a significant amount of organic matter was lost during the isolation process, and some original or neo-formed minerals remained in the sample. Loss of organic matter was probably exacerbated by the aim to remove all mineral matter. Elemental analysis was performed on isolated organic matter, for organic CHNOS, and inorganic elements to characterise remaining mineral matter. The stable carbon isotopic ratio was measured. Rock-Eval was applied to whole rock samples, to compare these results with those of elemental analysis of isolated OM. Optical analysis of smear slides of isolated organic matter included counting abundances of categories of organic matter, and was shown to be reasonably consistent at 300 points counted, and independent of the density of the slide. Image analysis was applied for particle size analysis.

Chemical and optical methods provide different information on OM: chemical analysis provides information on the bulk average composition of the OM but not on separate components; it provides no information on particle size or morphology. Techniques that can be applied to whole rock samples, such as Rock-Eval, do not suffer from the loss of

OM during isolation. Optical methods provide information on a size fraction limited by microscope resolution and maximum particle size for incorporation into microscope slides, and can only provide chemical information by inference. Used jointly, chemical and optical methods provide more comprehensive information and a fuller knowledge of sedimentary OM. The combination of both optical and geochemical methods is suggested to provide greatest information on the organic matter present in the rocks.

The results of organic matter isolation and analysis are presented in Chapters 7 and 8.

7. Organic matter geochemistry: results and discussion

7.1 Introduction

Organic matter (OM) was isolated from samples from cores of Glacial Till, Lincolnshire Limestone and from unconsolidated deposits underlying an industrial site (Site B), using the method described in Chapter 6. Isolated OM was made into slides for petrographic examination (Chapter 8) and dried residues for geochemical analysis (results in this chapter). Acid-insoluble carbon (AIC) between 0.01% and 2.9% has been measured in the Lincolnshire Limestone (Section 5.4) with between 0.035% and 1.5%, mean 0.3%, in the core from which samples were taken for OM isolation. Organic carbon content in limestone samples is increased when near marl bands; the marl and shale bands have much higher organic carbon content. Wide ranging AIC content has been measured in glacial tills from 0.03% to 0.95%, mean 0.25%, in North Sea Drift and from 0.1% to 1%, mean 0.5%, in Lowestoft Till (Section 5.6). Oxidised (weathered) glacial till has a reduced organic carbon content. Lower organic carbon content may be due to greater flow of oxidising water, or due to depositional differences. Samples selected from Site B cover a wide variety of material types, including made ground, and have material-dependent AIC concentrations which range from 0.01% to 27% (section 5.5.2). For each of these formations, many samples have sufficient total organic carbon content to suggest that those materials provide potentially significant sorbents.

In this chapter, the efficiency of the OM isolation is discussed (Section 7.2) together with the factors controlling the efficiency. Results of the elemental analysis of the isolated OM are presented and discussed (Section 7.3) and stable carbon isotope results are presented (Section 7.4). Results of Rock-Eval pyrolysis of whole rock samples (Section 7.6) are compared with directly analysed elemental ratios. Limitations of these methods are reviewed.

7.2 Isolation of organic matter

The carbon content of float and sink fractions of isolated OM are presented in Table 23 together with the percentage of the whole-rock AIC recovered in the float and sink fractions (summarised in Table 24).

Carbon contents between 47% and 59% in the glacial till floats suggest that the isolated OM is contaminated with little mineral matter. Isolation of OM from Lincolnshire

Chapter 7: Geochemistry Results and Discussion

Limestone (carbon content between 8.6% and 65%) and Site B samples (carbon content between 0.2% and 76%) was less consistently successful.

Little of the original OM is entrained in the sink fractions (under 5.2% of the original OM, arithmetic mean 2.8%), indicating that most non-recovered OM is lost during decanting as suspended or dissolved material. The low carbon content of the sink fractions (total carbon content under 6%, arithmetic mean 1.7%) indicates that the heavy liquid separation was an efficient purification stage, removing non-organic material without much loss of organic matter.

Table 23: Isolation of organic matter

Sample	original whole rock sample Description or suggested member	original whole rock sample		'float' residue			'sink' residue			Total AIC
		AIC %	Mass used g	TC %	Mass g	AIC % recovered	TC %	Mass g	AIC % recovered	
NTY1	sandy clayey SILT	0.46	49.935	51.5	0.13	29	1.37	0.200	1.7	31
NTY2	sandy silty CLAY	0.53	51.384	56.7	0.19	39	1.59	0.229	1.6	41
NTY3	silty CLAY	0.40	50.359	58.8	0.20	60	1.92	0.270	1.9	62
NTY4	very silty fine SAND	0.47	49.998	58.0	0.15	36	1.99	0.272	2.7	39
NTY5	silty fine SAND	0.28	49.538	57.5	0.16	68	1.32	0.297	1.7	70
NTY6	very silty fine SAND	0.27	50.856	56.0	0.14	57	2.48	0.266	4.8	62
NTY7	clayey SILT	0.94	50.853	46.0	0.17	17	1.86	0.184	2.5	20
NTY8	fine sandy SILT	0.34	49.988	51.2	0.19	57	1.72	0.248	0.90	58
NTY9	fine sandy silty CLAY	0.43	50.065	51.8	0.17	40	2.31	0.255	3.5	44
NTY10	fine sandy SILY	0.29	49.894	51.9	0.17	62	3.11	0.244	5.2	67
NTY11	clayey fine sandy SILT	0.30	50.879	50.2	0.19	62	1.76	0.299	3.4	65
NTY12	sandy very silty CLAY	0.33	48.923	55.1	0.19	64	1.63	0.301	3.2	67
GTL11	silty CLAY with gravel and straw fragments	0.20	50.122	48.46	0.15	75	1.25	0.376	4.7	79
GTL12		0.20	49.865	47.26	0.14	66	1.43	0.073	1.0	67
GTL81	dark grey CLAY with many chalk gravel	0.70	49.370	46.56	0.66	89	1.73	0.710	3.6	93
GTL82		0.70	49.553	54.04	0.73	113	1.83	0.717	3.8	117
L60.46-60.51	Overlying deposits	1.7	54.33	53.3	0.088	5.1	n.a.	n.a.	n.a.	5
L67.08-67.10	Sleaford Member	0.19	47.84	38.2	0.076	32	0.71	0.407	3.2	35
L67.54-67.56	Sleaford Member	0.20	42.76	14.2	0.222	36	2.43	0.335	9.4	46
L68.87-68.89	Sleaford Member	0.088	46.79	33.01	0.046	37	0.53	0.278	3.5	40
L68.97-68.99	Sleaford Member	0.10	42.878	25.80	0.033	19	0.56	0.530	6.8	28
L69.05-69.07	Blankney Member	0.079	53.733	22.3	0.063	33	0.06	0.406	0.54	34
L69.09-69.11	Blankney Member	0.056	67.605	15.4	0.070	28	0.37	0.077	0.75	29
L69.19-69.21	Blankney Member	0.086	43.162	36.93	0.008	8.0	0.76	0.241	4.9	13
L75.90-75.93	Metherington Member	2.0	43.631	31.5	0.522	19	2.74	5.673	18	37
L76.00-76.03	Lincoln Member	0.082	72.081	31.8	0.113	61	0.64	0.279	3.0	64
L79.35-79.37	Greetwell Member	0.084	67.388	n.d.	0.242	n.d.	2.41	2.356	100	100
L80.47-80.49	Greetwell Member	1.1	30.040	27.7	0.635	56	3.79	1.390	17	72
L81.50-81.525	Greetwell Member	0.10	51.339	8.64	0.089	14	0.87	1.092	16	32
L81.575-81.60	Greetwell Member	0.087	50.265	31.6	0.058	42	1.26	1.102	32	74
L82.17-82.19	Greetwell Member	0.21	43.240	60.25	0.030	20	1.42	2.066	33	53
L82.27-82.29	Greetwell Member	0.084	39.090	65.33	0.002	4.0	0.53	0.490	7.9	12
B 1.0m	made ground	13	57.216	75.54	7.24	72	4.2	2.819	1.6	73
B 2.0m	made ground	18	54.023	61.06	12.36	77	5.87	0.422	0.2	77
B 3m	made ground	1.1	59.879	47.93	1.37	104	5.94	0.415	3.9	108
B 6m	grey brown silty CLAY	0.98	59.140	41.34	1.07	77	1.43	0.861	2.1	79
B 11.3-11.4m	red brown sandy CLAY	0.088	55.170	47.88	0.11	104	1.17	0.216	5.2	109
B 12.8-13.25m	red brown silty SAND	0.089	52.025	6.18	0.11	14	0.466	0.246	2.5	17
B 13.5-13.95m	red brown sandy CLAY	0.060	57.119	11.98	0.08	26	0.574	0.204	3.5	30
B 15.1-15.8m	red brown sandy CLAY	0.011	59.505	25.88	0.12	480	1.48	0.189	43	523
B 17.5-17.95m	red brown silty SAND	0.041	55.910	3.27	0.08	11	0.149	0.728	4.6	16
B 20.7-21.15m	orange brown silty SAND	0.074	57.176	0.80	0.68	13	0.509	0.210	2.5	16
B 31.5m	orange brown silty SAND	0.028	58.497	0.22	0.06	0.66	0.15	0.104	1.0	1.8

NTY = North Sea Drift samples; GTL = Lowestoft Till samples

L = Lincolnshire Limestone samples; B = Site B samples; n.a. = not analysed (insufficient sample)

Mass of float residue includes an estimation of the amount removed to make slides.

Whole rock sample mass is the amount of sample used for OM isolation.

Table 24: Summary of recovery of carbon in isolated OM

	% recovery in float fractions			% recovery in float and sink		
	max.	mean	min.	max.	mean	min.
North Sea Drift	68%	49%	17%	70%	52%	20%
Lowestoft Till	113%	86%	66%	117%	89%	67%
Lincs. Limestone	60%	28%	5%	100%	42%	5%
Site B	104%	50%	0.8%	109%	53%	2%

It is likely that >100% recovery in Lowestoft Till and Site B samples is due to overestimation of the mass removed for slides, or to inaccuracies in measurement of acid-insoluble carbon (AIC) of the bulk sample, or of carbon content of the isolated OM.

Problems with isolating OM, using techniques such as that used in this work, lead to impure OM isolates. HF reacts with some inorganic elements (for example, calcium) to form insoluble fluoride salts (e.g. CaF_2) which are hard to remove. Addition of HCl during HF treatment reduces the dissociation of HF (a weak acid). This keeps fluoride ion activity low, thereby inhibiting and minimising fluoride salt formation (Durand and Nicaise, 1980). Whelan and Thompson-Rizer (1993) state that *'it is nearly impossible to obtain a mineral-free kerogen concentrate due to acid-resistant minerals, neoformed minerals from HF complex fluorides ... and minerals protected by OM coating'*.

Pyrite (FeS_2) can be intimately mixed with organic matter, and its complete removal is a well-known problem. Pyrite contents of up to 70% (mean 18%) in isolated kerogen¹⁹ have been reported (Durand and Monin, 1980). Pyrite may be removed by heavy liquid separation, or destruction by oxidising or reducing agents (Durand and Nicaise, 1980). However, heavy liquid separation can fractionate OM due to density differences, and may not completely remove pyrite. Chemical destruction of pyrite causes concurrent alteration of OM. In addition to residual pyrite, heavy oxides, sulphates and some silicates may remain; they have been reported to comprise up to 30% of isolated kerogen, with a mean of 5% (Durand and Monin, 1980). Minerals are sometimes protected from HF attack by OM coating. Some residues can interfere with OM geochemical analysis.

Whilst the HCl / HF preparation is widely used to concentrate and purify OM, it may alter the chemical or physical nature of the OM (Robl and Davis, 1993; Whelan and Thompson-Rizer, 1993). HCl, a strong acid, may hydrolyze the OM (as may HF to a lesser degree). Chlorine and fluorine may be incorporated into treated samples by halogenation reactions (Robl and Davis, 1993, Durand and Nicaise, 1980). Immature OM is the most susceptible to chemical alteration.

¹⁹ Kerogen is defined in Section 6.2.1 as organic matter remaining after treatment with both organic solvents and HCl and HF (Whelan and Thompson-Rizer, 1993; Senftle *et al.*, 1993).

It was found during this study that some OM in some samples was not recovered from the isolation procedure (Table 23 and Table 24). HCl / HF will dissolve some organic matter (such as sugars and amino acids) which will be removed in the decanting stage (Lichtfouse, pers. comm., 1999). Loss during decanting the supernatant from the samples was minimised in this study by pipetting rather than pouring (Wood *et al.*, 1996). The loss of organic matter dissolved in acids is thought to be less significant than loss of suspended OM during decanting (Bissada, pers. comm., 1999). Loss of OM suspended in decanted liquid may cause elemental fractionation, as the lighter, H-rich fraction which settles slowest is lost. It has been suggested that '*many problems with kerogen isolation relate to the lack of a standard procedure ... the methods employed ... vary significantly ... [with the result that] kerogen varied significantly*' (Senfle *et al.*, 1993).

7.3 Elemental content of isolated organic matter

An indication of the elemental ranges that may be found in OM is provided in Table 25. Ranges for isolated kerogen have been calculated assuming kerogen consists of CHNOS only. Humic and fulvic acids components are defined operationally as the fractions that dissolve in alkali, with humic acids being re-precipitated by acidification and fulvic acids remaining in solution.

Table 25: Elemental composition of kerogen, humic acid and fulvic acid

	kerogen			humic acid		fulvic acid	
	min. %	mean %	max. %	min. %	max. %	min. %	max. %
C	59.1	76.4	92.8	53.6	58.7	40.7	50.6
H	1.5	6.3	14.1	3.2	6.2	3.8	7.0
O	1.2	11.1	29.5	32.8	38.3	39.7	49.8
S org.	0	3.65	12.3	0.1	1.5	0.1	3.6
N	1.23	2.02	3.8	0.8	5.5	0.9	3.3

Kerogen composition after Durand and Monin (1980)

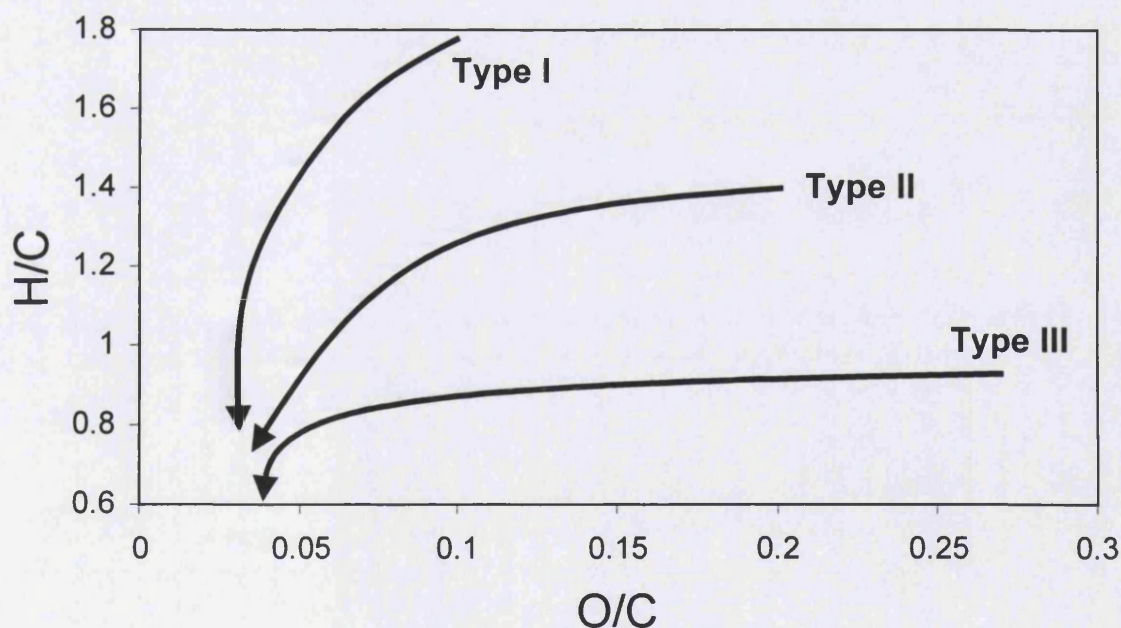
Humic acid and fulvic acid composition after Killops and Killops (1993)

For every 1000 C atoms in kerogen there are ~ 500 to 1800 H, ~ 25 to 300 O, ~ 5 to 30 S and ~ 10 to 35 N (Killops and Killops, 1993). The high sulphur content in kerogen,

compared to living organisms, may be due to the incorporation of inorganic sulphur into OM during diagenesis (Durand and Monin, 1980). Humic and fulvic acids both show low H/C, with both H/C and O/C lower in humic acid. Fulvic acid is more soluble as it contains more polar functional groups. Coal contains 1-2% N and generally <1% S. The C content increases with increasing coalification from ~55% in peats up to 100% in anthracites (Killops and Killops, 1993).

Van Krevelen diagrams are used to categorise OM components (kerogen or coal) on the basis of O/C and H/C atomic ratios. Such plots aid the identification of OM origin and illustrate geochemical evolution paths. Oxidative weathering causes a large increase in O/C and slight decrease in H/C. Kerogen typically forms most of the OM in a material, and therefore generally plots at a very similar location as the whole OM from the same sample. Three types of kerogen are defined on the van Krevelen diagram (Figure 34); type IV is not illustrated.

Figure 34: Van Krevelen diagram of kerogen types



based on Killops and Killops, 1993; Tyson 1995; Binger *et al.*, 1999

The following information on kerogen types is from Tyson (1995) and Killops and Killops (1993). Type I kerogen is rare, with initially high H/C (1.5-1.8) and low O/C

(generally <0.1). Type II, the most common, is usually formed in reducing conditions in marine environments, but may also be produced from concentrated transported plant material. It has relatively high H/C (1.0-1.3) and low O/C. It often contains substantial S; where organic S is 8-14% and organic S/C > 0.04 it may be referred to as type II-S. Type III is derived from continental plants and contains much identifiable plant debris and amorphous matter. It has relatively low initial H/C (<1.0) and high initial O/C (up to 0.2 or 0.3). Type IV is mainly wood and opaque coal debris, probably higher plant material oxidised on land and transported to its deposition location. It has an initial H/C <0.8 and O/C generally 0.2-0.3. Thermal evolution of kerogen can be tracked on the van Krevelen diagram (Figure 34) in reducing H/C and O/C as first CO_2 and H_2O are eliminated, then fuel hydrocarbons produced. The typing of kerogen, or other OM components, in this way ignores and disguises the fact that OM in any sample is a mix of organic components with differing composition and, possibly, different origins.

The carbon, hydrogen, nitrogen, oxygen and sulphur content of organic matter isolated in this study are listed in Table 26. The percentage of each sample that is accounted for by these elements is also given, as are the atomic S/C, O/C, H/C and H/O ratios.

Carbon content measured by the LECO[®] analyser for North Sea Drift samples is a mean of 3.8% relative lower than that measured by the Carlo-Erber analyser; that for the Lowestoft Till samples is 0.9% higher. This is likely to be due to variations in equipment calibration and is within the relative 5% variation between duplicates (Section 3.4.1). Differences between carbon content measured by LECO[®] analyser and Carlo-Erber analyser for the other samples were not consistently different.

Isolated OM from both North Sea Drift and Lowestoft Till samples show much lower organic sulphur / carbon ratios and organic sulphur content for the uppermost samples (S_{org}/C 0.06, S_{org} between 1.0% and 1.2%) than for samples from greater depth (S_{org}/C between 0.28 and 0.33, S_{org} 5.7%). As observed in Section 4.4, oxidative weathering in the Lowestoft Till removes both sulphur and organic carbon from the samples. Both organic sulphur (Table 26) and inorganic sulphur (Table 27) have been removed by weathering. The S content of these samples is within the range typical of kerogens (Table

25). S generally constitutes a lower proportion of fulvic and humic acids (Killops and Killops, 1993) than kerogen. S/C ratio of the Lincolnshire Limestone OM samples was relatively high, mostly above 0.26. No clear trend with depth was observed. S/C ratio of samples from Site B was generally low, under 0.03, except for grey silty samples from 3m bgl and 6 m bgl which had S/C ratios of 0.10 and 0.34 respectively.

Atomic H/C ratios mainly between 1.0 and 1.1 for North Sea Drift, and 1.0 and 1.2 for Lowestoft Till, indicate that the glacial till OM could be classified as Type II. Unweathered samples with high S content fall into the sub-classification Type II-S. Much of the glacial till material is reworked Kimmeridgian Clay, which was deposited in anoxic marine conditions, typical for production of Type II kerogen. However, the atomic O/C ratios (typically 0.2 to 0.3) are higher than would be expected for Type II samples: this may be due to re-incorporation of O during OM reworking prior to inclusion in the glacial sediments, or due to subsequent weathering. Atomic H/C ratios of up to 1.8, and O/C ratios of over 0.15 in Lincolnshire Limestone samples suggest classifications of Type II or Type III. O/C and H/C ratios from Site B samples are highly varied.

Table 26: Elemental analysis of isolated organic matter

sample	depth m bgl	C (LECO) %	C (CE) %	H %	N %	S org %	O %	CHNOSorg total %	atomic S/C	atomic H/O	atomic O/C	atomic H/C
NTY1	2	51.5	54.3	4.72	2.53	1.27	23.64	86.5	0.06	3.20	0.33	1.04
NTY2	3	56.7	59.3	4.99	1.76	1.90	18.09	86.0	0.09	4.42	0.23	1.01
NTY3	4	58.6	61.0	5.64	1.60	5.54	13.09	86.9	0.24	6.89	0.16	1.11
NTY4	5	58.0	59.4	5.34	1.50	5.92	14.18	86.4	0.27	6.03	0.18	1.08
NTY5	6	57.5	59.7	5.18	1.53	5.77	14.66	86.8	0.26	5.65	0.18	1.04
NTY6	7	56.0	57.7	2.19	1.47	6.55	16.13	84.0	0.30	2.17	0.21	0.46
NTY7	9	48.0	50.3	4.61	1.53	6.61	16.59	79.7	0.35	4.45	0.25	1.10
NTY8	11	51.2	54.1	4.63	1.62	7.26	18.95	86.5	0.36	3.91	0.26	1.03
NTY9	13	51.8	53.9	4.36	1.48	5.27	18.29	83.3	0.26	3.82	0.25	0.97
NTY10	15	51.9	53.1	4.46	1.51	6.79	17.31	83.2	0.34	4.13	0.24	1.01
NTY11	17	50.2	53.1	4.58	1.55	7.45	18.49	85.2	0.38	3.97	0.26	1.04
NTY12	19	55.1	55.5	4.63	1.54	5.23	17.76	84.6	0.25	4.18	0.24	1.00
GTL11	1.5-2.0	49.9	48.46	3.99	2.08	1.18	20.69	76.4	0.06	3.08	0.32	0.99
GTL12	1.5-2.0	46.6	47.26	3.81	2.06	0.98	20.02	74.1	0.06	3.04	0.32	0.97
GTL81	8.5-9.0	46.8	46.56	4.67	1.21	5.72	12.79	70.9	0.33	5.84	0.21	1.20
GTL82	8.5-9.0	54.8	54.04	5.30	1.44	5.68	11.62	78.1	0.28	7.30	0.16	1.18
L60.48-60.51	60.48-60.51	30.39	12.46	1.05	0.45	1.23	20.88	36.1	0.26	0.81	1.26	1.01
L62.02-62.05	62.02-62.05	n.a.	43.58	3.07	2.84	5.44	16.57	71.5	0.33	2.97	0.29	0.85
L67.08-67.10	67.08-67.10	38.2	38.75	3.54	1.25	3.66	17.02	64.2	0.25	3.33	0.33	1.10
L67.54-67.56	67.54-67.56	14.2	15.18	0.83	0.48	12.46	7.87	36.8	2.20	1.68	0.39	0.65
L68.87-68.89	68.87-68.89	n.a.	33.01	3.23	1.47	1.46	18.13	57.3	0.12	2.85	0.41	1.17
L68.97-68.99	68.97-68.99	n.a.	25.80	2.61	1.10	0.04	17.89	47.4	0.00	2.33	0.52	1.21
L69.05-69.07	69.05-69.07	22.3	22.19	2.25	0.82	1.96	18.60	45.8	0.24	1.94	0.63	1.22
L69.09-69.11	69.09-69.11	15.4	15.08	1.91	0.57	1.39	21.87	40.8	0.25	1.40	1.09	1.52
L69.19-69.21	69.19-69.21	n.a.	36.93	3.64	1.44	i.s.	13.53	55.6	n.a.	4.31	0.27	1.18
L75.90-75.93	75.90-75.93	31.5	32.84	2.92	0.86	2.97	18.33	57.9	0.24	2.55	0.42	1.07
L76.00-76.03	76.00-76.03	31.8	38.04	3.08	1.22	7.10	14.29	63.7	0.50	3.45	0.28	0.97
L79.35-79.37	79.35-79.37	n.a.	n.d.	0.70	0.31	i.s.	n.a.	1.0	n.a.	n.a.	n.a.	n.a.
L80.47-80.49	80.47-80.49	27.7	29.35	2.61	0.78	2.23	17.87	52.8	0.20	2.34	0.46	1.07
L81.50-81.525	81.50-81.525	8.64	8.06	1.25	0.27	3.82	19.71	33.1	1.27	1.01	1.83	1.86
L81.575-81.60	81.575-81.60	31.6	30.34	2.68	1.08	16.70	9.87	60.7	1.47	4.35	0.24	1.06
L82.17-82.19	82.17-82.19	n.a.	60.52	3.59	1.35	2.69	12.39	80.5	0.12	4.63	0.15	0.71
L82.27-82.29	82.27-82.29	n.a.	65.33	3.09	1.37	i.s.	n.a.	69.8	n.a.	n.a.	n.a.	0.57
B1	1	78.5	75.54	1.08	1.56	0.81	11.75	90.7	0.03	1.47	0.12	0.17
B2	2	62.35	61.06	0.92	1.35	0.49	12.39	76.2	0.02	1.19	0.15	0.18
B3	3	49.4	47.93	3.26	1.79	1.72	21.18	75.9	0.10	2.46	0.33	0.82
B6	6	41.2	41.34	3.59	1.81	5.19	21.98	73.9	0.34	2.61	0.40	1.04
B11	11	47.7	47.88	2.99	1.18	0.29	18.41	70.7	0.02	2.60	0.29	0.75
B12	12.8-13.25	n.a.	6.18	0.88	0.11	n.d.	17.05	24.2	n.d.	0.82	2.07	1.70
B13	13.25-13.95	n.a.	11.98	1.45	0.19	n.d.	13.84	27.4	n.d.	1.67	0.87	1.45
B15	15.1-15.8	n.a.	25.88	2.09	0.55	0.24	18.98	47.7	0.02	1.76	0.55	0.97
B17	17.5-17.95	n.a.	3.27	0.82	0.08	n.d.	8.53	12.7	n.d.	1.54	1.95	3.00
B20	20	0.774	0.80	0.81	0.02	n.d.	6.13	7.8	n.d.	2.13	5.72	12.17
B31	31.5	n.a.	0.14	0.62	0.02	n.d.	5.37	6.1	n.d.	1.86	29.23	54.40
B31A	31.500	n.a.	28.49	2.16	0.97	n.a.	n.a.	31.6	n.a.	n.a.	n.a.	0.91

NTY = North Sea Drift samples; GTL = Lowestoft Till samples

L = Lincolnshire Limestone samples; B = Site B samples;

n.d. = not detected. Detection limit 0.5% using Carlo-Erber

n.a. = not analysed (insufficient sample)

Bold indicates the mean of two analyses

Between 80% and 87% of the OM isolated from North Sea Drift samples, and 70% to 78% from Lowestoft Till is accounted for by its CHNOS_{org} content. This confirms reasonable success in OM isolation. Between 33% and 81% of the OM isolated from Lincolnshire Limestone samples, and 6% to 91% of the OM isolated from Site B samples is accounted for by its CHNOS_{org} content, indicating reasonably successful OM isolation

for some of these samples and less success for others. The analysis results of the residual mineral content are presented and discussed in Section 7.4. Some of the oxygen may be associated with mineral matter rather than organic molecules.

As described in Section 7.2, several problems introduced by the OM isolation may interfere with elemental analysis of the OM. Heterogeneous samples, with relatively large particles from made ground samples, required careful crushing and homogenisation prior to analysis of as large a sub-sample as acceptable for the analysis technique. Residual minerals may interfere with the analysis results. Pyrite and marcasite (both FeS_2) contribute to sulphur (S) analysis; S from pyrite and marcasite was accounted for in this study by analysing for iron (Fe). Pyrite and marcasite may oxidise in the presence of water to form hydrated iron oxides or sulphates, thus contributing to the O content; this can be avoided by using platinum or silver analysis vessels. Iron may form oxides with oxygen from the OM, leading to an under-measurement of O, which can be avoided by the use of specifically designed apparatus. Heavy oxides and silicates are very stable and may not contribute to the analysis results (Durand and Monin, 1980). Heavy sulphates may contribute to S and O content. Fluoride minerals formed during kerogen isolation contain water of constitution so will contribute O and H. Estimation of O by ‘the difference method’, as the remainder after CHNS analysis, is considered inadequate (Durand and Monin, 1980), especially in kerogen with high ash content, and so has been analysed directly; the identification of significant mineral component in these isolated OM samples confirmed the necessity of this.

7.4 Inorganic content of isolated organic matter

The major and minor elemental geochemistry of the isolated OM residues analysed using the methods detailed in Section 6.2.2 is presented as Table 27. Inorganic sulphur content has been calculated assuming that all Fe present is as FeS_2 ²⁰, and the difference between measured total sulphur and calculated inorganic sulphur taken to be organic sulphur (included in Table 26). In addition, P and Mn were analysed, but not detected at above the detection level of 0.01%. The inorganic analysis results show low Si and Al in most cases (Si usually below 2%, Al usually below 1%) indicating that little silicate materials (such

²⁰ Iron-sulphides may be present in other proportions, such as FeS or FeS_{1-2} .

Chapter 7: Geochemistry Results and Discussion

as quartz and clay) survive the isolation procedure. Higher Fe content (up to 25%, average 3%) indicates significant pyrite survives the isolation process. Difficulties with removing pyrite are detailed in Section 7.2. Sulphur content of isolated organic matter cannot be assumed to be organic, without iron analysis to correct for the inorganic sulphur. Barium, strontium and zinc content suggest the presence of barite, which has very low solubility. Titanium and zircon suggest the presence of remaining heavy minerals.

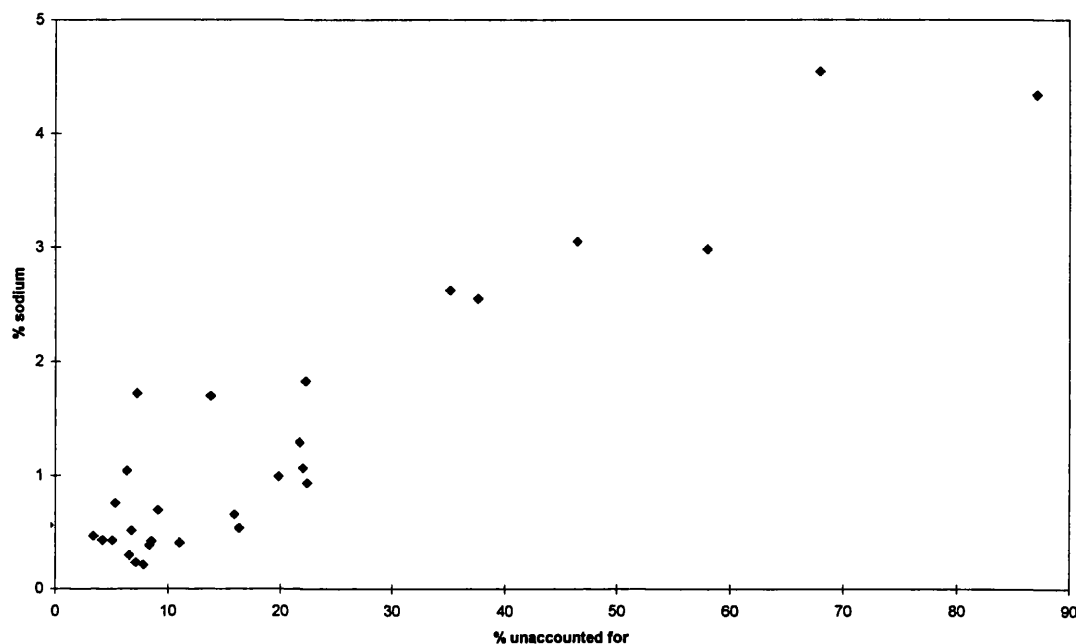
Where there was sufficient sample for all the analyses undertaken, the total organic content (C, H, N, O, S_{org}) and the total inorganic content together account for between 13% and 100% (arithmetic mean 79%) of the whole. The % material unaccounted-for is approximately proportional to the sodium content (Figure 35). It is therefore considered to be largely sodium salts, residual from the sodium polytungsten heavy liquid, despite the washing procedure following density separation. It was impossible to achieve 100% removal of the heavy liquid from the samples, as the settled material was easily disturbed when decanting the supernatant, and at low ionic strengths lack of flocculation of the suspension prevented settling. This problem may be minimised by using an ionic solution (such as NaCl_(aq)) for the final washes when removing the heavy liquid. For every 1wt% Na, there is between 4.2% and 36.8% unaccounted-for mass (mean 16.9%). Sodium polytungsten (chemical formula Na₆(H₂W₁₂O₄₀).H₂O) contains Na and W in the proportions 1:16 by weight, suggesting that much of the unaccounted-for mass may be tungsten. Analysis for tungsten content was not available.

Table 27: Inorganic geochemistry of isolated OM residues

n.d. = not detected (detection limit for n.d. S was 0.5%, see Section 6.2.2; for Mg 0.01%;
for other elements 1ppm)

i.s. = insufficient sample for analysis

	Si	Al	Fe	Mg	Ca	Na	K	Ti	Ba	Co	Cr	Cu	Li	Ni	Sc	Sr	V	Y	Zn	Zr	S total	S inorg	S org	inorganic total %	organic total %	inorg+org total %	
	NTY1	0.77	0.59	0.28	n.d.	0.08	0.69	0.07	1.44	1190	18	76	76	67	31	4	53	27	36	379	160	1.8	0.32	1.27	4.45	86.46	90.91
	NTY2	7.64	0.24	0.16	0.01	0.08	0.47	0.09	1.59	431	21	64	39	18	40	4	26	30	29	417	217	2.1	0.18	1.90	10.59	86.04	96.63
	NTY3	0.64	0.41	1.65	0.01	0.16	0.30	0.05	1.35	202	22	66	50	23	72	3	44	24	30	195	211	7.4	1.90	5.54	6.57	86.90	100.61
	NTY4	5.07	0.85	2.93	0.02	0.18	0.56	0.08	1.02	627	19	69	63	47	104	3	76	25	22	347	186	9.3	3.37	5.92	14.24	86.38	93.47
	NTY5	0.82	0.71	2.48	0.01	0.17	0.43	0.08	0.50	341	12	60	58	34	75	2	46	16	16	246	79	8.6	2.86	5.77	8.16	86.84	95.01
	NTY6	0.71	0.28	2.16	0.00	0.17	1.72	0.30	0.63	1320	16	53	69	57	77	n.d.	53	16	16	1007	108	9.0	2.48	6.55	8.74	84.05	92.79
	NTY7	1.16	0.25	3.90	0.01	0.13	0.38	0.05	1.54	264	34	79	167	27	106	3	34	34	21	204	170	11.1	4.49	6.61	12.02	79.68	91.70
	NTY8	0.43	0.64	2.90	0.02	0.16	0.43	0.07	1.22	245	28	90	80	22	67	3	53	27	18	242	194	10.6	3.34	7.26	9.32	86.54	95.86
	NTY9	0.83	0.17	2.13	0.00	0.03	0.42	0.04	2.01	563	34	115	74	34	63	5	41	41	50	237	340	7.7	2.45	5.27	8.23	83.27	91.50
	NTY10	0.72	0.62	3.05	0.01	0.10	0.23	0.03	1.36	221	33	62	92	21	74	4	40	30	28	138	234	10.3	3.51	6.79	9.74	83.18	92.92
	NTY11	1.04	0.18	2.65	0.01	0.06	0.75	0.13	1.56	240	34	93	98	26	67	3	40	34	29	505	235	10.5	3.05	7.45	9.58	85.15	94.79
	NTY12	1.08	0.47	2.27	0.01	0.10	0.52	0.07	1.37	697	25	82	78	14	67	5	49	30	37	331	211	7.8	2.61	5.23	8.65	86.64	93.29
	GTL11	1.26	0.25	0.21	n.d.	0.06	0.65	0.09	4.70	1067	61	510	146	44	30	8	113	69	108	367	549	1.4	0.24	1.18	7.77	76.40	84.17
	GTL12	1.16	0.28	0.26	0.01	0.07	0.54	0.06	6.64	860	86	448	175	33	28	7	138	124	138	270	828	1.3	0.30	0.98	9.63	74.13	83.76
	GTL81	0.34	0.15	2.02	n.d.	0.03	0.93	0.03	0.78	240	15	44	91	3	78	n.d.	34	15	9	160	88	8.0	2.32	5.72	6.69	70.94	77.63
	GTL82	3.10	0.18	2.70	n.d.	0.04	0.40	0.00	1.31	397	23	56	103	4	87	n.d.	43	25	14	35	163	8.8	3.10	5.68	10.93	78.08	88.02
	L60.48-60.51	1.32	0.09	0.60	n.d.	0.07	2.98	0.05	0.05	396	1	19	22	21	47	n.d.	16	7	4	187	22	1.93	0.69	1.23	5.94	36.09	42.02
	L62.02-62.05	i.s.	0.31	0.89	n.d.	0.05	0.46	0.03	4.01	564	51	484	113	55	29	18	76	69	335	317	1077	8.46	1.02	5.44	7.10	71.49	78.59
	L67.08-67.10	i.s.	0.48	2.32	n.d.	0.07	2.91	0.17	0.08	13454	0	60	60	20	70	n.d.	76	10	10	1004	205	6.33	2.67	3.66	10.14	64.23	74.37
	L68.54-67.56	0.93	0.10	24.98	0.03	0.92	1.04	0.08	0.03	85	3	24	29	20	56	n.d.	16	17	4	295	36	41.2	28.74	12.46	56.88	36.81	93.70
	L68.67-68.69	i.s.	0.17	6.82	n.d.	0.19	2.03	0.15	0.11	1034	n.d.	45	40	63	49	n.d.	36	n.d.	4	598	27	9.31	7.85	1.46	17.51	57.30	74.80
	L68.97-68.99	i.s.	0.30	8.29	n.d.	0.22	2.99	0.21	0.04	1542	n.d.	44	31	88	50	n.d.	57	6	6	944	25	7.28	7.24	0.04	17.57	47.44	65.02
	L69.05-69.07	i.s.	0.54	6.71	n.d.	0.24	4.69	0.37	0.00	1930	n.d.	68	45	158	90	n.d.	90	n.d.	11	1828	11	9.68	7.72	1.96	20.69	45.83	66.52
	L69.09-69.11	i.s.	0.21	2.22	n.d.	0.29	4.32	0.30	0.02	1577	n.d.	24	24	52	40	n.d.	44	n.d.	4	1063	8	3.94	2.55	1.39	10.19	40.82	51.01
	L69.19-69.21	i.s.	i.s.	i.s.	i.s.	i.s.	i.s.	i.s.	i.s.	i.s.	i.s.	i.s.	i.s.	i.s.	i.s.	i.s.	i.s.	i.s.	i.s.	i.s.	i.s.	i.s.	i.s.	i.s.	55.55	55.55	
	L75.90-75.93	0.46	1.07	0.60	0.42	0.52	2.62	0.10	0.45	252	4	37	15	15	24	2	69	20	11	116	88	3.66	0.69	2.97	6.99	57.93	64.92
	L76.00-76.03	0.94	0.12	8.95	n.d.	0.25	1.70	0.10	0.09	463	n.d.	28	56	44	59	n.d.	25	6	3	391	13	17.4	10.30	7.10	22.55	63.72	86.27
	L79.35-79.37	i.s.	i.s.	i.s.	i.s.	i.s.	i.s.	i.s.	i.s.	i.s.	i.s.	i.s.	i.s.	i.s.	i.s.	i.s.	i.s.	i.s.	i.s.	i.s.	i.s.	i.s.	i.s.	i.s.	55.55	55.55	
	L80.47-80.49	0.38	1.68	1.24	1.33	0.62	2.55	0.15	0.18	296	3	37	18	9	20	2	83	5	8	178	31	3.65	1.42	2.23	9.61	52.83	62.44
	L81.50-81.525	i.s.	0.10	1.84	n.d.	0.04	3.30	0.06	0.12	484	2	22	20	27	20	n.d.	20	5	2	347	22	5.94	2.12	3.82	7.67	33.11	40.78
	L81.575-81.60	i.s.	0.37	15.04	n.d.	0.43	1.82	0.18	0.69	964	27	38	87	78	120	n.d.	54	33	11	1078	87	34	17.30	16.70	36.08	60.67	96.75
	L82.17-82.19	i.s.	0.30	2.72	n.d.	0.12	2.59	0.20	0.39	2285	n.d.	49	32	113	57	n.d.	89	8	8	1428	65	5.82	3.13	2.69	9.85	80.55	90.40
	L82.27-82.29	i.s.	i.s.	i.s.	i.s.	i.s.	i.s.	i.s.	i.s.	i.s.	i.s.	i.s.	i.s.	i.s.	i.s.	i.s.	i.s.	i.s.	i.s.	i.s.	i.s.	i.s.	i.s.	i.s.	69.78	69.78	
	B 1.0m	0.33	0.13	0.08	n.d.	0.55	0.21	0.02	0.01	53	n.d.	264	17	2	12	1	17	3	2	15	4	0.90	0.09	0.81	1.46	90.74	92.20
	B 3.20m	0.34	0.12	0.07	n.d.	0.03	1.29	0.07	0.01	296	2	311	37	3	21	1	18	2	3	143	5	5.57	0.08	0.49	2.10	76.20	78.30
	B 9.3m	0.68	0.08	0.04	n.d.	0.06	1.07	0.03	0.08	163	3	216	31	3	23	n.d.	10	3	4	13	47	1.76	0.04	1.72	2.12	75.88	78.09
	B 8m	0.75	0.12	1.88	0.83	0.05	0.99	0.04	0.18	244	7	40	85	3	31	n.d.	15	6	9	137	55	7.36	2.17	5.19	6.28	73.91	80.19
	B 11.3-11.4m	1.35	1.95	0.30	0.07	0.40	1.82	0.20	0.33	1027	4	115	56	63	36	4	151	12	12	535	190	0.84	0.35	0.29	7.00	70.75	77.75
	B 12.8-13.25m	1.74	0.42	0.15	0.02	0.26	4.55	0.21	0.09	1362	n.d.	40	25	65	38	n.d.	43	4	4	537	29	n.d.	0.17	n.d.	7.82	24.21	32.03
	B 13.5-13.95m	1.76	2.72	0.48	0.21	1.71	9.91	1.42	0.41	10925	n.d.	205	68	514	68	n.d.	342	34	34	3870	137	n.d.	0.55	n.d.	20.79	27.44	48.23
	B 15.1-15.8m	1.50	0.17	0.16	0.02	0.22	3.05	0.21	0.08	1614	3	76	53	40	28	n.d.	28	5	5	641	66	0.42	0.18	0.24	5.64	47.74	53.57
	B 17.5-17.95m	i.s.	1.35	0.11	0.05	0.43	4.35	0.17	0.19	1179	3	45	16	42	10	3	63	5	8	547	52	n.d.	0.13	n.d.	6.97	12.70	19.67
	B 20.7-21.15m	0.64	0.11	n.d.	n.d.	0.04	4.34	0.01	0.03	32	n.d.	11	2	3	1	n.d.	6	n.d.	2	5	9	0.01	n.d.	n.d.	5.17	7.76	12.94
	B 31.5m	i.s.	0.52	0.12	0.03	0.55	4.87	0.21	0.03	1688	n.d.	26	9	68	9	n.d.	47	n.d.	n.d.	622	9	n.d.	0.14	n.d.	6.71	6.15	12.85

Figure 35: Correlation between sodium content and residue unaccounted-for

7.5 Stable carbon-isotope content of isolated organic matter

The stable carbon-isotope composition of kerogen depends on the isotopic composition of its biological precursors and any isotopic fractionation processes during formation and chemical evolution. Stable carbon-isotope analysis is widely used to determine the source of OM in Recent sediments (Tyson, 1995), particularly relative proportions of phytoplanktonic and terrestrial C. Carbon-isotope analyses are presented in δ notation relative to an international standard, PDB.

$$\delta^{13}\text{C} = \left(\frac{{}^{13}\text{C}_{\text{sample}}}{{}^{13}\text{C}_{\text{standard}}} - 1 \right) \times 1000$$

Different carbon reservoirs have different isotopic signatures. Biological favouring of the lighter isotope is preserved in sedimentary OM ($\delta^{13}\text{C} \sim -26\text{‰}$) (Killops and Killops, 1993). Proportions of inputs from terrestrial and marine sources are calculated as the product of mixing two end-members, typically with 5-9‰ enrichment in terrestrial plants for modern mid to low latitude OM. Care is required in selection of end-member values from published sources, as each end-member shows a range of about 4‰ or more, and will be affected by geographical variations. Recent marine sediments have $\delta^{13}\text{C}$ about -25‰, and kerogen has $\delta^{13}\text{C}$ about -27.5‰ due to the preferential loss of lighter CO_2

(Hoefs, 1997). The difference in $\delta^{13}\text{C}$ between terrestrial and marine plants is less marked in kerogen: that from terrestrial sources usually has $\delta^{13}\text{C}$ only 3-5‰ lower than that from marine organisms (Killops and Killops, 1993; Tyson, 1995). $\delta^{13}\text{C}$ is also affected by many biological, productivity and environmental impacts, and diagenetic alteration can cause $\delta^{13}\text{C}$ shifts of a few ‰ (Hoefs, 1997). The $\delta^{13}\text{C}$ measured in these samples is presented in Table 28.

Table 28: Stable carbon isotope results

Glacial Till samples			Lincolnshire Limestone samples			Site B samples		
Sample	$\delta^{13}\text{C}$ (‰)	% C	Sample	$\delta^{13}\text{C}$ (‰)	% C	Sample	$\delta^{13}\text{C}$ (‰)	% C
NTY1	-26.5	55.4	L60.48-60.51	-24.3	13.5	B1W1-1	-22.8	79.3
NTY2	-25.8	59.3	L62.02-62.05	-23.6	47.2	B2	-22.7	53.2
NTY3	-25.0	68.6	L67.08-67.10	-24.7	40.7	B3	-24.9	57.1
NTY4	-24.8	74.6	L67.54-67.56	-24.9	15.2	B6	-26.2	45.7
NTY5	-24.8	61.3	L68.87-68.89	-25.1	32.2	B11	-24.1	47.9
NTY6	-25.1	64.5	L68.97-68.99	-24.8	26.0	B12	-23.9	6.27
NTY7	-25.3	52.9	L69.05-69.07	-24.9	23.8	B13	-24.1	12.2
NTY8	-25.7	56.7	L69.09-69.11	-24.7	15.7	B15	-24.6	21.3
NTY9	-25.5	56.0	L69.19-69.21	-25.1	49.1	B17	-24.1	3.38
NTY10	-25.5	54.7	L75.90-75.93	-27.4	41.8	B20	-25.1	0.42
NTY11	-25.6	57.6	L76.00-76.03	-26.5	38.5	B31	-26.4	0.19
NTY12	-25.5	58.0	L80.47-80.49	-26.4	26.2			
GTL11	-24.8	50.4	L81.50-81.525	-24.7	8.39			
GTL12	-24.5	49.9	L81.575-81.60	-24.6	34.2			
GTL81	-24.9	50.6	L82.17-82.19	-24.2	66.9			
GTL82	-25.3	57.7	L82.27-82.29	-24.2	69.1			

NTY = North Sea Drift samples; GTL = Lowestoft Till samples

L = Lincolnshire Limestone samples; B = Site B samples;

Bold indicates the mean of two analyses

These results show very uniform $\delta^{13}\text{C}$, between -24.5‰ and -26.5‰ in glacial till samples, with wider variation for Lincolnshire Limestone ($\delta^{13}\text{C}$ from -23.6‰ to -27.4‰) and Site B samples ($\delta^{13}\text{C}$ from -22.7‰ to -26.4‰). The carbon content measured by gas pressure during the carbon-isotope analysis (not presented) is typically a few percent higher than that from analysis by Carlo-Erber and LECO equipment, probably due to calibration variation.

7.6 Rock-Eval pyrolysis of whole rock samples

Except where otherwise indicated, the following description of Rock-Eval pyrolysis has been compiled from Whelan and Thompson-Rizer (1993), Tyson (1995) and Killops and Killops (1993).

Organic matter isolation and elemental analysis are time consuming, and mineral residues may interfere with O and H analyses. In the petroleum industry, elemental analysis of isolated OM for kerogen classification schemes has therefore largely been replaced by pyrolysis techniques. In theory, Rock-Eval pyrolysis rapidly determines parameters that correlate with OM H/C and (depending on the equipment) O/C ratios, thus providing information on its amount, type and thermal maturity (Peters, 1986). Rock-Eval is now being superseded by pyrolysis techniques that enable identification of individual products.

TOC is usually greater than the sum of S_1^{21} , S_2 and S_3 , as not all organic carbon present will be pyrolysable; for example a rock with abundant graphite will have high TOC but no pyrolysis response. A sample containing oxidised, mature material, predominantly recycled inertinite, may produce very low S_1 and no S_2 peaks (Peters, 1986). This was observed in made ground samples analysed during this study (Site B samples from 1m bgl, 2m bgl and 3m bgl).

S_2 , S_3 and total organic carbon (TOC) values give the 'hydrogen index' (HI) (S_2 /TOC, mg hydrocarbons / g TOC) and 'oxygen index' (OI) (S_3 /TOC). HI is considered proportional to the kerogen elemental H/C ratio, and OI considered sometimes proportional to the kerogen elemental O/C ratio. A plot of HI against OI can be analogous to the van Krevelen diagram, indicating organic matter type and maturity. However, some coals produce pyrolysis HI and OI values that do not correspond to their elemental H/C and O/C ratios (Peters, 1986). Reliable correlation of HI and OI to H/C and O/C is required for the pyrolysis technique to replace elemental analysis. Espitalié *et al.* (1977) found good correlations for both HI and OI to elemental H/C and O/C from pyrolysis of whole rock samples, indicating that the mineral matrix did not obscure the relation. Other researchers

²¹ S_1 , S_2 , S_3 and Tmax are operationally defined in Section 6.2.2.

Chapter 7: Geochemistry Results and Discussion

have found good correlations of H/C to HI for isolated kerogen and for whole rocks with TOC > 5%, and weaker correlations for whole rock samples with TOC <5% (Tyson, 1995 and references therein). Crossey *et al.* (1984) linked whole rock HI ($HI_{(bulk)}$) to the HI of the isolated extract ($HI_{(extract)}$) via the relation:

$$HI_{(extract)} = 1.077HI_{(bulk)} + 76.95 \quad (\text{correlation coefficient } 0.87)$$

and the HI of the isolated kerogen to the elemental H/C ratio via

$$H/C = 0.00073HI_{(extract)} + 0.541 \quad (\text{correlation coefficient } 0.92).$$

Tyson (1995) gives two formulae to link HI to H/C and O/C:

$$HI = 694(H/C - 0.29) - (800O/C), \text{ and } HI = 667H/C - 570O/C - 333.$$

Samples with low TOC (<0.5%) may produce low S_2 (and thus HI). Retention of hydrocarbons (HC) on clay minerals (such as smectite and illite) will lead to artificially low HI and elevated T_{max} . Instrumentation problems may produce inaccurate T_{max} for samples with S_2 <0.2 mg HC/g rock. HI determined on isolated kerogen has been reported to be 67 to 200% higher than HI determined on whole rock samples, especially where whole rock HI values are <200.

While it has been generally assumed that pyrolysis OI data are proportional to elemental O/C and can be reliably obtained from isolated kerogens and low-carbonate whole rocks, Whelan and Thompson-Rizer (1993) report no further corroboration of this beyond work by Espitalié *et al.* (1977). Tyson (1995) claims that OI is now regarded as unreliable. S_3 from whole rock samples can be affected by carbonate decomposition and may be elevated in rocks with TOC <2% and high carbonate. S_3 is also susceptible to instrumentation problems (Peters, 1986). To avoid using OI from problematical S_3 values, kerogen typing can be undertaken by plotting HI versus T_{max} .

The results of Rock-Eval analysis for the S_1 , S_2 and T_{max} components of whole rock samples are listed in Table 29 below. The hydrogen index (HI; S_2/TOC), AIC content, IC content and atomic H/C ratio are also presented.

A positive linear correlation exists between the H/C ratio of the isolated OM and the HI of the whole rock sample over a small range for North Sea Drift samples. This is extended and reinforced by the two Lowestoft Till samples (Figure 36).

Chapter 7: Geochemistry Results and Discussion

Table 29: Rock Eval analysis results

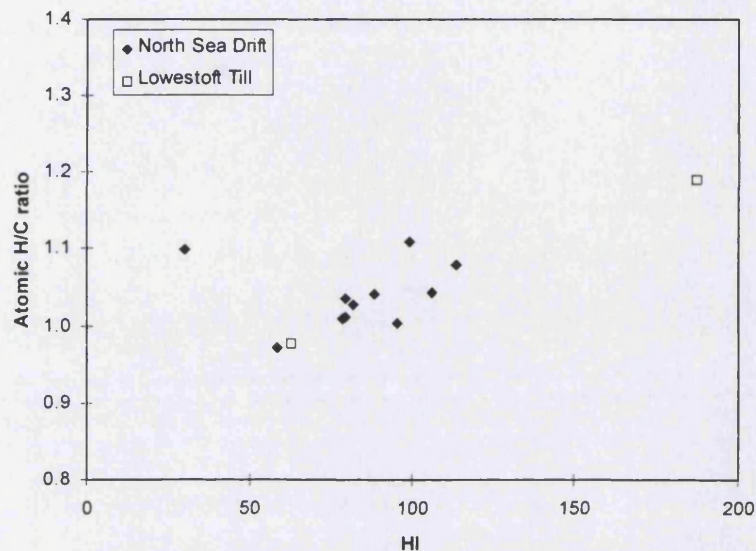
Sample	Depth m bgl	AIC %	IC %	S1 (mg/g)	S2 (mg/g)	Tmax (C)	HI (S2/TOC)	H/C atomic
NTY1	2	0.46	2.3	0.33	0.49	391	107	1.04
NTY2	3	0.526	2.6	0.17	0.42	416	80	1.01
NTY3	4	0.402	3.5	0.20	0.40	426	100	1.11
NTY4	5	0.465	2.8	0.25	0.53	424	114	1.08
NTY5	6	0.283	2.5	0.14	0.25	419	88	1.04
NTY6	7	0.273	3.0	0.30	0.44	419	161	0.46
NTY7	9	0.935	8.4	0.15	0.28	421	30	1.10
NTY8	11	0.341	2.2	0.16	0.28	416	82	1.03
NTY9	13	0.427	1.4	0.15	0.25	423	59	0.97
NTY10	15	0.293	1.9	0.18	0.23	401	78	1.01
NTY11	17	0.301	1.8	0.20	0.24	410	80	1.04
NTY12	19	0.325	2.0	0.24	0.31	402	95	1.00
GTL1.5-2	1.5-2.0	0.199	5.89	0.17	0.13	414	63	0.98
GTL8.5-9	8.5-9.0	0.704	5.8	0.16	1.32	426	188	1.19
L1	60.48-60.51	1.7	1.7	0.35	1.57	439	92	1.01
L2	62.02-62.05	0.188	0.25	0.29	0.11	340	59	0.85
L3	67.08-67.10	0.197	11	0.12	0.20	437	102	1.10
L4	67.54-67.56	0.203	10.7	0.18	0.21	431	103	0.65
L5	68.87-68.89	0.088	11.3	0.08	0.07	404	80	1.17
L6	68.97-68.99	0.102	11.3	0.09	0.09	376	88	1.21
L7	69.05-69.07	0.079	11.8	0.07	0.04	420	51	1.22
L8	69.09-69.11	0.056	11.3	0.05	0.05	391	89	1.52
L9	69.19-69.21	0.086	11.9	0.08	0.09	436	105	1.18
L10	75.90-75.93	1.99	9.3	0.33	2.51	428	126	1.07
L11	76.00-76.03	0.082	12.1	0.08	0.08	430	98	0.97
L12	79.35-79.37	0.084	11.8	0.07	0.08	434	95	0.93
L13	80.47-80.49	1.05	8.5	0.22	0.87	430	83	1.07
L14	81.50-81.525	0.104	11.3	0.06	0.04	436	38	1.86
L15	81.575-81.60	0.087	11.9	0.08	0.07	409	80	1.06
L16	82.17-82.19	0.207	10.7	0.12	0.12	392	58	0.71
L17	82.27-82.29	0.084	11.5	0.07	0.05	339	60	0.57
L18	66.98-67.04	0.16	11.3	0.07	0.19	434	119	n.a.
L19	LS	1.995	7.7	0.35	2.42	428	121	n.a.
B1	1	13.3	1.9	0.27	0.33	424	2	0.17
B2	2	18.2	3.9	0.65	0.54	400	3	0.18
B3	3	1.06	0.76	0.41	0.83	420	78	0.82
B6	6	0.98	0.90	0.32	1.02	420	104	1.04
B11	11.3-11.4	0.088	1.39	0.09	0.02	352	23	0.75
B12	12.8-13.25	0.089	1.1	0.15	0.07	341	79	1.70
B13	13.5-13.95	0.06	0.83	0.12	0.02	nm	33	1.45
B15	15.1-15.8	0.011	1.1	0.10	0.02	315	182	0.97
B17	17.5-17.95	0.041	0.58	0.16	0.02	nm	49	3.00
B20	20.7-21.15	0.074	0.87	0.25	0.07	331	95	12.17
B31	31.5	0.028	0.56	0.16	0.02	nm	71	0.91

NTY = North Sea Drift samples; GTL = Lowestoft Till samples

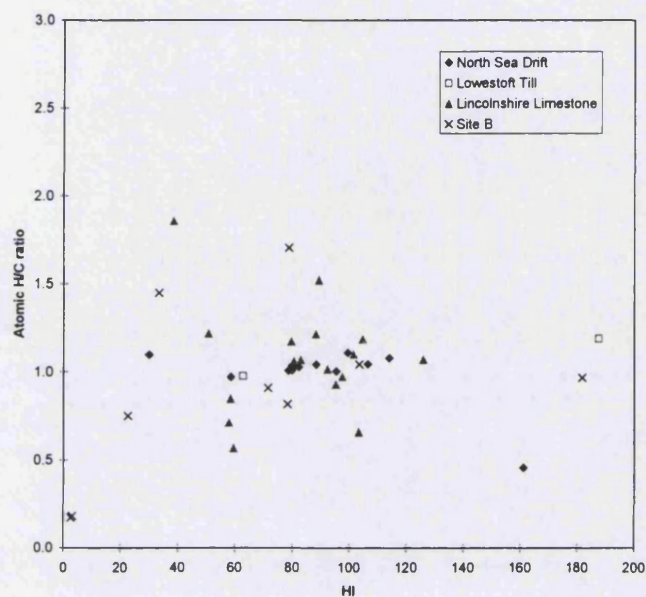
L = Lincolnshire Limestone samples; B = Site B samples;

Bold indicates the mean of two analyses

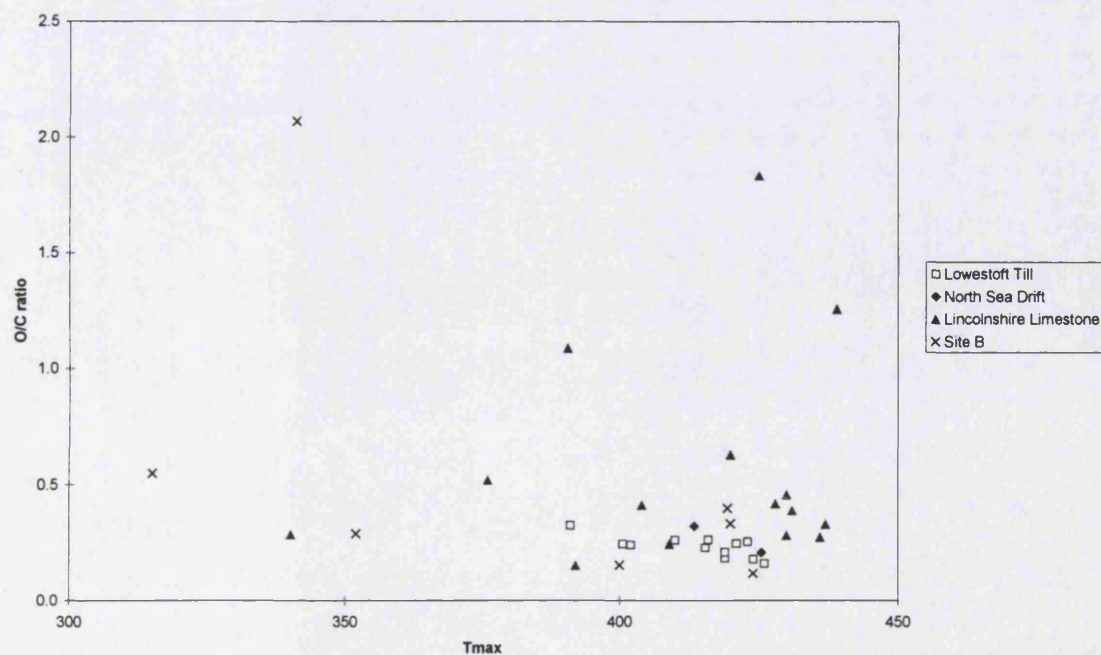
nm = Tmax not measurable due to evolution of insufficient gas

Figure 36: HI correlation with H/C for glacial till samples

Excluding the North Sea Drift samples with the lowest H/C ratio (NTY6) which had the highest HI, and with the lowest HI (NTY7) which had one of the highest H/C ratios, the 12 glacial till samples show the linear correlation between HI and H/C: $H/C = 0.0017HI + 0.8833$ (r^2 value 0.85). Additionally excluding the Lowestoft Till sample with high HI and H/C, the linear correlation $H/C = 0.0019HI + 0.8645$ has an r^2 value of 0.63. Much weaker positive trends are demonstrated by Lincolnshire Limestone and Site B samples (Figure 37).

Figure 37: HI plotted against H/C for all samples

As S_3 is not available from the Delsi analyser, OI could not be obtained. However, it has been suggested that T_{max} may be used in place of OI in kerogen typing (Tyson, 1995). The O/C ratio and T_{max} (plotted in Figure 38) indicate a possible negative correlation for the glacial till samples, but no correlation for the other samples, indicating that T_{max} cannot be consistently used as an appropriate proxy for O/C ratios for these samples.

Figure 38: Atomic O/C against T_{max} 

Chapter 7: Geochemistry Results and Discussion

As the S₃ component was not available using the Delsi analyser, selected samples were analysed using IFP II analyser (Section 6.2.2) to enable calculation of OI (Table 30). The results of IFP analysis differ from the results of the Delsi analysis by, on average, 41% deviation from the mean for S₁, 34% for S₂ and 2% for T_{max}, confirming the low accuracy of the Rock-Eval method.

Table 30: Rock Eval analysis results including S₃ data

sample	depth	AIC %	S1 mg/g	S2 mg/g	S3 mg/g	Tmax C	HI	OI	HI/OI	H/C atomic	O/C atomic	H/O atomic
NTY9	13	0.43	0.16	0.23	0.56	413	53	130	0.41	0.97	0.25	3.82
NTY12	19	0.33	0.33	0.51	0.50	410	155	152	1.02	1.00	0.24	4.18
GTL1.5-2	1.5-2.0	0.20	0.12	0.14	0.51	407	70	255	0.27	0.98	0.32	3.05
GTL8.5-9	8.5-9.0	0.70	0.18	1.31	0.34	425	187	49	3.85	1.19	0.19	6.44
L2	62.02-62.05	0.19	0.59	0.24	0.47	342	126	247	0.51	0.85	0.29	2.97
L5	68.87-68.89	0.09	0.06	0.11	0.16	414	125	182	0.69	1.17	0.41	2.85
L9	69.19-69.21	0.09	0.05	0.13	0.13	420	151	151	1.00	1.18	0.27	4.31
L18	66.98-67.04	0.16	0.06	0.31	0.21	427	194	131	1.48	n.a.	n.a.	n.a.
L19	LS	2.00	0.56	2.72	0.63	429	136	32	4.32	n.a.	n.a.	n.a.
W2	2	18.00	0.23	0.42	2.55	407	2	14	0.17	0.18	0.15	1.19
W3	3	1.10	0.22	0.74	1.25	415	67	114	0.59	0.82	0.33	2.46
W4	6	0.98	0.22	0.75	1.31	420	77	133	0.58	1.04	0.40	2.61
W6	12.8-13.25	0.09	0.23	0.18	0.15	353	202	169	1.20	1.70	2.07	0.82
IGCR		0.00	0.01	0.02	0.00	431	-	-	-	n.a.	n.a.	n.a.

IGCR = carbon free sample; n.a. = not analysed; - = not meaningful (divided by zero).

Hydrogen index and oxygen index both increase with increasing H/C and O/C ratios respectively (Figure 39), although linear correlations of the data are weak. H/O correlates linearly with the log of (HI/OI) (Figure 40) with the equation:

$$H/O = 1.5\ln(HI/OI) + 4.1 \quad r^2 = 0.79.$$

This suggests that Rock-Eval data may provide a useful proxy from whole rock samples for the H/O atomic ratio of the isolated OM.

Figure 39: Covariance of HI and OI with atomic ratios

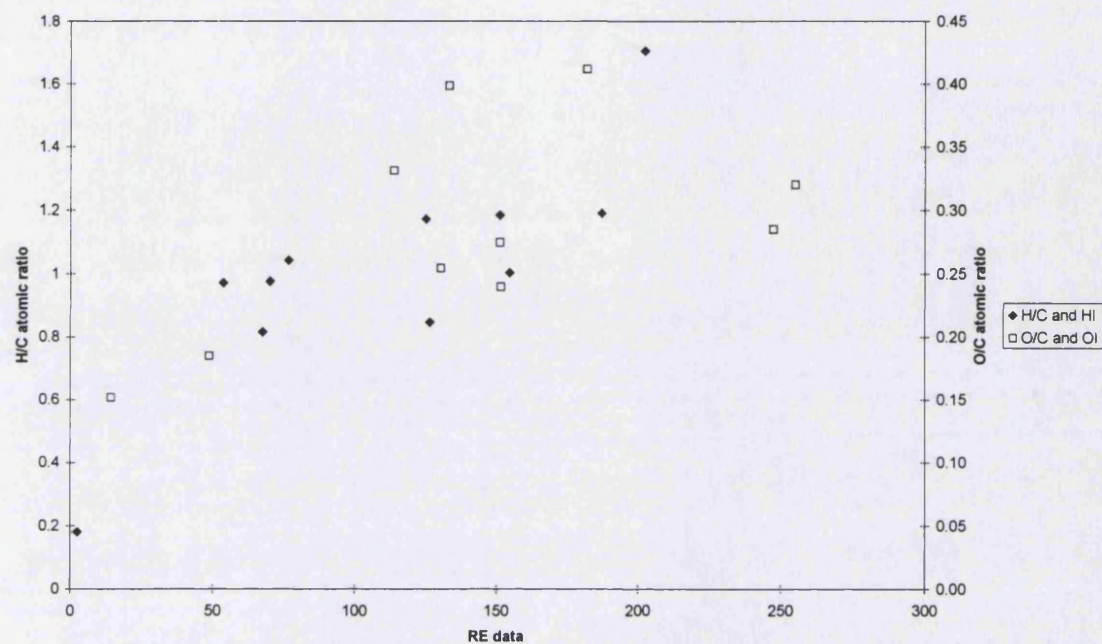


Figure 40: Covariance of HI/OI with H/O atomic ratio



7.7 Summary

- Organic matter isolation recovered about 80% of the original organic matter from North Sea Drift samples, and 50% of the original organic matter from other samples.
- The sum of C, H, N, O and S (as elements) accounted for about 85% of the isolated organic matter from glacial till samples, 61% from Lincolnshire Limestone samples and 46% from Site B samples.
- S/C ratios in oxidised glacial till samples were lower and O/C ratios higher than in unoxidised glacial till samples, confirming that chemical changes due to the weathering affected the OM in these samples. Lincolnshire Limestone samples had high sulphur content, and low oxygen and hydrogen. Site B samples had generally low sulphur content, and varied oxygen and hydrogen content.
- Rock-Eval analysis revealed weak correlations between HI and H/C ratios and OI and O/C ratios.

8. Organic matter morphology: results and discussion

8.1 Introduction

Organic matter was viewed optically after isolation according to the methods detailed in Chapter 6 and Appendix E. The optical examination was undertaken to measure the particle size distribution of the OM and identify its components, classified by morphology according to the scheme in Chapter 6 which was developed as suitable for the context and purpose of this study.

The results of the examination of the physical nature of the organic matter are presented in this chapter. Morphological classification results are included and discussed in Section 8.2. Particle size data are presented and discussed in Section 8.3: image analysis data is discussed in Section 8.3.1 and the distribution of organic carbon content with whole-particle size in a made ground sample in Section 0. Morphology results are summarised in Section 8.4.

8.2 Organic matter characterisation results

Components were classified morphologically according to the scheme in Chapter 6. Many other classification schemes have been published in which OM is divided into different ‘types’ using reflected or transmitted light microscopy, based on identifiable features, each specifically designed to provide maximum information for the purpose of the study in which they are used. Such schemes are presented by: Tyson (1995) for constructing palynofacies environments to assess hydrocarbon potential; Traverse (1994) for palynology; Boulter (1994) for palynofacies interpretation and sedimentary conditions; Durand (1980) for coal petrography; Batten (1996) for palynology / palynodebris classification.

The OM at 300 locations on 58 slides from 43 samples of isolated OM was classified and counted. Point counting will provide abundance as proportions of planar surface area. Percentage abundances of the components within samples of isolated OM are listed in Appendix F, and illustrated and summarised below (Figure 41 to Figure 44 and Table 31). Photographs of slides of material from selected samples (Figure 45) indicate the range of material types and particle sizes in these slides.

Figure 41: Components in organic matter from Lowestoft Till samples

Each slide is from a sub-sample isolated independently.

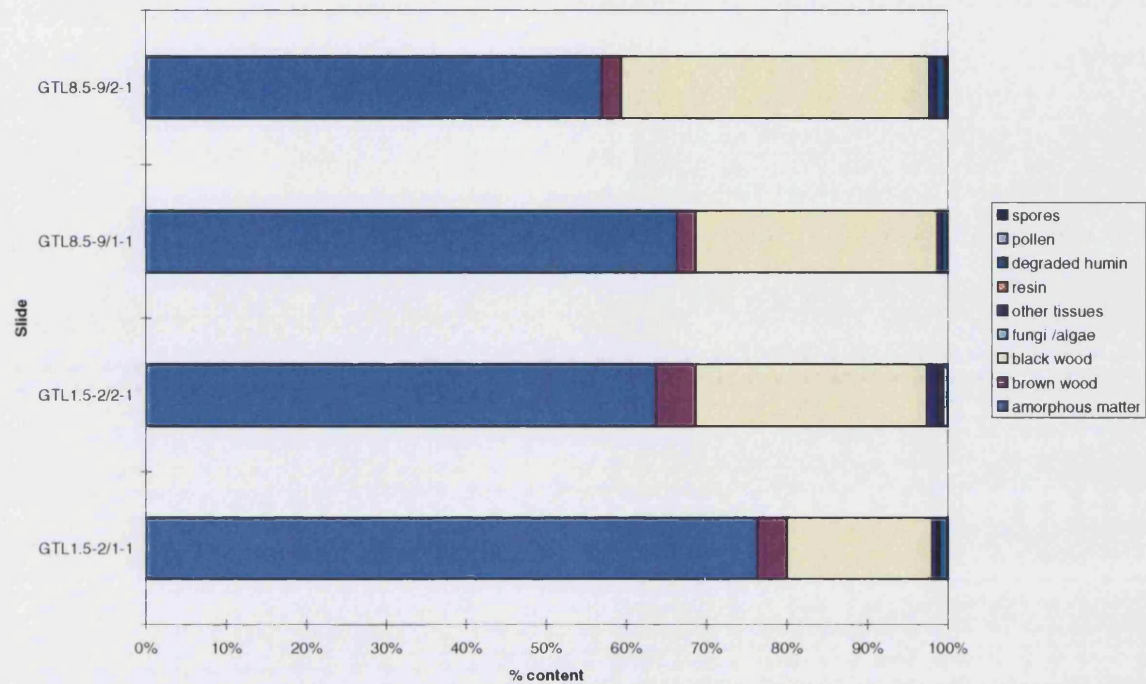


Figure 42: Components in organic matter from North Sea Drift samples

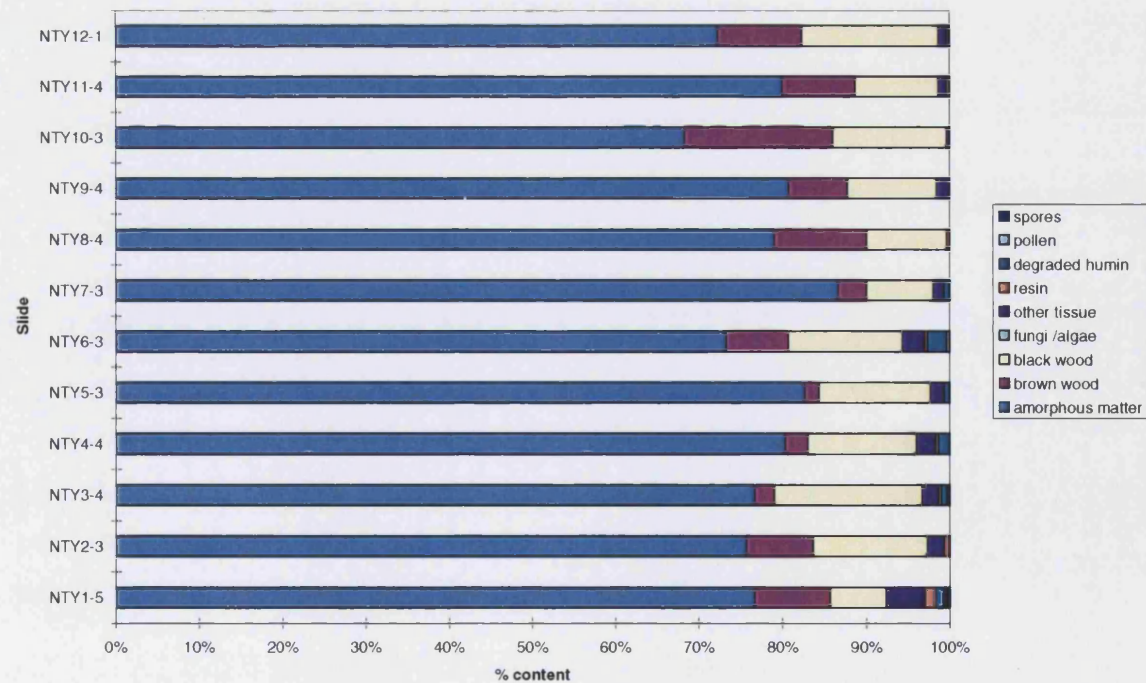


Figure 43: Components in organic matter from Lincolnshire Limestone samples

Samples are in increasing depth order. Label numbers are depth range (m bgl)

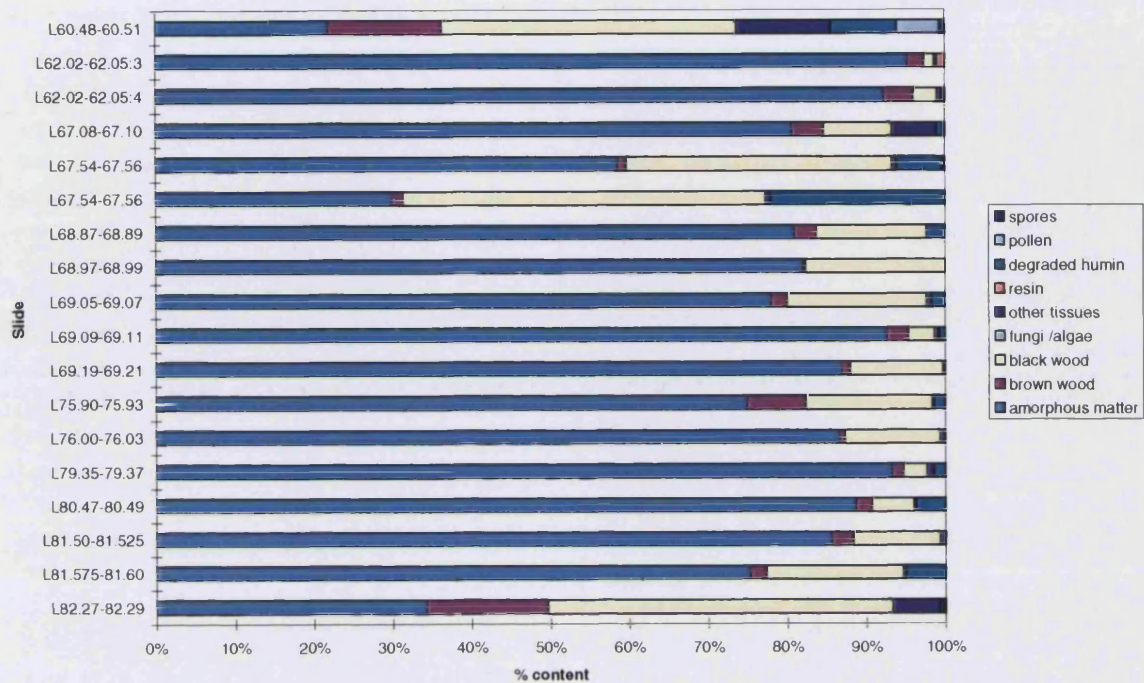


Figure 44: Components in organic matter from Site B samples

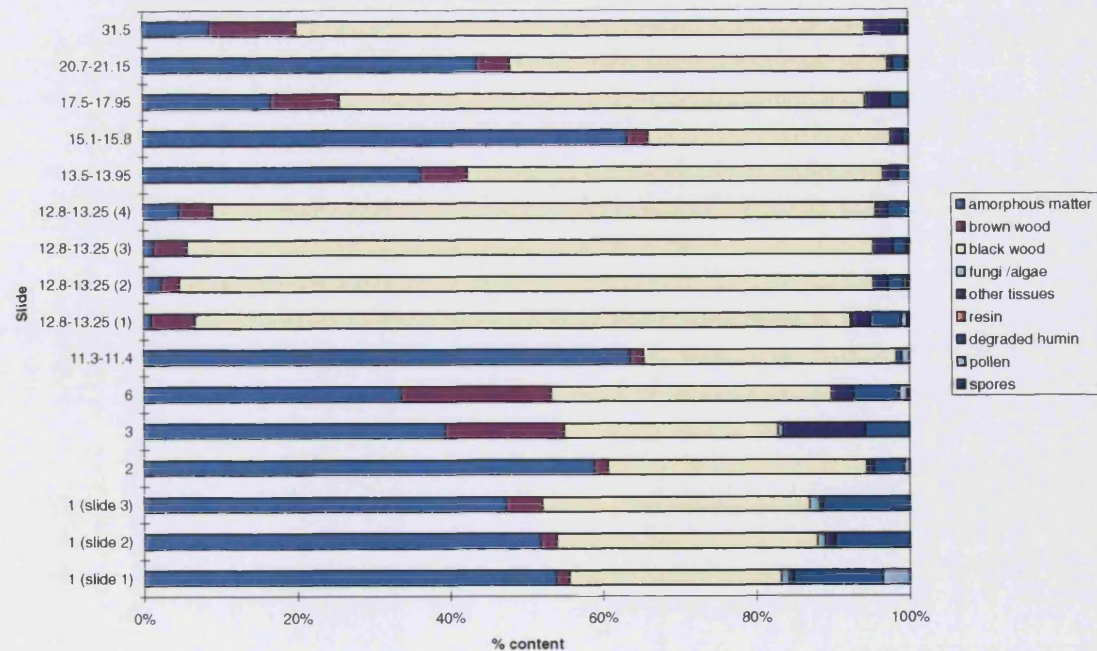
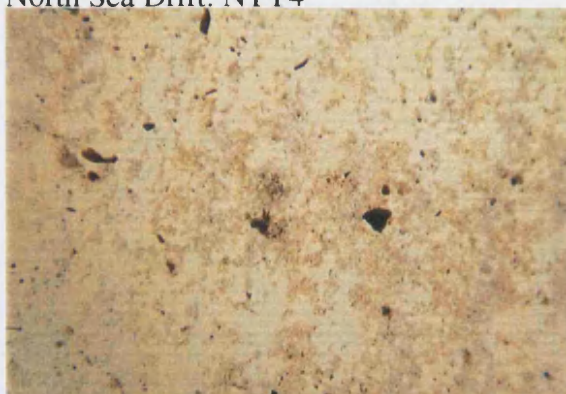


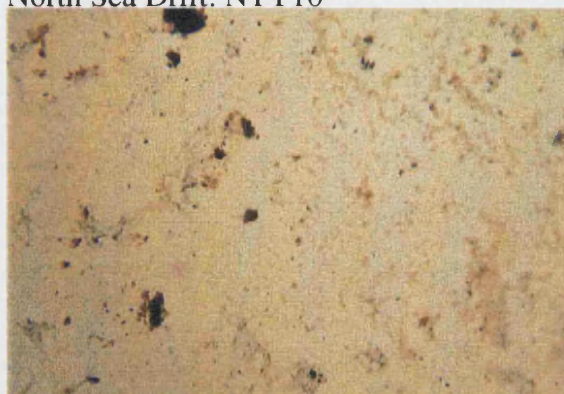
Figure 45: Photomicrographs of selected smear slides of isolated organic matter

All photomicrographs at $\times 115$

North Sea Drift: NTY4



North Sea Drift: NTY10



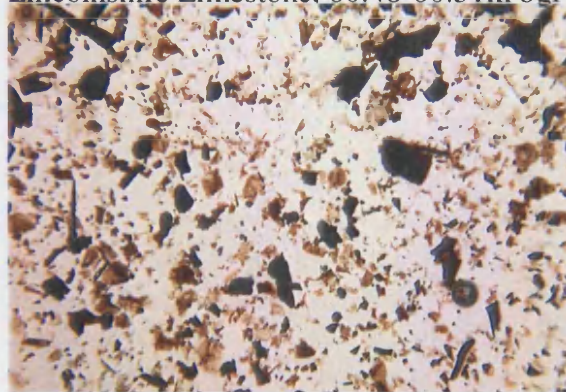
Lowestoft Till from 1.5-2m bgl



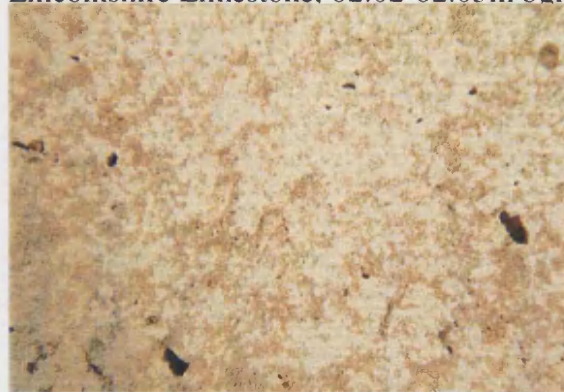
Lowestoft Till from 8.5-9m bgl



Lincolnshire Limestone, 60.48-60.51m bgl



Lincolnshire Limestone, 62.02-62.05m bgl



Site B, 6m bgl, grey-brown silty clay



Site B, 13.5-13.96m bgl, red-br. sandy clay

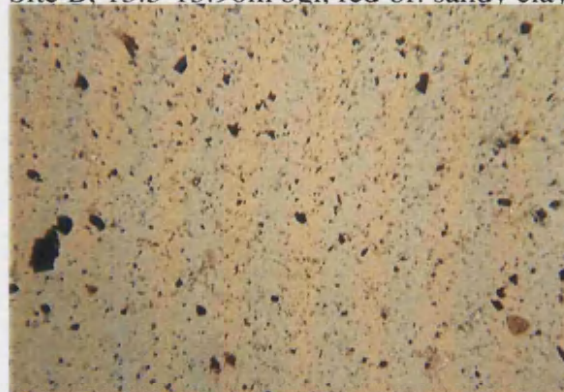


Table 31: Mean components in organic matter each material type

Unit	amorphous	brown wood	black wood	fungi / algae	other plant tissue	resin	degraded humin	pollen	spores
North Sea Drift	77.9	7.4	12.2	0.0	1.7	0.3	0.6	0.1	0.1
Lowestoft Till	65.8	3.3	28.8	0.0	1.0	0.2	0.8	0.0	0.0
Lincolnshire Limestone	74.4	3.7	16.8	0.02	1.7	0.1	3.0	0.3	0.1
Site B	33.0	6.0	53.7	0.3	2.3	0.0	4.1	0.5	0.1

For the Glacial Till samples and most of the Lincolnshire Limestone samples, the majority of the material is amorphous, with smaller contributions from black and brown wood and occasional pollen, spores, resin, degraded humic and other plant tissue. North Sea Drift samples contain a greater proportion of brown wood and amorphous matter and less black wood than Lowestoft Till samples. Differences between the two pairs of Lowestoft Till sub-samples (Figure 41) has been introduced during the organic matter isolation process (or by sub-sampling), but they do show similar proportions of each component. The uppermost Lincolnshire Limestone sample (from slide L60.48-60.51, L60.48 - 60.51 m bgl, the uppermost bar in Figure 43), which is from the overlying deposits rather than the Limestone, and the lowermost Lincolnshire Limestone sample (from slide L82.27-82.29, 82.27-82.29 m bgl, the lowermost bar in Figure 43) both contain large amounts of black wood and brown wood, with larger contributions from other tissue and degraded humin than the other samples. It is likely that these samples, from the ends of the formation series, were deposited under or subjected to different conditions than the other samples. The organic matter from Site B samples is widely varied between samples, which is not surprising given the wide variation in their material types. Organic matter isolated from samples at one and two metres depth had many larger particles (diameters of several millimetres or more) which were too large to be incorporated into the slides. Therefore the material characterisation from these samples is not representative of the whole sample. All samples had either black wood or amorphous matter as their predominant component. In general, black wood was predominant in sand rich samples, and amorphous matter predominant in samples with higher clay content. There is little diversity in the type of OM isolated from the samples. Total organic carbon content in Lincolnshire Limestone was found to be associated with clay content (Section 5.3) and these samples can be described as clay rich excluding the carbonate content. In the sandy samples (some Site B samples) a high proportion of black wood and other components was found; in other

samples (all glacial till, some Site B samples and the Lincolnshire Limestone), the OM was predominantly amorphous.

The OM type contained in the samples may influence sorption processes in two ways. Firstly, different types of OM may have different geochemical composition and therefore interact with organic solutes in different ways or to different extents. The different abundances of OM types in the samples could potentially dictate the samples' overall sorption behaviour. However, the properties of individual OM types has not been investigated. This could be a productive area for further research. The bulk geochemistry of these samples was analysed and the results have been presented and discussed in Chapter 7. Secondly, different types of particles may have different sizes: amorphous OM was composed of smaller particles than other components. The OM size together with its physical distribution in the formation will affect its surface area, and so possibly the area available for immediate sorption, and the ratio of surface area to internal volume, possibly affecting desorption characteristics. The sizes of particles in these slides has been investigated by image analysis, the results of which are presented and discussed in the next section.

8.3 Particle size analysis

Smear slides of isolated organic matter were analysed for their particle size distribution (PSD) by image analysis, following the method described in Chapter 6. This method was suitable for all till and limestone samples and samples from Site B, excepting samples of made ground from Site B, which contained organic particles too large to be incorporated in slides; PSD results would therefore be unrepresentative to the point of meaninglessness, and are therefore not included. One complete made ground sample (not isolated OM) was separated into size fractions, which were analysed for acid-insoluble carbon (AIC) content (Section 0). This does not, however, provide direct information on the size of the organic particles, but on the size of the particles containing organic matter.

8.3.1 Image analysis results

The results are presented as frequency distributions. The PSD of particles with areas (in plane projection) between 5 and 150 μm^2 , the PSD of particles with areas between 0.312 and 9.9 μm^2 , and the PSD of particles with areas between 0.078 and 9.9 μm^2 are the

results of image analysis of images obtained at different magnifications (objective lenses $\times 5$, $\times 20$ and $\times 40$ respectively). The distribution charts in Figure 46 and Figure 47 compare the PSD results at each magnification for each sample in the sets.

For each sample, at each scale, the PSD is strongly biased towards smaller particles²². Much more very fine material exists; this is possibly amorphous matter observed in the slides (Section 8.2). There is little variation within slides of North Sea Drift material, and within slides of Lowestoft Till material, except between slides deliberately created at different dilutions. Greater variation is observed within Site B samples and Lincolnshire Limestone samples, which both had greater variation in abundance of different types of organic matter and in abundance of amorphous OM. Between sample sets, broad similarity can be seen, with typically about 30% of particles falling in the finest bracket. This is most extreme for the Lowestoft Till at the greatest magnification (particles with areas between 0.078 and $10 \mu\text{m}^2$).

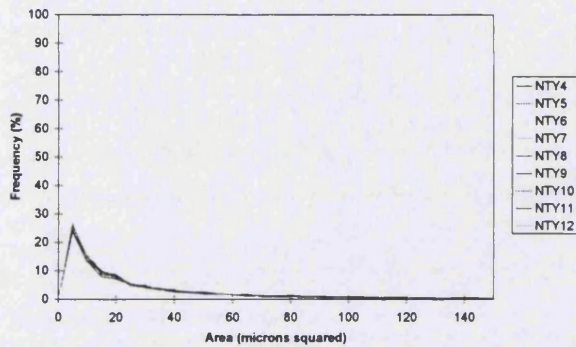
²² The resolvable size is calculated as pixel separation divided by magnification. Since the JVC KY-F55B camera used has a pixel size of $10\mu\text{m} \times 10\mu\text{m}$, resolution at magnification $\times 40$ is calculated to be $0.25\mu\text{m}$, close to the smallest particle diameter measured, $0.31\mu\text{m}$. The difference may be due to slight errors in calibration. Smallest diameters measured at $\times 20$ and $\times 5$ are $0.63\mu\text{m}$ and $2.5\mu\text{m}$ respectively, which scale inversely and linearly with the magnification as expected.

Chapter 8: Morphological results and discussion

Figure 46: Particle size distribution of Glacial Till samples

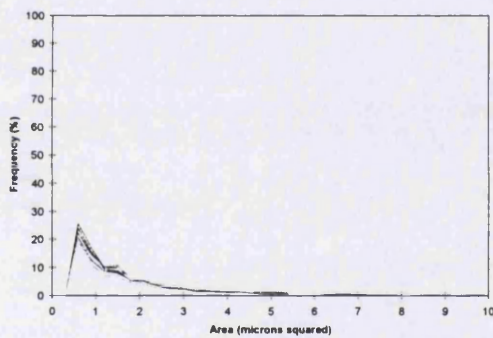
North Sea Drift

Results of particle areas, 5 to 150 μm^2



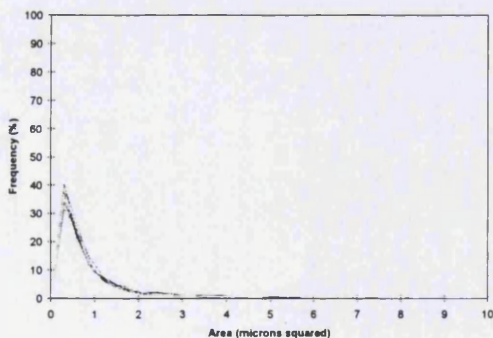
Between 6.3 and 11.4% of measured particles exceeded 150 μm^2 .

Results of particle areas, 0.312 to 9.9 μm^2



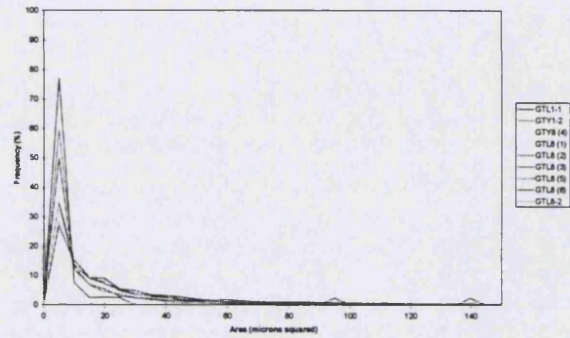
Between 4.8 and 16.0% of measured particles exceeded 9.9 μm^2 .

Results of particle areas, 0.078 to 9.9 μm^2

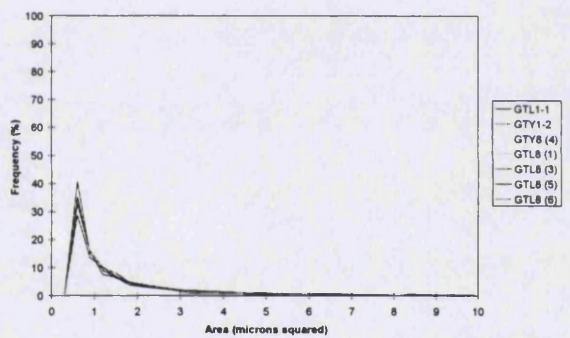


Between 1.3 and 4.5% of measured particles exceeded 9.9 μm^2 .

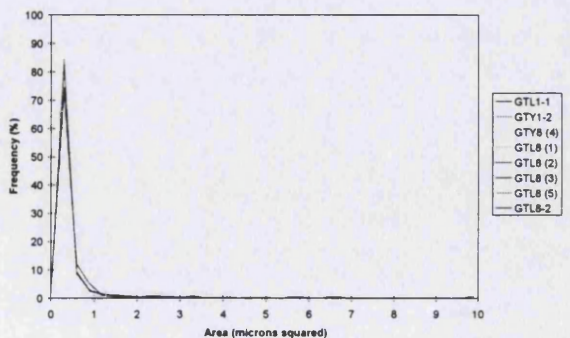
Lowestoft Till



Between 1.4% and 8.3% of measured particles exceeded 150 μm^2 .



Between 3.4 and 8.9% of measured particles exceeded 9.9 μm^2 .



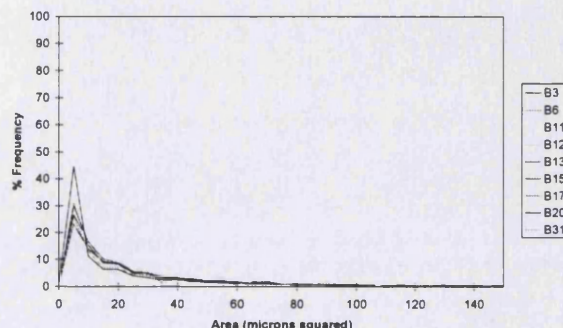
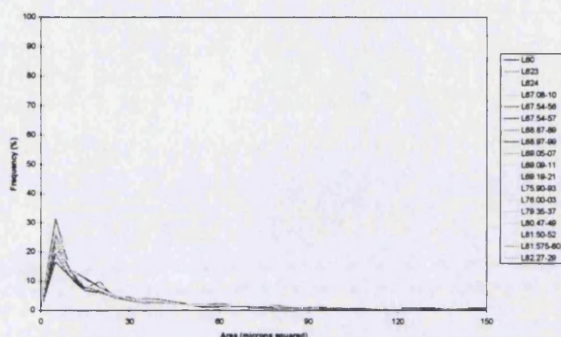
Between 0.2 and 2.8% of measured particles exceeded 9.9 μm^2 .

Figure 47: Particle size distribution of Lincolnshire Limestone and Site B samples

Lincolnshire Limestone

Site B

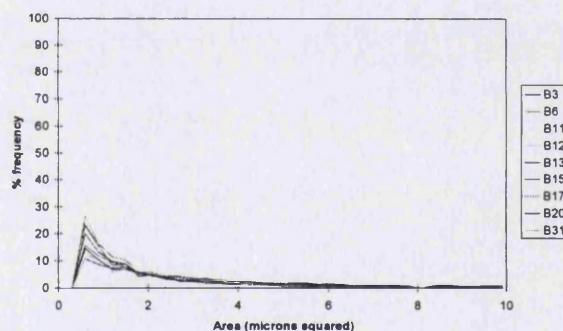
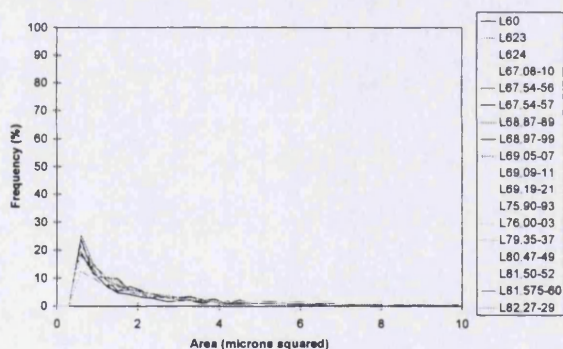
Results of particle areas, 5 to 150 μm^2



Between 5.8% and 22.0% of measured particles exceeded 150 μm^2

Between 3.8% and 12.1% of measured particles exceeded 150 μm^2

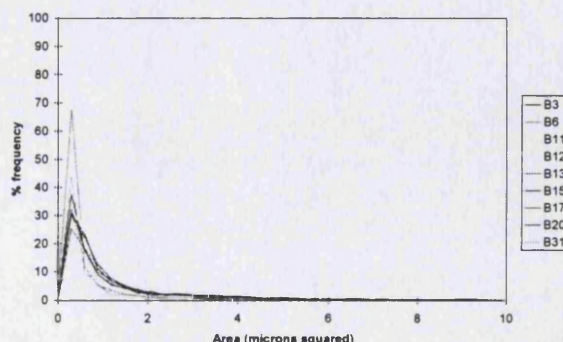
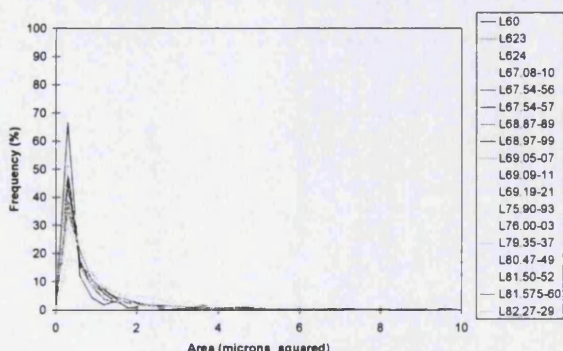
Results of particle areas, 0.312 to 9.9 μm^2



Between 4.9 and 25.5% of particles exceeded 9.9 μm^2

Between 5.5 and 18.8% of particles exceeded 9.9 μm^2

Results of particle areas, 0.078 to 9.9 μm^2



Between 1.4 and 8.8% of particles exceeded 9.9 μm^2

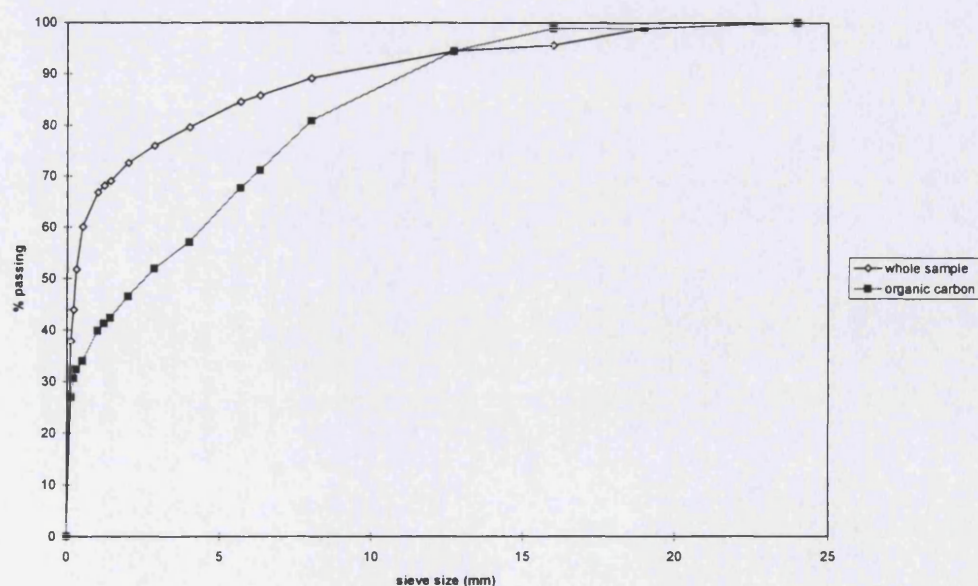
Between 1.1 and 27.7% of particles exceeded 9.9 μm^2

Particle size distribution by image analysis has been shown to be a rapid method to gain information on the isolated OM. Organic matter PSD in the Site B samples is related to the whole sample PSD. However, the PSD from image analysis is dependent on the slide density, and reveals little variation between most of the samples. This, therefore, does not provide as useful information as may be expected.

8.3.2 Made ground AIC distribution with particle size

The distribution of organic carbon with particle size was determined for made ground from Site B, 2 m bgl. The sample was dark grey, slightly ashy, slightly sandy clay with occasional angular to subangular gravel-size fragments of sandstone and clinker²³. A subsample (obtained by riffle splitting) was divided into particle size fractions by wet sieving. All water and material passing the finest sieve was retained, allowed to settle and much of the water removed by pipette. Each size fraction was oven-dried, weighed, and its acid-insoluble carbon content (AIC) determined. The sample's particle size distribution (PSD), and the PSD of the AIC (Figure 48) shows that 70% of the organic carbon in this sample is in particles greater than 1mm diameter. This does not provide the PSD of organic particles, but does indicate the OM content of different size ranges of particles.

Figure 48: PSD of particles and organic carbon content in made ground sample



²³ Consultant's description, confirmed by observation.

These made ground samples contained a significant amount of organic carbon in larger particles, greater than would be predicted based on the whole-rock PSD by weight. 50% of organic carbon was in particles with diameter greater than 2.5mm, compared to only 25% of the whole sample, by weight. Organic particles typically have lower density than inorganic particles, so the disparity between the organic carbon distribution with particle size and the whole sample PSD may be less if measured by volume rather than weight. Organic material included burnt coal fragments (shown in photographs Figure 49 to Figure 51). Coal fragments retained on the 19 mm sieve are contained within a larger particle (Figure 49) with total AIC 12.5%, but in other size fractions they form complete particles: coal fragments between 12.7 mm and 16 mm were revealed (Figure 50) with AIC 54.1%. Large inorganic fragments are found between 16 mm and 19 mm (Figure 51) with AIC 0.045%. Finer organic material may also be contained within other particles. Much of the organic material in this sample is present as or in particles of sand and gravel size, which have a corresponding lower surface area than would the same mass of smaller fragments. As the surface area per unit weight of organic carbon will be lower and the organic matter is more localised in larger particles than fine organic material would be, it is suggested that the organic matter may not be as available to solutes as a sorbent than the same amount of finer organic material.

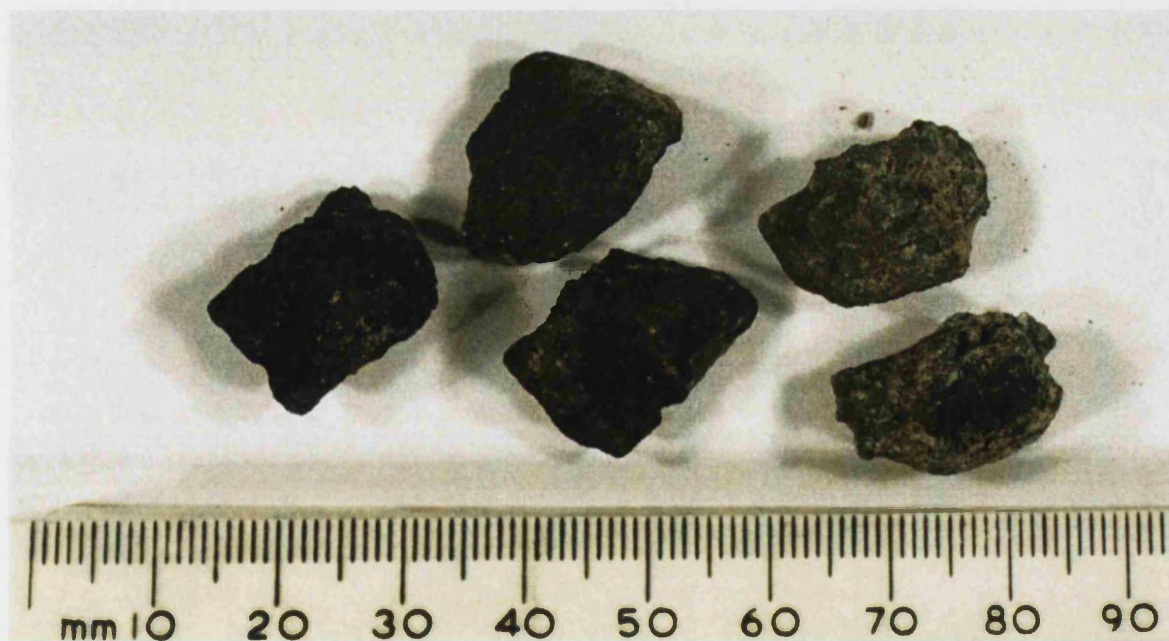
Figure 49: Photograph of made ground from 2m bgl, retained on 19 mm sieve



Figure 50: Photograph of made ground from 2m bgl, between 16 and 19 mm



Figure 51: Photograph of made ground from 2m bgl, between 12.7 and 16 mm



8.4 Summary

- Samples of North Sea Drift and Lowestoft Till contained mainly amorphous OM (37% to 87%), with more amorphous OM in the North Sea Drift (87% to 72%) than in the Lowestoft Till (37% to 82%). In most samples, the next most abundant material was black wood (15% to 53%). PSD analysis of glacial till samples revealed little difference between samples, and a great abundance of fine particles, considered to be the amorphous matter.
- Most Lincolnshire Limestone samples contained predominantly amorphous organic matter (22% to 95%), and had a high proportion of fine-grained particles (34% to 79% with area less than $0.6 \mu\text{m}^2$). The samples from the top and bottom of the formation had large proportions of brown wood, black wood and other tissues. These samples had the greatest and lowest proportion of very fine (area less than $0.6 \mu\text{m}^2$) material as seen under the highest magnification. Other samples showed similar PSDs to each other.
- Site B samples contained a larger proportion of non-amorphous organic matter than did other samples. Much of this other organic matter was black and brown wood fragments. Different sample materials (such as clayey compared to sandy samples) had different organic matter types and sizes. PSD image analysis of Site B samples revealed a greater proportion of larger particles in sandy samples. Samples of made ground contained a significant amount of organic carbon in larger particles (50% greater than 2.5mm diameter), greater than would be predicted based on the whole rock PSD by weight.
- It was found that the range of particle sizes and morphologies comprising the majority of the organic matter isolated from all the samples was not broad. The organic matter in most samples was predominantly amorphous. Larger proportions of other material types were observed in some samples, notably Site B samples with higher sand content. In all samples, fine grained organic matter predominated, although Site B samples with high sand content had a higher proportion of larger fragments than other samples.

9. Measuring Sorption: methods used

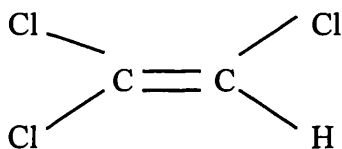
9.1 Introduction

Batch sorption experiments were undertaken to investigate the relation of organic matter type and content to trichloroethene sorption. Trichloroethene (TCE) is a common and persistent contaminant that causes significant groundwater contamination (see Section 9.2.3); it has been widely used in previous research on sorption of hydrophobic contaminants to organic carbon. Batch sorption experiments do not replicate natural conditions as well as other experimental set-ups such as column experiments, but are relatively quick to perform (Section 9.3) and results can be compared to results of previous batch experiments (Section 9.4). A method developed to undertake batch sorption measurements is described in Section 9.5.

9.2 TCE as a contaminant

9.2.1 TCE properties

The formula for trichloroethene (TCE, synonyms include trichloroethylene) is C_2Cl_3H :



It is a clear, colourless liquid, with a distinct odour. It is soluble in other organic solvents, but has low water solubility. Selected chemical and physical properties are given in Table 32.

Table 32: Chemical and physical properties of trichloroethene

Boiling point (°C)	87.2
Density at 0°C (g/cm ³)	1.4996
Density at 15°C (g/cm ³)	1.4762
Density at 20°C (g/cm ³)	1.464
Density at 30°C (g/cm ³)	1.4514
Diffusivity in water (10 ⁵ cm ² /sec)	0.94 at 20°C
Log K _{oc}	between 1.66 and 2.83; references given represent K _{oc} from 46 to 676 (presumably l/kg) additional values given in Section 9.4
Log K _{ow} (units not given)	2.29 to 3.30 - represent K _{ow} of 195 to 1995
water solubility	1.08 - 1.1 mg/l at 20°C

from Montgomery, 1996

A detailed discussion on the properties and fate of TCE, and other 'dense chlorinated solvents' is given in Pankow and Cherry, (1996). Bourg *et al.* (1992) also review aspects of the attenuation of TCE movement in the ground, including its movement as a free phase, degradation, sorption and vapour phase processes. The synopsis below is taken from Montgomery (1996).

Whilst TCE has low biodegradability, degradation products have been observed in anaerobic, and possibly in aerobic conditions. Degradation proceeds via progressive dehalogenation: from TCE to *cis*- and *trans*-1,2-dichloroethene to chloroethene and possibly ultimately to CO₂. The low biodegradability leads to persistence of TCE in groundwater.

TCE is potentially a carcinogen, and exposure causes dizziness, headache, fatigue and visual disturbances. It has been widely used: for dry cleaning; for degreasing and drying metals and electronic parts; as an extraction solvent for oils, waxes and fats; as a solvent for cellulose esters and ethers; for decaffeinating coffee; as a refrigerant and heat exchanger; as a fumigant; in paints and adhesives; in textile processing; in aerospace operations (flushing liquid oxygen); as an anaesthetic; in medicine; as a septic tank cleaner (Fetter, 1993) and in organic synthesis.

9.2.2 Trichloroethene use

Trichloroethene was first manufactured in the early 20th century and introduced on a large scale as a commercial solvent in 1929. Tetrachloroethene (perchloroethene, or PCE) was introduced as a less volatile alternative in 1950 (Ashley, 1998). Human toxicity lead to replacement of TCE and PCE from the early 1960s, and peak usage was in the early 1970s. From the mid 1970s it was realised that TCE and PCE presence in drinking water was potentially carcinogenic. The European Community set a limit for organochlorine compounds in drinking water of 1 µg/l, which was implemented in the UK in 1985; in 1984 the World Health Organisation introduced preliminary guideline concentrations of 30 µg/l and 10 µg/l for TCE and PCE respectively in drinking water, which were implemented in the UK in 1989 as maximum concentrations in revised drinking water

standards. TCE and PCE are on the EC Black List (List I Dangerous Substances Directive 76/464/EEC) which is implemented in UK via an environmental quality standard (EQS) for surface water of 10 µg/l for TCE and PCE (Banks, 1998). *'The chlorinated solvents ... are undoubtedly among the top 10 organic groundwater pollutants. They are quite persistent and mobile in groundwater, and may, therefore, lead to the contamination of large groundwater areas. ... for example, in Switzerland ... it would only take about 0.2% of the annual consumption of these chemicals ... to spoil the total annual water supply of 6 million people'* (Schwarzenbach *et al.*, 1993).

9.2.3 Case examples of trichloroethene contamination

'Researchers at Birmingham University caused considerable concern when they revealed that the unconfined Permo-Triassic Sandstone aquifer beneath Birmingham was subject to widespread solvent contamination, largely caused by engineering industries and dry cleaning.' (Mather *et al.*, 1998). In studies of Birmingham and Coventry, chlorinated solvents were found in 70 - 80% of sampled boreholes (Burston *et al.*, 1993, Rivett *et al.*, 1990): in Coventry, TCE concentrations of up to 1000 µg/l were detected in pumped waters and up to 6000 µg/l in investigation boreholes at local hotspots where metal degreasing and cleaning occurred (Lerner *et al.*, 1993, Bishop *et al.*, 1993); in Birmingham, maximum TCE concentrations of 5500 µg/l were found (Rivett *et al.*, 1990). Highest concentrations were seen on sites of heavy engineering companies, and concentrations increased towards the city centre. Harris (1998) claimed that *'beneath the majority of industrial premises that handle, manufacture or store organic chemicals in liquid of soluble form, the groundwater will be found to be polluted to some degree'*. In industrial areas, wide use of solvents used in motor, metal, electronics, plastics, textiles and components manufacturing and maintenance and dry-cleaning has resulted in many discrete sources coalescing to form a diffuse pollution problem, which, for urban areas over major aquifers, has had a significant impact on groundwater quality. Rural areas suffer from chlorinated solvent pollution from point sources. At least 14 public supply boreholes need treatment to maintain drinking water supplies below legal limits for TCE and PCE (30 µl/l TCE; 10 µl/l PCE) (Harris, 1998). Several examples of halogenated solvent contamination are given in Mather *et al.* (1998) who comment that *'chlorinated*

solvents are considered to be among the most problematic and pervasive groundwater contaminants in the industrialised world':

- the famous court case between Eastern Counties Leather and Cambridge Water Company involved contamination by PCE and TCE of a water supply from the Chalk aquifer;
- investigations of petroleum contamination unexpectedly found dissolved chlorinated solvent contamination in the Lincolnshire Limestone (Banks, 1998) from at least three sources, which contaminated a spring with TCE concentrations greater than the EQS of 10 µg/l;
- extensive chlorinated solvent contamination in the Chalk Downs may have been caused by chemical disposal into unlined lagoons in the Chalk (Mather *et al.*, 1998);
- TCE contamination of a groundwater source with 40 to 80 µg/l, and concentrations up to 100 µg/l in the Upper Chalk aquifer and 27 700 µg/l in localised hotspots in the overlying drift (Misstear *et al.*, 1998) was suggested to be caused by a number of chlorinated solvent pollution incidents from a number of sources over many years.

9.3 Methods to measure sorption

Sorption can be measured using laboratory and field experiments. Field experiments to measure contaminant sorption require locations where contaminants can be injected into the ground, and are therefore rare. One high profile example is the 'forced-gradient' test in the Borden aquifer (Mackay *et al.*, 1994), in which dissolved chlorinated solvents and conservative tracers were injected and their appearance in a pumping well monitored.

In the laboratory, batch experiments measure the partition of a solute between solid and solution under conditions designed to maximise the contact between solid and solution: a subsample of the solid is placed in a vial, together with a solution of the compound(s) under investigation, and the vial mixed for a set period of time (typically 24 or 48 hours) to allow equilibrium to be attained (Allen-King *et al.*, 1996a). Centrifugation is used to separate the phases, and the concentration of the compound in the water analysed. Vials are replicated and prepared over a concentration range to allow a temperature isotherm to be plotted.

Column experiments are a closer representation of field conditions; aquifer material is packed into a column, through which water flows. A solution of the compound of interest,

together with a conservative tracer, is injected and a transport model fitted to the concentration and time of appearance of these solutes in the water exiting the column. Non-equilibrium and transport effects can complicate these results (Allen-King *et al.*, 1996a). Some researchers (for example, Bourg *et al.*, 1993) have experimented on columns of undisturbed material, rather than repacked columns.

9.4 Literature review of trichloroethene sorption

Because of its widespread occurrence as a groundwater pollutant, sorption of TCE to aquifer materials has been extensively studied. Many K_{oc} values for TCE are summarised in a review by Allen-King *et al.* (1997b), who identified sorption nonlinearity in those experiments covering a wide concentration range, but calculated average linear K_d for each of the individual concentration points (following Ball and Roberts, 1991). Ascribing all the sorption to organic carbon and using the TOC values given in the original papers, they found K_{oc} values from 50 to 500 l/kg, excluding one K_{oc} of 9000 l/kg. These are much lower than the K_{oc} values they measured in till samples (7800 to 15700 l/kg). Other compilations of previously measured K_{oc} values for TCE are given in Spitz and Moreno (1996), who give K_d values, with TOC for some materials, and Bourg *et al.* (1993). Pankow and Cherry (1996) and Fetter (1993) both give a single TCE K_{oc} , 126 ml/g and 152 ml/g respectively.

Mouvet *et al.* (1993) found linear sorption isotherms with K_{oc} between 58 ml/g and 209 ml/g for a concentration range of 1 to 1000 $\mu\text{g/l}$ that were '*strongly but not systematically*' related to the TOC of the solids (between 0.13 to 1.2%); they conducted the experiments at $23 \pm 3^\circ\text{C}$, solid to solution ratios of 1.4 to 1.7, with vials mixed by rotation at 16 rpm, for an equilibration time of 2 days, followed by separation by centrifugation at 200g for 20 min. Analysis was by GC-ECD of headspace. They suggested that '*some of the unexplained discrepancies observed in the relationship between K_p [K_d] and f_{oc} may be due to the nature of the organic matter, both as particulate or dissolved compounds*'. For this reason, they did not present K_{oc} directly, but the K_d and TOC of the materials. Isotherm nonlinearity has been observed over large concentration ranges: Allen-King *et al.* (1996b) found Freundlich isotherms provided a better fit to their measured TCE sorption to aquitard materials than linear or Langmuir isotherms; Ball and Roberts (1991)

found deviation from linearity at over 1000 $\mu\text{g/l}$ PCE, with a measured K_d of 0.09 l/kg to 2.51 l/kg in materials with TOC of less than 0.1%.

Column experiments on undisturbed Coventry Sandstone rock columns (Bourg *et al.*, 1993) gave a much lower retardation factor than calculated from batch sorption studies on the same material. They found that the sorption reaction in the column was chemically rate-limited, but little affected by solute flow rate. They found that published retardation factors for TCE, trichloroethane (TCA) and PCE from batch sorption were similar to those from repacked column measurements, and both were much higher than for columns of undisturbed material.

9.5 Method applied

A method was developed to undertake batch sorption measurements on selected materials using TCE as the sorbate. This section describes method development prior to the undertaking of batch sorption experiments and details the method applied. The details investigated include the use of a methanolic stock solution of TCE, the ratio of solids to solution in each batch reactor, the time to equilibrium and centrifugation to separate the liquid from the solids after equilibration. The discussions below both review existing literature and present work undertaken for this study. Finally, the method applied for this study is described, together with the analytical method for TCE quantification.

9.5.1 Methanolic Solutions

Trichloroethene (TCE) dissolution in water is slow; TCE added to water did not dissolve completely over a period of several days, and provided a solution of much lower concentration than required. As dissolution is incomplete and volatilisation continuous, concentrations are unpredictable. This problem can be overcome by using a methanolic solution of TCE which dissolves quickly in water. Methanolic solutions are widely used in sorption studies (for example: Allen-King *et al.*, 1996b; Allen-King *et al.*, 1995; Ptacek and Gillham, 1992; Curtis *et al.*, 1986; Bourg *et al.*, 1993) because methanol does not interfere with TCE sorption at the concentrations used (Nkeddi-Kizza *et al.* 1985; Munz and Roberts, 1986).

Chapter 9: Measuring Sorption

The concern with this approach is that methanol may interfere with TCE sorption. It has been suggested that interferences between co-solutes are avoided in an ideal solution, which has no interactions between components and follows ideal thermodynamic rules (Munz and Roberts, 1986). To achieve an ideal solution, the mole fraction (X_i) of each co-solute should be less than 10^{-4} .

$$X_A = \frac{M_A}{\sum M_i}$$

where:

X_A = the mole fraction of component A

M_i = the molarity (concentration / molecular mass) of any component in the mixture

M_A = the molarity of component A ($M_{\text{water}} = \frac{1000}{18}$)

The molar fraction of methanol (MeOH) in an aqueous solution of TCE and methanol is:

$$X_{\text{MeOH}} = \frac{M_{\text{MeOH}}}{M_{\text{MeOH}} + M_{\text{TCE}} + M_{\text{water}}}$$

The molar fractions for a range of concentrations of TCE and methanol in water (Table 33) have been calculated for the methanol and TCE concentrations used in the batch sorption experiment (figures in bold) and for the maximum concentrations at these MeOH : TCE ratios that will maintain the molar fraction of each component below 10^{-4} (figures in italics).

Table 33: Molar fractions of methanol and TCE in water

TCE: MeOH by vol	Conc TCE g/l	Conc TCE ml/l	Molarity TCE $\times 10^3$	Conc MeOH g/l	Conc MeOH ml/l	Molarity MeOH $\times 10^{-3}$	Molar fraction MeOH $\times 10^{-5}$	Molar fraction TCE $\times 10^{-5}$
0.5	0.293	0.200	2.23	0.158	0.200	4.95	8.91	4.00
<i>0.5</i>	<i>0.329</i>	<i>0.225</i>	<i>2.50</i>	<i>0.178</i>	<i>0.225</i>	<i>5.57</i>	<i>10.00</i>	<i>4.51</i>
0.1	0.0146	0.0100	11.1	0.079	0.100	2.48	4.45	20.0
0.1	0.0293	0.0200	22.3	0.158	0.200	4.95	8.91	40.0
<i>0.1</i>	<i>0.0329</i>	<i>0.0225</i>	<i>25.0</i>	<i>0.178</i>	<i>0.225</i>	<i>5.57</i>	<i>10.00</i>	<i>45.1</i>
0.01	0.00293	0.00200	223	0.158	0.200	4.95	8.91	400
<i>0.01</i>	<i>0.00329</i>	<i>0.00225</i>	<i>250</i>	<i>0.178</i>	<i>0.225</i>	<i>5.57</i>	<i>10.00</i>	<i>451</i>
0.001	0.000293	0.000200	2230	0.158	0.200	4.95	8.91	4000
<i>0.001</i>	<i>0.000329</i>	<i>0.000225</i>	<i>2500</i>	<i>0.178</i>	<i>0.225</i>	<i>5.57</i>	<i>10.00</i>	<i>4510</i>

Chapter 9: Measuring Sorption

The maximum TCE concentration used was for a 1:1 by volume MeOH : TCE mixture, with TCE concentration of 0.3 g/l, just under 30% of TCE solubility (1.1 g/l). For this TCE : MeOH ratio, above 0.33g/l TCE the mole fraction of methanol exceeds $1e-4$. Higher TCE concentrations maintaining solution ideality could be attained using a greater TCE : MeOH ratio. However, the dissolution rate of the mixture in water was expected to increase as the TCE : MeOH ratio increases, leading towards the problems encountered when attempting to make a neat aqueous solution of TCE.

9.5.2 Batch sorption procedure

Batch sorption experiments were undertaken on two samples from the Lincolnshire Limestone, two samples of Lowestoft Till, two of made ground and an underlying unconsolidated clayey silt sample from Site B (descriptions in Table 34). Organic geochemistry of these samples is presented in Chapter 7 and organic morphology in Chapter 8. The samples were air-dried at less than 40°C and crushed gently to disaggregate them into their fine component particles. Lincolnshire Limestone samples were crushed in a disc mill to coarse sand sized particles or finer.

Table 34: Descriptions of samples used in sorption experiments

Sample	Description
Weathered Till	1.5 - 2.0m bgl, orange brown silty clay with chalk, straw, brown silty clay inclusions and gravel
Unweathered Till	8.5 - 9.0m bgl, soft dark grey clay with chalk gravel
Lincolnshire Limestone	Sleaford Member, light grey hard wackestone
Lincolnshire Limestone	Kirton Shale, marly shale
Made Ground, 2m bgl	ashy sand, clinker and rock
Made Ground, 3m bgl	orange ashy clayey silt
Silty clay	6m bgl, grey brown silty clay

All hardware that contacted experimental solutions (except microsyringes) was cleaned prior to use following a method based on USEPA Protocol B (USEPA, 1992). Microsyringes were rinsed repeatedly with methanol between each use. All water used was ultra-pure organic-free water (from an Elga Option 3 Water Purifier), TCE was Fischer Analytical Reagent (AR) grade, and methanol was Fischer Distol F 'for pesticide residue analysis' grade.

Chapter 9: Measuring Sorption

Experimental procedure follows that described by, for example, Ptacek and Gillham, (1992). Each batch reactor vial (40 ml nominal volume vials with Teflon lined septa) was filled as follows to eliminate air bubbles and minimise headspace: the vial was half-filled with 0.2g/l NaHCO₃ solution²⁴ before the solid was added; the vial was capped and shaken to saturate the solids and eliminate air bubbles; the vial was then filled up with the solution. Solid and liquid quantities were measured by weight. Control vials were filled with NaHCO₃ solution in one action. After filling all the vials, the methanolic TCE solution was dispensed into the vial using micro-syringes of appropriate volume, and the vial rapidly and tightly capped. The completed batch reactors were shaken and set upon the rotator. Initial TCE concentrations used are as shown in Table 33, and were selected to cover the range with a logarithmic distribution since pilot studies showed that, over this concentration range, Freundlich sorption isotherms were expected. Blank reactors, without TCE but containing methanol in NaHCO₃ solution, and with and without solids were run, to check for TCE contamination from the original samples or during the experimental procedure.

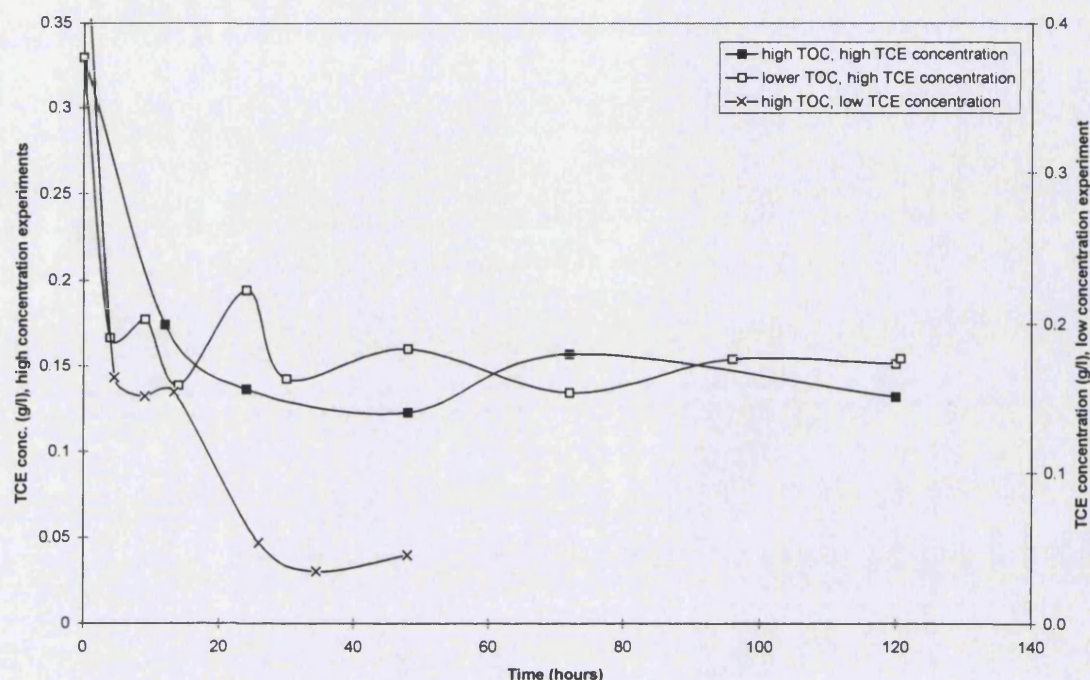
The higher the solid to solution ratio, the greater amount of TCE will be removed from the solution by sorption. Therefore a high solids to solution ratio reduces errors linked to loss of TCE from solution by other means (such as sorption to walls). In this study, 30 grams of solid was used in a 40 ml nominal volume vial with 31 ml water, giving a solids to solution ratio of approximately 1:1 by mass. This compares with solution to solid ratios reported in published literature of 2:1 (Mackay *et al.*, 1986), 3:2 in 60 ml vial (Ptacek and Gillham, 1992) and 18 g solid in 40 ml nominal volume vial (approximately 2:1, Allen-King *et al.*, 1997b).

²⁴ It was found that separation by centrifugation required the solution to be ionic. For this reason 0.2 g/l NaHCO₃ solution was used for batch sorption experiments, chosen as these ions are commonly present in groundwater. Many researchers use 'synthetic groundwater' (for example, Allen-King *et al.*, 1995) designed to approximate to the groundwater chemistry from the site of the sample under investigation. The samples in this study are from several locations with differing groundwater chemistry: using a different synthetic groundwater to represent each sampling location would have varied water chemistry between batch reactors.

Chapter 9: Measuring Sorption

The batch reactors were mixed at $22^{\circ}\text{C} \pm 1^{\circ}\text{C}$ for 48 hours by rotation at 33 rpm. Mixing ensures continued and intimate contact between the solid and the solution, removing dependence on diffusion: Ball and Roberts (1991) found that continuous mixing was required for short-term sorption measurements. After 48 hours the batch reactors were centrifuged at 2200 rpm for 30 minutes ($757 \times$ gravity) leaving a clear supernatant, and providing a Stoke's equivalent settling radius of just $0.013 \mu\text{m}$. This separation technique is commonly applied: Allen-King *et al.* (1997b) used 2000 rpm (828g) for 30 min on clay-rich glacial samples, and found results consistent with those from experiments which separated solids from liquids with dialysis tubing (Allen-King *et al.*, 1996b); other examples include Ball and Roberts, 1991; Allen-King *et al.*, 1998; Mackay *et al.*, 1986; Ptacek and Gillham, 1992.

Time to equilibrium was measured using high and low TCE concentrations on a high TOC sample ($\sim 18\%$ TOC), and at high TCE concentrations on a lower ($\sim 0.2\%$) TOC sample over a range of time periods (between 4.5 and 120 hours). These indicated that most of the sorption occurred in the first few hours, and that the extent of sorption did not change measurably between about 24 and 120 hours (Figure 52). This confirm other reports of 24 or 48 hour equilibration periods (for example, Allen-King *et al.*, 1997b; Mouvet *et al.*, 1993) and consequently time to equilibrium was not determined on all experimental conditions. A time period of 48 hours was used in batch experiments.

Figure 52: Concentration change in batch reactors over time

Sorption continues slowly over much longer time periods, possibly associated with changing bonding of sorbents to sorbate. Some studies using other chlorinated solvents have reported increasing sorption for tens or hundreds of days (Ball and Roberts, 1991). There is 'a growing body of evidence that sorption and desorption may not reach equilibrium within time scales characteristic of solute transport or degradation' (Ball and Roberts, 1991). Time constraints prevented an investigation of such long-term phenomena.

After centrifugation, the supernatant liquid was sampled through the septa using micro-syringes of appropriate volume, diluted into organic-free water in full 40 ml nominal volume vials to within the GCMS analysis range and the TCE concentration measured.

9.5.3 Loss into headspace

The careful filling of the batch reactors does not eliminate all headspace. Air bubbles of approximately 0.4 ml were measured after 48 hours equilibration and centrifuging, in contact with approximately 31 ml water. The effect of TCE volatilising into this headspace at room temperature is calculated using its Henry's Law constant (K_H), the air-

Chapter 9: Measuring Sorption

water distribution ratio of a neutral compound (such as TCE) at dilute concentrations in pure water:

$$K_H = \frac{P_i}{C_w} \text{ in (atm.l. mol}^{-1}\text{)}$$

where:

K_H = Henry's Law constant

P_i = partial pressure of the chemical in the gas (in atm; 1 atm = 10^5 Nm^{-2})

C_w = molar concentration of the dissolved chemical

To convert P_i to moles per total gas volume:

$$\frac{n_i}{V} = \frac{P_i}{RT}$$

where

n_i = no of moles

V = volume

R = gas constant (8.314 Nm/mol.deg)

T = temperature in Kelvin (295K)

As the methanol and TCE concentrations were selected to maintain solution ideality, it can be assumed that the TCE is present dissolved in pure water. Using K_H of 0.0085 atm-m³/mol for 22°C (between 0.00713 at 20°C and 0.00937 at 25°C, atm-m³/mol; Pankow and Cherry, 1996), it was calculated that less than 0.5% of the TCE present in the batch vials is volatilising into the headspace.

9.5.4 GC-MS analysis

Analysis was by GC-MS operating with an automatic purge and trap; analysis conditions are detailed in Appendix G. Analytical runs (up to 48 analyses) were calibrated with two sets of six TCE calibration standards, producing a linear calibration. For calibration standards, TCE dissolved in methanol was spiked into ultra-pure water in autosampler vials (USEPA recommended), for a concentration range of 1 to 20 µg/l. Known concentration standards and blanks (vials containing ultra-pure water only) were analysed throughout each run. The TCE degradation products dichloroethene and vinyl chloride were also searched for, but were not detected, indicating no degradation of TCE. Peak areas for blanks were less than 1% of typical sample peak areas, so blank corrections were

not made. Selective ion monitoring provides a very low detection level, enabling measurement of very low TCE concentrations in blanks. The small blanks were found to be due to memory effects from previous samples (Appendix G).

Analysis of liquid from solid-containing and solid-free blanks with methanol added, and of blanks of NaHCO_3 solution only, revealed TCE concentrations below the detection limit, indicating that no TCE contamination occurred from the experimental procedure or from the original samples.

The loss due to sorption was determined as the difference between amount lost from the batch sorption reactors and amount lost from the TCE-free batch vials (assumed to be sorption to the vial and diffusion through the septa). The sorbed concentration of TCE (as mass TCE per mass soil or per mass solid organic carbon) was plotted against concentration remaining in solution, to display the sorption isotherm. As the sorption isotherms over this concentration range were not linear, a single partition coefficient was not determined. The experimental data was fitted to Freundlich isotherms; results of the sorption experiments and calculated isotherms are presented and discussed in Chapter 10, with correlations with organic geochemistry and morphology, and implications for contaminant transport.

9.6 Conclusions and Summary

- Sorption measurements are necessary to compare differences in sorption coefficient, and relate these to changes in organic carbon type.
- TCE was chosen as the sorbate, as it is a common groundwater contaminant, it is persistent in subsurface environments, and a significant body of previous research on the sorption of TCE enables comparison with previous results.
- A batch sorption method was chosen as it is simpler and quicker than alternative methods to measure sorption. It therefore enables a greater number of samples and concentrations to be investigated, and sorption isotherms to be constructed.
- A method to undertake batch sorption experiments was developed.
 - It was found necessary to use an ionic solution to enable centrifugation separation of solids and liquids.

Chapter 9: Measuring Sorption

- Use of a methanolic TCE solution overcame difficulties in dissolving TCE directly in water; care was taken to maintain solution ideality.
- Measurement of sorption through time for two samples at high and low TCE concentrations supported the use of a 48 hour equilibration time, common in reported batch sorption studies.
- A high solid to solution ratio would enable greatest concentration change in the analysed solution.

The method developed was applied to seven samples, and the results detailed in Chapter 10.

10. Sorption: results and discussion

10.1 Introduction

Batch sorption experiments using trichloroethene (TCE) were undertaken in order to calculate sorption isotherms and hence K_{oc} values. Sorption isotherms indicate the relationship between sorption and solute concentration. The relationship between the distribution coefficient and the sample total organic carbon (TOC) content was examined to identify the extent to which TOC content controls sorption and any relationship with geochemistry and morphology. Results from sorption experiments have been used as inputs for contaminant transport modelling (Chapter 11) to identify the importance of these features.

Batch sorption experiments were undertaken on seven samples following the method described in Section 9.5. As seen from the results presented in Chapters 5, 7 and 8, samples of Glacial Till, Lincolnshire Limestone, made ground and silty clay represented a range of material types, TOC content and extent of oxidation / weathering. The two Lowestoft Till samples, from 1.5 to 2 m and 8.5 to 9m bgl, had different AIC²⁵ (0.2% and 0.7% respectively) and extent of weathering (judged visually and confirmed by differing H/O ratios). They both contained a large proportion of amorphous matter, slightly more in the shallower, oxidised sample, with 'black wood' as the next most abundant component. The three samples from Site B had different organic geochemistry. Two samples of made ground from 2m and 3m below ground level (bgl) had different AIC (18.5% and 1.1%), organic matter geochemistry and morphology. The other sample from Site B (6m bgl) was grey brown silty clay with 0.55% AIC. Samples from Site B all had greater brown and black wood content than Glacial Till or Lincolnshire Limestone samples. Two samples containing greater than 0.1% AIC were selected from the Lincolnshire Limestone, expected to display measurable sorption. A sample of Kirton Shale had 2.0% AIC content, associated with a greater clay content. The other was more pure limestone from the Sleaford member, with 0.2% AIC. The organic geochemistry of these samples is detailed further in Chapter 7 and the morphology of isolated organic matter presented in Chapter 8.

²⁵ These AIC results were measured on subsamples of the material used in sorption experiments.

Chapter 10: Sorption results and discussion

This introduction (Section 10.1) includes details of the samples selected for sorption study. The sorption isotherms resulting from the batch sorption experiments (Section 10.2) are presented both per gram of sample and after normalisation to the organic carbon content of the sample. Much of the difference in the extent of sorption between different samples is not accounted for by differences in their organic carbon content, and their geochemistry (Section 10.3) and morphology (Section 10.4) are examined to determine whether these details can be used to predict their varying sorption. Section 10.5 summarises the points made in this chapter.

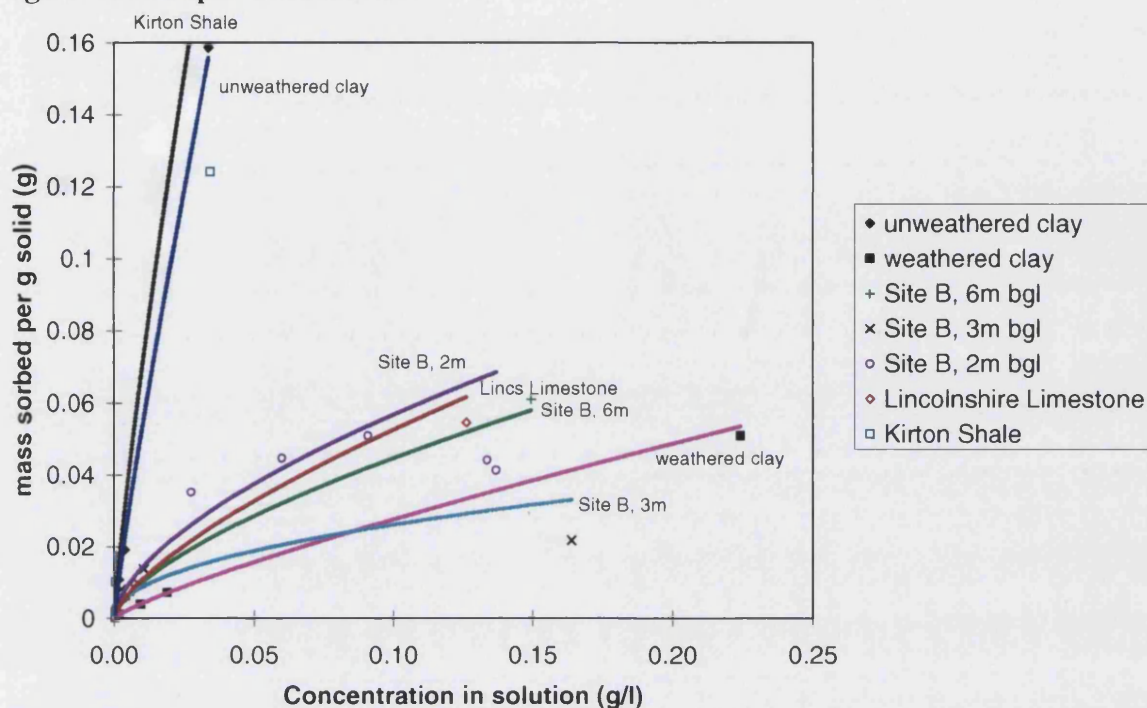
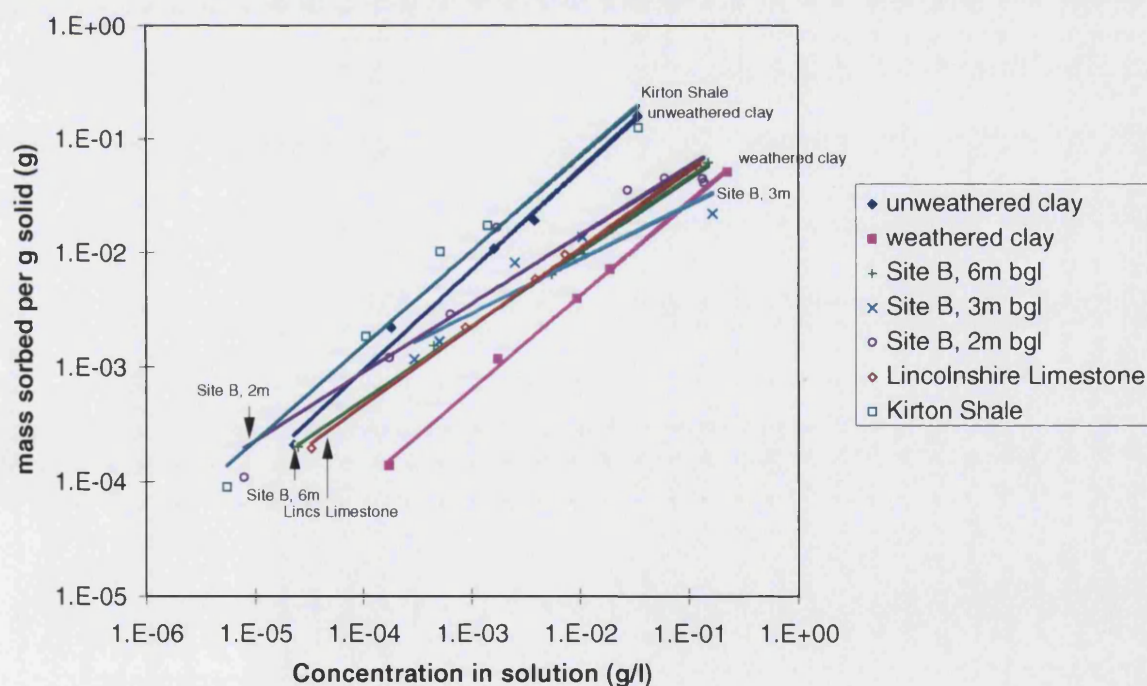
10.2 Sorption isotherms

The results are presented here graphically and data tabulated in Appendix H, and isotherms are fitted to the data (Figure 53 to Figure 56). It can be seen from these diagrams that the range of equilibrium trichloroethene (TCE) concentrations differ significantly between samples (Table 35). The starting concentrations used for each material were similar; the difference in equilibrium concentration is due to the different extent of sorption in each sample.

Table 35: Range of equilibrium trichloroethene concentrations

Sample	Minimum TCE concentration	Maximum TCE concentration
Weathered Till	1.7×10^{-4} g/l	0.22 g/l
Unweathered Till	2.3×10^{-5} g/l	0.034 g/l
Site B, 2m bgl	7.9×10^{-6} g/l	0.14 g/l
Site B, 3m bgl	2.9×10^{-4} g/l	0.16 g/l
Site B, 6m bgl	2.5×10^{-5} g/l	0.15 g/l
Lincolnshire Limestone	3.3×10^{-5} g/l	0.13 g/l
Kirton Shale	5.5×10^{-6} g/l	0.034 g/l

Measured sorption isotherms plotted on linear (Figure 53) and logarithmic (Figure 54) axes indicate non-linear sorption for all samples.

Figure 53: Sorption isotherms**Figure 54: Sorption isotherms, with logarithmic scale**

If organic carbon content were the only factor controlling the extent of sorption, differences in extent of sorption between samples would be removed by normalising the sorption to organic carbon content. Normalisation reduces but does not remove the wide variation (compare Figure 53 and Figure 54 with Figure 55 and Figure 56). This confirms

Rivett's view (Rivett, 2000) that '*measuring foc does not guarantee that the $foc \times K_{OC}$ calculation will work*'. Indeed, in the case of made ground, (Site B, 2m bgl and 3m bgl), such normalisation illustrates the very poor sorptive capacity of its organic carbon.

Figure 55: Sorption isotherms, per gram organic carbon

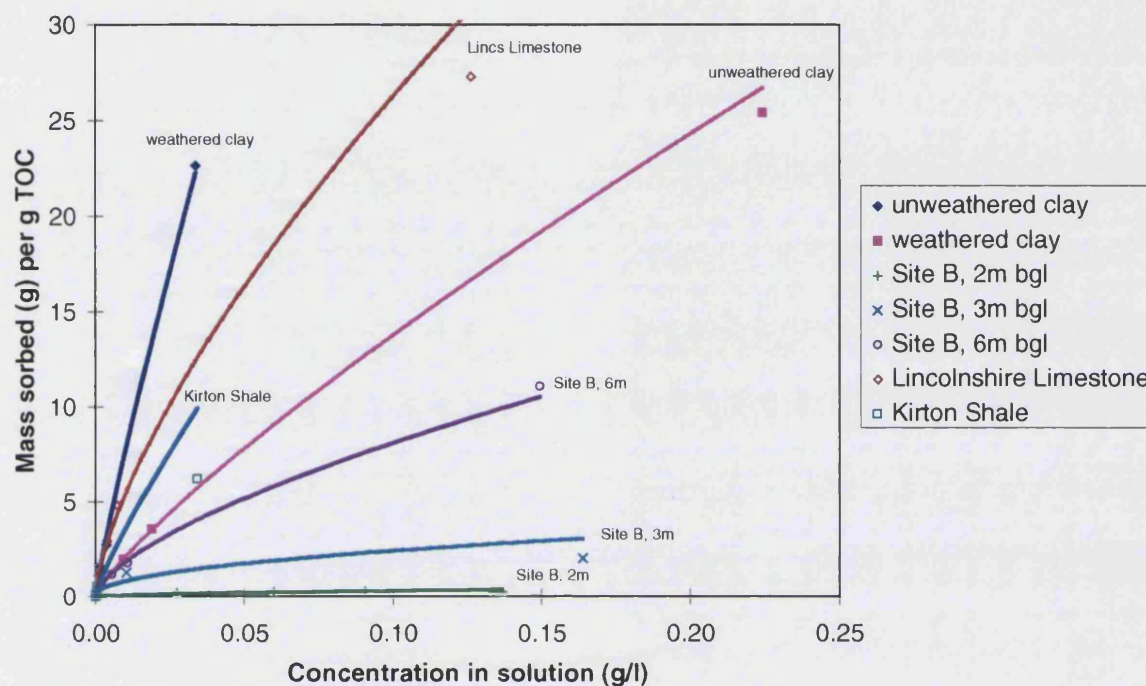
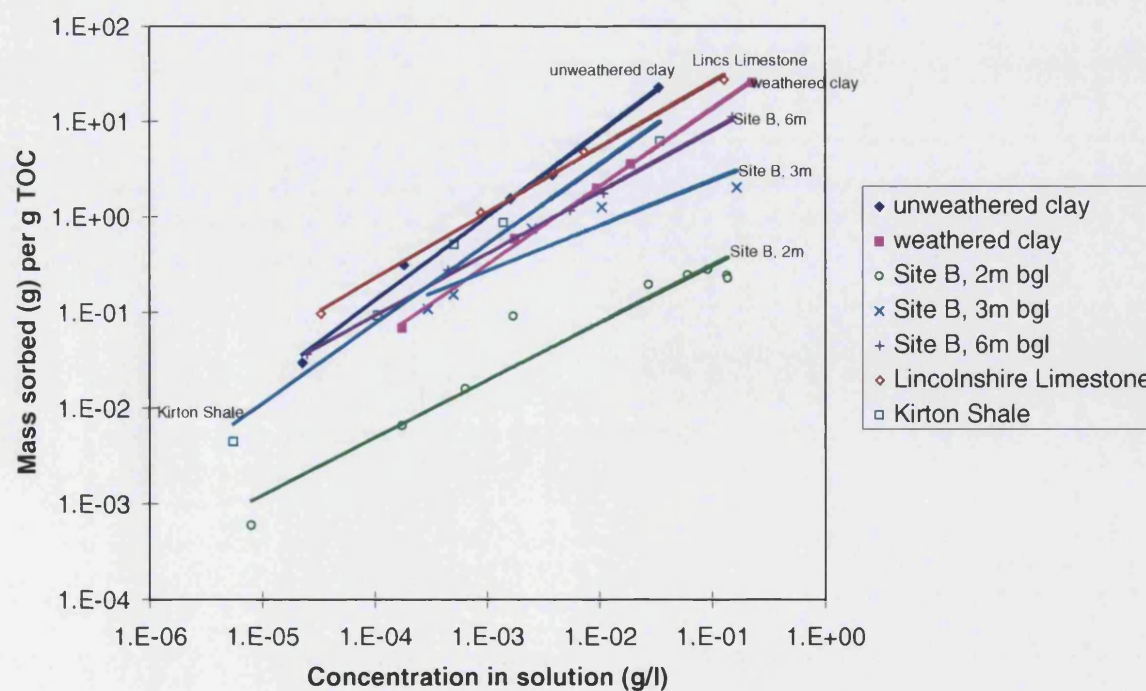


Figure 56: Sorption isotherms per gram organic carbon, with logarithmic scales

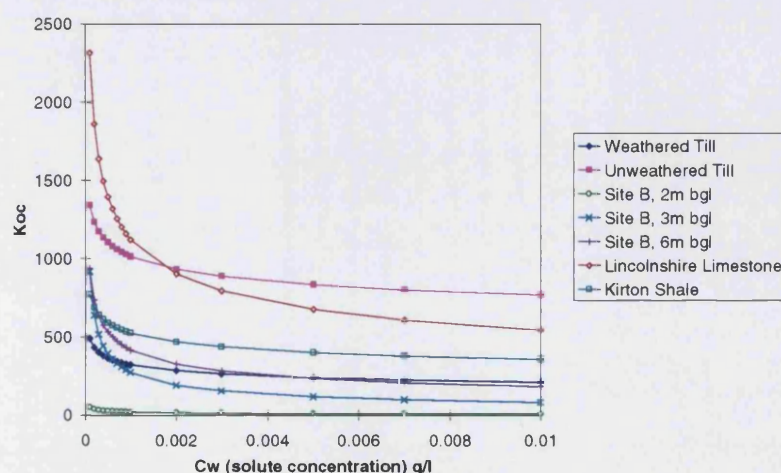


The observed range of K_{OC} values for each sample (Table 36) is due to sorption non-linearity, which produces concentration-dependent K_{OC} values. Because maximum and minimum K_{OC} values for each sample are not from the same equilibrium concentration, they cannot be directly compared. To enable direct comparison, K_{OC} values have been calculated from Freundlich isotherms fitted to the data (Table 37) at an equilibrium solute concentration of 0.01 g/l TCE. These show that K_{OC} at this concentration varies by a factor of one hundred between made ground (Site B, 2m bgl, $K_{OC} = 7.85$) and unweathered glacial till ($K_{OC} = 767$). Many of the measured K_{OC} values at this concentration fall within the 50 to 500 l/kg range from most previously published literature (Allen-King *et al.*, 1997b, see Section 7.4). At lower concentrations, K_{OC} values for many samples exceed 500 l/kg. K_{OC} values for each sample do not vary in proportion to each other, due to different isotherm non-linearity; this is illustrated in Figure 57, which shows that these curves converge or diverge at different concentrations.

Table 36: Range of K_{OC} values measured

Sample	Min. K_{OC} (l/kg)	K_{OC} at 0.01 g/l TCE (l/kg)	Max. K_{OC} (l/kg)
Weathered Till	113	211	401
Unweathered Till	674	767	1315
Site B, 2m bgl	1.66	7.85	75.2
Site B, 3m bgl	12.3	81.3	370
Site B, 6m bgl	74.3	184	1480
Lincolnshire Limestone	217	543	2966
Kirton Shale	181	356	813

Figure 57: Variation of K_{OC} with solute concentration



Chapter 10: Sorption results and discussion

Sorption data may be represented by a Freundlich isotherm of the form $C_s = K_F C_w^N$ (Section 2.2.1) where C_s is the sorbed concentration, C_w is the dissolved concentration and K_F and N are constants. Freundlich isotherms of the sorption data are plotted on Figure 53 to Figure 56 and given in Table 37, normalised both to gram of solid and to gram of organic carbon. The Freundlich constant normalised to organic carbon (K_{FOC}) is also provided; the slope and fit of the isotherms is not altered.

Table 37: Freundlich isotherms fitted to the experimental data

Sample	TOC (%)	Freundlich K_F	Freundlich N	Freundlich K_{FOC}	r^2
Lowestoft Till, 1.5-2m	0.2	0.18	0.82	90.6	0.998
Lowestoft Till, 8.5-9m	0.7	3.07	0.88	439	0.992
Site B, BH9, 2m bgl	18.5	0.23	0.60	1.24	0.937
Site B, BH9, 3m bgl	1.1	0.078	0.47	7.21	0.871
Site B, BH9, 6m bgl	0.55	0.20	0.65	36.0	0.998
Lincs Lmsth 67.5-67.6m	0.2	0.26	0.69	128	0.997
Kirton Shale 75.9-76.0m	2.0	3.3	0.83	165	0.974

The r^2 value is calculated by Excel using a transformed regression model.

Alternatively, sorption may be modelled with a Langmuir isotherm (Section 2.2.2) of the

form $\frac{C_w}{C_s} = \frac{1}{\alpha\beta} + \frac{C_w}{\beta}$ where α is the absorption constant related to binding energy and

β is the maximum amount of solute that can be sorbed by the solid. If the experimental points fitted this isotherm, a plot of C_w against C_w/C_s would be linear. This is not the case (Figure 58) for most samples; however the two made ground samples (Site B, 2 m bgl and 3 m bgl), and the Kirton Shale sample fit the Langmuir isotherm better than the Freundlich isotherm (Table 38).

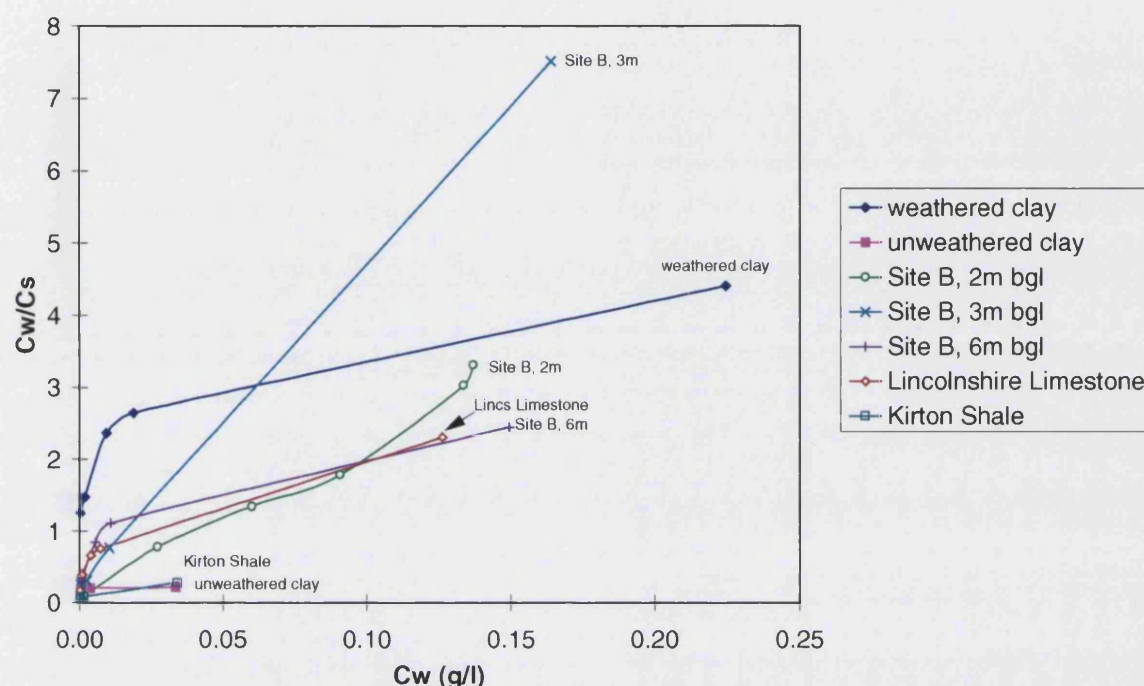
Table 38: Langmuir isotherms (per gram solid)

Sample	$1/\beta$ (slope of line)	$\alpha\beta$ (intercept of line)	r^2 value
Weathered Till	11.798	1.8278	0.84
Unweathered Till	2.7084	0.128	0.49
Site B, 2m bgl	21.913	0.101	0.99
Site B, 3m bgl	44.34	0.2517	0.99
Site B, 6m bgl	13.127	0.526	0.86
Lincolnshire Limestone	14.926	0.4431	0.95
Kirton Shale	6.3401	0.0591	0.99

Note: for some of these curves, r^2 values are fitted to data that is far from being normally distributed and are therefore dubious or possibly meaningless.

Figure 58: Plot of C_w against C_w/C_s

(lines are smoothed curves joining data points)



The data from the sorption experiments provides a range of sorption distribution coefficients that is not accounted for by the range of TOC in the samples analysed. It is therefore suggested that some characteristic of the organic matter affects the sorption of the materials. This is examined in the next two sections (10.3 and 10.4). Additionally, non-linear sorption isotherms have been observed, displaying a wide range of degrees of non-linearity. The Langmuir isotherm is based on the concept that the samples have a limited, potentially exhaustible, number of sorption sites. As discussed in Section 2.4.3, sorption processes may combine Langmuir-type and linear (dissolution-type) sorption, producing a Freundlich sorption isotherm as the sum of these two processes. The made ground samples may receive a relatively small contribution to sorption from dissolution-type partitioning, and 'binding sites' for Langmuir-type sorption may become exhausted, within the concentration range used.

10.3 Correlation with geochemical characteristics

It has been proposed that variations in K_{OC} of the same solute to different materials is due to variations in the composition of the organic matter (OM) (Section 2.4; Binger *et al.*, 1999 and references therein). To examine this, the organic carbon normalised K and N values of the Freundlich isotherms, and geochemical characteristics of the samples are presented in Table 39 and Figure 59. K_{OC} at 0.01 g/l TCE has been calculated from the Freundlich isotherms, and is used in Figure 59 to remove variation due to different degrees of non-linearity.

Table 39: Measured sorption and geochemical data

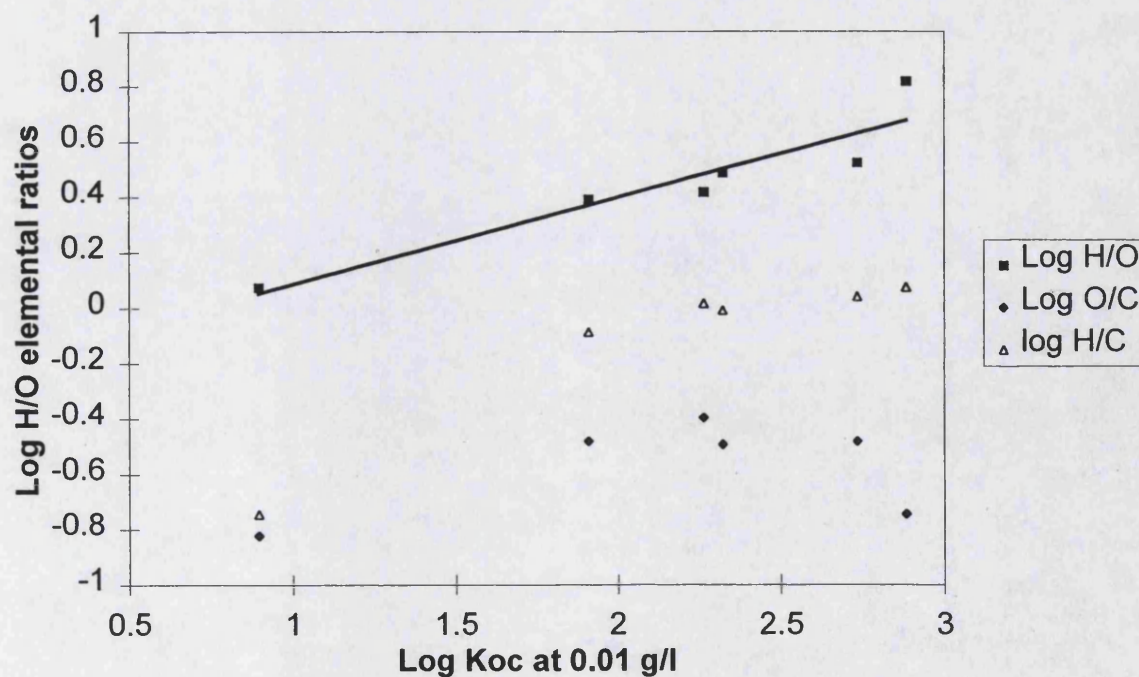
Sample	Freundlich Koc	Koc at 0.01 g/l TCE	Freundlich N	O/C	H/C	(O+N)/C	H/O	Tmax	HI
Weathered Till	90.6	211	0.8167	0.32	0.98	0.356	3.063	414	63
Unweathered Till	439	767	0.8788	0.18	1.19	0.2062	6.572	426	188
Site B, 2m bgl	1.2441	7.85	0.6001	0.15	0.18	0.1711	1.186	400	3
Site B, 3m bgl	7.2097	81.3	0.4738	0.33	0.82	0.3634	2.465	420	78
Site B, 6m bgl	36.001	184	0.6461	0.4	1.04	0.4362	2.614	420	104
Lincolnshire Limestone	127.6	543	0.6854	0.33	1.1	0.3571	3.332	434	119
Kirton Shale	164.56	356	0.8324	n.a.	n.a.	n.a.	n.a.	428	121

Elemental ratios presented in Section 7.3.

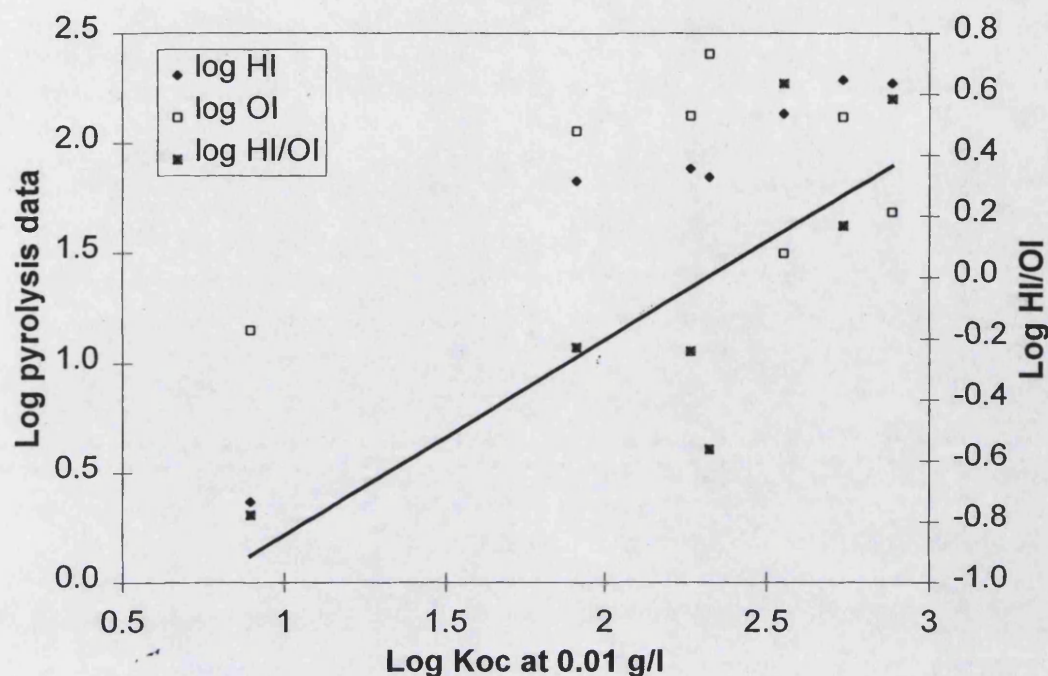
n.a. = not analysed. OM was not isolated from Kirton Shale due to insufficient sample.

Figure 59: Relationship between K_{OC} and geochemical results

Elemental ratios



Rock Eval results



A correlation between the oxidation state, represented by the H/O ratio and K_{OC} (at 0.01g/l TCE) corroborates Grathwohl (1990) and Binger *et al.* (1999), using a wider range of sample materials than in either of those earlier studies. The correlation has the equation $\text{Log } K_{fOC} = 3.63 \text{ Log (H/O)} - 0.10$ ($r^2=0.89$) where K_{fOC} is the carbon-normalised Freundlich coefficient or

$\text{Log } K_{OC} = 1.25 \text{ Log (H/O)} - 1.17$ ($r^2 = 0.93$) with K_{OC} 0.01g/l.

This is similar to a published correlation:

$\text{Log } K_{OC} = 1.52 \text{ Log (H/O)} + 1.54$ (Grathwohl, 1990).

Another correlations has been obtained using tetrachloroethene (PCE) rather than TCE as the sorbate. These are similar chemicals; PCE sorbs more strongly than TCE:

$\text{Log } K_{OC} = 2.57 \text{ log (H/O)} + 1.49$ (K_{OC} at about 80 μ g/l, Binger *et al.*, 1999).

The second chart in Figure 59 illustrates the relationship between $\log K_{OC}$ and the hydrogen index (HI) and oxygen index (OI) produced by Rock-Eval pyrolysis. As discussed in Chapter 7, the HI/OI ratio is approximately proportional to the elemental H/O ratio of isolated organic matter (Figure 40). Therefore, the relationship that is observed between elemental H/O and K_{OC} is also observed between HI/OI and K_{OC} . This indicates that Rock-Eval pyrolysis could provide a useful method to gain the oxidation details and predict sorption.

The correlation above indicates the dependence of sorption on the state of oxidation of the sample's organic matter. The two glacial till samples most closely represent samples with different oxidation states but otherwise similar source and mineralogy, and are therefore specifically discussed.

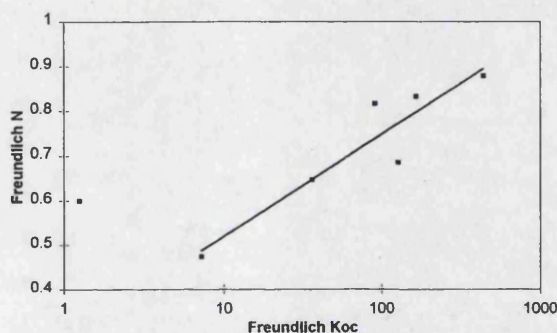
Greater sorption to unweathered glacial till than to weathered glacial till (independent of the TOC) specifically corroborates the greater sorption to unweathered till samples than to weathered till found by Binger *et al.* (1999). K_{OC} values previously measured in glacial till samples of 7800 to 15700 l/kg (Allen-King *et al.*, 1997) and 2240 to 38900 l/kg (Binger *et al.*, 1999) are much higher than those presented here. Allen-King *et al.* (1997) conclude that high K_{OC} in glacial till may be due to some characteristic of the organic material in the till. After conducting batch sorption experiments on samples with TOC content strongly reduced (up to 90% removed) by baking they concluded that minerals contribute very little sorption.

Binger *et al.* (1999) carried out batch sorption experiments over a very limited concentration range, and do not provide Freundlich N values, but do say that they are not significantly different between different samples. Huang and Weber (1997) found that sorption increases and sorption isotherms become more non-linear (lower N) as O/C decreases though diagenetic alteration. In this study, the reverse of Huang and Weber's observation on the non-linearity of the samples is found. Freundlich N increases with decreasing sorption (i.e. decreasing Freundlich K_{OC}), with the equation

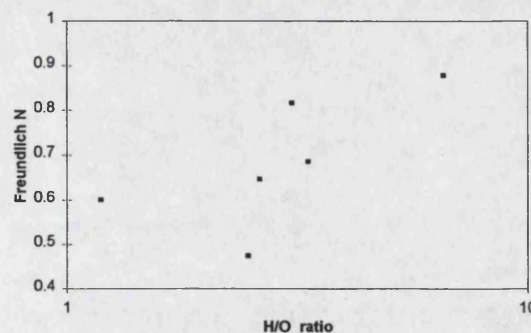
$N = 0.06 \ln K_{OC} + 0.5$, $r^2=0.65$ (Figure 60). The correlation is stronger if the made ground sample with very low K_{OC} (Site B, 2m bgl) is excluded ($N = 0.1 \ln K_{OC} + 0.3$, $r^2=0.87$). As K_{OC} is correlated to H/O, a weak correlation between Freundlich N and H/O ratios can be seen.

Figure 60: Correlation of Freundlich N with K_{OC} and H/O

Freundlich N with Freundlich K_{OC}



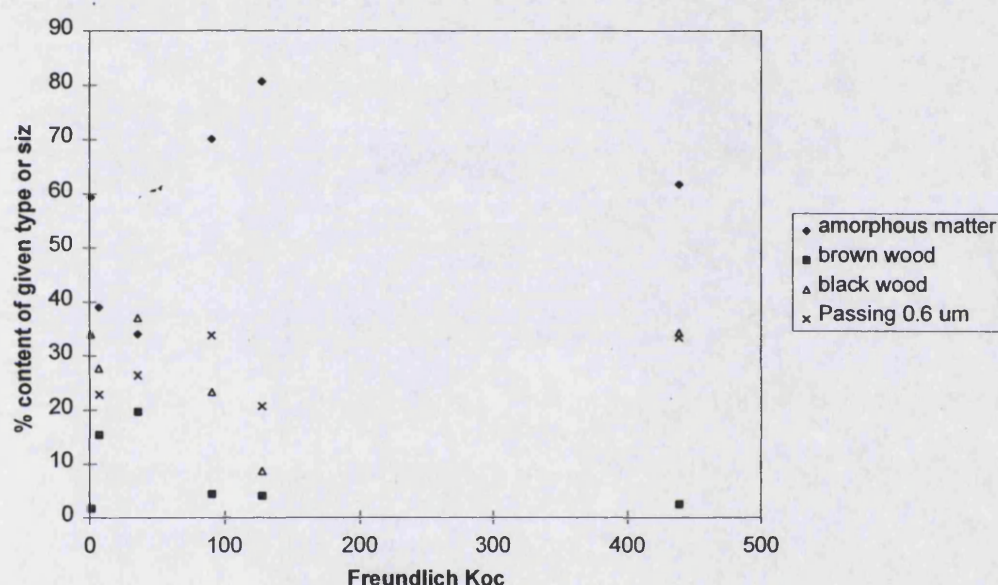
Freundlich N with H/O ratio



10.4 Correlation with physical characteristics

There is no clear correlation between the Freundlich K_{oc} and either the OM morphological types contained in or the particle size distributions of these samples. The % amorphous, brown wood and black wood content of the samples, and the % of organic particles finer than $0.6\mu\text{m}^2$, are plotted against the Freundlich K_{oc} (Figure 61). Whilst it is considered likely that different morphological types of OM have different chemical composition, no clear trend between atomic ratios and morphology or particle size is apparent. Variation in morphology between these samples is not extensive.

Figure 61: Sorption plotted with morphological type content and % passing $0.6\mu\text{m}$



10.5 Retardation factor

The retardation factor can be calculated from the sorption coefficients; the appropriate equations are presented in Section 2.2. Retardation factors based on Freundlich sorption isotherms have been calculated for the seven samples for which isotherms been experimentally determined (Table 39a). These use estimated bulk density of $1.2\text{g}/\text{cm}^3$ and effective porosity of 0.4 for the made ground samples, and bulk density of $1.7\text{g}/\text{cm}^3$ and porosity of 0.3 for the other samples.

Table 39a: Retardation coefficients

Sample	Retardation factor
Weathered till	2.92
Unweathered till	27.6
Site B, 2m bgl	3.61
Site B, 3m bgl	2.26
Site B, 6m bgl	4.69
Lincolnshire Limestone	5.24
Kirton Shale	4.40

10.6 Summary

- Sorption isotherms for TCE measured in this study were non-linear. For most samples, the Freundlich isotherm provided the best fit to the data, although the Langmuir isotherm better fitted made ground samples and Kirton Shale. In general, samples with lower organic carbon normalised Freundlich K values have greater Freundlich N values (i.e. are more non-linear). This may be because when sorption is more limited, saturation of the sorbed chemical is reached more rapidly, and greater non-linearity is observed. Alternatively, referring to the DRDM model (Section 2.4.3), materials with lower sorption capacity may have a proportionately smaller capacity for linear dissolution-type partitioning and a greater influence from Langmuir binding-site-type partitioning, leading to both a better fit to Langmuir isotherms and greater non-linearity.
- The sorption partition coefficient differed by several orders of magnitude between samples. Such differences were accounted for to only a small degree by variation in the TOC content of the samples. The remaining variation in K_{oc} was found to be proportional to the oxidation state of the samples' OM, represented by the H/O ratio of the OM.
- Rock-Eval pyrolysis has been seen to produce HI/OI ratios that are correlated with organic matter H/O ratios. This method can therefore produce results that indicate the oxidation state of the material. Rock-Eval has been widely used as a screening tool for petroleum sample geochemistry. It is less time consuming than OM isolation for elemental analysis, and avoids the problems associated with the isolation procedure. It is therefore considered likely to provide an accessible method for commercial organisations and environmental consultants to measure sample oxidation and thereby estimate K_{oc} values for samples of materials from investigation sites.
- Current methods to estimate sorption, typically based on a linear partition of the sorbate, dependent on the TOC content of the material only, will not predict the extent of sorption. The published K_{oc} value chosen may be an order of magnitude or more different to that of the sample. The impact of the error introduced by using published K_{oc} values rather than sample-specific values is examined in Chapter 11 using computer simulations.

11. Computer Modelling

11.1 Introduction

In order to place the results of the batch sorption experiments in the context of contaminant transport, simulations of contaminant transport have been undertaken. Three materials were selected for the simulations, to represent the range of material types studied experimentally (Chapters 9 and 10). These were made ground, and both unweathered and weathered glacial till, simulating the empirical sorption isotherms. These materials were simulated for the same reasons they were studied experimentally: the made ground represents a material type typical of that encountered on industrial sites; and the glacial till represents an aquitard, likely to have significant sorption, that protects the major Chalk aquifer from contamination from the surface. The made ground was found to have much lower sorption than predicted from widely published values, and the unweathered till much more sorption. The experimentally measured weathered till K_{OC} values were similar to those widely published (Chapter 10).

The types of isotherms used and their retardation coefficients are described more fully in Chapter 2. The sorption isotherms applied in the models are based on empirical results presented in Chapter 10, and the physical properties of the glacial till simulated are based on literature reviewed in Chapter 4.

The impact of varying parameters on the retardation factor have been calculated (Section 11.2) and simulations of linear and non-linear sorption isotherms run using Bio1d software (a one-dimensional transport model that can simulate non-linear sorption, Section 11.3). The sensitivity of the Bio1d results to variation in input sorption and physical parameters has also been studied (Section 11.4).

11.2 Retardation factor

The retardation coefficient (R) represents the increase in rate of unretarded solute transport compared to solute transport retarded by sorption. For a linear isotherm, R is calculated as:

$$R = 1 + \frac{K_{OC} f_{OC} B_d}{n_e}$$

where R = retardation factor [dimensionless]

K_{OC} = partition coefficient to organic carbon [dimensions: L^3/M]

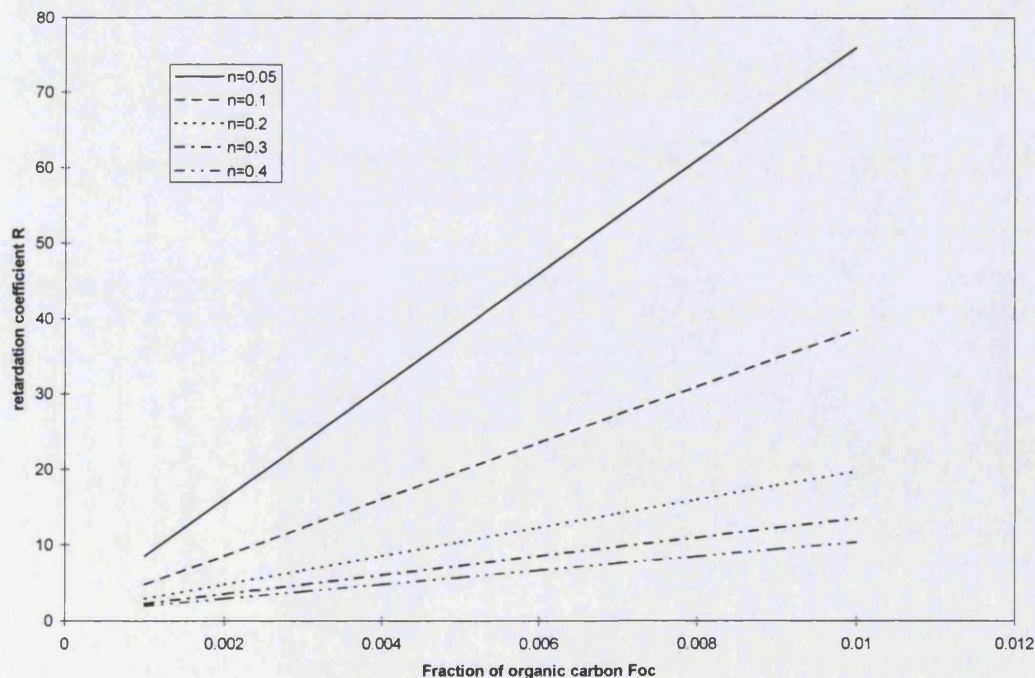
f_{OC} = fraction of organic carbon [dimensionless]

B_d = bulk density of porous medium [M/L^3]

n_e = effective porosity [dimensionless]

The greatest variation in R with TOC variation occurs at lowest porosity (n_e) (Figure 62) (Mouvet *et al.*, 1993). In a low porosity material, small variations in TOC may have a significant impact.

Figure 62: Variation of R with n and TOC for a linear isotherm



The retardation factor for Freundlich isotherms is:

$$R_F = 1 + \frac{B_d K_F N C_w^{N-1}}{n_e} \text{ giving a contamination velocity (v) of } v = \frac{K_i}{n_e + B_d K_F N C_w^{N-1}}$$

where symbols are as before, with:

R_F = Freundlich retardation coefficient (dimensionless)

K_F = Freundlich coefficient (dimensions depend on N; dimensionless when N=1)

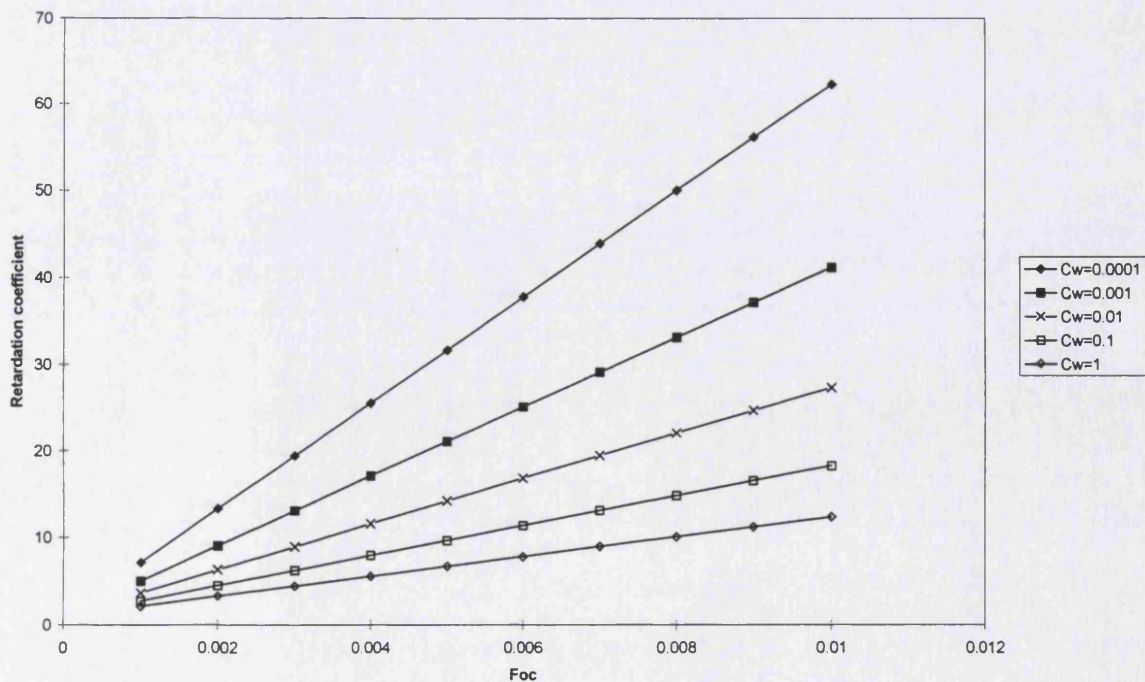
N = Freundlich exponent (dimensionless)

C_w = solute concentration [M/L³]

These formulae indicate the dependence of R_F and therefore v on C_w and N as well as K_F .

The variation of R with solute concentration (C_w in g/l) has been calculated (Figure 63) for the Freundlich isotherm generated experimentally for weathered glacial till (see Chapter 10), assuming mineral density of 2.5 g/cm³ and n_e of 0.2. Over the TOC range 0.1% to 1%, the retardation coefficient generated is between 3.3 and 5 times greater for low concentration solutions (0.0001 g/l) than for high concentration solutions (1 g/l). Low concentration solutions have the greatest K_d and thus the greatest R, and the greatest variation with TOC changes.

Figure 63: Variation of Freundlich retardation coefficient with concentration



Low Freundlich N (greatest non-linearity) gives greater retardation, which is more sensitive to TOC variation. This is modelled in Figure 64 and Figure 65 for $C_w=0.01$ g/l, $n_e=0.2$, mineral density $=2.5$ g/cm³, $K_{OC} = 90.6$ (as for weathered glacial clay).

Figure 64: Variation of R with TOC for varying Freundlich N

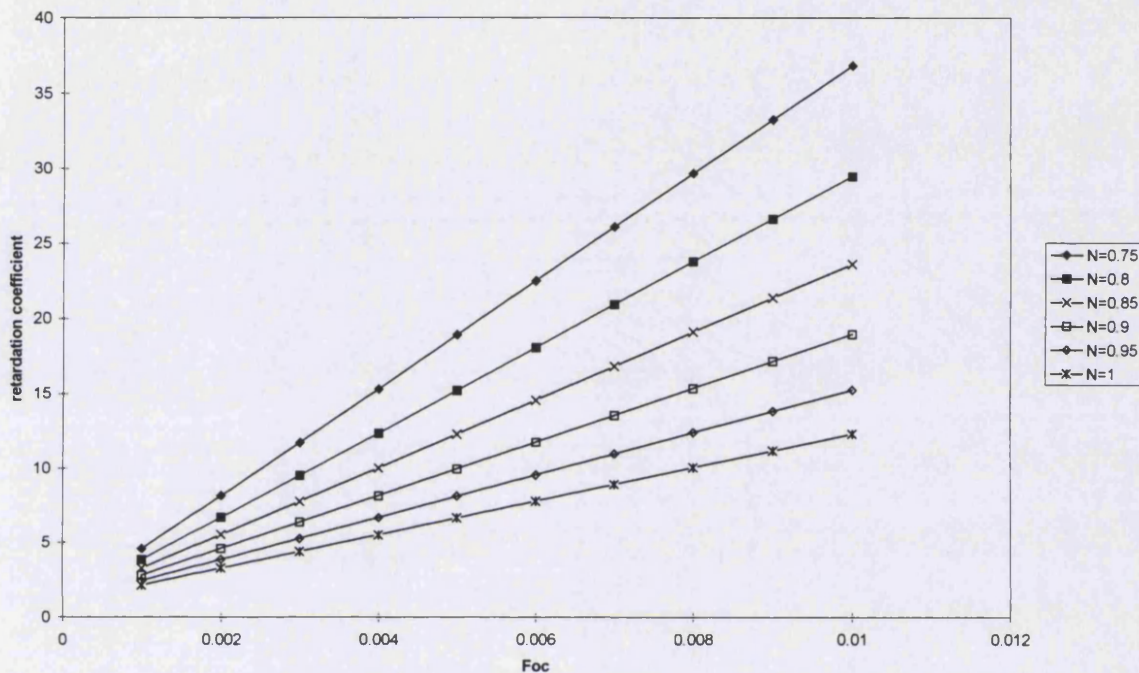
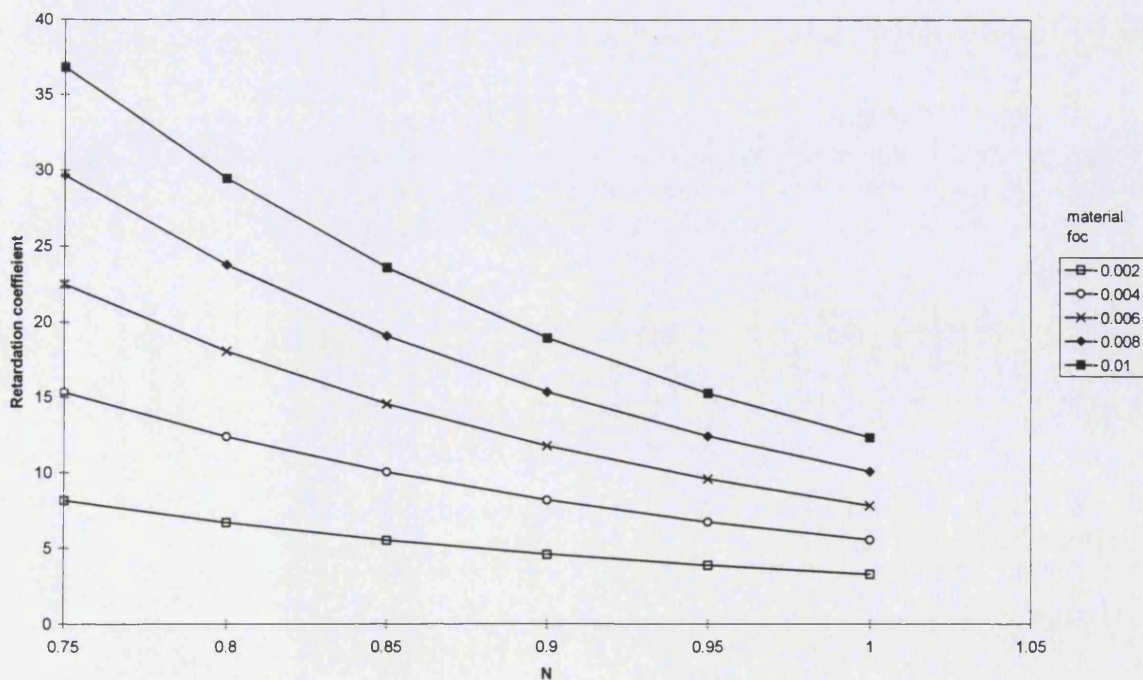


Figure 65: Variation of R with Freundlich N for varying TOC



As already noted, in low porosity materials, small variations in TOC may have a significant impact. Therefore, accurate TOC values are most important in low porosity materials. When modelled using a concentration-dependent isotherm, accurate TOC values are most important at low solute concentration and greatest non-linearity.

11.3 Bio1d simulations

Sorptive transport through three of the materials tested during this study was simulated using Bio1d (version 1.2, 1999, Srinivasan and Mercer, published by Geotrans, Inc.; Srinivasan and Mercer, 1988). Bio1d is a one-dimensional, finite difference model that can simulate sorption using linear, Freundlich and Langmuir sorption isotherms. It incorporates advective and dispersive transport of the solute and sorbate, in a porous sorbent. As only the liquid phase concentrations of the sorbate is simulated, desorption is disregarded, and sorption is assumed to be permanent. This will have the effect of removing the sorbate from the system completely, so that as its dissolved concentration decreases, the simulated concentration will not be supplemented by desorbing solute.

The scenario simulated was transport into either a 0.2m thick glacial till layer or a 4m thick made ground layer, based on materials tested in batch sorption experiments. The contaminant solute was forced into the ground under a hydraulic gradient of 1, such as would be produced by gravity driven flow (for the transport equations, saturation must be assumed). Simulations were run for 500 days for glacial till and 0.125 days for made ground. The time periods, layer thickness and hydraulic gradient were selected to provide contaminant peaks that had migrated from the boundary and that had not decreased to very low concentrations by sorption and dispersion. The low time periods used for the made ground indicate that at such high hydraulic conductivity with hydraulic gradient of 1, advection of the contamination will be so fast, that (even assuming that equilibrium sorption is reached) sorption will not usefully delay contaminant migration. However, understanding the sorption behaviour under these conditions for the brief period will indicate what input data has significant impacts on the modelling results and in which properties accuracy is important. Contaminant concentrations of 300 mg/l and 5 mg/l were applied to the boundary for 60 days for glacial till and 0.005 days for made ground. The input values of intrinsic velocity, dispersion coefficient (D) and effective porosity were calculated from physical properties presented in Table 40. D was calculated as

Chapter 11: Computer modelling

$D=0.1 \times L \times v$ (Spitz and Moreno, 1996) where v = intrinsic velocity and L = distance travelled by the contaminant peak (0.04m for till; 1m for made ground, the approximate distance travelled by the contaminant peaks, from iterative modelling and adjustment of the model).

Table 40: Properties used in simulations

Property	unweathered till	weathered till	made ground
bulk density (g/cm^3)	1.7 ^a	1.7	1.2 ^b
hydraulic conductivity (m/d)	8.6×10^{-6} ^c	8.6×10^{-6} ^c	5 ^d
effective porosity (%)	0.3	0.3	0.4
TOC (%)	0.7	0.2	20

a: from mineral density of 2.65 g/cm^3 , porosity of 0.3

b: mineral density of 2.0 g/cm^3 , porosity of 0.4

c: from laboratory hydraulic conductivity of 10^{-9} to 10^{-11} m/s (Lloyd *et al.*, 1981)

d: one rising head test in made ground at this site gave $K=5.8\text{m/d}$

Sorption isotherms investigated (Table 41) were based on experimental results (Chapter 10) and included the Freundlich isotherm and linear isotherm fitted over the complete experimental concentration range (referred to as Linear AC in the following discussion). Many published empirical data result from experiments undertaken at low concentrations only, and therefore another linear isotherm was fitted to data gathered at equilibrium TCE concentrations below 20 mg/l (referred to as Linear LC in the following discussion). In addition, a linear isotherm was investigated using K_{OC} of 152 ml/g (Fetter, 1994; see Section 9.4) and TOC measured for these materials during this study (Table 40). Made ground sorption results were well fitted by a Langmuir isotherm, so this was also investigated for the made ground simulation.

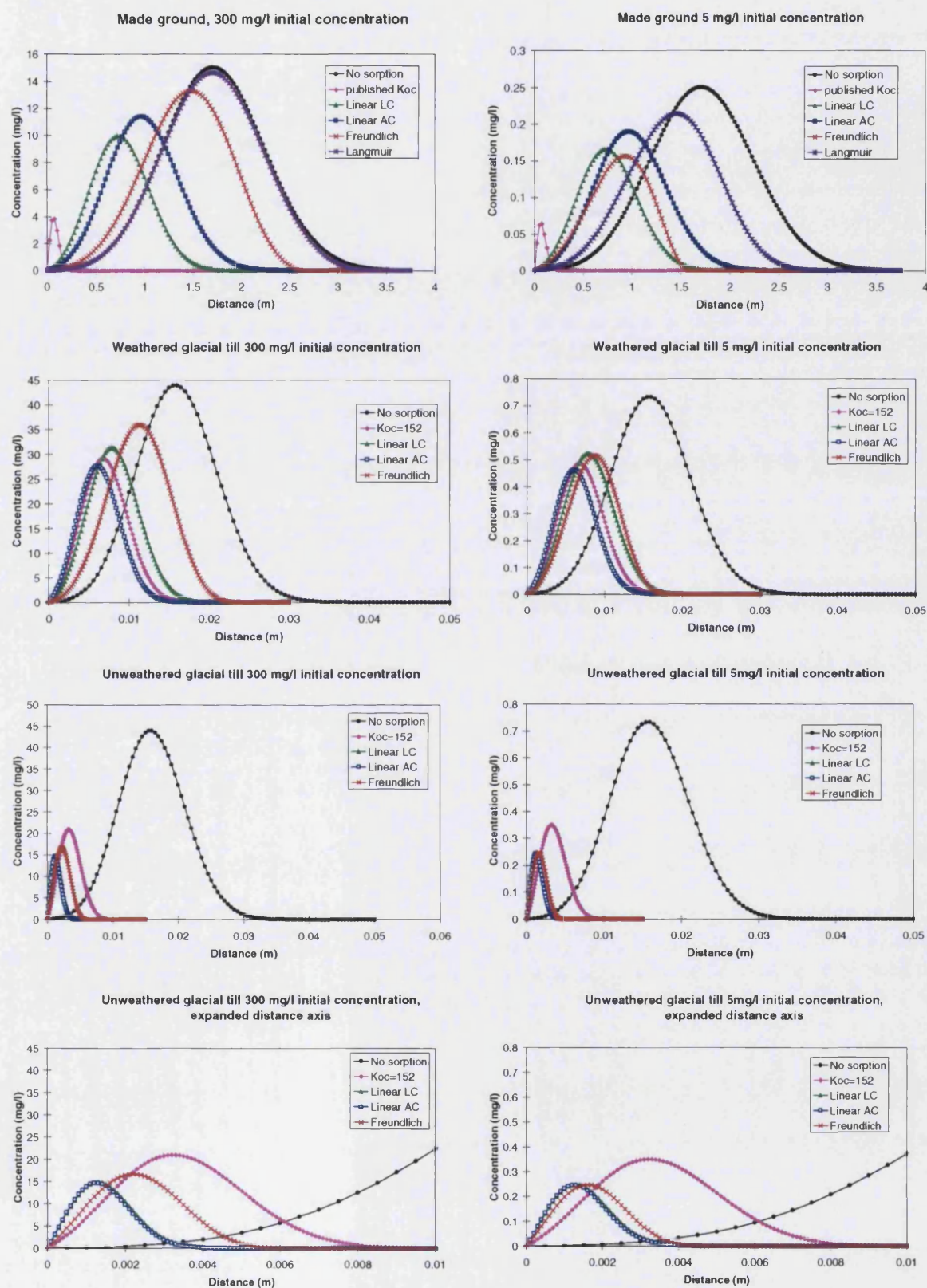
Table 41: Isotherms used in simulations

Isotherm	unweathered till	weathered till	made ground
Linear LC	$C_s=4.67C_w$	$C_s=0.22C_w$	$C_s=0.55C_w$
Linear AC	$C_s=4.94C_w$	$C_s=0.37C_w$	$C_s=0.30C_w$
Linear, $K_{OC}=152$	$C_s=1.06C_w$	$C_s=0.30C_w$	$C_s=30.5C_w$
Freundlich	$C_s=0.07C_w^{0.88}$	$C_s=0.18C_w^{0.82}$	$C_s=0.23C_w^{0.60}$
Langmuir	n/a	n/a	$\frac{C_w}{C_s} = \frac{1}{2.8 \times 0.053} + \frac{C_w}{0.053}$

n/a = not applied

The concentration profiles with distance from these three modelled scenarios are illustrated in Figure 66.

Figure 66: Concentration profiles from Bio1d simulations



Where the proportion sorbed decreases with increasing solute concentration (i.e. where the Freundlich isotherm has $N < 1$) linear sorption isotherms fitted to data over a lower concentration range will have higher K_d than linear isotherms fitted to data measured at higher concentrations. Therefore Linear LC isotherms have higher K_d s than Linear AC, and simulate greater sorption. For the unweathered till the Linear AC and Linear LC isotherms are very similar, and produce practically identical concentration profiles in the modelled scenario. For the other materials modelled the different concentration profiles produced by these two isotherms are distinguishable, but not very different. The unweathered till Freundlich isotherm leads to a similar peak concentration after 500 days as the empirical linear isotherms, but one which has travelled further. In weathered glacial till, the Freundlich isotherm leads to significantly less sorption at high concentrations than the linear isotherms. Freundlich isotherms predict proportionally greater partitioning onto the solid phase at low concentrations, hence the concentration profile in weathered till at low concentration is closer to that produced by the linear isotherms. In made ground, both peak concentration and distance travelled by the peak were clearly dependent on the isotherm. At high concentrations, the Langmuir isotherm produced solute transport very close to that from no sorption at all. The Freundlich isotherm produced the next smallest sorption, before the Linear AC then Linear LC isotherms. At a lower concentration (5 mg/l input), the Freundlich and Langmuir sorption isotherms both demonstrate proportionally much greater sorption.

These concentration profiles have been generated using material specific sorption isotherms, rather than published K_{OC} values, and they demonstrate the importance of doing so. Weathered glacial till produced empirical isotherms that are similar to those from published values, but the unweathered glacial till proved to be more strongly sorbing and the made ground sample much less so (Table 41). The impact of this variation can be clearly observed in the concentration profiles. Solute transport in the made ground sample with sorption based on published values produces a solute peak of much lower concentration and that has travelled a much smaller distance. In such a case, use of published sorption distribution coefficients would lead to a significant underestimate of the solute concentrations at a receptor. Conversely, sorption to unweathered till samples was found to be greater than expected from the published K_{OC} values, and the

concentration profile predicted from empirical data had a lower concentration peak that had travelled a smaller distance.

Modelling solute transport in these materials indicates that in neither case does sorption have a significant impact on the solute movement. In the made ground, high hydraulic conductivity results in rapid movement, such that at the modelled gradient solutes will have travelled several metres within a few hours. In the glacial till, transport through the matrix will enable movement of only a few centimetres in years. However, flow through fractures in glacial till will lead to more rapid solute transport with little delay from sorption. Fracture flow is beyond the scope of this study and has not been incorporated in the model. Rather, these materials have been modelled as examples to determine the extent to which choosing an accurate isotherm may affect solute transport results. The modelling confirms that accurate, material-specific, distribution coefficients are very important for even approximate sorption modelling.

The difference in outputs predicted by the linear isotherm from all the data and that from the lower concentrations varies with the non-linearity of the Freundlich isotherm. Unweathered till produced the most linear Freundlich isotherm, with $N=0.88$. The two linear isotherms fitted to this data produced very similar concentration profiles. The Freundlich isotherm fitted to the made ground data was the most non-linear, with $N=0.6$, and produced the greatest difference in concentration profiles from the two linear isotherms. The variation produced by concentration-dependent isotherms at different concentrations is less significant than the impact of using an accurate distribution coefficient. It is therefore more important to use an accurate K_d , even in a linear isotherm, than to use a concentration-dependent isotherm with an inaccurate K_d .

11.4 Sensitivity to inputs

To test sensitivity to the values selected for input into the simulation, simulations were run based on the Freundlich isotherm at the lower input concentration (5 mg/l) in made ground and weathered glacial till with varied input values. In turn, values for bulk density (Bd), effective porosity (n_e), hydraulic conductivity (K), Freundlich K_d and Freundlich N were altered by $\pm 20\%$ (Marsland and Carey, 1999, Environment Agency methodology document) and to maximum and minimum realistic values. Bd maximum and minimum

Chapter 11: Computer modelling

values were the result of combining likely maximum and minimum values of total porosity and mineral density. Changes in n_e and K affected input velocity and dispersion coefficient; changes in n_e were also input directly and used by Bio1d in adsorption calculations. The values used and their results are presented in Table 42 and Table 43, and Figure 67.

Table 42: Input values used for made ground

parameter varied		minimum	-20%	modelled	+20%	maximum
Bd	parameter value	0.75	0.96	1.2	1.44	1.75
	peak concentration	0.179	0.168	0.157	0.148	0.138
	peak distance	1.125	1.025	0.925	0.85	0.8
ne	parameter value	0.2	0.32	0.4	0.48	0.5
	peak concentration	0.167	0.161	0.157	0.153	0.152
	peak distance	1.225	1.025	0.925	0.85	0.85
K	parameter value	3	4	5	6	8
	peak concentration	0.126	0.142	0.157	0.17	0.194
	peak distance	0.6	0.75	0.925	1.1	1.45
Kd	parameter value	0.14	0.18	0.23	0.28	0.32
	peak concentration	0.181	0.169	0.157	0.147	0.141
	peak distance	1.15	1.025	0.925	0.85	0.8
N	parameter value	0.2	0.48	0.6	0.72	1
	peak concentration	0.066	0.129	0.157	0.175	0.204
	peak distance	0.7	0.875	0.925	0.975	1.075

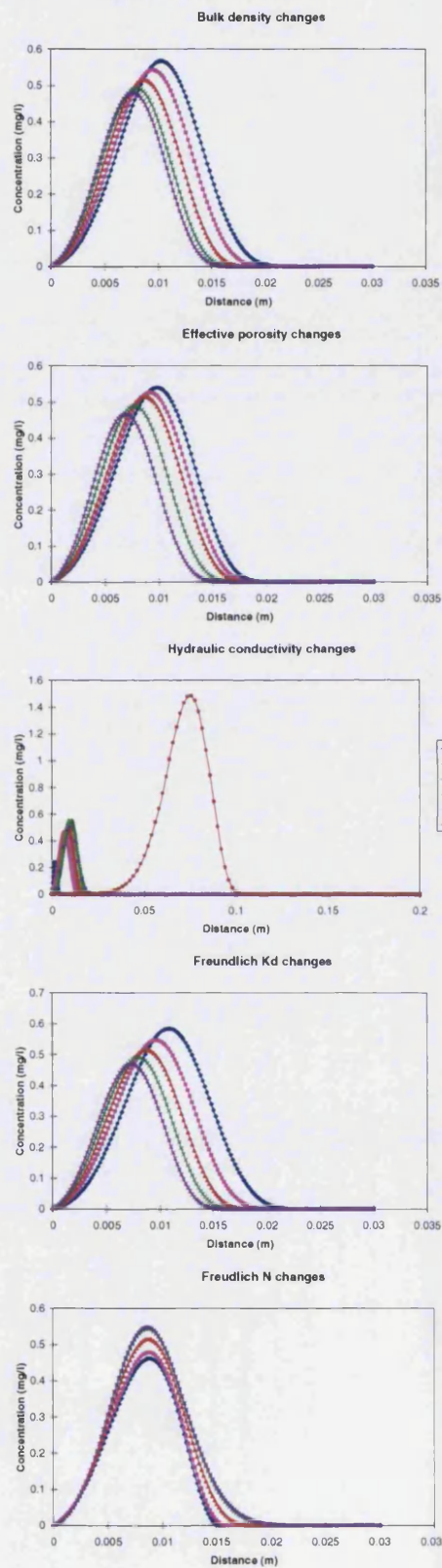
‘modelled’ indicates the value used in the models described in Section 11.3.

Table 43: Input values used for weathered glacial till

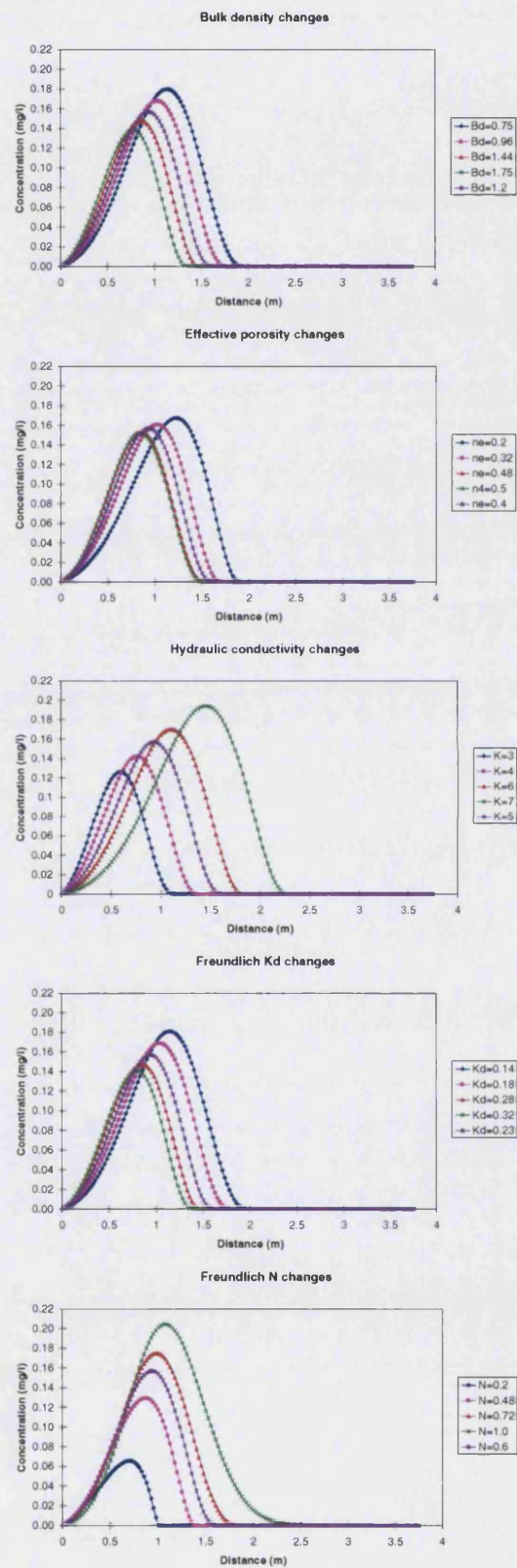
parameter varied		minimum	-20%	modelled	20%	maximum
Bd	parameter value	1.10	1.36	1.70	2.04	2.25
	peak concentration	0.558	0.543	0.516	0.493	0.481
	peak distance	0.0110	0.0096	0.0086	0.008	0.0076
ne	parameter value	0.20	0.24	0.30	0.36	0.45
	peak concentration	0.541	0.527	0.516	0.490	0.467
	peak distance	0.0098	0.0092	0.0086	0.0076	0.0068
K	parameter value	8.64x10 ⁻⁷	6.91x10 ⁻⁶	8.64x10 ⁻⁶	1.04x10 ⁻⁵	8.64x10 ⁻⁵
	peak concentration	0.240	0.462	0.510	0.551	1.485
	peak distance	0.0014	0.0070	0.0084	0.0100	0.0760
Kd	parameter value	0.10	0.14	0.18	0.22	0.26
	peak concentration	0.585	0.547	0.516	0.491	0.469
	peak distance	0.0108	0.0096	0.0086	0.0078	0.0070
N	parameter value	0.60	0.66	0.82	0.98	1.00
	peak concentration	0.462	0.479	0.516	0.545	0.548
	peak distance	0.0088	0.0088	0.0086	0.0086	0.0086

Figure 67: Results of parameter changes

Weathered Glacial Till



Made Ground



These results indicate the great significance of accurate hydraulic conductivity values in this scenario (Allen-King *et al.*, 1998 and references therein), particularly since the measured or published range in K may vary by considerably greater proportions than the 20% suggested by the Environment Agency (Marsland and Carey, 1999) for sensitivity checks. 20% change in hydraulic conductivity created nearly 10% change in peak concentration and 20% change in the distance travelled in the time period. Changes in the Freundlich N value led to significant concentration changes, 20% change in N caused 18% change in peak concentration, but with little change (5%) in distance travelled. While inaccuracies of $\pm 20\%$ may be reasonable for most parameters, some may be more inaccurate, especially depending on the source of the values: whether they have been measured on material from the site or whether they have been taken from published data. K_{OC} is usually taken from published values, and many common sources provide a single value, implying that it is well-known. However, much wider variations in K_{OC} have been encountered (Section 9.4 and Chapter 10).

11.5 Conclusions and summary

- Accurate TOC values and understanding of TOC distribution and variation is most important at low porosity, low solute concentration and greatest non-linearity.
- An accurate sorption distribution coefficient for the material being modelled is of utmost importance. Published sorption coefficients for TCE of around 150 ml/g were shown to be appropriate fits for only one of the three materials modelled. In the made ground scenario, sorption based on published K_{OC} values and measured TOC would have vastly overestimated the sorption occurring, compared to the results of the batch sorption experiments.
- While of less impact than the need for an accurate, material-specific partition coefficient, use of different isotherms will produce different transport model results. In particular, use of linear sorption isotherms is only valid where the isotherm is an empirical fit to data over the same, limited concentration range that the simulation covers. In these simulations, input concentrations of 300 mg/l were reduced by sorption and dispersion to approximately 10 to 35 mg/l. Therefore, the sorption isotherms should be appropriate to cover such a concentration range, as would only be the case for concentration-dependent isotherms.

12. Conclusions

Sorption of dissolved hydrophobic organic contaminants is controlled by the organic matter in the rock through which the contaminants are flowing. The extent of sorption is usually modelled as proportional to the total organic carbon (TOC) content of the rock. The rock's TOC may be measured or a value taken from published data. As described in the Introduction (Chapter 1), this research aimed to examine the methods used to analyse geological samples for TOC and to increase the database of TOC values in UK aquifers. These aims were undertaken by experimentation, sample collection and analysis. In addition, the research aimed to improve the knowledge of the impact of the type or size of the organic matter on its capacity to sorb organic contaminants. This was undertaken by isolating the organic matter from samples, to inspect its geochemistry and micro-morphology, and comparing this to the results of batch sorption experiments. The results of the batch sorption experiments were used as inputs to computer simulations of organic contaminant transport, to examine the significance of the findings. The following conclusions have been drawn from the work:

1. TOC should be measured by high temperature oxidation following removal of inorganic carbon by acid pre-treatment. The method of acid pre-treatment should be chosen to minimise errors from either incomplete carbonate removal or partial removal of organic carbon. As discussed in Chapter 3, incomplete carbonate removal has been found to be a particular problem for carbonate-rich UK aquifer materials. The acid pre-treatment method should be reported by commercial laboratories, and likelihood of over- or under-measurement of TOC be borne in mind by the data users. A consistently applied TOC analysis method may be of benefit.
2. In the context of limited published data, a substantial new body of organic carbon measurements has been presented for UK aquifer and aquitard materials, taken from over 1000 samples. As described in Chapter 4, these measurements have shown that most UK aquifer materials have low organic carbon content (less than 0.1% in the Chalk and Triassic Sandstone), which is unlikely to be sufficient significantly to sorb organic contaminants. Higher amounts of TOC are found in the Lincolnshire Limestone (up to 2.5%), particularly associated with clay-rich layers. Glacial Tills

analysed have greater TOC content, and are likely to provide significant sorbents. TOC content was depleted by oxidative weathering in glacial tills and on a regional scale in the Lincolnshire Limestone. Other samples had widely ranging TOC content, over 20% in some made ground samples.

3. Sorption experiments using TCE on seven samples have shown that the extent of equilibrium sorption partitioning does not depend on samples' TOC content alone. As seen in Chapter 10, the variation in sorption partitioning can be correlated to the organic matter geochemistry. Distribution coefficients normalised to organic carbon content for each sample correlated with the H/O ratio of the sample's organic matter, consistent with the small body of previously published results. However, as described in Chapters 7 and 8, the organic matter isolated from 43 samples (including those used for batch sorption experiments) showed generally little variety in size and in carbon stable isotope ratios. The limited variations in the morphology of the organic matter contained in the samples did not correlate with the sorption partition coefficients.
4. Isolation of organic matter from geological samples is time-consuming and has been found neither to recover all the organic matter nor to eliminate all the mineral matter. As discussed in Chapter 10, Rock-Eval pyrolysis provides data from whole-rock samples which correlates with the bulk organic matter H/O ratio. Rock-Eval may prove a useful commercial technique to gain rapidly a parameter that correlates with the sorption coefficient.
5. Sorption isotherms plotted from empirical data in Chapter 10 were non-linear, and mostly fitted the Freundlich isotherm well. Those that fitted the Langmuir isotherm better were more non-linear (had a lower Freundlich N exponent); these had lower partition coefficients, demonstrating their lower capacity to sorb the contaminant. The correlation of lower sorption capacity with greater sorption non-linearity may be due to a reduced proportion of the sorption provided by dissolution type partitioning, or to imperfect dissolution type binding becoming exhausted. Both these explanations would result in a greater proportion of the sorption binding being binding site specific and the Langmuir isotherm being a better fit.
6. Computer sorption simulations using Biold indicated that accurate knowledge of TOC values and distribution is most important at low porosity, low solute concentration and greatest non-linearity. As shown by the batch sorption experiments,

K_{OC} values are material-specific. Modelling presented in Chapter 11 indicated that using published K_{OC} values for materials which they do not represent could lead to very significant under- or over-estimation of the travel time and concentration of the dissolved contaminant. Use of non-linear rather than linear isotherms did not make a large impact on the contaminant travel time or arrival concentration. Sorption modelling *must* apply material-specific K_{OC} values to gain a reasonable prediction of contaminant transport. However, modelling undertaken as part of this research indicated that the use of non-linear isotherms produced similar results to linear isotherms; within the confines of the situations simulated, use of linear isotherms does not lead to significant errors. Almost all widely used commercial reactive transport models permit only linear isotherms.

Much work remains to be done:

- additional data needs to be compiled on the variation of TOC in major aquifers and also in major aquitards;
- further work confirming the correlation between organic matter geochemistry and its sorptive properties, in a range of rock types, would increase confidence on the correlations given and the breadth of their application;
- this additional work could also confirm the usefulness of the Rock-Eval pyrolysis technique as a geochemical tool in the context of sorption capacity;
- further modelling could confirm the range of situations in which sorption has a significant effect on contaminant transport and in which non-linearity can be disregarded.

Never-the-less, the work presented in this thesis fulfils the aims of the research. A significantly greater database of TOC values is now available to sorption modellers. The requirement for the use of sorbent-specific distribution coefficients is clear. The dependence of such distribution coefficients on the geochemistry of the organic matter is also clear, and the correlation with the oxidation of the organic matter has been shown. These conclusions increase knowledge of the sorption process, and should improve predictive modelling of solute transport.

References

- Allen-King R.M., Gillham R.W. and Mackay D.M., 1996a, *Sorption of dissolved chlorinated solvents to aquifer materials* p233-266 in Pankow J.F. and Cherry J.A., *Dense chlorinated solvents and other DNAPLS in groundwater*, Waterloo Press, 522p.
- Allen-King R.M., Albanese C.L. and Martin J.P., 1997a, *Discussion of Papers on "Determination of Nonvolatile Organic Carbon in Aquifer Solids after Carbonate Removal by Sulfurous Acid"* by G. Heron, M.J. Barcelona, M.L. Anderson, and T.H. Christensen, *January-February 1997 issue*, v. 35, no.1: 6 - 11, together with Authors' Reply, *Ground Water* 35 (6), 1107 - 1109.
- Allen-King R.M., Groenveldt H. and Mackay D.M., 1995, *Analytical method for the sorption of hydrophobic organic pollutants in clay-rich materials*, *Environ. Sci. Technol.*, 29 (1) 148-153.
- Allen-King R.M., Groenveldt H., Warren C.J. and Mackay D.M., 1996b, *Non-linear chlorinated solvent sorption in four aquitards*, *J. Contam. Hydrol.*, 22 203-221.
- Allen-King R.M., Halket R.M., Gaylord D.R. and Robin M.J.L., 1998, *Characterizing the heterogeneity and correlation of perchloroethene sorption and hydraulic conductivity using a facies-based approach*, *Water Resources Research* 34 (3) 385-396.
- Allen-King R.M., McKay L.D. and Trudell M.R., 1997b, *Organic carbon dominated trichloroethene sorption in a clay-rich deposit*, *Ground Water*, 35 (1) 124-130.
- Ashley R.P., 1998, *Foreseeability of environmental hazards: the implications of the Cambridge Water Company case* p23-26 In: Mather J., Banks D., Dumbleton S. and Fermor M. (eds) *Groundwater contaminants and their migration*, Geol. Soc. London Sp. Publ. 128, 368p.
- Ashton M., 1980, *The Stratigraphy of the Lincolnshire Limestone Formation (Bajocian) in Lincolnshire and Rutland (Leicestershire)*, *Proc. Geol. Assoc.*, 91, 203-223.
- Ball W.P. and Roberts P.V., 1991, *Long-term sorption of halogenated organic chemicals by aquifer material. 1. Equilibrium*, *Environ. Sci. Technol.* 25 (7), 1223-1237.
- Banerjee P., Piwoni M.D. and Ebeid K., 1985, *Sorption of organic contaminants to a low carbon subsurface core*, *Chemosphere*, 8, 1057-1067.
- Banks D., 1998, *Migration of dissolved petroleum hydrocarbons, MTBE and chlorinated solvents in a karstified limestone aquifer, Stamford, UK* p123-145 In: Mather J.,

References

-
- Banks D., Dumbleton S. and Fermor M. (eds) Groundwater contaminants and their migration, Geol. Soc. London Sp. Publ. 128, 368p.
- Batten D.J., 1996, *Palynofacies and palaeoenvironmental interpretation*, Chapter 26A, p 1011-1064 in Jansonius J. and McGregor D.C. (ed.), *Palynology: principles and applications*, Vol 3. Publ. American Association of Stratigraphic Palynologists Foundation.
- Bein A. and Sandler A., 1983, *Early diagenetic oxidation and maturation trends in organic matter from Eocene Chalks and Cherts*, *Chemical Geology* 38, 213-224.
- Binger C.A., Martin J.P., Allen-King R.A. and Fowler M., 1999, *Variability of chlorinated-solvent sorption associated with oxidative weathering of kerogen*, *J. Contam. Hydrol.* 40, 137-158.
- Bishop P.K. and Lloyd J.W., 1990, *Chemical and isotopic evidence for hydrogeochemical processes occurring in the Lincolnshire Limestone*, *J. Hydrology*, 121, 293-320.
- Bishop P.K., Lerner D.N., Jakobsen R., Gosk E., Burston M.W. and Chen T., 1993, *Investigation of a solvent polluted industrial site on a deep sandstone-mudstone sequence in the UK. Part 2. Contaminant sources, distributions, transport and retardation*, *J. Hydrology* 149, 231-256.
- Bissada A., 1999, Petroleum Geochemistry Institute, Petroleum Research Centre, University of Houston, pers. comm.
- Bostick N.H. and Alpern B., 1977, *Principles of sampling, preparation and constituent selection for microphotometry in measurement of maturation of sedimentary organic matter*, *J. Microscopy*, 109 (1) 41-47.
- Boulter M.C., 1994, *An introduction to a standard terminology for palynodebris*, p199-216 in Traverse A. (ed.), *Sedimentation of Organic Particles*, Publ. Cambridge University Press, Cambridge, 544p.
- Bourg A.C.M., Degrange P., Mouvet C. and Sauty J.P., 1993, *Migration of chlorinated hydrocarbon solvents through Coventry sandstone rock columns*, *J. Hydrology* 149, 183-207.
- Bourg A.C.M., Mouvet C. and Lerner D.N., 1992, *A review of the attenuation of trichloroethylene in soils and aquifers*, *Quart. J. Eng. Geol.* 25, 359-370.
- Bown P.R. (ed.), 1998, *Calcareous Nannofossil Biostratigraphy*, Publ. Chapman and Hall.
-

References

- British Geological Survey, 1997, *The physical properties of major aquifers in England and Wales*, BGS Technical Report WD/97/34, Publ. British Geological Survey, Keyworth. 312 p.
- British Geological Survey, 1971, *Geological Sheet 76*, Solid Geology of Rochdale.
- British Standard BS 1377: Part 3, 1990, *Soils for civil engineering purposes Part 3: Chemical and electro-chemical tests* Publ. British Standards Institution.
- British Standard BS 7755:Section 3.8, 1995, *Soil Quality Part 3. Chemical Methods. Section 3.8 Determination of organic and total carbon after dry combustion (elemental analysis)* 7pp. Publ. British Standards Institution.
- Burston M.W., Nazari M.M., Bishop P.K. and Lerner D.N., 1993, *Pollution of groundwater in the Coventry region (UK) by chlorinated hydrocarbon solvents*, J. Hydrology 149, 137-161.
- Caughey M.E., Barcelona M.J., Powell R.M., Cahill R.A., Grøn C., Lawrenz D. and Meschi P.L., 1995, *Interlaboratory study of a method for determining nonvolatile organic carbon in aquifer materials*, Environmental Geology, 26, 211 - 219.
- Churcher P.L. and Dickhout R.D., 1989, *Analysis of Ancient Sediments for Total Organic Carbon - Some New Ideas*, J. of Geochemical Exploration, 29, 235 - 246.
- Crossey L.J., Frost B.R. and Surdam R.C., 1984, *Secondary porosity in Laumanite bearing sandstones*. p225-237 in *Clastic Diagenesis* ed. McDonald D.A. and Surdam R.C. AAPG Memoir 37, Publ. AAPG, Oklahoma, 434p.
- Curtis G.P., Roberts P.V. and Reinhard M., 1986, *A natural gradient experiment on solute transport in a sand aquifer 4. Sorption of organic solutes and its influence on mobility*, Water Resources Research 22 (13) 2059-2067.
- Day J.B.W., 1986, *The Occurrence of Groundwater in the United Kingdom*, pp 5 - 48 in Brandon T.W., (ed.) *Groundwater: Occurrence, Development and Protection*, Publ. The Institution of Water Engineers and Scientists, London, England pp 615.
- Dobson J. and Kinghorn R.R.F., 1987, *Dispersed sedimentary organic matter in Coal Measure Horizons, East Midlands, UK*, J. Petroleum Geology 10 (4) 453-474.
- Downing R.A. and Williams B.P.J., 1969, *The groundwater hydrology of the Lincolnshire Limestone with special reference to groundwater resources*. Water Resources Board Publication 9.

References

- Durand B. and Monin J.C., 1980, *Elemental analysis of kerogens (C, H, O, N, S, Fe)*, in Durand B. (ed.), *Kerogen: Insoluble Organic Matter from Sedimentary Rocks*, publ. Technip., Paris, 519p.
- Durand B. and Nicaise G., 1980, *Procedures for kerogen isolation*, in Durand B. (ed.), *Kerogen: Insoluble Organic Matter from Sedimentary Rocks*, publ. Technip., Paris, 519p.
- Durand B., 1980, *Sedimentary organic matter and kerogen. Definition and quantitative importance of kerogen*. pp 13-33 in Durand B. (ed.), *Kerogen: Insoluble matter from sedimentary rocks*. Pub. Technip, Paris 519p.
- Ebukanson E.J. and Kinghorn R.R.F., 1985, *Kerogen facies in the major Jurassic mudrock formations of Southern England and the implication on the depositional environments of their precursors*, *J. Petroleum Geology*, 8 (4) 435-462.
- Edmunds W.M., Bath A.H. and Miles D.L., 1982, *Hydrochemical evolution of the East Midlands Triassic Sandstone aquifer, England*, *Geochimica and Cosmochimica Acta*, 46, 2069-2081.
- Ehlers J., Gibbard P and Whiteman C.A., 1991, *The glacial deposits of northwestern Norfolk*, p223-232 in Ehlers J., Gibbard P.L. and Rose J. (ed.) *Glacial Deposits in Great Britain and Ireland*, publ. A.A. Balkema, Rotterdam.
- Emery D. and Dickson J.A.D., 1991, *The subsurface correlation of the Lincolnshire Limestone Formation in Lincolnshire*, *Proc. Geol. Assoc.* 102 (2), 109-122.
- Espitalié J., Madec M., Tissot B., Mennig J.J. and Leplat P., 1977, *Source rock characterization method for petroleum exploration* Preceedings of the 9th Annual Offshore Technology Conference, Houston pp439-444.
- Fetter C.W., 1993, *Contaminant Hydrogeology*, Publ. Prentice Hall, 458pp.
- Fretwell B.A., 1999, *The distribution of contaminants in the seasonally unsaturated zone of the Chalk aquifer*, PhD Thesis, University of London.
- Froelich P.N., 1980, *Analysis of organic carbon in marine sediments*, *Limnology and Oceanography* 25 (3), 564 - 572.
- Gauthier T.D., Setlz W.R. and Grant C.L., 1987, *Effects of structural and compositional variations of dissolved humic materials on pyrene K_{oc} values*, *Environ. Sci. Technol.* 21, 243-248.

References

- Gehman H.M., 1962, *Organic matter in limestones*, *Geochimica et Cosmochimica Acta*, 26, 885-897.
- George M.A., 1998, *High precision stable isotope imaging of groundwater flow dynamics in the chalk aquifer systems of Cambridgeshire and Norfolk*, PhD Thesis, University of East Anglia, 206p plus appendices.
- George M.A., Hiscock K.M., Dennis P.F., Corbett W.M. and Steventon-Barnes H., in prep., *Stable isotope evidence for groundwater flow through a glacial till aquitard system*.
- Gibbs R.J., 1977, *Effect of combustion temperature and time, and of the oxidation agent used in organic carbon and nitrogen analyses of sediments and dissolved organic material*, *Journal of Sedimentary Petrology* 47 (2), 547 - 550.
- Golder Associates, 1999, Consim, version 2.04 Demonstration Copy (June 1999).
- Grathwohl P., 1990, *Influence of organic matter from soils and sediments from various origins on the sorption of some chlorinated aliphatic hydrocarbons: implications on K_{OC} correlations*, *Environ. Sci. Technol.*, 24, 1687-1692.
- Greswell R., Yoshida K., Tellam J.H. and Lloyd J.W., 1998, *The micro-scale hydrogeological properties of the Lincolnshire Limestone, UK*, *Quart. J. Eng. Geol.*, 31 (3), 181-197.
- Harris R.C., 1998, *Protection of groundwater quality in the UK: present controls and future issues* p3-13 In: Mather J., Banks D., Dumbleton S. and Fermor M. (eds) *Groundwater contaminants and their migration*, *Geol. Soc. London Sp. Publ.* 128, 368p.
- Hart J.K. and Boulton G.S., 1991, *The glacial drifts of northeastern Norfolk*, p233-243 in Ehlers J., Gibbard P.L. and Rose J. (ed.) *Glacial Deposits in Great Britain and Ireland*, publ. A.A. Balkema, Rotterdam.
- Hendry M.J. and Wassenar L.I., 1999, *Implications of the distribution of δD in pore waters for groundwater flow and the timing of geologic events in a thick aquitard system*, *Water Resources Research*, 35 (6) 1751-1760.
- Heron G., Barcelona, M.J., Anderson M.L. and Christensen T.H., 1997, *Determination of nonvolatile organic carbon in aquifer solids after carbonate removal by sulfuric acid*, *Ground Water*, 35 (1) 6 - 11.
- Hoefs J., 1997, *Stable isotope geochemistry*, Publ. Springer, 201p.

References

- Huang W. and Weber W.J. 1997, *A distributed reactivity model for sorption by soils and sediments. 10. Relationships between desorption, hysteresis, and the chemical characteristics of organic domains*, Environ. Sci. Technol. 31 (9) 2562-2569.
- Jackson D. and Rushton K.R., 1987, *Assessment of recharge components for a Chalk Aquifer unit*, J. Hydrology, 92, 1-15.
- Karickhoff S.W., 1984, *Organic pollutant sorption in aquatic systems*, J. Hydraul. Eng., 110, 707-735.
- Kenig F., Hayes J.M., Popp B.N. and Summons R.E., 1994, *Isotopic biogeochemistry of the Oxford Clay Formation (Jurassic), UK*, J. Geol. Soc. Lond., 151, 139-152.
- Kent P., 1980, *British Regional Geology: eastern England, from the Tees to the Wash*, publ. HMSO, London, 115p.
- Killops S.D. and Killops V.J., 1993, *An introduction to organic geochemistry*, publ Longman Scientific and Technical, Harlow, 265p.
- Kim A., McArthur J.M. and Burgess W.G., undated, *Organic matter in aquifer rocks*, in Pollutant transport in soils and rocks in Pollutant Transport in soils and rocks, meeting, NERC and BBSRC.
- Klinck B.A., Barker J.A., Noy D.J. and Wealthall G.P., 1996, *Mechanisms and rates of recharge through glacial till: experimental and modelling studies from a Norfolk site*, Fluid Processes Series Technical Report WE/96/1. Publ. British Geological Survey, Keyworth, 32 p.
- Lawrence A.R. and Foster S.S.D., 1986, *Denitrification in a limestone aquifer in relation to the security of low nitrate groundwater resources*, JIWEM 40, 159-172.
- Lee C.M. and Macalady D.L., 1989, *Towards a standard method for the measurement of organic carbon in sediments*, Intern. J. Environ. Anal. Chem., 35, 219 - 225.
- Lerner D.N., Gosk E., Bourg A.C.M., Bishop P.K., Burston M.W., Mouvet C., Degranges P. and Jakobsen R., 1993, *Postscript: summary of the Coventry groundwater investigation and implications for the future*, J. Hydrology 149, 257-272.
- Lichtfouse E., 1999, Soils and Environment Laboratories, INRA-ENSAIA / INPL, pers. comm.
- Lloyd J.W., Greswell R., Williams G.M., Ward R.S., Mackay R. and Riley M.S., 1996, *An integrated study of controls on solute transport in the Lincolnshire Limestone*, Quarterly Journal of Engineering Geology 29 (4) 321-339.

References

- Lloyd J.W., Harker D. and Baxendale R.A., 1981, *Recharge mechanisms and groundwater flow in the Chalk and drift deposits of southern East Anglia*, Quart. J. Eng. Geol. 14, 87-96.
- Mackay D.M., Ball W.P. and Durant M.G., 1986, *Variability of aquifer sorption properties in a field experiment on groundwater transport of organic solutes: methods and preliminary results*, J. Contam. Hydrol. 1, 119-132.
- Mackay D.M., Bianchi-Mosquera G.C., Kopania A., Kianjah H. and Thorbjarnson K., 1994, *A forced-gradient experiment on solute transport in the Borden aquifer. 1. Experimental methods and moment analysis of results*, Water Resources Research 30, 369-383.
- MAFF (Ministry of Agriculture, Fisheries and Food), 1986, *The Analysis of Agricultural Materials*, Publication reference RB427, Publ. HMSO Books.
- Marsland P.A. and Carey M.A., 1999, *Methodology for the derivation of remedial targets for soil and groundwater to protect resources*, Environment Agency R&D publication 20.
- Mather J., Banks D., Dumbleton S. and Fermor M. (eds), 1998, *Groundwater contaminants and their migration*, Geol. Soc. London Sp. Publ. 128, 368p.
- McArthur J.M., Tyson R.V., Thomson J., Mathey D., 1992, *Early Diagenesis of marine organic matter; alteration of the carbon isotope composition*, Marine Geology, 150, 51 - 61.
- McLeod A.C., 1998, *Dissolved Organic Carbon in UK Aquifers*, PhD Thesis, University of London.
- Missteart B.D.R., P.W. Rippon and Ashley R.P., 1998, *Detection of point sources of contamination by chlorinated solvents: a case study from the Chalk of eastern England* p217-228 In: Mather J., Banks D., Dumbleton S. and Fermor M. (eds) *Groundwater contaminants and their migration*, Geol. Soc. London Sp. Publ. 128, 368p.
- Moncaster S.J., 1993, *Sulphur isotope geochemistry of the Central Lincolnshire Limestones*. PhD thesis, University of Birmingham, UK.
- Montgomery J.H., 1996, *Groundwater Chemicals Desk Reference*, 2nd edition, Publ. CRC Lewis, 1345p.

References

- Mouvet C., Barberis D. and Bourg A.C.M., 1993, *Adsorption isotherms of tri- and tetrachloroethylene by various natural solids*, J. Hydrology, 149, 163-182.
- Munz C. and Roberts P.V., 1986, *Effects of solute concentration and cosolvents on the aqueous activity of halogenated hydrocarbons*, Environ. Sci. Technol., 20 (8) 830-836.
- Murphy A., Jarvis I. and Edmunds W.M., 1997, *Geochemistry of the Banterwick Barn Chalk Borehole*, Hydrogeological Series Technical Report WD/97/37 Publ. British Geological Survey, Keyworth, Nottinghamshire.
- Murphy E.M., Zachara J.M. and Smith S.C., 1990, *Influence of mineral-bound humic substances on the sorption of hydrophobic organic compounds*, Environ. Sci. Technol., 24, 1507-1516.
- Myrand D., Gillham R.W., Sudicky E.A., O'Hannesin S.F. and Johnson R.L., 1992, *Diffusion of volatile organic compounds in natural clay deposits: Laboratory tests*, J. Contam. Hydrol. 10, 159-177.
- Nkedi-Kizza P., Rao P.S.C. and Hornsby A.G., 1985, *Influence of organic co-solvents on sorption of hydrophobic organic chemicals by soils*, Environ. Sci. Technol., 19, 975-979.
- Norri M.J., Dunham A.C. and Hudson J.D., 1994, *Mineralogy and geochemistry of the Peterborough Member, Oxford Clay Formation, Jurassic, UK: element fractionation during mudrock sedimentation*, J. Geol. Soc. Lond., 151, 195-207.
- Pacey N.R., 1989, *Organic Matter in Cretaceous Chalks from Eastern England*, Chemical Geology, 75, 191-208.
- Pankow J.F. and Cherry J.A., 1996, *Dense chlorinated solvents and other DNAPLS in groundwater: history, behaviour and remediation*, Publ. Waterloo Press, Ontario, 522p.
- Parker B.L., Gillham R.W. and Cherry J.A., 1994, *Diffusive disappearance of immiscible-phase organic liquids in fractured geologic media*, Ground Water, 32 (5) 805-820.
- Perrin R.M.S., Davies H. and Fysh M.D., 1973, *Lithology of the Chalky Boulder Clay*, Nature Physical Science, 245, 101-104.
- Perrin R.M.S., Rose J. and Davies H., 1979, *The distribution, variation and origins of pre-Devensian tills in eastern England*, Phil. Trans. R. Soc. London Ser. B, 287, 535-570.

References

- Peters K.E., 1986, *Guidelines for evaluating petroleum source rock using programmed pyrolysis*, AAPG Bull. 70 (3) 318-329.
- Pickering K.T., Souter C., Oba T., Taira A., Schaaf M. and Platzman E., 1998, *Glacio-eustatic control on deep-marine clastic forearc sedimentation, Pliocene - mid Pleistocene (c1180 - 600 ka) Kazusa Group, SE Japan*, J Geol Soc, 156 (1) 125 - 136.
- Powell R.M., Bledsoe B.E. Curtis G.P. and Johnson R.L., 1989, *Interlaboratory methods comparison for the total organic carbon analysis of aquifer materials*, Environ. Sci. Technol., 23 (10) 1246 - 1249.
- Ptacek C.J. and Gillham R.W., 1992, *Laboratory and field measurements of non-equilibrium transport in the Borden aquifer, Ontario, Canada*, J. Contam. Hydrol., 10, 119-158.
- Rivett M.O., 2000, *From Borden to Birmingham*, presentation at the Contaminated land meets groundwater meeting, 18 July 2000, University of Birmingham.
- Rivett M.O., Lerner D.N., Lloyd J.W. and Clark L., 1990, *Organic contamination of the Birmingham aquifer, U.K.*, J. Hydrology, 113, 307-323.
- Robertson W.D., Russell B.M. and Cherry J.A., 1996, *Attenuation of nitrate in aquitard sediments of southern Ontario*, Journal of Hydrology, 180, 267-281.
- Robl T.L. and Davis B.H., 1993, *Comparison of the HF-HCl and HF-HBF₃ maceration techniques and the chemistry of the resultant organic concentrates*, Organic Geochemistry, 20 (2) 249-255.
- Rushton K.R., Smith E.J. and Tomlinson L.M., 1982, *An improved understanding of flow in a limestone aquifer using field evidence and mathematical models*, J. Inst. Water and Environ. Sci. 36, 369-387
- Rutherford D.W., Chiou C.T. and Kile D.E., 1992, *Influence of soil organic matter on the partitioning of organic compounds*, Environ. Sci. Technol. 26, 336-340.
- Schwarzenbach R.P. and Westall J., 1981, *Transport of non-polar organic compounds from surface water to groundwater. Laboratory sorption studies*, Environ. Sci. Technol., 15 (11), 1360-1367.
- Schwarzenbach R.P., Gschwend P.M. and Imboden D.M., 1993, *Environmental Organic Chemistry*, (John Wiley and Sons, NY), 681 pp.

References

- Senftle J.T., Landos C.R. and McLaughlin R.L., 1993, *Organic Petrographic Approach to Kerogen Characterisation*, in Engel M.H. and Macko S.A. (ed.), *Organic Geochemistry: Principles and Applications*, publ. Plenum Press, 861p.
- Smith-Carrington A.K., Bridge L.R., Robertson A.S. and Foster S.S.D., 1983, *The nitrate pollution problem in groundwater supplies from Jurassic limestones in central Lincolnshire*. Report of the Institute of Geological Science No. 83/3.
- Spitz K and Moreno J., 1996, *A practical guide to groundwater and solute transport modelling*, Publ. John Wiley and Sons, In, 461p.
- Srinivasan P. and Mercer J.W., 1988, *Simulation of biodegradation and sorption processes in ground water*, *Ground Water*, 26 (4) 475-487.
- Stuart M.E., 1991, *Organic Carbon in British Aquifers, A Review*, Technical Report, Hydrogeological Series, WD/91/5, Pub. British Geological Survey, Keyworth, Nottingham.
- Traverse A., 1988, *Paleopalynology*, publ. Unwin Hyman, Boston, 600p.
- Traverse A., 1994, *Sedimentation of palynomorphs and palynodebris: an introduction* p1-8 in Traverse A. (ed.), *Sedimentation of Organic Particles*, Publ. Cambridge University Press, Cambridge, 544p.
- Tucker M.E., 1983, *Sedimentation of organic-rich limestones in the Late Precambrian of southern Norway*, *Precambrian Research*, 22, 295-315.
- Tyson R.V., 1995, *Sedimentary Organic Matter: Organic facies and palynofacies*. Publ Chapman and Hall.
- USEPA, 1992, *Specifications and guidance for contaminant-free sample containers*, USEPA publication no. 9240,0-05A, EPA640/R-93/-051, PB93-963316, Dec. 1992.
- Weber W.J., Huang W. and Yu H., 1998, *Hysteresis in the sorption and desorption of hydrophobic organic contaminants by soils and sediments 2. Effects of soil organic matter heterogeneity*, *J. Contam. Hydrol.* 31, 149-165.
- West C.C., Lyon W.G., Ross D.L. and Pennington L.K., 1994, *Investigation of vertical distribution and morphology of indigenous organic matter at Sleeping Bear site, Michigan*, *Env. Geol.* 24, 176-187.
- Whelan J.K. and Thompson-Rizer C.L., 1993, *Chemical Methods for Assessing Kerogen and Protokerogen Types and Maturity*, in Engel M.H. and Macko S.A. (ed.), *Organic*

References

- Geochemistry: Principles and Applications, publ. Plenum Press, New York and London, 861p.
- Whitelaw K. and Edwards R.A., 1980, *Carbohydrates in the unsaturated zone of the Chalk, England*, Chemical Geology, 29, 281-291.
- Williamson D.J., 1993, *Controls on the transport of organic pollutants through Permo-Triassic sandstone aquifers: low concentration sorption of selected species on mineral substrates*, PhD thesis, University of Birmingham.
- Wood G.D., Gabriel A.M. and Lawson J.C., 1996, *Palynological Techniques - Processing and Microscopy*, in Jansonius J. and McGregor D.C. (ed.), Palynology: principles and applications; American Association of Stratigraphic Palynologists Foundation, Vol. 1, p29 - 50.
- Woodcock N., 1994, *Geology and environment in Britain and Ireland*, publ. UCL press, London 164pp.
- Wright W.B., Sherlock P.L., Wray D.A., Lloyd W. and Tonks L.H., 1927, *The geology of the Rossendale Anticline*, publ. HMSO.
- Xing B. and Pignatello J.J., 1997, *Dual-mode sorption of low-polarity compounds in glassy poly(vinyl chloride) and soil organic matter*, Environ. Sci. Technol. 31, 792-799.
- Xing B., McGill W.B. and Dudas M.J., 1994, *Cross-correlation of polarity curves to predict partition coefficients of nonionic organic matter contaminants*, Environ. Sci. Technol., 28, 1929-1933.

A. TOC analysis methods

A.1 Commercial laboratories' method details

Laboratory A

Laboratory A summarise their method for the determination of the carbon content of geological samples as: *'A powdered sample is combusted in oxygen over a temperature gradient from around 700 °C to around 1600 °C. The carbon dioxide produced is passed ... into an infra-red detector previously calibrated ... When the determination is restricted to organic carbon only, the samples are pre-treated with acid to remove carbonates.'*

Carbonates are removed with a 50% solution of concentrated HCl added to crushed dried powders of the samples in beakers until effervescence has ceased, followed by evaporation to dryness; acid addition and evaporation is repeated. The sample is washed on a glass fibre filter pad with distilled water. The filter pad is removed, folded, used to wipe any sample adhering to the filter walls and replaced in the beaker and dried in an oven at approximately 110°C for about two hours under reduced pressure. The folded filter is transferred into a crucible for analysis.

Analysis is performed by high temperature oxidation (HTO) using a LECO® carbon analyser, calibrated with 0.6% carbon standards and a blank. Calcium carbonate (CaCO₃) standards (0.25 g) are analysed. The method claims reproducibility of ±0.2% of the total on a 0.5% carbon standard. They comment that allowing for heterogeneity of rock samples, and the low weight used, duplicate results should not vary by more than 10%.

Laboratory B

Laboratory B claim their method is derived from a United States Environmental Protection Agency (USEPA) method, but were unable to provide a reference. The sample is homogenised, treated with acid to remove inorganic carbon, and washed and dried. The sample is then analysed by HTO. They declined to provide further details of the acidification step.

Laboratory C

Laboratory C remove inorganic carbon from dried rock powders and soil samples with hot and cold dilute and concentrated HCl, which is filtered from the sample through porous crucibles. The samples are then rinsed with deionised water and dried. Analysis is carried out by HTO using a LECO® CS444 Carbon Analyser. Quality control includes a daily calibration check and accuracy is checked against standard samples every 10 analyses.

Laboratory D

When surveyed, Laboratory D were developing a method based on Heron *et al.* (1997) and were unable to provide a method statement or further details.

Laboratory E

Laboratory E remove the carbonate with phosphoric acid and remove remaining acid by filtration. Analysis is by HTO.

Laboratory F

Laboratory F use the British Standard 1377 wet-chemical oxidation method (Chapter 3, Section 3.2.1.2) for soil TOC analysis.

Laboratory G

Laboratory G analyse for TOC by leaching. The sample is acidified and purged to remove carbonate carbon. The solids are shaken in a volume of water 10 times the weight of the sample. Organic carbon in the leachate is oxidised by sodium persulphate to carbon dioxide, which is determined by infra-red detection.

Laboratory H

Laboratory H use a wet chemical oxidation method based on Method 56, Organic Matter in Soil, from MAFF 1986. Soil organic matter is almost completely oxidised by gently boiling with a solution of potassium dichromate, sulphuric acid and orthophosphoric acid; excess dichromate is determined by titration with ferrous sulphate solution. Organic carbon is assumed to be completely oxidised; conversion to organic matter (OM) assumes that OM is 1.724 times the organic carbon.

A.2 Wolfson Geochemistry Laboratory, UCL

Samples are dried and ground. Approximately 0.7g (depending on expected TOC) is weighed into a porous LECO[®] crucible that had been ignited at 800°C to remove any organic carbon. Carbonate is removed by treatment with dilute HCl (10% of concentrated HCl) in filtering crucibles under low vacuum until after all signs of effervescence has ceased (typically two to three hours for a carbonate-rich sample). When acid-resistant carbonates are suspected, concentrated HCl is used and the samples are left to stand until all effervescence, however weak, has ceased. The samples are then washed with distilled water, and dried at 40 to 50°C for over 16 hours. Blank (empty) crucibles are treated in the same way.

Weight percentage of remaining carbon and sulphur are analysed in the laboratory's LECO[®] CS125 analyser, calibrated with steel ring standards and blanks, calibration confirmed with calcite standards. Carbon is oxidised to carbon dioxide and carbon monoxide and sulphur converted to sulphur dioxide, at over 1000°C in a high frequency induction furnace in an oxygen stream. The gaseous combustion products are passed through traps to remove chlorine and water vapour. Sulphur dioxide is then detected by infra-red. Carbon monoxide is converted by a platinised silica gel catalyst to carbon dioxide; all carbon dioxide is then quantified by infra-red detection. Carbon and sulphur contents are corrected for the calibration factors and given as percentages of the input sample weight.

A.3 Commercial Laboratories Surveyed

The following commercial laboratories were surveyed. They are listed here in alphabetic order which does not correspond to the order in which they are presented above.

Analytical and Environmental Services	Scientific Analysis Laboratories Ltd.
Cottage Leap	Medlock House
Rugby CV21 3XP	New Elm Road
01788 552244	Manchester M3 4JW
	0161 827 1400

Chemex International Plc	
Bar Hill Business Park	Severn Trent Laboratories Ltd.
37 Saxon Way	STL Business Centre
Bar Hill	Torrington Avenue
Cambridge CB3 8EL	Coventry CV4 9GU
01954 789700	01203 692692

Geochem Group Limited	Severn Trent Laboratories Ltd.
Chester Street	Lancots Lane
Chester CH4 8RD	St. Helens
01244 671121	Merseyside WA9 3ES
	01744 611553

Robertson Research International Ltd.	
Llanrhos	TES Brethby
Llandudno	Brethby Business Park
Gwynedd LL30 1SA	Ashby Road
01492 581811	Burton upon Trent
	Staffordshire DE15 0XD
	01283 554416

B. Dissolved Organic Carbon in acid

To determine the loss of organic carbon by acid dissolution, acid was added to selected samples, and the leachate tested for dissolved organic carbon (DOC). The sample weight used was based on the sample's AIC content. Samples were dried and ground.

B.1 Method

Glassware was cleaned with chromic acid. Samples were weighed into beakers and 10 ml dilute hydrochloric acid (10% dilution of concentrated HCl in ultra-pure water) added to each sample, except the chalk which received 20 ml HCl, which is a 100% excess. Two method blanks had only HCl added to the beaker. Beakers were covered and mixed intermittently for 20 hours. At the end of this time perceptible effervescence had ceased, although incomplete dissolution of chalk was observed despite 200% excess acid for 20 hours, due to rate limited dissolution (possibly related to original particle size). The samples were then filtered through a Whatman GF/B glass microfibre filter (1.0 μm particle retention), into 100 ml standard flasks. The beakers were rinsed out into the filter paper, and an additional 50 ml ultra-pure water washed through the filter paper into the standard flask; flasks were then made to the mark with ultra-pure water. Prior to use, filter papers were baked at 400°C for 2 hours and washed with 200 ml of ultra-pure water and 200 ml HCl.

Subsamples from the flasks were adjusted to pH 3 using 10 normal sodium hydroxide solution before analysis for DOC using a calibrated Shimadzu 5000 TOC analyser. Each sample was analysed for total dissolved carbon and for dissolved inorganic carbon and the difference taken to be dissolved organic carbon. The quantity of organic carbon that had dissolved from the original solid samples was calculated after correction for blanks.

B.2 Results

The method blank results (Table 44) comprised approximately 25% of the sample results for organic carbon. Blank-corrected sample results (Table 45) are shown as acid-soluble organic carbon (ASOC) as a percentage of the solid sample weight.

Appendix B: Dissolved organic carbon in acid

Table 44: Total and Inorganic carbon measured in blanks

	Machine blank (ppm)	Method blank 1 (ppm)	Method blank 2 (ppm)
Total carbon	0.3	12.5	n.m.
Inorganic carbon	0.02	11.8	11.5
Organic carbon	0.3	0.7	n.m.

n.m. = not measured due to equipment failure

ASOC values are compared to the samples' acid-insoluble carbon values, and also given as a percentage of total organic carbon (TOC), where total organic carbon is taken as the sum of the previously measured acid-insoluble carbon and the dissolved organic carbon measured in this experiment.

Table 45: Acid-soluble organic carbon as a percentage of original sample weight

Sample reference	Sample description	AIC (%)	Mass used (mg)	ASOC (%)	ASOC as % of TOC
WH-3-23	Mudstone	3.1	65.63	0.51	14
T 22.83	Lower Chalk	0.038	5005.89	0.0074	16
W9D 6.0m	grey silty clay	0.96	201.15	0.13	12
W9D 10.4m	red-brown sandy clay	0.29	599.77	0.032	9.8
W9D 2m	Made Ground	7.5	29.54	1.5	16
LL 67.48-67.70	Lincolnshire Limestone	0.16	1014.12	0.028	15

Some conclusions drawn from this experiment are discussed in Chapter 3, Section 3.4.3.

C. Acid-evaporation pre-treatment method

To determine the difference between TOC measured in samples from which the acid has been evaporated and AIC measured by the UCL method, samples were analysed after pre-treatment by both methods. The eight samples selected represented a range of organic carbon content, inorganic carbon content and ratio of organic carbon to carbonate carbon and included a carbon-free blank. This experiment was designed to confirm the results of the measurements of DOC in acid filtrate (Appendix B and Chapter 3, Section 3.4.3) and to test evaporation to remove acid from samples.

Additionally, as a carbon-free sample (referred to as IGCR), a porous LECO[®] crucible was baked at 800°C ('ignited') to remove all carbon, then processed and analysed identically to geological samples. Samples were dried and crushed with a pestle and mortar. Each was analysed three times using the UCL standard method (results reported as AIC), and three times using the experimental method (results reported as TOC), and was also analysed three times for total carbon content.

The experimental acid-evaporation pre-treatment method applied was adapted from Heron *et al.* (1997). Greater quantities of acid were used to facilitate complete carbonate dissolution. H₂SO₃ was used, as presence of halogens in residual salts (from HCl) would interfere with the operation of the LECO[®] analyser. A similar published method (Caughey *et al.*, 1995) uses non-filtering LECO[®] crucibles (LECO[®] # 528-018) together with crucible liners (LECO[®] # 529-036) as the reaction vessels for the addition of acid. In testing this, it was found that both the 'non-filtering' crucibles and the crucible liners are porous, and liquid was lost through them. Because they leak acid, they are inappropriate reaction vessels.

All glassware was washed in 'Decon 90', a surface active cleaning agent. The samples were weighed into 50 ml glass beakers (amount used dependant on expected TOC). An (at least three times) excess of 0.78M H₂SO₃ (between 3 ml and 27 ml) was added dropwise to each beaker. BDH 5% w/v sulphur dioxide (SO₂) solution was used; this is not a specified quality grade; SO₂ solution of specified grade is not available from standard

Appendix C: Acid evaporation pre-treatment method

laboratory reagent suppliers (BDH and Fisher). The acid evaporated at room temperature, precipitating sulphite salts; little liquid remained in the beakers after 24 hours. Additional acid was added daily in 5 ml aliquots, with vigorous stirring, until no further effervescence was apparent. 5 ml to 30 ml additional H_2SO_3 brought the total acid per sample to between 8 ml and 49 ml.

When the addition of further acid elicited no perceptible signs of effervescence the samples were dried at room temperature, before being transferred into analysis crucibles. As transfer of samples from glass beakers to analysis crucibles may not be complete, material remaining in beakers was weighed and results adjusted accordingly. The crucibles were oven-dried overnight at 40°C , and carbon content measured using the LECO[®] CS analyser.

D. Measured AIC Content

Samples were collected from cores or disturbed material soon after drilling where possible, and dried at below 50°C, usually at room temperature to minimise loss of organic compounds by volatilisation.

Notes and abbreviations:

AIC	Acid-insoluble carbon
AIS	Acid-insoluble sulphur
TC	Total Carbon
TS	Total Sulphur
IC	Inorganic Carbon
m bgl	metres below ground level
n.d.	not detected (analysis results below detection limit)
~	not determined
detection limit	0.0027% AIC
	0.0022% AIS
	0.0005% TC
	0.0018% TS
bold figures	indicate the mean of the results of at least two analyses

D.1 Upper Chalk

Layer de la Haye

Samples were taken a few days after drilling and stored in cling-film or plastic bags. Samples were cut on a water-lubricated diamond wheel to obtain a fresh face which was sub-sampled either by chipping or cutting a one to three centimetre thick slice, and oven-dried at 40 to 45°C. All samples were taken from the centre of the core, except those to assess the intrusion of drilling fluid into the core. Sample descriptions are based on borehole logs made and provided by CH2MHill, verified by observation.

bold figures indicate the mean of the results of at least two analyses

Depth (m bgl)	AIC (%)	Sample descriptions
92.20	0.030	Pale creamy white medium soft chalk with closely spaced fractures becoming hard with widely spaced fractures
94.83	0.028	
97.11	0.034	
103.56	0.030	Pale creamy white medium hard to hard chalk with widely spaced fractures and occasional flint bands
108.16	0.025	
111.12	0.040	Pale creamy white medium hard to hard chalk with widely spaced joints
112.16	0.037	
115.88	0.034	
118.09	0.046	
119.99	0.048	Medium soft chalk with a little putty chalk
121.99	0.031	
123.92	0.040	Pale creamy white medium hard chalk
126.04	0.050	
128.18	0.028	
130.28	0.035	Pale creamy white medium hard chalk putty chalk
132.00	0.058	
134.35	0.028	moderately hard chalk
137.33	0.030	
140.36	0.033	
143.80	0.032	
146.76	0.015	
150.17	0.024	moderately hard chalk with thin moderately weak bands
153.56	0.049	
156.75	0.035	
159.49	0.038	
162.38	0.039	moderately hard chalk with occasional soft bands
165.67	0.040	
167.96	0.034	
170.86	0.056	
170.67	0.036	
178.03	0.033	medium hard chalk
180.05	0.056	moderately strong chalk with moderately weak bands occasional flint nodules
180.08	0.065	
184.95	0.044	
185.40	0.053	
190.70	0.033	
191.21	0.049	
195.71	0.039	moderately strong chalk with moderately weak bands
198.69	0.054	

Appendix D: Measured AIC content

Banterwick Barn

Samples were supplied dried.

Upper Chalk

Depth (m bgl)	AIC (%)	CaCO ₃ (%)
1.52	0.021	96.00
2.90	0.018	96.90
6.23	0.013	96.60
10.33	0.028	93.90
12.47	0.010	95.30
13.87	0.019	95.20
15.78	0.025	96.90
17.23	0.045	95.00
22.29	0.039	95.20
25.73	0.022	95.50
29.14	0.026	95.90
33.28	0.023	95.10
35.58	0.018	95.30
36.86	0.043	95.90
38.22	0.063	n.g.
38.96	0.021	93.80
39.57	0.047	93.60
40.28	0.017	97.00
40.76	0.046	90.30
41.15	0.023	95.00
41.37	0.052	83.60

Middle Chalk

Depth (m bgl)	AIC (%)	CaCO ₃ (%)
43.02	0.050	92.30
46.10	0.042	82.30
46.86	0.026	90.70
48.07	0.034	93.40
49.49	0.051	92.90
50.84	0.036	85.80
52.04	0.015	92.20
53.08	0.027	95.00
55.02	0.023	97.30
56.18	0.027	95.90
56.64	0.015	93.90
59.61	0.016	93.60
60.34	0.015	94.80
61.75	0.041	91.60
63.53	0.016	97.30
64.84	0.019	96.10
66.45	0.048	92.10
67.86	0.025	96.50
68.85	0.013	95.20
70.63	0.030	95.40
72.11	0.026	95.50
73.23	0.022	91.30
74.27	0.029	93.40
75.23	0.030	97.60
76.34	0.019	95.20
77.36	0.028	93.30
78.51	0.025	96.50
79.27	0.022	93.70
80.52	0.022	97.80
81.61	0.023	95.90
82.41	0.016	96.80
83.65	0.018	97.30
84.77	0.013	94.10
85.93	0.027	98.30
86.89	0.015	95.60
87.34	0.028	93.80
88.02	0.026	95.50
89.51	0.017	97.70
90.49	0.016	94.90
91.38	0.062	90.20
91.83	0.021	95.70
92.50	0.028	95.40
93.41	0.023	96.60
94.48	0.014	94.00
95.80	0.068	88.80
97.00	0.015	96.40

CaCO₃ measured at Kingston University by A. Murphy (Murphy *et al.*, 1997)

n.g. CaCO₃ content was not given for this sample.

Figure 68: Lithological log of Banterwick Barn Upper and Middle Chalk core

Sedimentary log of the Banterwick barn core, showing core recovery and sample positions. Shaded blocks in column to the left of the lithology indicate gaps in core. Filled and open circles indicate lithological samples, with depth in metres. See Figure 69 for key to symbols. From Murphy *et al.*, 1997.

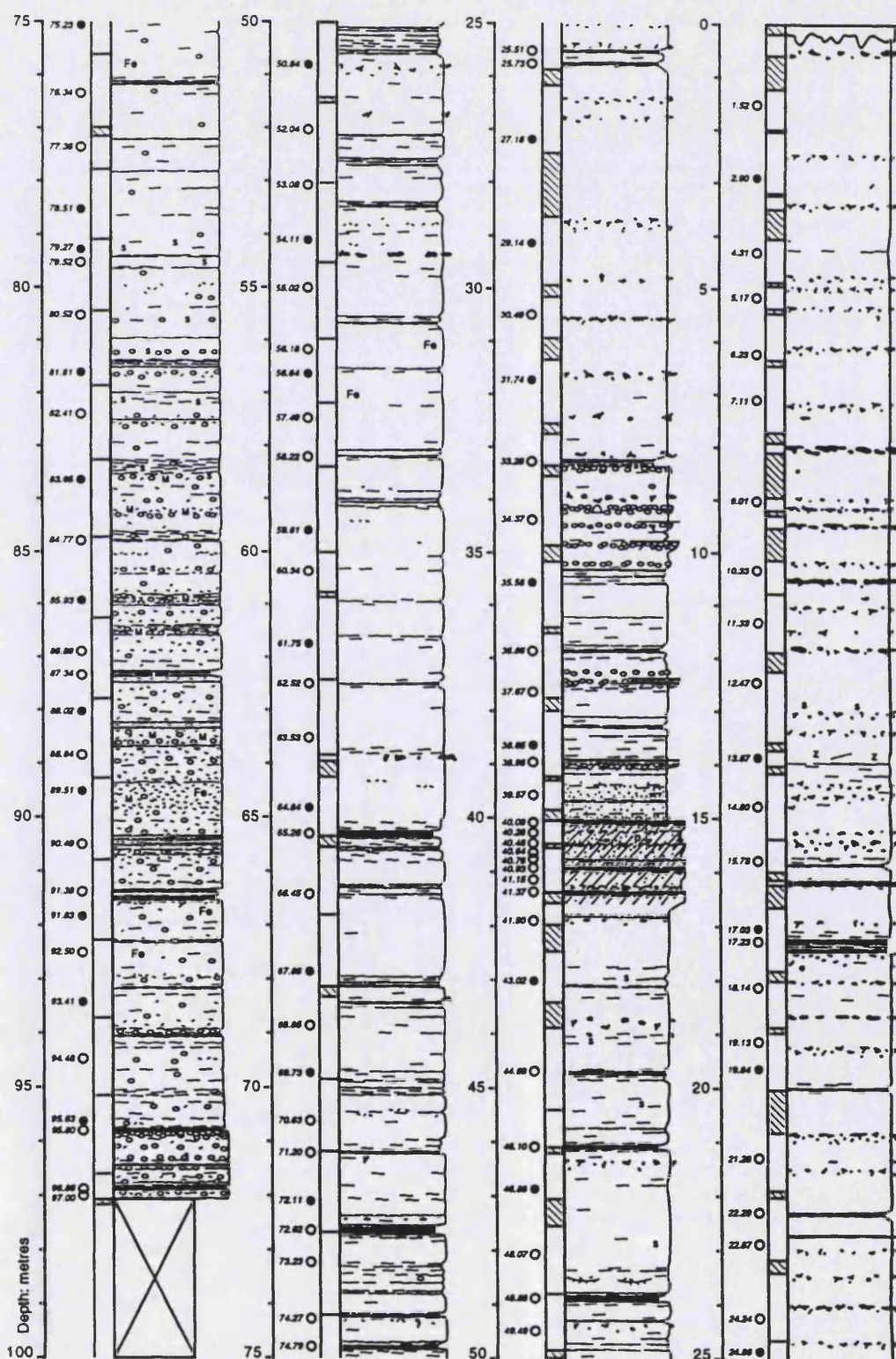
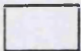
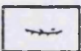
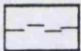

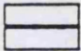
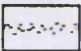
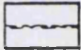
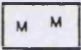
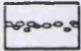
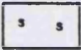
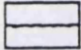
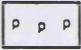
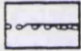
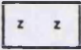
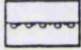
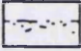
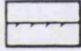
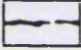
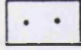
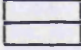

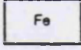



Figure 69: Key to lithological and other symbols used in Figure 68

From Murphy *et al.*, 1997.

Lithology

	white chalk		erosional scour
	marly chalk		granular glauconite
	marl seam		shell fragments
	omission surface		<i>Mytiloides</i>
	nodular chalk		sponge debris
	mineralised surface		phosphatic intraclasts
	exposed nodular chalk		<i>Zoophycos</i>
	nodular hardground		nodular flint
	massive hardground		semi-tabular flint
	pyrite		tabular flint
	sediment sample		iron oxyhydroxide staining
			porewater and sediment sample

D.2 Lower Chalk

Thriplow

Sample descriptions are based on a borehole log made and provided by the British Geological Survey and confirmed by observations.

bold figures indicate the mean of the results of at least two analyses

Depth (m bgl)	A.I.C. (%)	A.I.S. (%)	Sample description
4.70	0.020	n.d.	Firm to hard rubbly chalk with occasional shell fragments
7.00	0.12	n.d.	
9.30	0.018	n.d.	fractured chalk core with local iron staining
9.88	0.020	n.d.	
10.56	n.d.	n.d.	
11.20	0.016	n.d.	
12.58	0.025	n.d.	
13.88	0.037	n.d.	patchily hard, nodular shelly chalk with iron staining
16.11	0.0077	n.d.	patchily hard chalk with marl bands
17.35	0.055	n.d.	
19.60	0.029	0.0082	greenish grey marly chalk
20.54	0.042	0.0085	pale grey chalk with occasional burrows infilled with marly chalk
22.83	0.038	n.d.	pale grey chalk with bioturbation infilled with paler chalk
23.25	0.012	n.d.	pale grey chalk
23.60	0.024	n.d.	pale grey chalk with bioturbation infilled with paler chalk
24.13	0.047	n.d.	pale grey chalk, locally bioturbated, marly horizons
25.17	0.032	n.d.	pale to medium grey chalk
25.86	0.0068	n.d.	pale grey chalk
27.90	0.025	n.d.	pale grey chalk with dark grey marly chalk layers
28.04	0.027	n.d.	pale grey chalk with bands of orange staining
28.25	0.054	n.d.	
28.51	0.042	n.d.	pale grey bioturbated chalk
29.08	0.033	n.d.	pale grey, patchily bioturbated chalk with marly layers
29.55	0.033	n.d.	
30.38	0.035	n.d.	
30.70	0.028	n.d.	
31.47	0.052	n.d.	
34.40	0.016	n.d.	
35.00	0.013	n.d.	pale grey chalk with strong bioturbation
35.35	0.053	n.d.	darker marly chalk with bioturbation with paler infill
36.14	0.044	n.d.	
36.45	0.055	n.d.	pale brownish-grey chalk
37.12	0.049	n.d.	
39.04	0.057	n.d.	pale brownish-grey chalk in very broken core with local bioturbation
39.85	0.034	n.d.	pale brownish-grey weakly marly shelly chalk
40.11	0.066	n.d.	conspicuously bioturbated medium grey-brown marly chalk
41.92	0.082	0.0038	bioturbated pale brown silty chalk
42.80	0.066	n.d.	pale brownish grey chalk
43.80	0.034	n.d.	pale brownish grey chalk with marly horizons
44.25	0.049	n.d.	chalk with corroded marcasite nodule
46.49	0.076	0.0043	pale brownish grey chalk, patchily iron stained
47.53	0.068	0.0035	highly fragmented core, medium-grey marly chalk
49.40	0.047	n.d.	medium grey marly bioturbated chalk
50.50	0.056	0.0053	pale brownish grey chalk
53.60	0.053	n.d.	firm pale creamy grey bioturbated chalk, locally shelly
54.00	0.019	n.d.	
55.00	0.035	n.d.	medium grey marl, patchily iron stained
55.63	0.050	0.013	medium grey marly bioturbated chalk with patchy iron staining
56.58	0.037	n.d.	medium to pale grey marly bioturbated chalk
56.87	0.070	0.0033	firm pale grey creamy grey chalk with patchy iron staining
57.73	0.090	0.027	pale buffish grey marly chalk with local bioturbation and iron staining
59.08	0.099	0.011	pale buffish grey chalk with marly burrow infills, shelly and iron stained

D.3 Lincolnshire Limestone from Quarry exposures

Brauncewell Quarry

Depth (m bgl)	A.I.C. (%)	A.I.S. (%)	Sample description
4.70	0.020	n.d.	Firm to hard rubbly chalk with occasional shell fragments
7.00	0.12	n.d.	
9.30	0.018	n.d.	fractured chalk core with local iron staining
9.88	0.020	n.d.	
10.56	n.d.	n.d.	
11.20	0.016	n.d.	
12.58	0.025	n.d.	patchily hard, nodular shelly chalk with iron staining
13.88	0.037	n.d.	
16.11	0.0077	n.d.	patchily hard chalk with marl bands
17.35	0.055	n.d.	
19.60	0.029	0.0082	greenish grey marly chalk
20.54	0.042	0.0085	pale grey chalk with occasional burrows infilled with marly chalk
22.83	0.038	n.d.	pale grey chalk with bioturbation infilled with paler chalk
23.25	0.012	n.d.	pale grey chalk
23.60	0.024	n.d.	pale grey chalk with bioturbation infilled with paler chalk
24.13	0.047	n.d.	pale grey chalk, locally bioturbated, marly horizons
25.17	0.032	n.d.	pale to medium grey chalk
25.86	0.0068	n.d.	pale grey chalk
27.90	0.025	n.d.	pale grey chalk with dark grey marly chalk layers
28.04	0.027	n.d.	pale grey chalk with bands of orange staining
28.25	0.054	n.d.	
28.51	0.042	n.d.	pale grey bioturbated chalk
29.08	0.033	n.d.	pale grey, patchily bioturbated chalk with marly layers
29.55	0.033	n.d.	
30.38	0.035	n.d.	
30.70	0.028	n.d.	
31.47	0.052	n.d.	
34.40	0.016	n.d.	
35.00	0.013	n.d.	pale grey chalk with sporadic bioturbation
35.35	0.053	n.d.	pale grey chalk with strong bioturbation
36.14	0.044	n.d.	darker marly chalk with bioturbation with paler infill
36.45	0.055	n.d.	pale brownish-grey chalk
37.12	0.049	n.d.	
39.04	0.057	n.d.	pale brownish-grey chalk in very broken core with local bioturbation
39.85	0.034	n.d.	pale brownish-grey weakly marly shelly chalk
40.11	0.066	n.d.	conspicuously bioturbated medium grey-brown marly chalk
41.92	0.082	0.0038	bioturbated pale brown silty chalk
42.80	0.066	n.d.	pale brownish grey chalk
43.80	0.034	n.d.	pale brownish grey chalk with marly horizons
44.25	0.049	n.d.	chalk with corroded marcasite nodule
46.49	0.076	0.0043	pale brownish grey chalk, patchily iron stained
47.53	0.068	0.0035	highly fragmented core, medium-grey marly chalk
49.40	0.047	n.d.	medium grey marly bioturbated chalk
50.50	0.056	0.0053	pale brownish grey chalk
53.60	0.053	n.d.	firm pale creamy grey bioturbated chalk, locally shelly
54.00	0.019	n.d.	
55.00	0.035	n.d.	medium grey marl, patchily iron stained
55.63	0.050	0.013	medium grey marly bioturbated chalk with patchy iron staining
56.58	0.037	n.d.	medium to pale grey marly bioturbated chalk
56.87	0.070	0.0033	firm pale grey creamy grey chalk with patchy iron staining
57.73	0.090	0.027	pale buffish grey marly chalk with local bioturbation and iron staining
59.08	0.099	0.011	pale buffish grey chalk with marly burrow infills, shelly and iron stained

Continued on next page. Each result is the mean of two analyses. Samples collected, prepared and analysed by A. Kim

Appendix D: Measured AIC content

Brauncewell Quarry: Continued from previous page

Depth (m bgl)	AIC (%)	AIS (%)	TC (%)	TS (%)	Description
12.900	0.061	0.10	11.3	0.25	redox block, reduced blue grey side
12.905	0.057	0.080	11.1	0.25	
12.910	0.032	0.082	10.7	0.26	
12.915	0.050	0.072	11.8	0.26	
12.920	0.042	0.086	11.5	0.21	
12.925	0.040	0.12	11.4	0.33	
12.930	0.029	0.080	11.6	0.29	
12.935	0.045	0.11	11.5	0.30	
12.940	0.045	0.085	11.3	0.33	
12.945	0.052	0.087	11.9	0.34	
12.950	0.081	0.094	11.7	0.31	
12.955	0.040	0.079	11.6	0.30	
12.960	0.074	0.098	11.3	0.26	
12.965	0.054	0.12	11.2	0.35	
12.970	0.070	0.097	10.9	0.28	
12.975	0.056	0.12	11.9	0.36	
12.980	0.054	0.10	11.4	0.35	
12.985	0.048	0.10	11.6	0.40	
12.990	0.045	0.066	11.4	0.38	
12.995	0.065	0.15	11.6	0.36	
13.000	0.039	0.058	11.2	0.24	redox block, mid point
13.005	0.048	0.016	11.0	0.018	redox block, oxidised bleached buff side
13.010	0.032	0.011	11.0	0.021	
13.015	0.044	0.015	11.1	0.014	
13.020	0.038	0.012	11.1	0.0081	
13.025	0.030	0.0090	11.2	0.0060	
13.030	0.032	0.0084	11.5	0.014	
13.035	0.035	0.0071	11.5	0.0044	
13.040	0.041	0.0091	11.4	0.0068	
13.045	0.052	0.0096	11.4	0.0031	
13.050	0.041	0.0094	11.3	0.0071	
13.055	0.034	0.0061	11.4	0.013	
13.060	0.042	0.0098	11.1	0.015	
13.80	0.16	0.013	6.27	0.028	red brown marl
14.60	0.040	n.d.	11.0	n.d.	bleached cream white lime mudstone with some small shell fragments
14.62	0.044	n.d.	11.2	n.d.	
15.80	0.027	n.d.	11.5	0.0049	bleached buff coloured limestone peloidal packstone
15.82	0.037	n.d.	11.2	0.0073	
15.84	0.045	n.d.	11.3	0.0042	
15.86	0.036	n.d.	11.3	0.0038	

Each result is the mean of two analyses

Samples collected, prepared and analysed by A. Kim

Appendix D: Measured AIC content

Harmston Quarry

Depth (m bgl)	AIC (%)	AIS (%)	TC (%)	TS (%)	Description
0.50	0.022	0.0073	10.7	0.0059	bleached buff coloured peloidal packstone
0.51	0.024	0.0078	11.0	0.0021	
0.52	0.020	0.0094	11.2	0.0062	
0.53	0.029	0.0091	11.0	0.0040	
0.54	0.028	0.016	10.7	0.0047	
0.55	0.025	0.015	10.8	n.d.	
2.70	0.025	0.014	11.6	0.0049	bleached buff coloured peloidal packstone with small shell fragments
2.72	0.020	0.0091	11.6	0.0040	
4.00	0.016	0.0023	11.3	0.0080	
4.02	0.022	n.d.	11.0	0.0060	
4.04	0.017	n.d.	11.5	0.0090	
4.06	0.022	0.0023	11.5	0.0080	
6.70	0.034	0.0069	11.8	0.0021	
6.72	0.032	0.0078	11.8	0.0069	
6.74	0.027	0.0050	11.8	0.0066	
6.76	0.025	0.0038	11.8	0.0046	
7.80	2.5	1.2	9.12	2.1	black marl with small shell fragments
8.80	0.044	0.11	11.6	0.16	blue-grey lime mudstone with small and large shell fragments and calcite spars
8.82	0.073	0.12	11.6	0.16	
8.84	0.071	0.15	11.5	0.14	
8.86	0.067	0.15	11.4	0.16	
9.30	0.15	0.21	11.5	0.20	blue grey coloured peloidal packstone limestone
9.31	0.061	0.098	11.4	0.11	
9.32	0.11	0.19	11.6	0.15	
9.33	0.11	0.21	11.6	0.13	
10.05	0.15	0.20	12.3	0.18	black marl composed mainly of shell fragments in layers
10.07	0.26	0.37	12.1	0.27	
10.15	1.5	2.2	6.27	3.5	black marl
10.30	1.7	2.4	6.41	4.1	
10.30	0.75	1.4	8.81	1.4	black marl - stone like
10.40	0.16	0.31	11.0	0.19	blue grey lime mudstone
10.42	0.15	0.30	10.7	0.17	
10.44	0.15	0.29	11.0	0.20	
10.46	0.14	0.30	10.7	0.24	
10.48	0.14	0.30	10.6	0.24	
10.50	0.15	0.30	10.1	0.19	
10.60	0.95	1.4	7.21	2.5	black marl
11.80	0.067	n.d.	10.8	n.d.	bleached cream white lime mudstone with small and large shell fragments
11.82	0.041	n.d.	11.3	0.0063	
11.84	0.043	n.d.	11.4	0.0029	
11.86	0.047	0.0033	11.3	0.0054	

Each result is the mean of two; Samples collected, prepared and analysed by A. Kim

Figure 70: AIC, TS and TC in oxidised Lincolnshire Limestone, Harmston Quarry

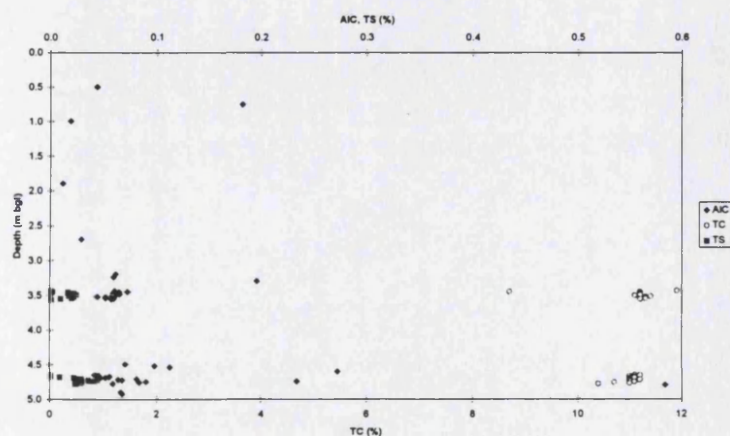


Figure 71: AIC, AIS and TS in redox block 1 from Harmston Quarry

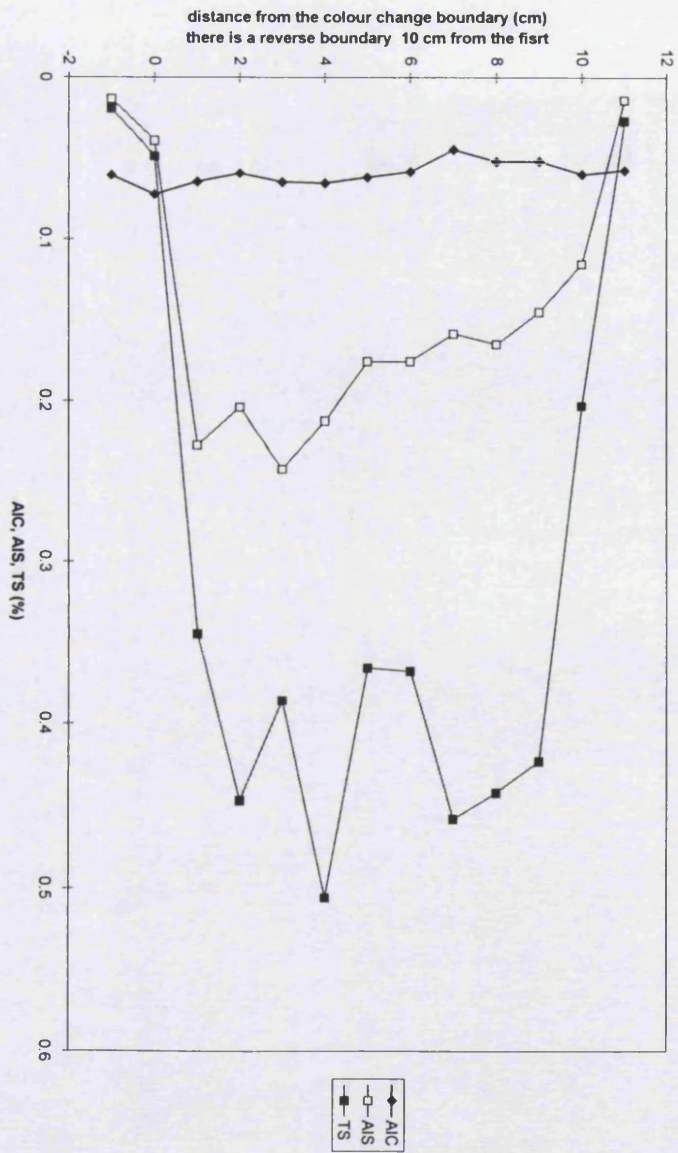
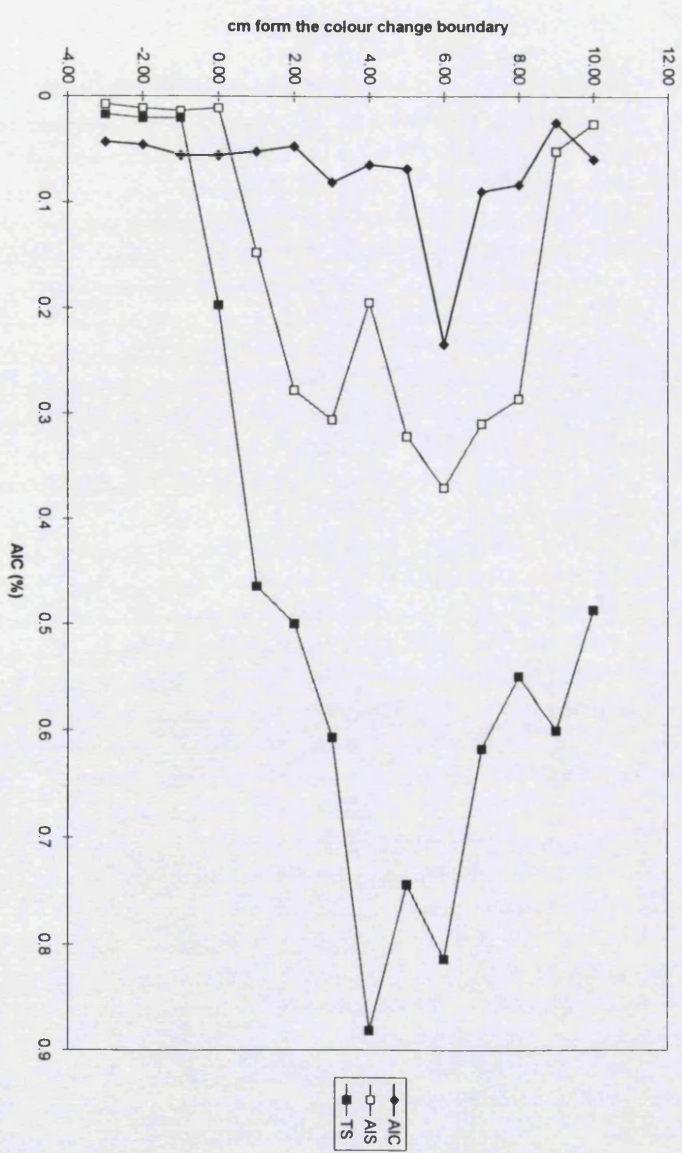


Figure 72: AIC, AIS and TS in redox block 2 from Harmston Quarry



Appendix D: Measured AIC content

Leadenham Quarry

Depth (m bgl)	AIC (%)	AIS (%)	Description
0.10	0.032	0.0039	bleached buff (light grey) lime mudstone with small shell fragments
0.40	0.035	0.0031	bleached buff (light grey) lime mudstone with large shell fragments
0.42	0.029	0.0035	
0.50	0.25	0.015	dark brown marl with 1mm weathering
0.60	0.052	0.0022	buff lime mudstone with small shell fragments
0.62	0.035	n.d.	
0.70	0.17	0.0060	brown marl (8cm thick section)
0.90	0.035	n.d.	bleached buff (light grey) lime mud stone with small shell fragments
0.94	0.018	0.0023	
1.50	0.23	0.0024	bleached buff peloidal wackestone with various sized shell fragments
1.52	0.023	n.d.	
1.54	0.020	n.d.	
1.56	0.018	n.d.	
2.50	0.21	0.0051	red brown marl (5cm thick section)
2.70	0.015	0.0040	bleached buff / sand-coloured lime mudstone with small shell fragments
2.73	0.052	n.d.	
2.76	0.018	n.d.	
3.80	0.018	n.d.	buff lime mudstone with large suspended peloids
3.84	0.020	n.d.	
4.60	0.024	n.d.	bleached buff coloured lime mudstone with shell fragments
4.62	0.021	n.d.	
4.64	0.024	n.d.	
4.66	0.014	n.d.	
5.35	0.16	n.d.	red brown coloured marl with distinctive grey streaks
6.00	0.045	n.d.	bleached buff coloured peloidal packstone
6.02	0.023	n.d.	
6.04	0.023	n.d.	
6.06	0.027	n.d.	
7.50	0.15	n.d.	
7.53	0.019	n.d.	
8.40	0.014	n.d.	bleached buff coloured lime mud stone with few suspended peloids
8.43	0.018	n.d.	
8.46	0.047	n.d.	
8.49	0.0095	n.d.	
9.70	0.13	n.d.	red brown coloured marl
10.10	0.019	n.d.	bleached buff coloured wackestone with some shell fragments
11.00	0.020	n.d.	
11.03	0.015	n.d.	
12.00	0.022	n.d.	bleached buff coloured coarse grained, peloidal packstone with some shell fragments
12.02	0.027	n.d.	
12.04	0.033	0.0024	
12.06	0.034	n.d.	

Each result is the mean of two analyses

Samples collected, prepared and analysed by A. Kim

Appendix D: Measured AIC content

Ropesley Quarry

Depth (m bgl)	AIC (%)	AIS (%)	TC (%)	TS (%)	Description
0.00	0.039	0.013	~	~	bleached buff peloidal packstone
0.02	0.029	0.012	~	~	
1.00	0.022	0.0090	~	~	
1.02	0.030	n.d.	~	~	
2.90	0.025	0.0025	~	~	
2.91	0.032	n.d.	~	~	
2.92	0.024	n.d.	~	~	
2.93	0.025	n.d.	~	~	bleached cream white mud stone
4.30	0.040	n.d.	~	~	
4.31	0.035	n.d.	~	~	
4.32	0.046	n.d.	~	~	
4.33	0.041	n.d.	~	~	bleached buff coloured peloidal packstone interspersed with clay mudstone
5.30	0.044	n.d.	~	~	
5.31	0.035	n.d.	~	~	
5.32	0.045	n.d.	~	~	
5.33	0.037	n.d.	~	~	bleached buff peloidal packstone with shell fragments
6.30	0.018	n.d.	~	~	
6.32	0.027	n.d.	~	~	
6.34	0.025	0.0033	~	~	
6.36	0.025	0.0024	~	~	yellow sand buff coloured peloidal packstone
7.30	0.079	0.0045	~	~	
7.32	0.047	0.0040	~	~	
7.34	0.031	0.0055	~	~	
7.36	0.036	0.0039	~	~	dark brown stiff marl
9.60	1.2	1.1	~	~	
9.625	0.060	n.d.	11.3	n.d.	redox block (oxidised side) lime mudstone with few small shell fragments
9.635	0.051	n.d.	11.2	n.d.	
9.645	0.050	n.d.	10.9	n.d.	
9.655	0.050	n.d.	11.3	n.d.	
9.665	0.052	0.0031	11.5	n.d.	
9.675	0.063	0.0057	11.6	0.0046	
9.685	0.062	0.0063	11.5	0.0047	
9.695	0.067	0.020	11.5	0.012	
9.705	0.061	0.11	11.5	0.14	
9.715	0.067	0.13	11.5	0.21	
9.725	0.088	0.13	11.5	0.18	
9.735	0.069	0.16	11.3	0.22	
9.745	0.13	0.27	11.3	0.28	
9.755	0.25	0.24	10.4	0.21	black marl , 5-10 cm thick
9.90	1.5	1.2	~	~	
10.30	0.041	0.041	~	~	blue grey lime mudstone some calcite spar
10.32	0.064	0.052	~	~	
10.34	0.064	0.074	~	~	
10.36	0.084	0.098	~	~	
10.40	0.38	0.019	~	~	black marl laminated with shell fragments
12.40	0.038	0.0026	~	~	bleached sand buff coloured peloidal packstone
12.42	0.035	0.0029	~	~	
12.44	0.026	n.d.	~	~	
12.46	0.028	0.0041	~	~	
12.48	0.035	0.012	~	~	
12.50	0.031	0.0054	~	~	
12.52	0.035	n.d.	~	~	
12.54	0.033	0.0042	~	~	cream white coloured peloidal packstone
17.00	0.037	n.d.	~	~	
17.02	0.029	0.0037	~	~	

Each result is the mean of two analyses

Samples collected, prepared and analysed by A. Kim



Appendix D: Measured AIC content

Walcott Quarry

m bct metres below core top

Depth (m bct)	AIC (%)	AIS (%)	Description
58.00	0.11	0.94	mid blue grey very coarse grained limestone, many shell fragments
58.04	0.096	0.87	
58.08	0.083	0.76	
58.12	0.068	0.11	mid blue grey fine grained limestone
58.14	0.054	0.082	
58.16	0.058	0.096	
58.18	0.047	0.078	
62.00	0.046	0.73	
62.03	0.028	0.63	mid blue grey coarse grained peloidal packstone, much shell debris
62.06	0.033	0.78	
62.09	0.054	0.75	
62.12	0.048	0.84	
62.15	0.038	0.93	
62.18	0.037	0.67	
62.21	0.036	0.51	
62.24	0.038	0.84	
62.27	0.038	0.84	
62.30	0.030	0.85	
62.33	0.035	0.84	
62.36	0.019	0.65	
62.39	0.032	0.68	
64.00	0.056	0.29	mid grey coarse grained peloidal packstone, many small shell fragments
64.03	0.052	0.47	
64.06	0.083	0.87	
64.09	0.11	0.40	
64.12	0.11	0.37	
66.50	0.057	0.091	dark grey peloidal packstone
67.50	0.061	0.095	light grey / buff coloured peloidal packstone
67.54	0.068	0.073	
67.58	0.087	0.084	
67.62	0.050	0.070	
67.66	0.075	0.084	
67.70	0.074	0.093	
68.50	0.18	0.33	mid grey, very coarse grained bioclastic wackestone
68.54	0.15	0.26	
68.58	0.082	0.13	mid grey, coarse grained bioclastic wackestone
68.62	0.098	0.17	
68.66	0.061	0.092	light grey, fine grained peloidal packstone
68.70	0.073	0.094	
68.74	0.093	0.11	light grey lime mudstone
70.50	0.11	0.12	
70.54	0.10	0.10	
70.58	0.093	0.083	
70.62	0.12	0.086	
70.66	0.092	0.067	
70.70	0.089	0.080	
70.74	0.10	0.076	
70.78	0.079	0.056	
70.82	0.076	0.064	
70.86	0.063	0.069	light grey coarse grained, many shell fragments

Continued on next page.

Each sample was analysed twice and the average of the results is presented.

Samples collected, prepared and analysed by A. Kim

Appendix D: Measured AIC content

Walcott Quarry: Continued from previous page

Depth (m bct)	AIC (%)	AIS (%)	Description
71.30	0.25	0.19	mid blue grey lime mudstone with suspended peloids and dark grey striations
71.34	0.13	0.11	
71.38	0.15	0.10	
71.42	0.22	0.16	
71.46	0.22	0.21	
71.50	0.41	0.36	
74.10	0.11	0.18	mid blue grey, fine grained peloidal packstone
74.14	0.11	0.15	
74.18	0.14	0.16	
74.22	0.11	0.12	
74.26	0.10	0.10	
74.30	0.097	0.091	
74.34	0.077	0.064	dark blue grey peloidal wackestone with large shell fragments
75.10	0.059	0.085	
75.14	0.076	0.17	
75.18	0.071	0.075	
75.22	0.061	0.051	
75.26	0.059	0.043	
75.90	2.2	1.7	black / dark grey marl
77.40	0.13	0.078	dark blue grey peloidal packstone with black oolites
77.44	0.49	0.059	
77.48	0.54	0.059	
77.52	0.038	0.091	mid blue grey lime mudstone
77.56	0.042	0.086	
77.60	0.031	0.095	
77.64	0.034	0.075	
77.68	0.029	0.080	
78.68	0.70	0.31	mid blue grey lime mudstone with much shell debris
78.72	0.95	0.67	mid blue grey lime mudstone
78.76	1.0	0.62	hard dark grey marl
78.80	0.95	0.67	
78.84	1.0	0.62	
80.00	0.67	0.79	dark grey almost black marl
80.50	0.072	0.19	mid blue grey limestone no peloids, many small shell fragments
80.54	0.051	0.20	
80.58	0.057	0.19	
80.62	0.074	0.25	
80.66	0.079	0.24	
81.60	0.085	0.12	
81.64	0.056	0.093	light grey almost buff coloured peloidal packstone, some secondary calcitification
81.68	0.058	0.064	
81.72	0.060	0.091	
81.76	0.062	0.13	
81.80	0.062	0.14	
83.20	0.11	0.71	
83.24	0.088	0.46	mid blue grey lime mudstone with many various sized shell fragments
83.28	0.073	1.0	
83.32	0.14	1.6	
83.36	0.14	2.9	mid blue grey coarse grained lime mudstone slightly silty
83.40	0.077	0.38	mid blue grey peloidal packstone
83.44	0.094	0.22	
83.48	0.18	0.66	

Each sample was analysed twice and the average of the results is presented.

Samples collected, prepared and analysed by A. Kim

Appendix D: Measured AIC content

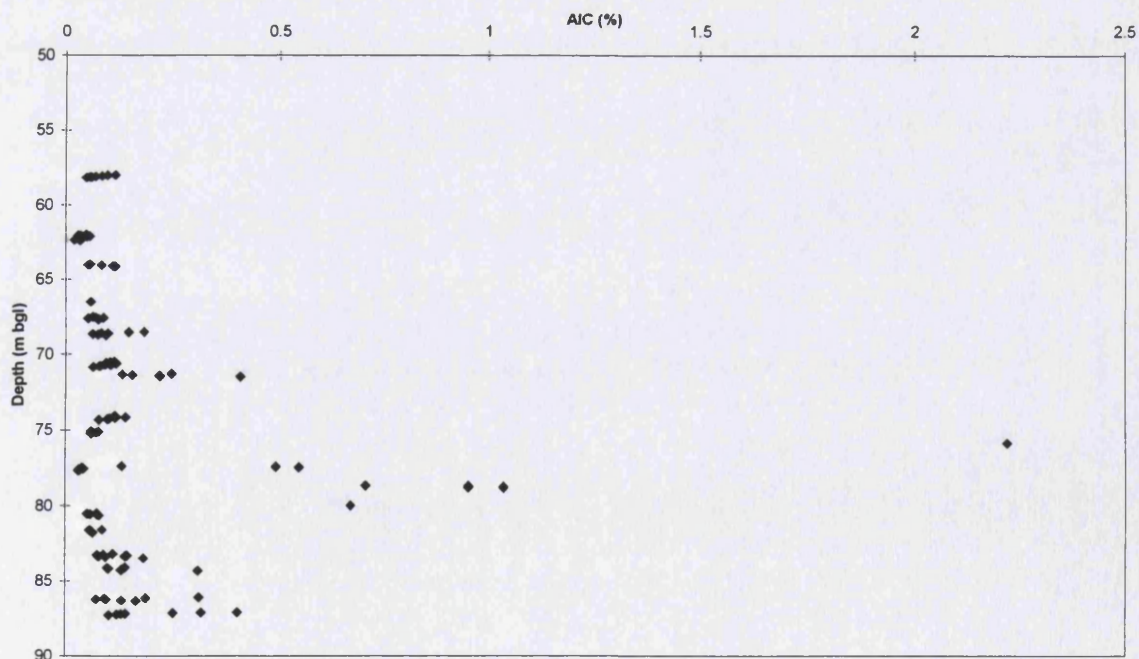
Walcott Quarry: Continued from previous page

Depth (m bct)	AIC (%)	AIS (%)	Description
84.10	0.14	0.47	mid blue grey peloidal wackestone with lime mud patches
84.14	0.097	0.34	
84.18	0.10	0.32	
84.22	0.13	0.22	
84.26	0.13	0.29	
84.30	0.13	0.24	
84.34	0.31	0.90	dark grey peloidal wackestone with lime mud patches
86.10	0.31	0.93	mid blue grey peloidal packstone, many shell fragments
86.14	0.19	0.58	
86.18	0.091	0.25	mid blue grey silty layer
86.22	0.072	0.23	mid blue grey lime mudstone
86.26	0.095	0.25	
86.30	0.13	0.54	mid blue grey peloidal packstone
86.34	0.16	0.65	
87.10	0.40	1.4	mid blue grey very coarse grained peloidal packstone with many small shell fragments
87.12	0.32	2.0	
87.14	0.25	0.73	
87.18	0.14	0.34	mid blue grey coarse grained peloidal packstone
87.22	0.13	0.76	
87.26	0.12	0.27	mid blue grey fine grained peloidal packstone
87.30	0.10	0.27	

Each sample was analysed twice and the average of the results is presented.

Samples collected, prepared and analysed by A. Kim

Figure 74: AIC in oxidised Lincolnshire Limestone, Walcott Quarry



D.4 Unoxidised Lincolnshire Limestone

Longholt Core

Depth (m bgl)	AIC (%)	AlS (%)	TC (%)	TS (%)	Description
60.38	0.27	0.033	0.293	0.10	light to dark grey soft crumbly mudstone
60.47	0.53	0.030	0.545	0.043	
60.56	2.0	1.4	2.09	1.9	
60.96	2.7	2.6	2.94	4.1	
61.02	0.84	1.2	0.991	0.95	
61.11	0.64	2.4	0.700	2.8	
61.17	0.65	3.4	0.784	4.7	
62.01	0.15	0.27	0.211	0.42	
62.10	1.4	0.35	1.62	0.22	
62.16	0.18	0.22	0.217	0.31	
62.49	0.24	1.3	0.290	1.9	
62.56	0.21	0.78	0.283	0.82	
62.67	0.18	0.58	0.216	0.59	
62.72	0.15	0.32	0.160	0.32	
63.75	1.2	2.2	10.2	3.0	dark grey (almost black) silt / limestone with many shell fragments (1-5% of rock), peloidal packstone, peloids are carbonate (10-20%) possibly quartz / lithic grains
63.77	1.3	2.4	10.3	3.1	
63.79	1.1	2.6	10.4	3.3	
63.81	1.2	2.1	10.4	2.9	
63.83	1.4	2.3	10.4	3.3	
63.85	1.5	3.0	10.5	3.8	
66.86	0.26	0.99	11.0	1.3	mid grey bioclastic / clastic siltstone poorly sorted, approx. 5-10% coarse shell debris with a few whole shells
66.88	0.23	0.65	11.3	1.0	
66.90	0.26	0.67	11.1	0.86	
66.92	0.33	1.4	11.1	1.5	
66.94	0.64	1.8	10.4	1.9	
66.96	0.95	1.8	9.93	2.3	marl/silt partings with undulating bedding planes of darker material
67.00	1.1	1.7	9.95	1.7	
66.99	0.16	0.57	11.3	0.44	light grey hard wackestone
67.07	0.24	0.42	11.3	0.37	light to mid grey hard peloidal packstone with some shell fragments
67.12	0.23	0.49	11.5	0.39	
67.22	0.49	3.2	10.5	3.6	light grey hard coarse wackestone with some shell fragments
67.49	0.11	0.37	11.6	0.41	
67.59	0.26	1.0	11.1	0.72	light grey hard peloidal wackestone with some shell fragments
67.69	0.19	0.88	11.1	0.87	
68.66	0.090	0.14	11.0	0.28	mid blue grey lime / silt stone fine peloidal packstone approx. 10% black grains, slightly marly layer (darker & finer)
68.68	0.22	0.53	9.76	0.81	
68.70	0.094	0.22	11.2	0.47	mid grey blue medium grade slightly coarser than overlying layers, bioclastic peloidal packstone with very large shell fragments and clasts
68.72	0.097	0.18	11.3	0.32	
68.74	0.061	0.13	11.4	0.31	
68.76	0.067	0.17	11.5	0.35	
68.78	0.11	0.20	11.4	0.32	
68.80	0.11	0.21	10.8	0.32	
68.80	0.087	0.20	11.5	0.19	light to mid grey hard coarse peloidal packstone with some shell fragments
68.90	0.081	0.17	11.3	0.28	
69.00	0.17	0.48	~	~	very light grey hard wackestone
69.06	0.080	0.14	11.5	0.14	
69.14	0.060	0.11	11.9	0.17	light grey hard peloidal packstone
69.22	0.079	0.13	12.0	0.11	
69.28	0.092	0.17	12.0	0.22	light blue grey packstone with many shell fragments
69.72	0.10	0.18	11.5	0.36	
69.74	0.11	0.22	11.5	0.38	
69.76	0.11	0.24	11.5	0.37	
69.78	0.074	0.23	11.5	0.41	
69.80	0.085	0.19	11.5	0.30	
69.82	0.068	0.14	11.6	0.21	
69.84	0.068	0.15	11.6	0.22	
69.86	0.080	0.15	11.8	0.32	

Continued on next page

Some samples prepared and analysed by the author, others by A. Kim.

bold figures indicate the mean of the results of at least two analyses

Appendix D: Measured AIC content

Longholt Core: Continued from previous page

Depth (m bgl)	AIC (%)	AIS (%)	TC (%)	TS (%)	Description
69.86	0.11	0.33	11.7	0.26	light grey hard peloidal packstone with shell fragments
69.90	~	~	11.1	0.68	
69.92	0.11	0.29	11.7	0.30	
69.98	0.076	0.17	11.7	0.23	
70.04	0.13	0.25	11.7	0.32	
70.12	0.071	0.18	11.6	0.22	mid blue grey lime / silt stone with many small shell fragments, peloidal packstone
70.85	0.11	0.26	11.7	0.48	
70.87	0.11	0.28	11.5	0.60	
70.89	0.053	0.13	11.6	0.52	
70.91	0.10	0.31	11.7	0.53	
70.93	0.091	0.21	11.6	0.50	
70.95	0.073	0.17	11.7	0.52	
70.97	0.12	0.31	11.6	0.61	
72.88	0.091	0.27	10.6	0.32	mid blue grey fine grain limestone
72.90	0.19	0.47	8.32	0.75	
72.92	0.46	0.73	6.87	1.1	dark grey marl partings (mm) parted at approx. 2cm, well bedded quartzite laminae
72.94	1.4	1.2	6.76	1.4	
72.96	1.0	1.1	6.27	1.5	
72.98	1.2	1.1	5.88	1.4	
73.00	0.91	1.0	6.42	1.4	
73.02	1.6	1.1	6.23	1.3	mid grey peloidal packstone oncolites, very coarse grained, uniform grained, few large shell fragments
73.96	0.24	0.31	11.1	0.35	
73.98	0.25	0.38	11.0	0.45	
74.00	0.27	0.50	11.0	0.57	
74.02	0.20	0.45	10.8	0.45	
74.04	0.17	0.37	11.1	0.40	
74.06	0.18	0.38	10.6	0.48	
74.08	0.22	0.39	10.1	0.39	
74.10	0.36	0.47	10.4	0.49	dark grey crumbly shale / mudstone
75.87	2.7	2.3	8.61	2.6	
75.99	1.3	1.2	10.3	1.3	light to mid grey crumbly mudstone with shell fragments
76.08	0.075	0.17	11.8	0.28	light grey hard peloidal wackestone with some shell fragments
78.17	0.50	0.29	11.5	0.41	mid blue grey lime mudstone with many shell fragments
78.18	0.62	0.24	11.5	0.42	
78.19	0.43	0.22	11.9	0.50	dark grey shale / marl band
78.20	0.18	0.26	11.9	0.45	
78.21	0.28	0.28	12.0	0.46	
78.22	0.33	0.32	11.8	0.33	mid blue grey peloidal wackestone with black oolites
78.23	0.22	0.038	11.7	0.33	
78.24	0.12	0.0024	11.7	0.25	
78.25	0.11	0.021	11.9	0.18	
78.26	0.090	0.053	12.0	0.20	
79.13	0.071	0.15	12.0	0.19	light grey hard peloidal packstone locally with some shell fragments
79.19	0.085	0.081	12.0	0.094	
79.24	0.085	0.084	11.8	0.17	
79.31	0.070	0.13	11.9	0.15	
79.40	0.068	0.26	11.8	0.43	light to mid grey grain supported coarse peloidal packstone
80.44	0.89	1.4	10.0	1.25	mid to dark grey crumbly shale / marl band with shell fragments
80.50	0.77	1.5	9.36	1.49	
80.56	0.53	0.73	10.1	0.77	
81.28	0.055	0.41	11.3	0.89	mid blue grey peloidal packstone with lime mud patches (interclasts), few shell fragments oolites / oncolites
81.30	0.044	0.25	11.4	0.73	
81.32	0.065	0.41	11.1	0.53	
81.34	0.063	0.46	11.4	0.69	
81.36	0.12	0.54	11.3	0.68	
81.38	0.069	0.54	11.4	0.72	
81.40	0.064	0.41	11.6	0.66	
81.41	0.064	0.27	11.5	0.41	light grey hard peloidal wackestone
81.48	0.065	0.40	11.6	0.48	light grey hard peloidal packstone / wackestone
81.56	0.077	0.44	11.6	0.59	mid grey peloidal packstone
81.64	0.080	0.57	11.4	0.63	

Continued on next page

Some samples prepared and analysed by A. Kim, some by the author

bold figures indicate the mean of the results of at least two analyses

Appendix D: Measured AIC content

Longholt Core: Continued from previous page

Depth (m bgl)	AIC (%)	AIS (%)	TC (%)	TS (%)	Description
82.08	0.15	0.54	10.9	0.48	light grey hard mudstone with rare 5mm areas of peloids and rare shell fragments
82.16	0.11	0.40	11.3	0.45	
82.24	0.084	0.24	11.4	0.25	
82.30	0.071	0.29	11.6	0.39	light grey hard peloidal wackestone
83.46	0.077	0.13	11.6	0.23	light blue grey peloidal packstone, very uniform, few small shell fragments + 1-2% cemented bioclastic material
83.47	0.086	0.13	11.7	0.26	
83.48	0.087	0.12	11.8	0.18	
83.49	0.076	0.087	11.6	0.25	
83.50	0.077	0.13	11.7	0.26	
83.51	0.096	0.19	11.5	0.25	
83.52	0.083	0.14	11.5	0.29	
83.53	0.068	0.11	11.7	0.25	
84.57	0.081	0.30	11.2	0.61	mid grey peloidal packstone, few small shell fragments, with oolites and patches of lime mud
84.59	0.054	0.14	11.1	0.60	
84.61	0.076	0.33	10.9	0.62	
84.63	0.081	0.043	11.0	0.58	
84.65	0.096	0.0097	11.1	0.64	
84.67	0.051	0.14	11.2	0.62	
84.69	0.098	0.22	10.8	0.72	
85.07	0.077	0.31	11.3	0.40	light blue grey peloidal packstone, few small shell fragments, oncolites with some patches of diffuse and irregular lime mud
85.08	0.060	0.29	11.2	0.49	
85.09	0.062	0.22	11.4	0.44	
85.10	0.12	0.54	11.3	0.48	
85.11	0.085	0.57	11.5	0.53	
85.12	0.081	0.63	11.4	0.73	
85.13	0.088	0.82	11.7	0.71	
85.14	0.042	0.33	11.4	0.89	
86.06	0.045	0.16	12.0	0.24	light blue grey wackestone with some shell fragments
86.07	0.042	0.16	12.0	0.26	
86.08	0.056	0.17	12.1	0.39	darker blue grey wackestone with some shell fragments
86.09	0.039	0.14	11.8	0.35	
86.10	0.077	0.22	12.1	0.36	light blue grey oncolites with lime mud patches
86.11	0.035	0.14	12.0	0.31	
86.12	0.057	0.19	11.9	0.32	
86.13	0.047	0.16	11.6	0.27	
89.00	0.13	0.50	6.91	0.90	dark to mid grey silt limestone, fine mudstone with some bioclasts (shell fragments)
89.02	0.21	0.044	7.26	0.68	
89.04	0.11	0.083	8.62	0.54	
89.06	0.060	0.0071	8.90	0.52	
89.08	0.086	0.24	9.08	0.46	
89.10	0.051	0.16	6.84	0.84	
89.12	0.24	0.24	4.72	0.99	
92.38	0.37	0.75	4.52	1.0	dark to mid grey silt limestone, fine mudstone, some grey striations across the bedding plain
92.39	0.43	0.74	4.53	1.0	
92.40	0.50	1.0	4.07	1.3	
92.41	0.43	0.95	4.75	1.4	dark grey almost black silt limestone, fine mudstone, some lighter grey striations across the bedding plain
92.42	0.42	0.61	4.84	0.93	
92.43	0.31	0.58	5.56	0.86	
92.44	0.25	0.49	5.58	0.78	
92.46	0.39	0.64	5.07	0.86	

Some samples prepared and analysed by A. Kim, some by the author

bold figures indicate the mean of the results of at least two analyses

D.5 Triassic Sandstone

Middlesbrough Core

Sample descriptions from: D.I. Jackson, *Details of strata above the Sherburn Anhydrite* and D.B. Smith *Details of strata from the top of the Sherburn Anhydrite to the Seaham Formation* confirmed by inspection of the samples.

bold figures indicate the mean of the results of at least two analyses

Sample depth (m bgl)	A.I.C. (%)	Sample description
28.40-28.42	0.014	Siltstone, brown-red, with interbedded
28.42-28.45	0.018	mudstone of similar colour and listric
28.45-28.48	0.040	surfaces
28.48-28.50	0.023	
34.73-34.76	0.008	
40.60-40.63	0.003	Sandstone, slightly orange-red,
40.65-40.67	0.012	fine-grained (fine- to medium-grained
45.08-45.12	0.049	above 40.45); argillaceous and decalcified;
45.08-45.22	0.010	downward-coarsening cycles
45.12-45.15	0.054	
45.15-45.18	0.002	
45.18-45.22	0.014	
51.23-51.25	0.016	Lag breccia: red brown siltstone
51.25-51.28	0.019	
51.25-51.28	0.016	as 40.60 - 45.22, micaceous
51.28-51.30	0.011	
62.40-62.42	0.003	Sandstone, orange-red, slightly weathered
70.10-70.14	0.016	dull red mudstone
80.00-80.04	0.001	dull green mottled sandstone
90.26-90.28	0.013	lag breccia: red brown sandstone
90.28-90.30	0.014	
90.30-90.32	0.015	Sandstone, dominantly brown-red and
90.32-90.34	0.005	fine-grained, sporadic micaceous and lag breccia bedding-plane
99.88-100.04	0.009	partings; sporadic mica-rich layers in 99.25 to 100.05
113.52-113.54	0.014	laminates, sandstone facies (thinly
113.54-113.57	0.016	interlaminated and interlayered fine-grained
113.57-113.59	0.022	sandstone, very fine-grained sandstone,
113.59-113.62	0.017	gritty siltstone and silty mudstone)
126.15-126.20	0.012	Lag breccia partings, red brown sandstone
139.80-139.82	0.018	pale green-white well cemented quartzose sandstone
149.81-149.91	0.010	sandstone, thinly-bedded, medium- and
149.87-149.91	0.006	fine-grained, containing large and very
149.91-149.94	0.007	large (greater than core diameter) mudstone
149.94-149.97	0.011	clasts and possible rafts
149.97-150.00	0.058	
159.85-159.87	0.013	sandstone, brown-red, dominantly
159.87-159.90	0.013	fine-grained, in downward coarsening
170.00-170.03	0.006	cycles
170.03-170.06	0.004	
178.00-178.02	0.004	sandstone, brown-red, dominantly
178.02-178.05	0.002	fine-grained and monotonous
190.12-190.20	0.011	dull red brown siltstone, silty mudstone and
190.14-190.17	0.002	fine grained sandstone
190.17-190.20	0.011	
202.42-202.47	0.007	mudstones and siltstones
276.52-276.60	0.006	red-brown silty mudstone occ reduction spot
290.05-290.08	0.034	mudstone, red-brown with scattered mainly
290.08-290.11	0.034	very small pale grey-green reduction
290.11-290.14	0.033	patches, mainly blocky (within the
290.14-290.17	0.020	Sherburn Anhydrite)
290.17-290.20	0.053	

Appendix D: Measured AIC content

Gamston Core

No sample descriptions were available. Samples were prepared and analysed by A. Kim

Depth (m bgl)	AIC (%)	AIS (%)	TC (%)	TS (%)
15.24	0.040	0.3410	0.982	0.42
31.76	0.038	n.d.	0.432	0.0030
37.49	~	~	0.534	0.0090
39.01	~	~	0.737	n.d.
43.13	~	~	0.524	0.0034
44.78	~	~	0.744	0.0048
47.12	~	~	0.581	n.d.
49.07	~	~	0.593	0.0027
50.60	~	~	0.619	n.d.
53.64	~	~	0.701	0.0036
56.08	~	~	1.05	n.d.
60.35	0.031	n.d.	0.647	n.d.
63.40	~	~	0.506	n.d.
69.19	~	~	0.675	n.d.
74.07	0.036	0.0076	0.532	0.012
77.72	~	~	0.767	n.d.
80.16	~	~	0.472	n.d.
82.30	~	~	0.513	n.d.
82.30	~	~	0.334	n.d.
86.26	~	~	0.943	n.d.
90.53	~	~	1.11	n.d.
93.57	0.046	0.0031	0.877	n.d.
98.45	~	~	0.500	n.d.
101.50	~	~	0.514	n.d.
104.24	~	~	0.451	n.d.
107.29	0.036	n.d.	0.363	n.d.
111.25	~	~	0.458	n.d.
117.04	~	~	0.408	n.d.
128.02	0.043	n.d.	0.451	n.d.
142.95	0.054	0.0065		
149.05	0.037	n.d.	0.936	n.d.
150.88	~	~	0.391	0.0038
153.62	0.030	n.d.	0.556	n.d.
158.19	0.041	0.0059	0.107	0.011
162.46	~	~	0.780	n.d.
168.86	~	~	0.559	n.d.
175.56	~	~	0.514	n.d.
176.78	~	~	1.68	n.d.
177.70	0.033	0.015	0.101	n.d.
179.53	~	~	0.672	n.d.
182.27	~	~	0.419	n.d.
184.10	~	~	0.337	n.d.
186.84	~	~	0.730	0.0059
191.41	~	~	0.744	n.d.
194.16	~	~	0.663	n.d.
197.51	~	~	0.489	n.d.
197.82	~	~	0.995	0.0076
199.03	~	~	2.60	n.d.
199.03	0.029	n.d.	0.139	n.d.
200.86	0.026	n.d.	0.867	n.d.
203.91	~	~	0.806	n.d.
207.26	~	~	0.545	0.0026
209.70	~	~	0.424	n.d.
210.92	~	~	0.156	0.0059
211.23	~	~	0.285	n.d.
213.06	0.024	0.0086	0.896	0.0065
213.66	~	~	1.10	n.d.
214.88	~	~	1.42	n.d.
214.88	~	~	0.0539	n.d.

D.6 Site A

Boreholes 1, 2, 3: Sands and gravels

BH	Depth (m)	AIC (%)
1	0.5	0.36
1	1.5	0.094
1	2	0.035
1	3	0.090
1	4.5	0.062
2	0.25	0.18
2	1.5	0.070
2	3	0.048
2	3.7	0.11
2	4	0.090
2	5	0.11
2	7.5	0.17
3	0.5	0.13
3	1	0.18
3	2	0.18
3	3	0.11
3	4	0.42
3	5	0.11

Borehole 4: estuarine silts

BH	Depth (m)	AIC (%)
4	1.5	6.2
4	3	0.99
4	4	0.59
4	5	0.16
4	6	0.17

Figure 75: AIC in samples from BH 1, Site A

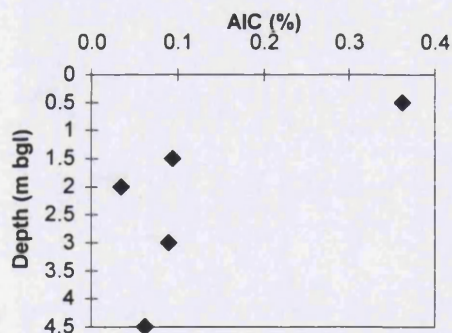


Figure 76: AIC in samples from BH 2, Site A

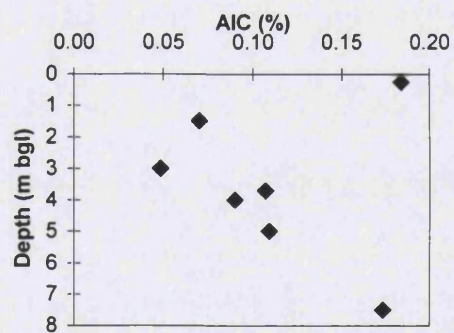


Figure 77: AIC in samples from BH 3, Site A

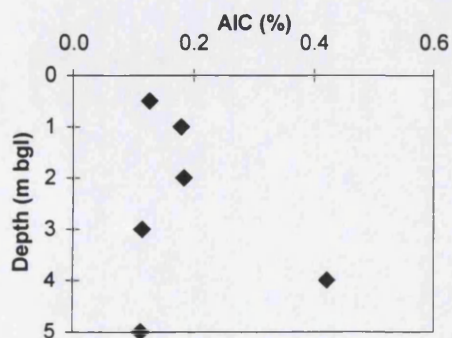
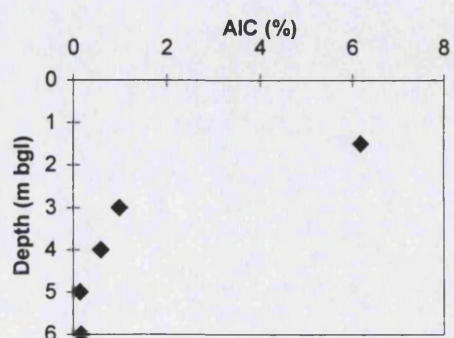


Figure 78: AIC in samples from BH 4, Site A



D.7 Site B

Samples with a single depth reference were taken from 100 mm diameter undisturbed (U100) cores. Where a depth range is given samples were taken from bulk samples, either from formations in which U100 samples could not be obtained, or from previously extruded U100 samples.

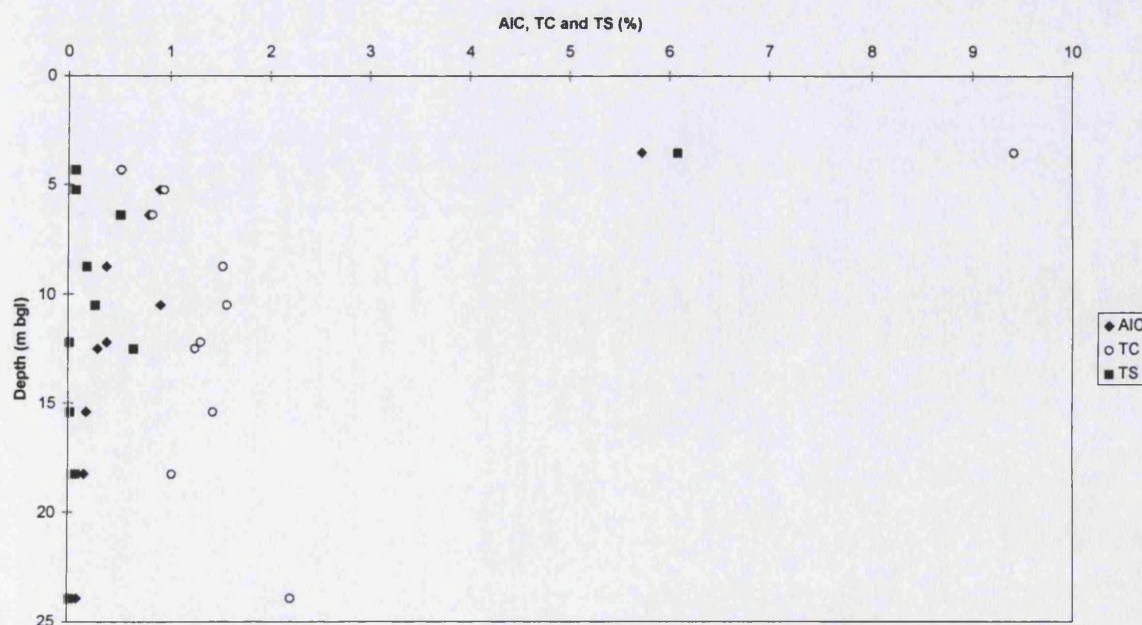
Sample descriptions are based on borehole logs prepared and supplied by consulting engineers, confirmed and corrected on inspection of the received samples.

MG made ground

Borehole 2D

Depth (m bgl)	AIC (%)	TC (%)	TS (%)	Material description
3.55	5.7	9.42	6.1	MG: Grey ashy slightly sandy clay with gravel
4.1-4.6	0.51	0.515	0.069	Stiff grey clayey SILT with occasional rootlets
5.25	0.90	0.939	0.070	
6.4	0.79	0.825	0.51	Stiff grey very silty CLAY with plant fragments
8.75	0.38	1.53	0.18	Stiff grey brown fine sandy SILT
10-11	0.90	1.57	0.26	Very soft grey very sandy SILT with occ gravel
12-13	0.29	1.25	0.64	red brown silty CLAY with rare fine gravel
15.4	0.18	1.43	0.016	Stiff reddish brown sandy CLAY with occ gravel
18-18.5	0.16	1.02	0.072	Red-brown clayey SAND with some gravel
21.2	0.38	1.31	0.013	Stiff brown slightly sandy CLAY with occasional
23.7-24.2	0.088	2.20	0.021	fine gravel and bands of very silty clay

Figure 79: AIC, TC and TS in Site B Borehole 2D

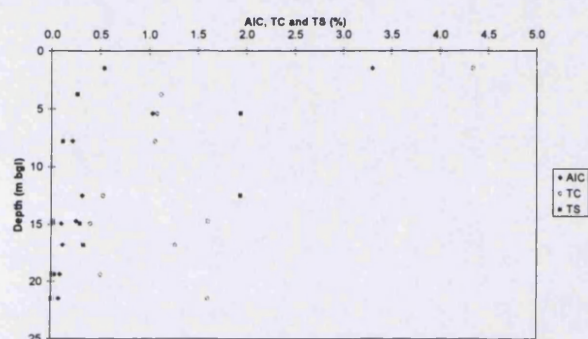


Appendix D: Measured AIC content

Borehole 4D

Depth (m bgl)	AIC (%)	TC (%)	TS (%)	Material description
1.5	3.3	4.34	0.54	MG: Firm brown and black sandy ashy clay
3.5-4.0	1.1	1.12	0.26	Firm brown and black clayey organic SILT
5.4	1.0	1.08	1.9	with occasional fine to medium black gravel
7.6-8	0.21	1.06	0.12	Brownish grey slightly silty fine SAND
12.5	0.32	0.532	1.9	Brownish grey silty SAND with some gravel
14.75	0.25	1.61	0.020	Brown very clayey silty fine to medium SAND
14.95	0.10	0.402	0.30	with occasional subangular medium gravel
16.8	0.12	1.27	0.33	Firm brown very clayey SILT with occ gravel
19.4	0.090	0.510	0.033	Stiff brown very sandy SILT with some gravel
21.5	0.076	1.61	0.006	Firm brown slightly sandy clayey SILT

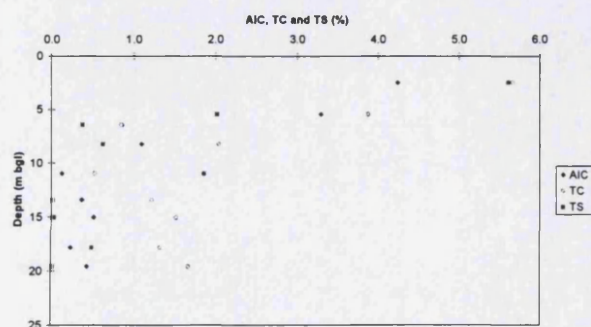
Figure 80: AIC, TC and TS in Site B Borehole 4D



Borehole 5D

Depth (m bgl)	AIC (%)	TC (%)	TS (%)	Material description
2.5	4.2	5.66	5.6	MG: brown / grey clayey sand with rubble
5.3-5.6	3.3	3.88	2.0	Firm brown / black very silty fine sandy CLAY
6.45	0.86	0.853	0.38	with occasional fine to medium gravel,
8.25	1.1	2.04	0.63	from 6m soft with occasional silt partings
10.5-11.5	0.13	0.529	1.9	Grey brown silty SAND with occasional gravel
13.45	0.37	1.22	0.015	Very stiff reddish brown CLAY with occ silt
15.05	0.52	1.52	0.031	Very stiff reddish brown CLAY with silt bands
17.85	0.24	1.32	0.50	Stiff reddish brown very fine sandy CLAY
19.6	0.44	1.67	0.013	Brown fine to medium very clayey SAND

Figure 81: AIC, TC and TS in Site B Borehole 5D

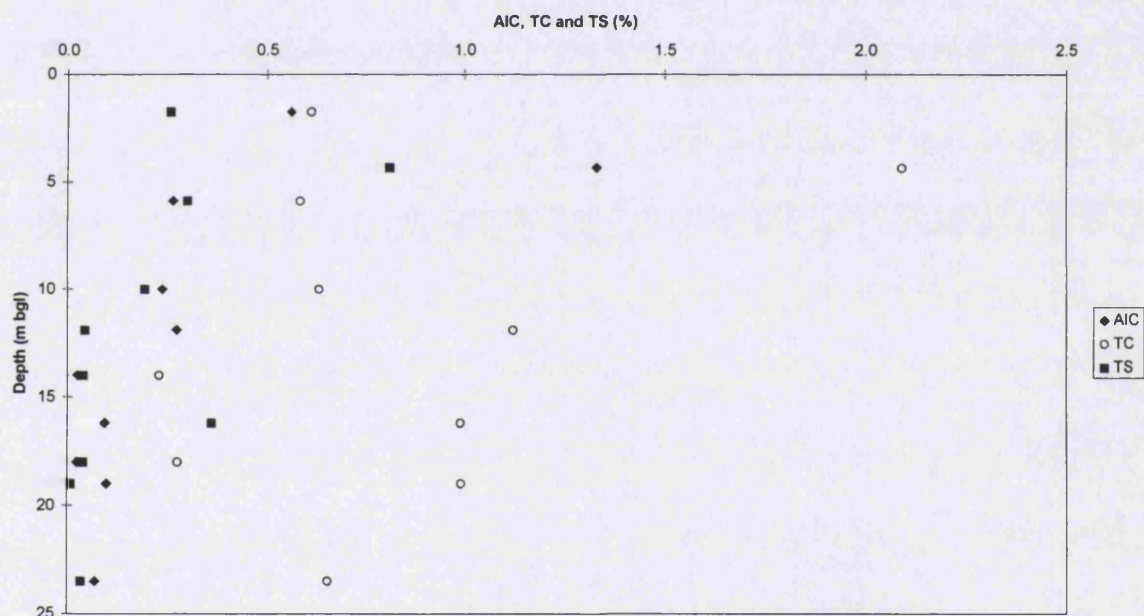


Appendix D: Measured AIC content

Borehole 6D

Depth (m bgl)	AIC (%)	TC (%)	TS (%)	Material description
1.5-2.0	0.56	0.611	0.26	Firm grey / brown slightly sandy CLAY
4.35	1.3	2.09	0.81	Firm reddish brown CLAY with silt partings
5.9	0.26	0.584	0.30	Brown slightly silty fine SAND
9.5-10.5	0.24	0.631	0.19	Red-brown clayey silty SAND with occ gravel
11.9	0.27	1.12	0.043	Stiff red-brown slightly sandy CLAY with silt
14	0.025	0.228	0.039	Brown fine to coarse SAND with some gravel
16.2	0.093	0.989	0.36	Stiff red-brown very sandy CLAY with gravel
17.5-18.5	0.023	0.275	0.039	Brown slightly clayey silty SAND with gravel
19	0.10	0.990	0.008	Stiff red-brown very sandy CLAY with occ gravel
23-24	0.070	0.653	0.034	Brown slightly clayey silty SAND with gravel

Figure 82: AIC, TC and TS in Site B Borehole 6D



Borehole 7S

Depth (m bgl)	AIC (%)	TC (%)	TS (%)	Material description
1.4-1.65	3.5	3.90	0.35	Firm brownish mottled grey very silty CLAY with occasional fine to coarse black gravel
1.4-1.65	3.3	4.01	0.43	
1.4-1.65	3.6	4.15	0.46	
1.4-1.65	3.5	3.86	0.41	
1.4-1.65	3.6	3.90	0.39	
1.4-1.65	3.5	3.77	0.046	
mean	3.5	3.93	0.35	

bold figures indicate the mean of the results of at least two analyses

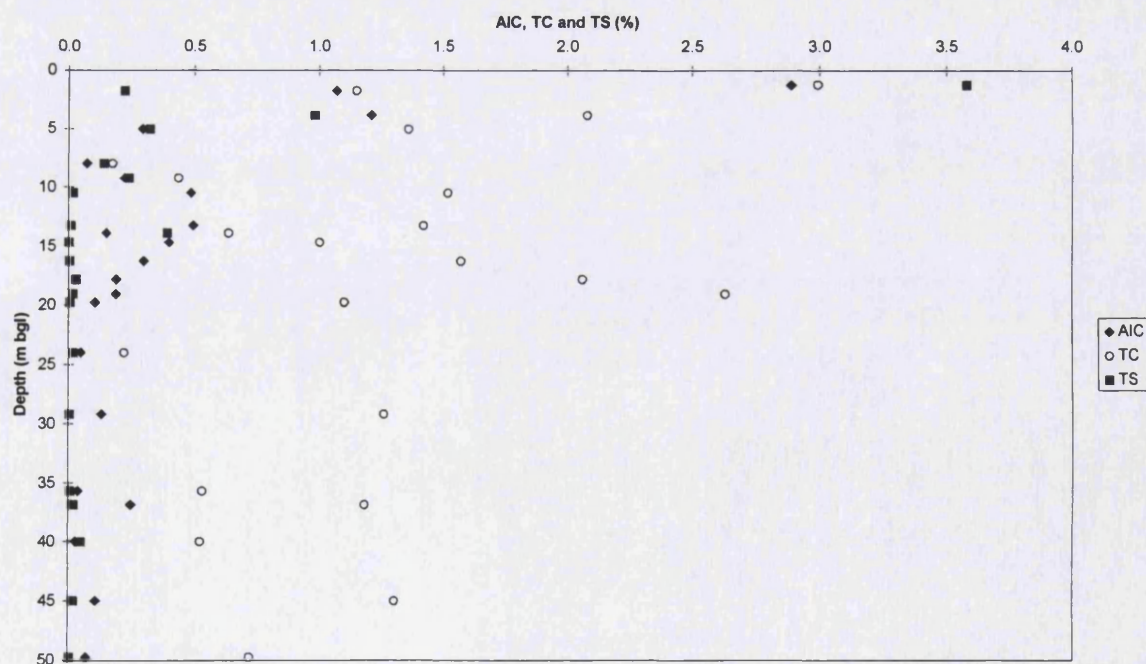
Appendix D: Measured AIC content

Borehole 8D

Depth (m bgl)	AIC (%)	TC (%)	TS (%)	Material description
1-1.5	2.9	2.99	3.6	MG: grey ashy CLAY with occ rubble gravel
1.5-2.0	1.1	1.15	0.22	Firm grey / brown silty sandy CLAY with roots
3.85	1.2	2.08	0.98	Grey brown clayey SILT with occ roots
5.05	0.29	1.36	0.32	Dark grey brown very silty fine to coarse SAND
7.5-8.5	0.073	0.175	0.14	with occ sandy clay
9-9.5	0.22	0.435	0.24	Brown slightly clayey SAND and GRAVEL
10.5	0.49	1.52	0.018	Firm to stiff brown laminated silty CLAY
13.25	0.49	1.42	0.0090	occasional partings of fine brown silty sand
13.9	0.15	0.636	0.39	and rare black fine gravel
14.7	0.40	1.00	n.d.	
16-16.45	0.30	1.57	0.0036	
17.8	0.19	2.06	0.029	Firm red-brown very clayey slightly sandy SILT
19.05	0.19	2.63	0.016	Soft reddish brown fine clayey SILT
19.75	0.11	1.10	0.0049	Reddish brown silty SAND with some gravel
24	0.048	0.220	0.018	Reddish brown fine to coarse silty SAND
29.2	0.13	1.26	0.0046	Firm reddish brown fine sandy clayey SILT
35.7	0.037	0.531	0.0077	Reddish brown silty clayey fine to coarse
36.7-37	0.25	1.18	0.020	SAND with occasional gravel
39.5-40.5	0.026	0.522	0.050	Reddish brown SAND with some gravel
44.5-45.5	0.11	1.30	0.019	Stiff red-brown fine sandy SILT
49.5-50	0.071	0.720	0.0048	Stiff red-brown sandy CLAY with occ gravel

bold figures indicate the mean of the results of at least two analyses

Figure 83: AIC, TC and TS in Site B Borehole 8D



Appendix D: Measured AIC content

Borehole 9D

Depth (m bgl)	AIC (%)	TC (%)	TS (%)	Material description
1	13	~	~	M.G. slightly ashy sand, clinker and rock cobbles
2	7.5	12.4	4.2	M.G. ashy sand and clinker and rock cobbles
2	18	~	~	
3	1.0	1.76	0.27	M.G. orange ashy clayey silt
3.6	0.0092	0.0187	0.015	M.G. red sandstone
5	0.011	0.0170	0.023	
6	0.97	1.87	0.90	grey brown silty clay
6.45	1.1	1.94	0.17	
6.8	0.19	0.835	0.12	
7 - 8	0.14	0.399	0.21	grey silty sand
8 - 9	0.28	0.424	0.33	
10.4	0.29	1.00	0.016	reddish brown silty sandy clay
10.8	0.22	1.63	0.015	
11.3 - 11.45	0.16	1.41	0.011	
11.3 - 11.4	0.089	~	~	
11.9	0.13	2.43	0.018	
12.33	0.12	1.41	n.d.	
13	0.055	0.994	0.011	reddish brown silty sand
13	0.089	~	~	
13.8	0.090	0.944	0.014	reddish brown sandy clay
13.8	0.060	~	~	
14.65	0.054	0.320	n.d.	reddish brown silty sand
15.34	0.095	1.12	0.021	reddish brown sandy clay
16.95	0.11	1.06	n.d.	
17.6	0.047	0.579	0.013	reddish brown silty sand
18 - 19	0.18	0.440	0.018	
19.7	0.097	1.49	0.018	reddish brown sandy clay
20.9	0.071	0.289	0.0068	orange brown silty sand
21.5	0.020	0.378	0.014	
28.5	0.042	0.216	0.0074	
29.6 - 30.2	0.13	1.77	n.d.	brown sandy clay
31.5	0.074	0.419	0.012	orange brown silty sand
31.5	0.028	~	~	

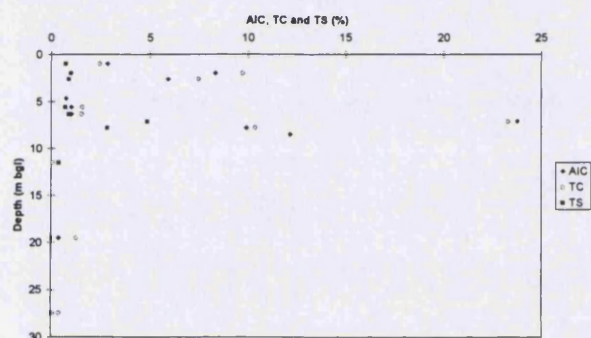
bold figures indicate the mean of the results of at least two analyses

Appendix D: Measured AIC content

Borehole 10D

depth (m bgl)	AIC (%)	TC (%)	TS (%)	Material description
1	2.8	2.45	0.73	M.G. stone and sandstone
2	8.3	9.71	1.0	M.G. mottled sandy silty clay
2.4 - 2.85	5.9	7.47	0.89	M.G. slag, clinker, concrete and mudstone
4.4 - 5.0	0.74	~	~	grey clay with plant fragments
5.2 - 5.85	1.0	1.58	0.70	grey clay with plant fragments
6.0 - 6.65	1.0	1.54	0.88	grey clay / brown peat
6.75 - 7.4	24	23.3	4.9	brown black clayey peat
7.55 - 8.05	9.9	10.4	2.8	brown clayey peat
8.25 - 8.7	12	~	~	brown peat / silty sand
11 - 12	0.062	0.0693	0.37	grey silty sand
19.4 - 19.7	0.39	1.28	0.0071	brown sandy clay
27 - 28	0.073	0.419	0.03	brown silty sand

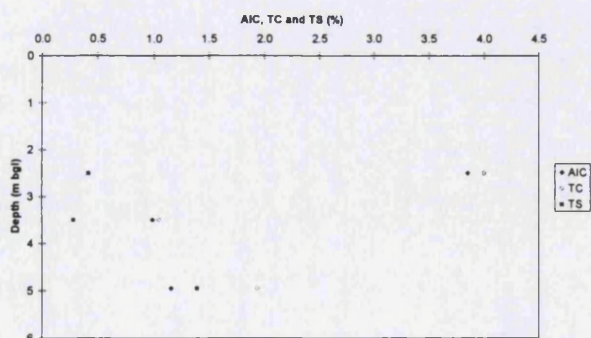
Figure 84: AIC, TC and TS in Site B Borehole 10D



Borehole 11D

depth (m bgl)	AIC (%)	TC (%)	TS (%)	Material description
2.5	3.9	4.00	0.42	Grey silt with plant fragments
3.5	0.99	1.05	0.28	Grey clayey silt
4.95	1.2	1.94	1.4	

Figure 85: AIC, TC and TS in Site B Borehole 11D

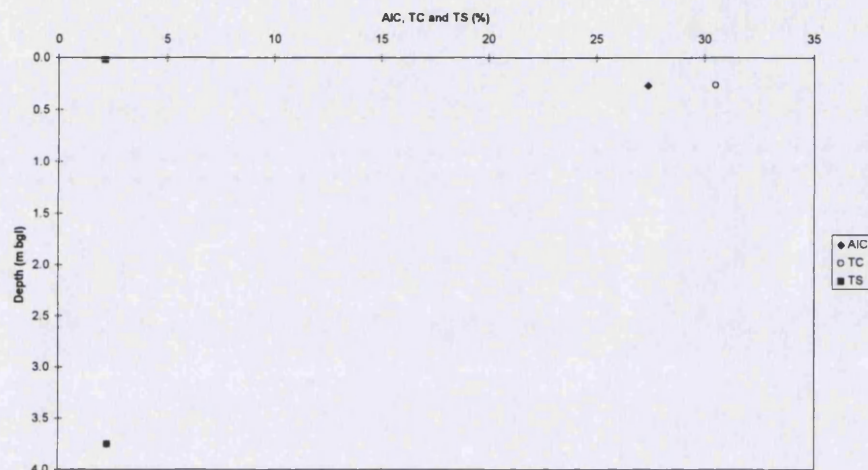


Appendix D: Measured AIC content

Borehole 12SA

Depth (m bgl)	AIC (%)	TC (%)	TS (%)	Material description
2.-2.5	27	30.5	2.1	MG: black clayey ashy sand and rubble gravel
3.5-4	0.27	0.262	0.019	Firm brown / grey very silty clayey SAND

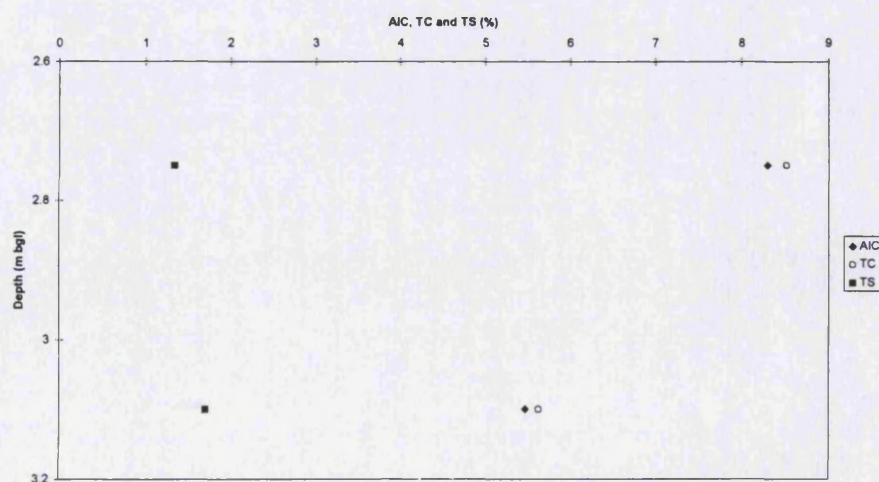
Figure 86: AIC, TC and TS in Site B Borehole 12SA



Borehole 13S

Depth (m bgl)	AIC (%)	TC (%)	TS (%)	Material description
2.5-3.0	8.3	8.52	1.3	MG: brown / black sandy ashy clay and rubble
3.1	5.5	5.63	1.7	brown / grey slightly sandy CLAY with gravel

Figure 87: AIC, TC and TS in Site B Borehole 13S



D.8 Lower Coal Measures

All sample descriptions based on borehole logs made by Geotechnical Engineering Limited, supplied by Entec UK Limited, confirmed by observation of the cores.

Borehole A

Depth (m bgl)	AIC (%)	Sample Description
6.17	1.9	Dark grey and black locally thinly laminated slightly, locally moderately, weathered MUDSTONE, moderately weak. Subhorizontal very closely to medium spaced planar smooth and rough open fractures.
6.56	4.3	
8.02	6.3	
7.30	5.0	
9.78	6.9	
10.96	1.5	clay-bound broken rock
11.65	1.8	
12.45	1.5	Light grey and grey fine and medium grained thinly laminated slightly weathered micaceous SANDSTONE interbedded with grey micaceous siltstone moderately weak and moderately strong. Subhorizontal very closely to medium spaced planar and undulating smooth and rough open fractures
13.02	1.9	
13.91	1.5	
16.00	1.2	

Borehole C

Depth (m bgl)	AIC (%)	Sample Description
17.80	0.44	Grey and dark grey thinly laminated slightly weathered MUDSTONE, moderately weak and moderately strong. Subhorizontal fractures with a little broken rock fill very closely spaced fractures with some clay bound mudstone gravel
18.30	0.74	
23.15	0.38	
23.90	0.43	
25.40	1.4	
25.72	0.47	Grey thinly laminated moderately weathered MUDSTONE, moderately weak. Subhorizontal very close and closely spaced planar and undulating open tight and smooth fractures. Some weathered brown rock.
27.06	0.46	
27.56	1.1	
27.83	0.58	
28.35	0.53	
29.20	0.86	Dark grey and black thinly laminated slightly weathered MUDSTONE, moderately weak. Subhorizontal very closely and closely spaced planar open smooth fractures
31.90	6.5	
33.77	7.3	Grey and dark grey slightly weathered SILTSTONE locally with sandstone
35.52	1.7	
36.20	0.88	Light grey and dark grey fine to medium grained thinly laminated slightly weathered locally micaceous SANDSTONE, moderately strong and strong. Subhorizontal closely to medium spaced planar and undulating open rough fractures.
37.50	3.1	
39.00	1.4	
39.90	1.5	

Borehole E

Depth (m bgl)	AIC (%)	Sample Description
60.10	0.42	Grey and dark grey locally thinly laminated moderately weathered MUDSTONE moderately weak. Subhorizontal very close to closely spaced planar open fractures.
60.90	0.81	
61.50	0.55	
62.45	4.2	Dark grey and black locally thinly laminated slightly weathered MUDSTONE moderately weak to moderately strong. Subhorizontal very closely to closely spaced planar smooth open fractures locally with broken rock
63.34	6.8	
63.88	6.7	
64.67	4.4	
68.38	5.2	Grey and light grey fine and medium grained thinly laminated slightly weathered micaceous SANDSTONE interbedded with grey micaceous siltstone, moderately strong. Subhorizontal very close to medium spaced planar / undulating smooth and rough open fractures occasionally with broken rock infill.
66.85	1.8	
67.15	1.8	
67.90	1.8	
68.18	1.6	
70.64	1.3	
71.76	1.4	

Appendix D: Measured AIC content

Borehole G

Depth (m bgl)	AIC (%)	Sample Description
53.35	0.38	Grey and dark grey locally thinly laminated slightly and moderately weathered MUDSTONE moderately weak. Subhorizontal very closely and closely spaced planar / undulating smooth open fractures with a little broken clay bound infill
54.60	0.41	
55.79	0.59	
56.90	0.71	
58.62	0.44	Dark grey and black locally thinly laminated slightly weathered MUDSTONE moderately weak. Subhorizontal planar / undulating smooth open fractures
60.47	0.64	
64.56	5.3	Light grey and grey fine and medium slightly weathered micaceous SANDSTONE locally interbedded with grey siltstone. Subhorizontal open fractures
66.38	1.5	
68.23	1.1	

Figure 88: AIC in Borehole A, Lower Coal Measures

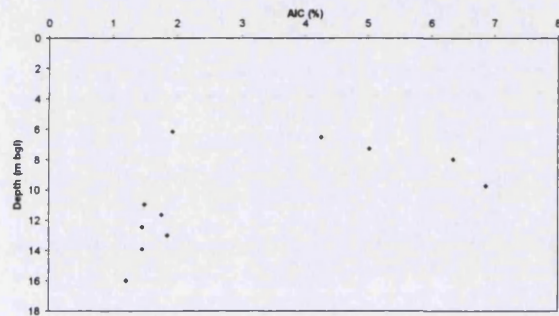


Figure 89: AIC in Borehole C, Lower Coal Measures

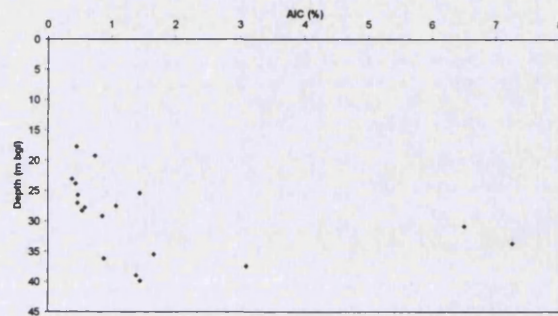


Figure 90: AIC in Borehole E, Lower Coal Measures

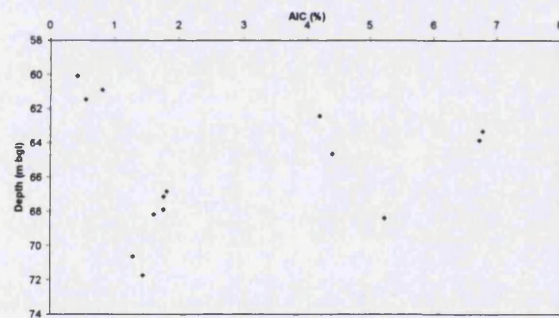
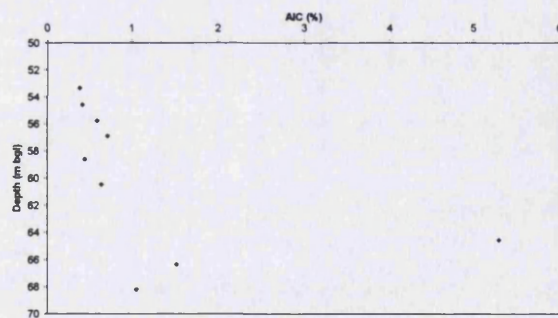


Figure 91: AIC in Borehole G, Lower Coal Measures



D.9 Bure Catchment Glacial Till

After coring, the cores were stored below 4°C. On extrusion from the sampling barrel, some cores clearly contained two different material types (for example, sandy and clayey materials) which were separated on extrusion, and treated as separate samples (marked by #). As the direction of the tubes was not known, it cannot be told which of the subsamples was uppermost. Samples were dried at 45°C, and crushed to homogenise them.

*= clay contents for these subsamples estimated on extrusion

all other clay content from George, 1998

Appendix D: Measured AIC content

Primrose Farm

Depth (m bgl)	AIC (%)	AIS (%)	Clay (%)	Sample Description
1	0.17	0.0039	70	Orange brown stiff very silty CLAY with many fine to medium subrounded gravel of chalk
2	0.090	0.0038	55	Orange brown clayey fine SAND with some fine to medium subrounded gravel of chalk and rare fine to medium subangular gravel of flint
3#	0.038	0.0024	30	Orange slightly clayey fine to coarse SAND with rare medium to coarse gravel of chalk
3#	0.092	0.017	50*	Orange slightly sandy very clayey SILT with some fine to coarse subrounded gravel of chalk
5	0.16	0.008	80	Brown clayey fine SAND with rare fine to medium gravel of chalk
6	0.25	0.005	80	Grey fine sandy very clayey SILT with rare fine subrounded gravel of chalk
9	0.14	0.0022	50	Orange slightly clayey fine SAND with rare coarse gravel
11	0.50	0.23	90	Dark grey fine sandy very clayey SILT with rare fine to medium subrounded gravel of chalk
15	0.10	0.014	20	Grey brown fine to coarse SAND
18	0.14	0.020	20	Grey brown fine to medium SAND with occasional fine to medium subangular gravel of mixed lithologies
20	0.12	0.032	20	Grey fine to coarse SAND with occasional to some fine to coarse subrounded gravel of mixed lithologies

Page's Farm

Depth (m bgl)	AIC (%)	AIS (%)	Clay (%)	Sample Description
2	0.46	0.008	50	Soft grey / light brown and dark brown mottled fine sandy clayey SILT with occasional subrounded fine gravel of chalk
3	0.53	0.011	55	greeny brown slightly fine sandy silty CLAY with many fine and occasional medium subangular gravel of chalk and occasional fine subrounded black gravel
4	0.40	0.28	100	Firm brownish grey silty CLAY with many fine and medium subrounded gravel of chalk and rare fine subangular gravel of flint
5	0.47	0.33	100	Soft grey clayey very silty fine SAND / very fine sandy SILT with many fine to medium subrounded gravel of chalk and rare medium subangular gravel of flint
6	0.28	0.22	95	Firm grey silty fine SAND with occasional fine to medium subrounded gravel of chalk
7	0.27	0.38	90	Soft grey clayey very silty fine SAND / fine sandy SILT with many fine subrounded gravel of chalk and subangular gravel of flint
9	0.94	0.23	50	Soft light grey and light brown mottled clayey SILT with rare fine subrounded gravel of chalk and subangular gravel of flint
11	0.34	0.26	55	Firm grey fine sandy SILT with occasional fine to medium subrounded gravel of chalk and rare medium subangular gravel of flint
13	0.43	0.19	55	Brownish grey fine sandy silty CLAY with occasional fine gravel of chalk and rare fine to medium black gravel
15	0.29	0.21	85	Firm grey fine sandy SILT with occasional fine subrounded gravel of chalk and medium subangular gravel of flint
17	0.30	0.17	90	Firm grey slightly clayey slightly fine sandy SILT with rare to occasional fine subrounded gravel of chalk and rare medium subangular gravel of flint
19	0.33	0.19	65	Brownish grey slightly sandy very silty CLAY with occasional fine to medium subangular gravel of flint and subrounded gravel of chalk

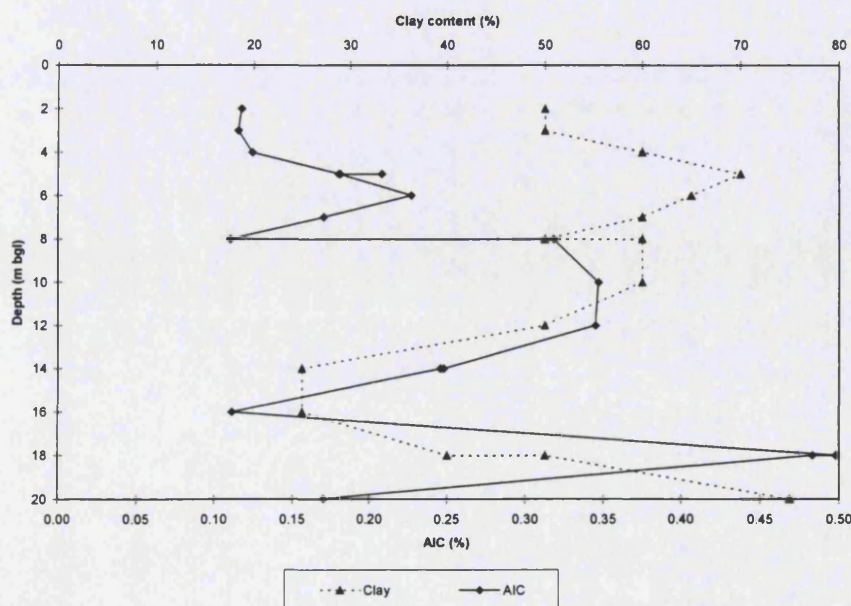
Appendix D: Measured AIC content

Bates Moor Farm

Depth (m bgl)	AIC (%)	AIS (%)	Clay (%)	Sample Description
2	0.12	0.0040	50	Very stiff orange silty fine SAND with rare medium gravel of chalk
3	0.12	n.d.	50	Soft orange brown clayey fine sandy SILT with occasional fine subrounded gravel of chalk and rare subangular fine to medium gravel of flint
4	0.12	0.0074	60	Soft brown clayey fine SAND with occasional fine subrounded chalk gravel and rare subangular flint gravel
5	0.19	0.0060	70	Soft brown clayey fine SAND with occasional subrounded fine gravel of chalk
6	0.23	0.012	65	Brown very silty fine SAND with many fine to medium subrounded gravel of chalk and flint
7	0.17	0.0022	60	Grey brown silty fine to medium SAND with rare subangular fine to medium gravel of flint
8#	0.11	0.017	60	Brown fine to medium SAND with occasional subangular to subrounded gravel of mixed lithologies
8#	0.32	0.15	50*	Firm dark grey clayey SILT with occasional fine subangular to subrounded gravel of chalk
10	0.35	0.17	60	Grey slightly silty fine SAND with occasional subrounded fine gravel of chalk
12	0.35	0.34	50	Soft brown very clayey fine SAND with occasional fine subrounded gravel of chalk
14	0.25	0.12	25	Soft / loosely consolidated brown slightly clayey fine to medium SAND with rare subrounded flint gravel
16	0.11	0.099	25	Brown slightly to very clayey fine to medium SAND with rare fine subrounded gavel of chalk and medium subangular gravel of flint
18	0.50	0.077	50	Brown slightly clayey fine to medium SAND with occasional fine to medium black gravel
18	0.48	0.26	40*	Soft dark grey fine to medium sandy clayey SILT with occasional subrounded fine chalk gravel and rare subangular gravel of flint
20	0.17	0.011	75	Very stiff light grey sandy clayey SILT with many subangular fine to medium gravel of flint and occasional fine subrounded gravel of chalk

bold figures indicate the mean of the results of at least two analyses

Figure 92: AIC and clay in North Sea Drift, Bates Moor Farm



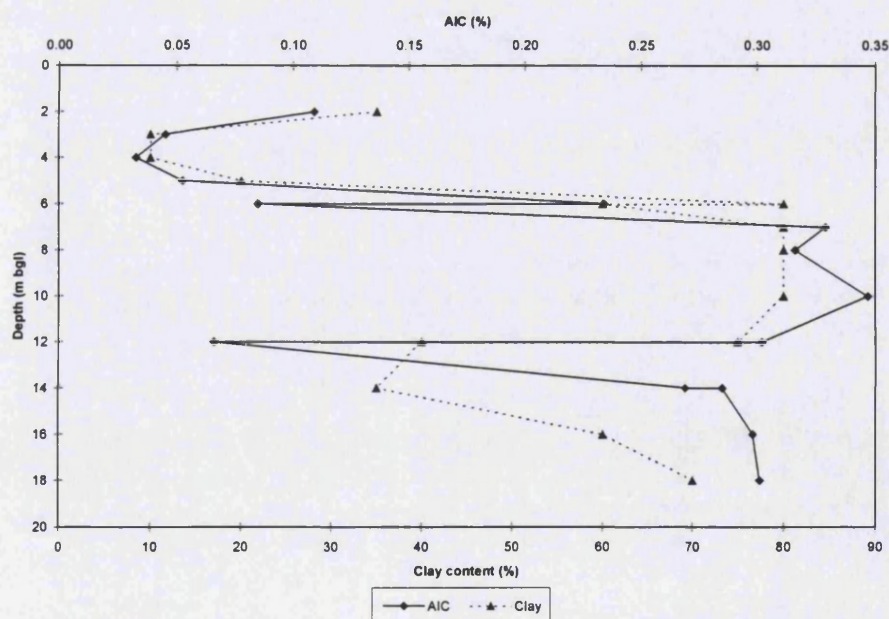
Appendix D: Measured AIC content

Crabgate Farm

Depth (m bgl)	AIC (%)	AIS (%)	Clay (%)	Sample Description
2	0.11	n.d.	35	Orange very stiff very fine sandy silt CLAY
3	0.045	n.d.	10	Orange very fine sandy CLAY / very clayey fine SAND with rare fine subrounded gravel of chalk
4	0.033	0.0024	10	Orange medium SAND with slightly clayey pockets and with occasional subangular to subrounded gravel of mixed lithology
5	0.053	0.0040	20	Orange brown clayey fine to medium SAND with some fine to coarse subrounded to subangular gravel of mixed lithology
6#	0.23	0.0034	80	Stiff grey CLAY
6#	0.08	0.0038	60*	Orange brown fine sandy silty CLAY with some to occasional fine subrounded gravel of chalk
7	0.33	0.12	80	Grey very stiff very clayey SILT and occasional subrounded fine gravel of chalk
8	0.32	0.11	80	Very stiff grey very clayey SILT / very silty CLAY
10	0.35	0.062	80	Stiff grey very clayey SILT / very silty CLAY
12#	0.30	0.088	75	Orange very sandy soft grey CLAY
12#	0.066	0.029	40*	Orange fine SAND with occasional medium to coarse gravel sized grey clay inclusions
14	0.28	0.086	35	Grey firm silty CLAY with much orange fine to medium SAND and occasional fine to medium subangular to subrounded gravel of mixed lithology
16	0.30	0.20	60	Dark grey brown clayey SILT / fine SAND with some fine subrounded gravel of chalk and rare medium to coarse subangular gravel of flint
18	0.30	0.18	70	Brown slightly clayey fine sandy SILT / silty fine SAND with some fine and occasional medium subrounded gravel of chalk and occasional medium subangular gravel of flint

bold figures indicate the mean of the results of at least two analyses

Figure 93: AIC and clay in North Sea Drift, Crabgate Farm

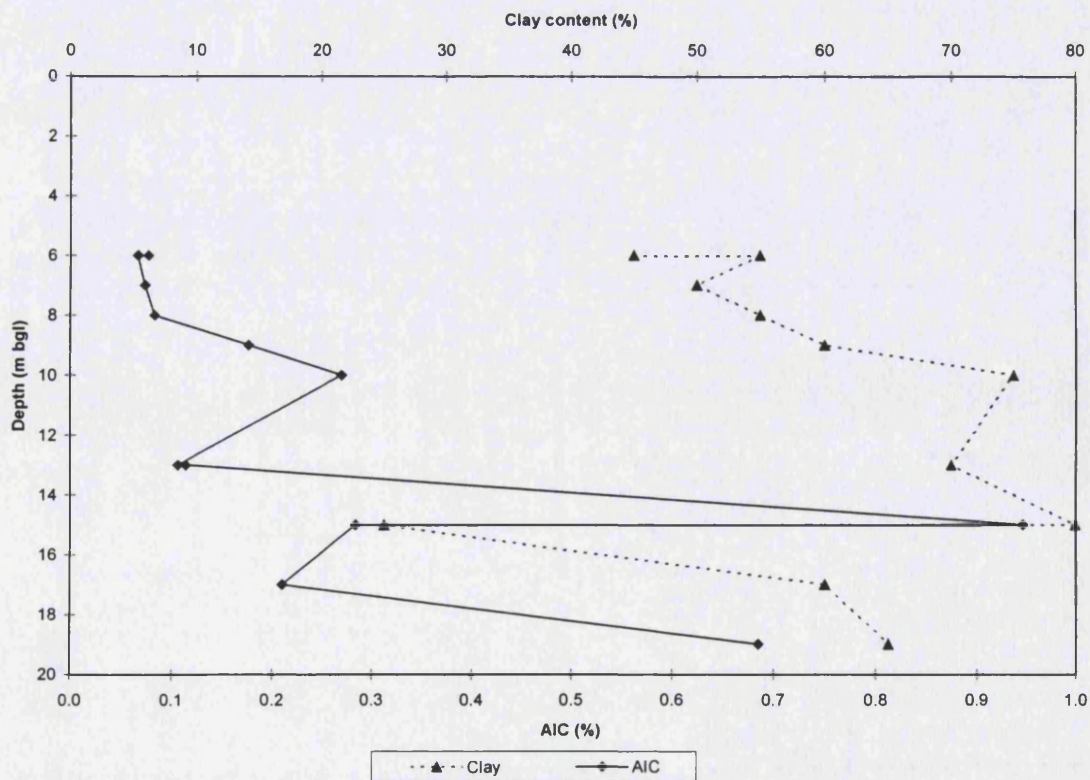


Appendix D: Measured AIC content

Ropers Farm

Depth (m bgl)	AIC (%)	AIS (%)	Clay (%)	Sample Description
6#	0.077	n.d.	45	Orange brown fine to coarse SAND with occasional fine to medium subangular flint gravel
6#	0.066	0.0024	55*	Light orange brown clayey fine sandy SILT with occasional subangular fine to medium gravel of chalk
7	0.073	0.0022	50	Orange brown very clayey fine SAND with many fine subrounded and occasional medium subrounded to subangular gravel of chalk and rare medium subrounded to subangular gravel of mixed lithology
8	0.083	0.0020	55	Brown very clayey fine SAND with occasional to some fine to medium subangular to subrounded gravel of chalk and rare medium subangular gravel of flint
9	0.18	0.0072	60	Firm brown slightly clayey fine to medium SAND with fine to medium subangular gravel of yellow chalk
10	0.27	0.23	75	Browny grey firm clayey fine sandy SILT with many fine and occasional medium subrounded gravel of chalk and rare subrounded medium gravel of mixed lithologies
11	0.11	0.047	70	Grey fine sandy CLAY with occasional fine to medium white subrounded gravel of chalk
13	0.11	0.051	70	Grey fine to coarse SAND with clayey pockets and with occasional fine to medium subangular to subrounded gravel of chalk
15#	0.95	0.13	25	grey fine to coarse SAND with occasional to rare subrounded fine to medium gravel of mixed lithologies
15#	0.28	0.13	25	Light grey slightly silty CLAY with rare fine to medium subrounded gravel of chalk
17	0.21	0.12	60	Soft grey silty CLAY with occasional fine and rare medium subrounded gravel of chalk
19	0.69	0.22	65	Very soft light grey clayey SILT with occasional to some fine to medium subrounded gravel of chalk

Figure 94: AIC and clay in North Sea Drift, Ropers Farm



D.10 Morley Glacial Till

The samples were collected from the outside of the drilling core barrel, bagged and stored at below 4°C. Samples were dried at room temperature and riffle split to gain smaller representative fractions, which were crushed to homogenise them.

Depth (m bgl)	TC (%)	TS (%)	AIC (%)	IC (%)	CaCO3 (%)	Sample description
0.8 - 1.0	4.68	0.0090	0.29	4.39	36.6	Orangey-brown silty CLAY with many chalk and occasional straw fragments, mottled with rare dark brown gravel sized inclusions, rare grey gravel sized silty CLAY inclusions; rare subrounded medium gravel of chalk; rare coarse gravel sized sandy inclusions
1.5 - 2.0	6.09	0.017	0.20	5.89	49.1	as 0.8 - 1.0 m with rare subangular medium to coarse flint gravel
2.5 - 3	6.46	0.011	0.24	6.22	51.8	soft brown slightly silty CLAY with many fine subrounded to subangular chalk gravel, rare straw fragments, rare medium to coarse flint gravel, and rare dark brown mottling
3.5 - 4	6.86	0.017	0.28	6.58	54.8	very soft light brown silty CLAY with many fine and rare medium to coarse subangular to subrounded chalk gravel
6	6.45	0.33	0.95	5.50	45.8	soft dark grey CLAY with many fine to medium subangular to subrounded chalk gravel
8	6.78	0.94	1.0	5.74	47.9	firm dark grey CLAY with many fine to medium subangular to subrounded chalk gravel
8.5 - 9	6.50	0.61	0.70	5.80	48.3	soft dark grey CLAY with many fine to medium subangular to subrounded chalk gravel
10#	4.66	0.020	0.12	4.54	37.8	soft to firm orange-brown very clayey SILT with some fine chalk gravel
10#	5.32	0.015	0.33	4.99	41.6	orange brown very clayey fine SAND

Samples referenced 10# were recovered from the same sample bag, and on inspection appeared to be different materials. These materials were separated before drying, and treated as separate samples.

bold figures indicate the mean of the results of at least two analyses

E. Organic matter isolation

Initial attempts to isolate organic matter (OM) from geological samples led to the identification of various problems and incorporation of improvements into the method applied, which are outlined here. Additionally, it should be noted that both liquid and gaseous states of hydrofluoric acid are **extremely dangerous**. The acid is extremely corrosive to the skin, although, depending on concentration, burns may not be felt for several hours. The acid is readily absorbed and often affects tissues beneath the skin (Wood *et al.*, 1996). Exposure can be fatal and may be carcinogenic. Precautions taken included wearing rubber apron, face visor, rubber gloves and gauntlets. Shower facilities and calcium gluconate gel were available.

E.1 Method details

Approximately 50g of each sample was weighed into a plastic beaker. Concentrated HCl was added until 24 hours after effervescence ceased. The sample was washed with distilled water six times, then covered with 90% concentrated HF, 10% concentrated HCl and stirred continuously for up to 14 days, until it no longer felt gritty. It was repeatedly washed with distilled water and concentrated HCl added to dissolve any CaF_2 formed. Dedicated pipettes were used to remove supernatant at each change of liquid. A heavy liquid separation of the residue with sodium polytungstenate (s.g. 2.0) produced a float and a sink fraction. The sink fraction was subjected to further heavy liquid separation to recover further OM, with the additional float added to the initial float. The float portion was repeatedly washed in distilled water. This was considered to be the final OM isolate and used to make slides, then freeze-dried and crushed in an agate pestle and mortar.

Slides were prepared by diluting an aliquot of the suspended OM in polyvinyl alcohol solution (a dispersant) to produce a suspension judged visually to have appropriate density. 1 ml of this was spread on a cover slip and slowly dried on a hot-plate. The cover slip was mounted on a microscope slide using petropoxy resin, and cured on a hot-plate at higher temperature. Slides were prepared before drying the material, as this was found to be more successful (consistent with Durand and Nicaise, 1980).

E.2 Mineral matter in residues

After initial processing attempts (on Site B samples), low carbon content of the residues (between 1.32% and 54.5%) indicated that significant amounts of mineral matter remained. Microscopic inspection of slides, X-ray diffraction and major element analysis of the residues indicated that most of the non-organic matter present was undissolved and unseparated siliceous material (Si up to 37%, arithmetic mean 8%; total Si, Al, Ca, Mg, Fe, Na content up to 42%, arithmetic mean 17%). The other non-organic components were pyrite (indicated by high S content, with Fe content up to 3.5%, arithmetic mean 1%), and possibly sodium polytungstenate crystals (Na content up to 9%, arithmetic mean 3%). The following procedures were adopted to minimise this problem:

- Teflon-coated magnetic stirrers were used to stir samples continuously when under HCl and HF; this also prevented cross-contamination of samples by stirring rods;
- the samples remained under HCl for 24 hours after visible effervescence had stopped;
- greater time was allowed for HF dissolution: carbonate samples were treated for at least a week; siliceous samples for at least two weeks, decanting and refreshing the HF after one week;
- heavy liquid separation was included in the processing, and applied to all samples.

OM isolated from Site B samples utilising these improvements had total carbon up to 75.5%, with an arithmetic mean of 30%. Lower recovery was from samples with low AIC.

E.3 Loss of organic matter

The calculation of recovery percentages indicated that significant amounts of OM were ‘lost’ during the processing. The following procedures were adopted to minimise this:

- the heavy liquid separation of the ‘sink’ fraction was repeated: significant OM was found in the sink fraction of initial separations (C content of the sink up to 20%, with more C recovered in the sink than in the float for some samples), either entrained with the settling mineral matter or intimately associated with mineral matter giving it a specific gravity greater than 2;
- the time period for centrifugation during heavy liquid separation was increased to at least 30 minutes.

Appendix E: OM isolation method development

OM is also lost as suspended particles during decanting of acid and water; this may preferentially remove fine-grained and low density particles which settle more slowly and are more easily disturbed. This was minimised by:

- removing supernatant liquid by pipetting rather than decanting;
- taking care to eliminate spillage and loss of particles, especially avoiding effervescence overflowing;
- increasing the settling time between repeated decanting.

In addition, an estimation was made of the material incorporated into slide preparation, based on the volume proportion removed from the sample before drying. Additional OM may be lost during the isolation procedure sorbed to the apparatus, particularly the beakers, and dissolved in the acids used and decanted. Further sample isolation using these improvements provided very low C content in the sink fraction, and greater % recovery of organic carbon in the float fraction.

No published data was found on recovery from organic matter isolation following similar procedures. However, discussion revealed that such losses were expected: *'in most of these procedures, you lose a significant fraction of your kerogen literally down-the-drain'* (Bissada, pers. comm., 1999) *'the reagents used may solubilise the humic and fulvic acids in modern sediments and soils, but these losses don't compare to the physical-mass losses in the decantation steps'*.

E.4 Use of HCl with HF

The presence of insoluble fluorite salts after HF treatment led to the addition of HCl with the HF in a 1:9 ratio (suggested by colleagues of D. Jolley, Centre for Palynology, Sheffield University). This minimised, but did not eradicate, fluorite salt production, which were removed by washing the sample in HCl for 24 hours.

E.5 Drying

Oven drying at 50°C of initial OM isolations resulted in aggregated OM that adhered to the glass container. Freeze-drying was more successful in preparing a loose OM residue.

E.6 Limitations

The method is not applicable to samples with very low organic carbon content. Given 50% recovery of the organic carbon present in the whole rock sample (Section 7.2, Table 23), recovery of 100mg of organic carbon (a workable minimum for slide preparation and chemical analysis) would require 200mg organic carbon to be present in the original sample. For a sample with 0.1% TOC, for example, 200g of original sample would be required. Operational restrictions, such as the volume of hydrofluoric acid used and the length of time the extraction would take would make this infeasible. Therefore isolation of organic matter from Triassic Sandstone and Chalk was not successfully attempted.

E.7 Slide preparation

Slides of early samples were created using both the technique described in Chapter 6 and Section E.E.1, and by mixing an aliquot of the material with molten glycerine spiked with safranin (which preferentially stains palynomorphs), spreading this on a microscope slide and sealing with a cover slip. This produces better photographs, as the contrast is greater. However, it was found that glycerine-mounted stained slides do not show amorphous OM clearly. Additionally, the OM is located throughout the depth of the glycerine, and not at a single focal depth when inspected by microscope. In slides made by drying the strewn smear on the cover-slip and mounting with petropoxy resin, the OM is in one focal plane. This method was used for all subsequent slides.

F. Results from point counting

F.1 Repeated counts on the same slide

Lincolnshire Limestone, Slide LL60.48, magnification ×400

count	amorphous matter	brown wood	black wood	fungi /algae	other tissues	resin	degraded humin	pollen	spores
1	53	89	114	0	12	2	15	12	3
2	78	81	109	0	10	2	11	8	1
3	85	83	94	0	11	1	13	13	0
4	71	76	121	0	10	2	10	10	0
5	68	83	106	0	15	3	16	9	0
6	67	77	104	0	14	0	23	15	0
mean	70.33	81.50	108.00	0.00	12.00	1.67	14.67	11.17	0.67
mean %	23.44	27.17	36.00	n.a	4.00	0.56	4.89	3.72	0.22
sd of counts	10.88	4.72	9.19	n.a	2.10	1.03	4.68	2.64	1.21

Glacial Till, slide NTY10-3, magnification ×400

count	amorphous matter	brown wood	black wood	fungi /algae	other tissues	resin	degraded humin	pollen	spores
1	221	36	35	0	6	0	2	0	0
2	219	40	34	0	4	0	3	0	0
3	215	37	41	0	6	0	1	0	0
4	225	31	38	0	4	0	2	0	0
5	220	38	35	0	4	0	3	0	0
6	218	41	36	0	3	0	2	0	0
mean	219.7	37.2	36.5	0	4.5	0	2.2	0	0
mean %	73.2	12.4	12.2	n.a.	1.5	n.a.	0.7	n.a.	n.a.
stdev	3.3	3.5	2.6	n.a.	1.2	n.a.	0.8	n.a.	n.a.
sd as % of mean	4.5	28.6	21.3	n.a.	81.6	n.a.	104.2	n.a.	n.a.

Site B, initial slides, slide W9D, 6.45, Counted 200, magnification ×500

count	amorphous matter	brown wood	black wood	fungi /algae	other tissues	resin	degraded humin	pollen	spores
1	44	28.5	16	0	2.5	0	9	0	0
2	46.5	29.5	13	0	3	0	8	0	0
3	45.5	24.5	12	0	6	0	12	0	0
4	47	23	16	0	3.5	0	10.5	0	0
5	45	17.5	17.5	0.5	4	0	15.5	0	0
6	52	23.5	12	0	2	0	10.5	0	0
mean	46.7	24.4	14.4	0.1	3.5	0	10.9	0	0
s.d.	2.8	4.3	2.4	0.2	1.4	n.a.	2.6	n.a.	n.a.
s.d. as % of mean	6.0	17.7	16.5	244.9	40.4	n.a.	24.1	n.a.	n.a.

Appendix F: Point counting results

Site B initial slides, slide W10D 2.0:1, Counted 300, magnification ×500

count	amorphous matter	brown wood	black wood	fungi /algae	other tissues	resin	degraded humin	pollen	spores
1	47.3	5	39.3	0	0	0	8.3	0	0
2	42.6	4.3	44.3	0	0.3	0	8	0	0
3	41.6	2.3	43.9	0	1.3	0	10.6	0	0
4	38.6	2.3	48.6	0	0	0	10.3	0	0
5	46	2	46.6	0	0	0	5.3	0	0
6									
mean	43.2	3.2	44.5	0.0	0.3	0	8.5	0	0
s.d.	3.5	1.4	3.5	0.0	0.6	n.a	2.1	n.a	a.
s.d. as % of mean	8.1	43.1	7.8	n.a.	175.9	n.a	25.1	n.a	n.a.

Site B initial slides, slide W10D 2.0:2, Counted 300, magnification ×500

count	amorphous matter	brown wood	black wood	fungi /algae	other tissues	resin	degraded humin	pollen	spores
1	47.3	5	39.3	0	0	0	8.3	0	0
2	42.6	4.3	44.3	0	0.3	0	8	0	0
3	41.6	2.3	43.9	0	1.3	0	10.6	0	0
4	38.6	2.3	48.6	0	0	0	10.3	0	0
5	46	2	46.6	0	0	0	5.3	0	0
6									
mean	43.2	3.2	44.5	0.0	0.3	0	8.5	0	0
s.d.	3.5	1.4	3.5	0.0	0.6	n.a	2.1	n.a	a.
s.d. as % of mean	8.1	43.1	7.8	n.a.	175.9	n.a	25.1	n.a	n.a.

F.2 Counts on duplicated slides of the same sample

Site B, Counted 300, magnification ×400

count	amorphous matter	brown wood	black wood	fungi /algae	other tissues	resin	degraded humin	pollen	spores
1/1:3	167	5	86	3	2	0	36	11	0
1/1:2	155	6	102	3	4	0	29	0	0
12.8-13.25:5	3	17	256	1	7	0	12	2	1
12.8-13.25:6	7	7	271	0	6	0	6	1	1
12.8-13.25:7	4	13	269	0	8	0	5	1	0
12.8-13.25:8	14	13	259	1	4	0	8	0	0

Glacial Till, magnification ×400

Slide	amorphous matter	brown wood	black wood	fungi /algae	other tissues	resin	degraded humin	pollen	spores
GTL1.5-2/1-1	229	11	54	0	2	1	3	0	0
GTL1.5-2/2-1	191	15	86	0	5	1	2	0	0
GTL8.5-9/1-1	199	7	90	0	2	0	2	0	0
GTL8.5-9/2-1	171	7	115	0	3	0	3	0	1

Samples GTL1.5-2 /1 and GTL1.5-2 /1 were subsamples from 1.5 to 2 m bgl, and treated for separation of OM separately, as were GTL8.5-9/1 and GTL8.5-9/2, from 8.5 to 9 m bgl.

Appendix F: Point counting results

F.3 Impact of density

Slide	dilution	amorphous matter	brown wood	black wood	fungi /algae	other tissues	resin	degraded humin	pollen	spores
GTL8.5-9/1-1	3.3E-03	199	7	90	0	2	0	2	0	0
GTL8.5-9/1-2	3.3E-04	211	19	64	0	2	0	4	0	0
GTL8.5-9/1-3	3.3E-05	245	5	46	0	1	0	2	0	0
GTL8.5-9/1-5	8.3E-06	113	17	160	0	5	1	4	0	0
GTL8.5-9/1-4	3.3E-06	217	9	66	0	5	0	3	0	0
GTL8.5-9/1-6	3.3E-07	too sparse to count								

F.4 Lincolnshire Limestone

Results from isolated OM from unoxidised Lincolnshire Limestone samples from the Longholt core are tabulated below:

Slide	amorphous matter	brown wood	black wood	fungi /algae	other tissues	resin	degraded humin	pollen	spores
L82.27-82.29	103	46	131	0	18	0	1	1	0
L81.575-81.60	226	6	52	0	1	0	15	0	0
L81.50-81.525	257	8	33	0	2	0	0	0	0
L80.47-80.49	266	6	16	0	1	0	11	0	0
L79.35-79.37	280	4	9	0	3	0	4	0	0
L76.00-76.03	260	2	36	0	2	0	0	0	0
L75.90-75.93	225	22	48	0	1	0	4	0	0
L69.19-69.21	261	3	35	0	1	0	0	0	0
L69.09-69.11	278	8	10	1	1	0	2	0	0
L69.05-69.07	234	6	53	0	2	0	5	0	0
L68.97-68.99	246	1	53	0	0	0	0	0	0
L68.87-68.89	243	8	42	0	0	0	7	0	0
L67.54-67.56	90	4	138	0	2	0	66	0	0
L67.54-67.56	176	3	101	0	2	0	17	0	1
L67.08-67.10	242	12	26	0	17	0	2	1	0
L62.02-62.05 (1)	277	11	9	0	2	0	1	0	0
L62.02-62.05 (2)	286	6	4	0	1	3	0	0	0
L60.48-60.51	66	43	112	0	36	0	25	16	2

Much of the opaque 'black wood' material in L82.27-82.29 may be pyrite.

Other plant tissues included 'flower like' structures and honeycomb structures in some samples.

F.5 Glacial Till

Results from isolated OM from North Sea Drift samples from Pages Farm:

Slide	amorphous matter	brown wood	black wood	fungi /algae	other tissue	resin	degraded humin	pollen	spores
NTY1-5	230	27	20	0	14	4	3	1	1
NTY2-3	227	24	41	0	6	2	0	0	0
NTY3-4	230	7	53	0	6	1	2	0	1
NTY4-4	241	8	39	0	7	1	4	0	0
NTY5-3	248	5	40	0	5	0	2	0	0
NTY6-3	220	22	41	0	8	1	7	1	0
NTY7-3	260	10	24	0	4	0	2	0	0
NTY8-4	237	33	29	0	0	1	0	0	0
NTY9-4	251	22	33	0	5	0	0	0	0
NTY10-3	205	53	41	0	1	0	0	0	0
NTY11-4	240	26	30	0	3	1	0	0	0
NTY12-1	217	30	49	0	3	0	1	0	0

notes: NTY3-4: 'black wood' opaque material may include pyrite

Results from isolated OM from Lowestoft Till samples from Morley are included in Sections F.2 and F.3.

F.6 Site B

Results from isolated OM from samples from Site B:

Slide	amorphous matter	brown wood	black wood	fungi /algae	other tissues	resin	degraded humin	pollen	spores
1/1:3	167	5	86	3	2	0	36	11	0
1/1:2	155	6	102	3	4	0	29	0	0
1/2:2	141	14	104	4	1	0	34	0	0
2/2:1	178	5	102	1	2	0	12	2	0
3:1	117	46	83	2	32	0	17	0	0
6:1	102	59	111	0	9	0	18	3	1
11.3-11.4:2	191	5	99	0	0	0	2	3	0
12.8-13.25:5	3	17	256	1	7	0	12	2	1
12.8-13.25:6	7	7	271	0	6	0	6	1	1
12.8-13.25:7	4	13	269	0	8	0	5	1	0
12.8-13.25:8	14	13	259	1	4	0	8	0	0
13.5-13.95:5	109	18	163	0	6	0	4	0	0
15.1-15.8:4	190	8	95	0	5	0	2	0	0
17.5-17.95:3	50	27	206	1	9	0	7	0	0
20.7-21.15:3	131	13	148	0	2	0	5	0	1
31:2	26	34	223	0	14	0	2	0	1

G. TCE analysis

G.1 TCE analysis method details

GC-MS analysis was by a method based on U.S. Geological Survey Open File Report 94-708 *Methods of analysis by the U.S. Geological Survey National Water Quality Laboratory: Determination of Volatile Organic Compounds in Water by Purge & Trap Capillary Gas Chromatography / Mass Spectrometry*. Instrumentation was a Tekmar 3000 Purge & Trap using a Precept II autosampler linked to a Fisons 8000 Series gas chromatograph interfaced to a MD 800 quadrupole mass spectrometer (ionisation voltage 70 eV; detector voltage 300V; source temperature 250 °C; interface temperature 250 °C). Separation was performed using a fused silica capillary column (25 mm × 0.32 mm i.d., SGE) coated (0.5 µm) with 5% phenyl polysiloxane (BP5). Helium was used as carrier gas with a head pressure of 110 pK_a. Initial oven temperature for the analytes was 35 °C for 4 minutes, subsequently increasing at 45 °C/min to 180 °C. TCE elutes at about 1.3 minutes.

Selective-ion monitoring was used to gather the TCE data. The following masses were analysed during the time period 1 to 2.5 minutes to look for TCE: 60, 62, 95, 97, 130, 132. DCE and VC, potential degradation products of TCE were also scanned for between 1 and 2.5 minutes; the following masses were selected: 62, 64 and 96. The following masses were analysed from 2.5 to 13 minutes to look for potential contamination products: 55, 77, 78, 91, 92, 112, 114 (these would reveal alkane and aromatic products). For all masses, the interchannel delay time was 0.02 min, the dwell time 0.1 min and the span time 0.5 min.

5 ml of each sample was purged for 6 minutes and then desorbed for 3 minutes at 250°C from a VOCARB 3000 Purge Trap (K). The sample was then swept onto the GC column via the transfer line held at 130 °C. The trap was baked after each sample for 4 minutes at 260 °C to minimise carryover.

G.2 Standards

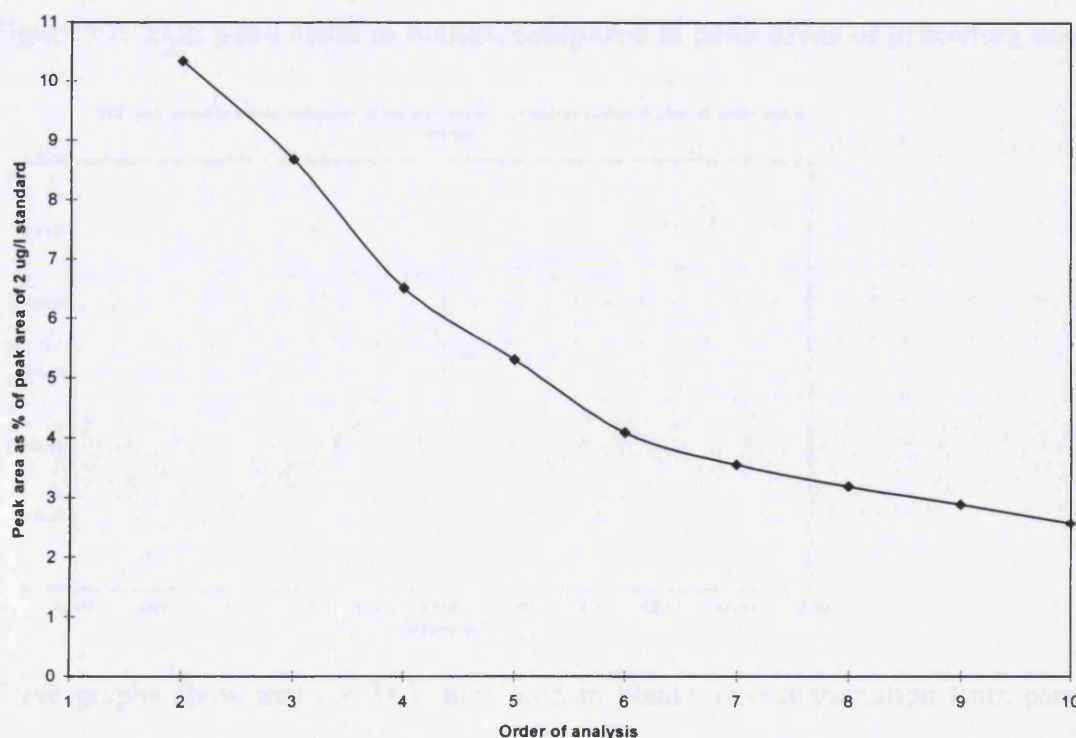
Standard solutions were prepared as follows: stock solution 1 comprised 38 µl TCE in 10.96 ml methanol, producing a solution of 5.054 g/l TCE. Stock solution 2 comprised

11 μl of stock solution 1 in 10.99 ml methanol, producing a solution of 0.005054 g/l TCE. The six calibration standards comprised approximately 42 ml water (to fill the vial, measured exactly) with a measured volume of stock solution 2. Calibration standards were prepared from stock solutions on the day that they were analysed.

G.3 Blank values

Carry-over between samples was confirmed by analysis of ten consecutive blank samples, and by comparing the peak areas of blanks analysed within sample analysis runs to the peak area of the preceding sample. The consecutive blank samples (Figure 95) clearly show a decline in measured peak area. (The first analysis of every sample run was found to be elevated, and so discarded; therefore the results from the first of the blank run was also excluded). These peak areas fell far below the calibrated range, and so have not been converted into a concentration of TCE, but have been compared to the peak area typical of the lowest standard (approximately $2\mu\text{g/l}$ TCE). The asymptote of the declining curve indicates a machine blank peak area around 2% of the lowest standard ($2\mu\text{g/l}$).

Figure 95: Decrease in TCE contamination in blanks with repeated analysis



Appendix G: TCE analysis

The peak areas measured for blanks in analysis runs (of time series experiments) containing samples and standards are plotted on Figure 96 against the peak area of the preceding sample. The same plot is also given for the run of consecutive blanks (Figure 97).

Figure 96: TCE peak areas in blanks, compared to peak areas of preceding samples

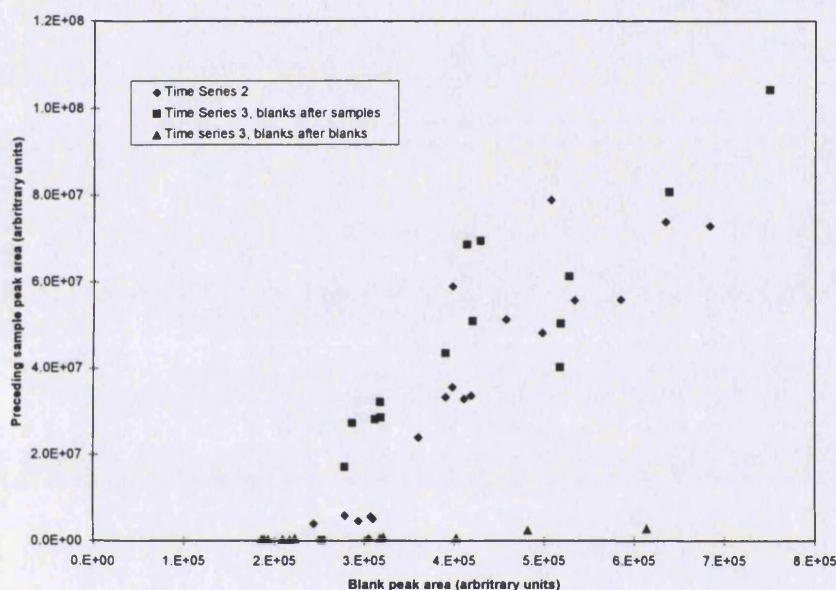
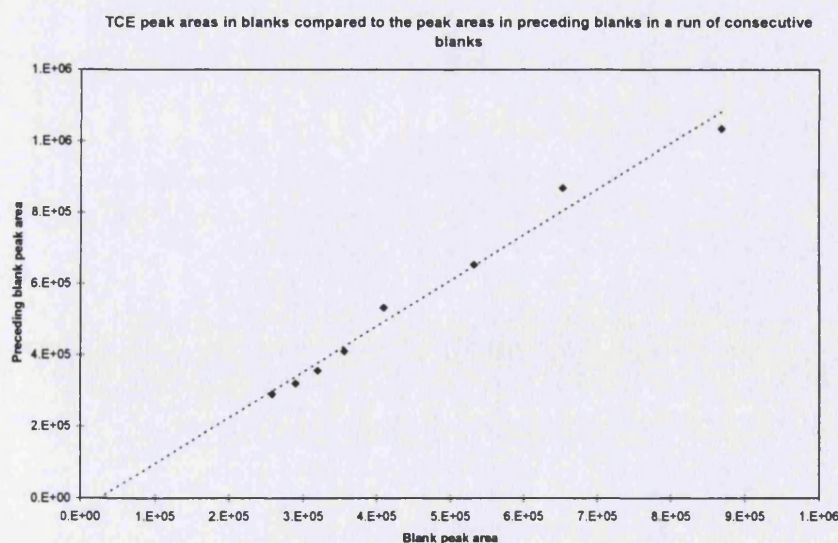


Figure 97: TCE peak areas in blanks, compared to peak areas of preceding blanks



These graphs show that the TCE measured in blanks is contamination from carry-over from the preceding sample. In the analysis of consecutive blanks, each peak area was on average 84% of the preceding peak area. An extension of the trendline of the points of

Appendix G: TCE analysis

Figure 97 indicates that a 'machine blank', uninfluenced by a preceding sample, would have a peak area of approximately 3×10^4 , about 10% of that in the last of the ten consecutive blanks analysed. This suggests that almost all of the TCE measured in blanks is carry-over from the preceding sample. Contamination remaining on the gas capillary column would not be detected at the same retention time as the TCE from the sample being analysed, so the constant retention time indicates that the contamination is being held somewhere within the autosampler or purge and trap module.

The contamination from runs containing standards and samples varies between about 2×10^5 and 8×10^5 with an arithmetic mean of about 4×10^5 . These are about 4% of the peak area of the lowest end of the concentration range analysed and about 0.4% of the peak area of a typical sample concentration and are therefore relatively insignificant.

H. Results of Sorption Experiments

Cw g/l	Cs mg/g	Kd l/kg	Koc l/kg
Weathered Glacial Till, TOC = 0.2%			
2.24E-01	5.09E-02	0.23	113
1.89E-02	7.13E-03	0.38	189
9.35E-03	3.96E-03	0.42	212
1.74E-03	1.18E-03	0.68	339
1.72E-04	1.38E-04	0.80	401
Unweathered Glacial Till, TOC = 0.7%			
3.36E-02	1.59E-01	4.72	674
3.78E-03	1.92E-02	5.07	724
1.59E-03	1.08E-02	6.80	971
1.79E-04	2.20E-03	12.32	1760
2.26E-05	2.08E-04	9.21	1315
Lincolnshire Limestone, TOC = 0.2%			
1.26E-01	5.46E-02	0.43	217
7.21E-03	9.62E-03	1.33	667
3.87E-03	5.88E-03	1.52	759
8.65E-04	2.22E-03	2.56	1281
3.27E-05	1.94E-04	5.93	2966
Kirton Shale, TOC = 2.0%			
3.43E-02	1.24E-01	3.62	181
1.39E-03	1.72E-02	12.36	619
5.04E-04	1.02E-02	20.22	1013
1.06E-04	1.84E-03	17.38	871
5.49E-06	8.91E-05	16.23	813

Cw g/l	Cs mg/g	Kd l/kg	Koc l/kg
Site B, made ground, 2m bgl, TOC = 18.2%			
1.37E-01	4.13E-02	0.30	1.7
1.34E-01	4.41E-02	0.33	1.8
9.07E-02	5.08E-02	0.56	3.1
5.99E-02	4.46E-02	0.75	4.1
2.73E-02	3.51E-02	1.29	7.1
1.70E-03	1.66E-02	9.78	53.7
6.27E-04	2.88E-03	4.59	25.2
1.73E-04	1.19E-03	6.88	37.8
7.91E-06	1.08E-04	13.68	75.2
Site B, made ground, 3m bgl, TOC = 1.1%			
1.64E-01	2.18E-02	0.13	12
1.05E-02	1.37E-02	1.31	121
2.50E-03	8.12E-03	3.25	301
4.95E-04	1.66E-03	3.36	311
2.92E-04	1.16E-03	3.99	370
Site B, silty clay, 6m bgl, TOC = 0.6%			
1.49E-01	6.11E-02	0.41	74
1.08E-02	9.74E-03	0.90	164
5.43E-03	6.45E-03	1.19	216
4.42E-04	1.53E-03	3.46	630
2.47E-05	2.01E-04	8.14	1480

The batch experiment on made ground from 2m bgl, Site B, was repeated using different concentrations, providing twice the results to the other samples. Results from the two batch experiments were in good agreement.